A CESIUM - 133 NMR STUDY OF THE STATICS AND DYNAMICS OF CESIUM ION COMPLEXATION BY CROWNS AND CRYPTANDS IN VARIOUS SOLVENTS

Dissertation for the Degree of Ph. D.
MICHIGAN STATE UNIVERSITY
ELIZABETH HUN-I MEI
1977





This is to certify that the

thesis entitled
A CESIUM-133 NMR STUDY OF THE STATICS AND
DYNAMICS OF CESIUM ION COMPLEXATION BY
CROWNS AND CRYPTANDS IN VARIOUS SOLVENTS.
presented by

ELIZABETH HUN-I MEI

has been accepted towards fulfillment of the requirements for

Ph. D. degree in Chemistry

Date Nov. 4, 1976

O-7639

JUL 14 (C.3) ,OCT | 9 (993) (DCT | 4 (9)

G101009

deviation esti

tetraphenylbor

popaqueous solv

Cesium-13

ABSTRACT

A CESIUM-133 NMR STUDY OF THE STATICS AND DYNAMICS OF
CESIUM ION COMPLEXATION BY CROWNS AND CRYPTANDS IN
VARIOUS SOLVENTS

By

Elizabeth Hun-I Mei

Chemical shifts of the cesium-133 nucleus were measured in six nonaqueous solvents relative to 0.5 M aqueous cesium bromide. Cesium tetraphenylborate (CsTPB), triiodide and thiocynate were used to determine the infinite dilution chemical shifts in pyridine (PY), propylene carbonate (PC), dimethylformamide (DMF), dimethylsulfoxide (DMSO), acetonitrile (MeCN), and acetone. The corresponding ion-pair formation constants were determined from chemical shift concentration data with the aid of a weighted nonlinear least squares program (KINFIT). The association constant for CsSCN in pyridine is 900±200 while for CsTPB in pyridine it is 370±20, in PC it is 16±7, in MeCN it is 40±10, and in acetone it is 22±3. The uncertainties given are standard deviation estimates.

Cesium-133 NMR studies were also performed on cesium tetraphenylborate complexes with five ligands in the six nonaqueous solvents mentioned. These ligands were 18-Crown-6

(18C6), dibenzotand-C222 (C222) have different t complexation abi 1:1 and 2:1 (lig solvents with th 10³. A new EQN to analyze data (2:1) formation. fected by the ge It was also show in the equilibri complexation by in PC $R_1 = (1.5\pm$ $R_2 = 34 \pm 0.5$, in $^{\text{DMSO}} K_1 = (1.1 \pm 0)$ 10^5 , $R_2 = 4.4 \pm 0$. ring of 18C6 yie DBC. However, p values are in th dine). A thorough

dine was made at for the purpose reference was de was used to show give temperature

(18C6), dibenzo-18C6 (DBC), dicyclohexyl-18C6 (DCC), cryptand-C222 (C222), and monobenzo-C222 (C222B). These liqands have different topologies and substituents which affect the complexation ability. Cesium tetraphenylborate forms both 1:1 and 2:1 (ligand/Cs⁺) complexes with 18C6 in all six solvents with the first formation constant (K_1) larger than 10³. A new EQN subroutine of the KINFIT program was written to analyze data which show both 1:1 and sandwich complex (2:1) formation. It was found that both K_1 and K_2 are affected by the geometry and substituents of the crown ligands. It was also shown that the solvent plays an important role in the equilibrium process. For example, the K values for complexation by 18C6 in pyridine are $K_1 > 10^8$, $K_2 = 71 \pm 1$, in PC $K_1 = (1.5\pm0.6) \times 10^4$, $K_2 = 8\pm2$, in acetone $K_1 > 10^7$, $K_2 = 34\pm0.5$, in DMF $K_1 = (9\pm3) \times 10^3$, $K_2 = 2.44\pm0.05$, in DMSO $K_1 = (1.1\pm0.1) \times 10^3$, $K_2 = (1\pm0.4)$ and in MeCN $K_1 > 0$ 10^5 , $K_2 = 4.4 \pm 0.3$. The attachment of a substituent on the ring of 18C6 yielded values of K₁ in the order 18C6 > DCC > DBC. However, probably because of steric effects, the K2 values are in the order DBC > 18C6 > DCC (at least in pyridine).

A thorough study of 18C6 complexes with CsTPB in pyridine was made at various temperatures (from 25° to -44°C). For the purpose of this study a new temperature independent reference was designed. Its validity was tested and it was used to show that ion-ion and ion-solvent interactions give temperature-dependent chemical shifts. The values of

the first format too large to be a were determined changes for the $LE_2 = -6.2 \pm 0.1 \text{ K}$ $LS_2 = -11.2 \pm 0.3$ reaction of Cs⁺. Kcal/mole.

The formati were also obtain formation consta sclvents. For i (10±1) x 10³ (PC x 10² (DMF), (27 222B, with a ben weaker complexes (PY) to zero (DM $^{ ext{dependent}}$ studie of kinetics. Bo $^{ ext{in}}$ the solution. of the formation of Cs⁺ by C222. also calculated that both quanti

complexation of

complex. The co

complex is much

the first formation constant at various temperatures were too large to be determined by NMR techniques but K_2 values were determined and used to obtain the enthalpy and entropy changes for the second complexation step. The results are: $\Delta H_2 = -6.2 \pm 0.1 \text{ Kcal/mole } (\Delta G_2^O)_{298} = -2.83 \pm 0.004 \text{ Kcal/mole,}$ $\Delta S_2 = -11.2 \pm 0.3 \text{ e.u. A kinetics study of the decomplexation reaction of Cs}^+ \cdot 18C6 \text{ gave an activation energy of } 8 \pm 0.3 \text{ Kcal/mole.}$

The formation constants of C222 and C222B complexes were also obtained from the NMR chemical shift data. The formation constants showed the same trends with various solvents. For instance, K_1 values for C222 are >10⁵ (PY), $(10\pm1) \times 10^3$ (PC), $(10.8\pm0.8) \times 10^3$ (acetone), (1.5 ± 0.1) \times 10² (DMF), (27±3) (DMSO), and (4±1) \times 10⁴ (MeCN). Cryptand-222B, with a benzo group on one of the ether chains forms weaker complexes, with K values ranging from (5.7 ± 0.8) x 10^3 (PY) to zero (DMSO). Chemical shift-mole ratio temperature dependent studies were also carried out, as well as studies of kinetics. Both gave evidence for two types of complexes in the solution. The results are interpreted on the basis of the formation of both inclusive and exclusive complexes of Cs⁺ by C222. Enthalpies and entropies of formation were also calculated by using the KINFIT program and it was found that both quantities are sensitive to the solvent for the complexation of free cesium ions to form the exclusive complex. The conversion of the exclusive to the inclusive complex is much less sensitive to solvent. The activation

energy (E_a) for the CSTPB in PC is 1-contained from kinare $E_a = 8.5 \pm 0.5$ (for 18C6). It at restricted geomethe largest actition.

energy (E_a) for the complexation reaction of C222B with CSTPB in PC is 14 ± 0.6 Kcal/mole. By comparison the values obtained from kinetics studies of crown complexes in PC are $E_a=8.5\pm0.5$ Kcal/mole (for DCC) and $E_a=8\pm4$ Kcal/mole (for 18C6). It appears that the higher rigidity and restricted geometry of the ligand combine to give C222B the largest activation energy for removal of a cesium ion.

A CESIUM

DYNAMI

CROWNS

in par

A CESIUM-133 NMR STUDY OF THE STATICS AND DYNAMICS OF CESIUM ION COMPLEXATION BY CROWNS AND CRYPTANDS IN VARIOUS SOLVENTS

Ву

ELIZABETH HUN-I MEI

A DISSERTATION

Submitted to

Michigan State University

in partial fulfillment of the requirement

for the degree of

DOCTOR OF PHILOSOPHY

Department of Chemistry

To My Parents.

The author Professors Jam guidance, enco out this study Gratitude Michigan State Administration financial aid. Special th brother Dr. Ho ment and sugge to the members and Professor moral support. Many thank

Frank Bennis f eter in operat

I am deepl love and cordi I dedicate thi

ACKNOWLEDGMENTS

The author wishes to express her sincere gratitude to Professors James L. Dye and Alexander I. Popov for their guidance, encouragement and whole-hearted support throughout this study.

Gratitude is also extended to the Department of Chemistry,
Michigan State University, the U.S. Energy and Development
Administration and the National Science Foundation for
financial aid.

Special thanks go to my Uncle Dr. Tony S. Shen and my brother Dr. Howell H. Mei for their constant encouragement and suggestions in many ways. Thanks are also extended to the members of the research groups of both Professor Dye and Professor Popov for their constant stimulation and moral support.

Many thanks also go to Mr. Wayne Burkhardt and Mr. Frank Bennis for their efforts in keeping the NMR spectrometer in operating condition.

I am deeply grateful to my parents for their great love and cordial concern throughout all my life. To them I dedicate this thesis.

- 1. INTROD
- II. HISTOR
 - A. Ma
 - pl
 - B. Co Ma
 - c. Nι
 - (:
 - (:

(i:

- III. CONCLU
- CHAPTER II. 1
 - I. SYNTHI
 - II. SOLVEN PREPAI
 - III. THE NY AND DA
- CHAPTER III.
 CESIUM TET
 COMPLEXES
 VARIOUS SO
 - I. INTROD
 - II. INVEST

TABLE OF CONTENTS

Chapter		Page
LIST OF	TABLES	vii
LIST OF	FIGURES	xiv
CHAPTER	I. HISTORICAL	1
1.	INTRODUCTION	2
II.	HISTORICAL BACKGROUND	3
	A. Macrocyclic Polyether-Crown Complexation of Alkali Metal Ions	3
	B. Complexation of Metal Ions by Macroheterocyclic Ligands-Cryptands	15
	C. Nuclear Magnetic Resonance	25
	(i) Introduction	25
	(ii) Chemical Shift Studies of Electrolyte Solutions	27
	(iii) Cesium Nuclear Magnetic Resonance	38
III.	CONCLUSIONS	43
CHAPTER	II. EXPERIMENTAL PART	44
I.	SYNTHESIS OF CESIUM TETRAPHENYLBORATE AND LIGAND PURIFICATION	45
II.	SOLVENT PURIFICATION AND SAMPLE PREPARATION	47
III.	THE NMR SPECTROMETER; MEASUREMENT AND DATA HANDLING	52
CES	III. STUDY OF FORMATION CONSTANTS OF IUM TETRAPHENYLBORATE ION PAIR AND OF PLEXES WITH MACROCYCLIC LIGANDS IN	
	IOUS SOLVENTS	57
I.	INTRODUCTION	58
-	INVESTIGATION OF CESIUM SALTS IN	50

A. C:

B.

CHAPTER IV. CESIUM TE WITH CROW

I. INTRO

II. DETER THE L

A. M

B. E

III. RESUL

A.

B. s P

c. D

CHAPTER V. A
COMPLEXAT
COMPLEXES

I. INTRO

Chapter		Page
III.	FORMATION CONSTANTS OF CESIUM TETRA- PHENYLBORATE COMPLEXES WITH CROWNS AND CRYPTANDS IN VARIOUS SOLVENTS	68
	(i) Complexation Reactions with Crowns	89
	(ii) Complexation Reactions with Cryptands	99
IV.	TEMPERATURE DEPENDENCE OF THE CHEMICAL SHIFT AND ITS RELATIONSHIP TO THE THERMO-DYNAMICS OF COMPLEXATION REACTIONS	109
	A. CESIUM TETRAPHENYLBORATE COMPLEXES WITH 18C6 IN PYRIDINE	109
	B. CESIUM TETRAPHENYLBORATE COMPLEXES WITH C222 IN VARIOUS SOLVENTS	125
CES	IV. A STUDY OF THE DYNAMICS OF IUM TETRAPHENYLBORATE COMPLEXES H CROWNS AND CRYPTANDS	142
ī.	INTRODUCTION	143
II.	DETERMINATION AND INTERPRETATION OF THE LINESHAPES	143
	A. MEASUREMENTS IN THE ABSENCE OF EXCHANGE	144
	B. EVALUATION OF EXCHANGE TIMES	151
III.	RESULTS AND DISCUSSION	152
	A. LIGAND EFFECT ON EXCHANGE RATE	152
	B. SOLVENT EFFECT ON THE EXCHANGE PROCESSES	168
	C. DISCUSSION	183
COM	V. A CESIUM-133 NMR STUDY OF THE PLEXATION OF CESIUM TETRAPHENYLBORATE C222: DISCUSSION OF THE TYPES OF	
	PLEXES	186
I.	INTRODUCTION	187

CHAPTER VI. SU FUTURE STU:

I. SUMMARY

II. SUGGEST

APPENDICES

APPENDIX A.

APPENDIX B.

APPENDIX C.

APPENDIX D.

REFERENCES. . .

Chapter																				Page
-	EVIDE COMPL			-			T .	Y P	ES	•	F	CR	YP •	TA •	TE	:	•	•	•	187
CHAPTER V	VI.	SUM	MA	RY	Α	ND	S	UG	GE	ST	'IC	NS	F	OR	2					
FUTUI	RE ST	UDI	ES	•	•	•	•	•	•	•	•	•	•	•	•	•	•	•	•	201
I. S	SUMMA	.RY	•	•	•	•	•	•	•	•	•	•	•	•	•	•	•	•	•	202
II.	SUGGE	STI	ON	S	FC	R	FU	TU	RE	S	TU	DI	ES	•	•	•	•	•	•	205
APPENDICES																				
APPE	NDIX	A.	•		•	•	•	•	•	•	•	•		•	•	•		•	•	208
APPE	NDIX	В.	•	•	•	•	•	•	•	•	•	•	•	•	•	•	•	•	•	212
APPE	NDIX	c.	•	•	•	•	•	•	•	•	•	•	•	•	•	•	•	•	•	221
APPE	NDIX	D.	•	•	•	•	•	•	•	•	•	•	•	•	•	•	•	•	•	235
DEEEDENCES 220								220												

Thermodyna Cryptate (

by Caloria

3 Trends in Cryptands

4 Values of

 Δ , and the

Alkali Me

Values of

Techniques

The Physic

Nucleus .

7 Physical :

Correction on DA-60.

8 Cesium-13

Salt Solu:

On Pair sealts in sealts i

Mole Ration With Cesi

ру Са-133

LIST OF TABLES

Table	Page
1 Thermodynamic Quantities for Com	plexation
Reactions of Macrocyclic Polyeth	ers 11
2 Thermodynamic Quantities for Alk	ali
Cryptate Complexation Reaction M	easured
by Calorimetry at 25°C in Water	22
3 Trends in Thermodynamic Paramete	rs with
Cryptands	21
4 Values of the Average Excitation	Energy,
Δ , and the Expectation Value $< r_i^-$	³ > _p for
Alkali Metals	33
5 Values of σ_{aq}^{O} Obtained by Various	s
Techniques	37
6 The Physical Properties of the Ca	s-133
Nucleus	38
7 Physical Properties of Solvents	and
Correction for Magnetic Susception	bility
on DA-60	55
8 Cesium-133 Chemical Shifts of Ces	sium
Salt Solution at 25°C	60
9 Ion Pair Formation Constants of	Cesium
Salts in Various Nonaqueous Solve	ents 67
10 Mole Ratio Study of 18C6 Complex	es
with Cesium Salts in Various Sol	vents
by Cs-133 NMR at 25°C	72

12 Mole Ratio

NMR at 25

CsTPB in v

CsTPB in v

15 Formation

with Ligar

with CsTPi

l7 Limiting (
Solvents.

Half-heig

log K Valligands i:

Tak	ole	Page
11	Mole Ratio Study of DBC Complexes with	
	CsTPB in various Solvents by Cs-133 NMR	
	at 25°C	75
12	Mole Ratio Study of DCC Complexes with	
	CsTPB in Various Solvents by Cs-133	
	NMR at 25°C	77
13	Mole Ratio of C222B Complexes with	
	CsTPB in Various Solvents by Cs-133 NMR	
	at 25°C	79
14	Mole Ratio Study of C222 Complexes with	
	CsTPB in Various Solvents by Cs-133 NMR	
	at 25°C	81
15	Formation Constants of CsTPB [0.01 M]	
	with Ligands in various Solvents (25°C)	88
16	Mole Ratio Study of 18C6 Complexes	
	with CsTPB in Pyridine at 24°C, -6°C,	
	-38°C	93
17	Limiting Chemical Shifts in Various	
	Solvents	97
18	Half-height Linewidth (Δν, Hz) of	
	Cs ⁺ -Ligand Complexes at 24°C	101
19	Log K, Values of Cesium Salts with	
	Ligands in Various Solvents (25°C)	108

21 Data fro Reference

22 Mole rat

Chemical

of 18C6 :

23 The Simuland Least

for the C

borate by

Temperatu

24 Limiting

Complex a

in Pyridi

25 Mole Rati

Chemical

Presence

Mole Rati

Chemical

the Prese

Nole Rati

Chemical

presence

**

Concentration Dependence of the Chemical	
Shift at 25°C for CsTPB and its 1:1	
Complex with 18C6 in Pyridine	111
Data from the Test of the Insulated	
Reference Tube	119
Mole ratio-Temperature Data for the	
Chemical Shift of CsTPB in the Presence	
of 18C6 in Pyridine	121
The Simulated Formation Constant (K ₁)	
and Least-Squares Adjusted Constant (K ₂)	
for the Complexation of Cesium Tetraphenyl-	
borate by 18C6 in Pyridine at Various	
Temperatures	123
Limiting Chemical Shift of the Cs+ (18C6)	
Complex and the Thermodynamic Parameters	
for the Reaction Cs ⁺ ·18C6 + 18C6 ‡ Cs ⁺ ·(18C6),	
in Pyridine at Various Temperatures	126
Mole Ratio-Temperature Data for the	
Chemical Shift of CsTPB [0.02 M] in the	
Presence of C222 in PC	128
Mole Ratio-Temperature Data for the	
Chemical Shift of CsTPB [0.01 M] in	
the Presence of C222 in PC	129
Mole Ratio-Temperature Data for the	
Chemical Shift of CsTPB [0.02 M] in the	
	130
	Shift at 25°C for CsTPB and its 1:1 Complex with 18C6 in Pyridine

Table

Page

Presence

30 Formation

Chemical of CsTPB

Temperatu

31 Formation

Shifts fo C222 in D

32 Formation Chemical

cf CsTPB

Acetone a

33 Thermodyn

Complexat

Various S

34 Temperatu

Transverse

Free and (in Propyle

28	Mole Ratio-Temperature Data for the	
	Chemical Shift of CsTPB [0.01 M] in the	
	Presence of C222 in DMF	131
29	Mole Ratio-Temperature Data for the	
	Chemical Shift of CsTPB [0.02 M] in the	
	Presence of C222 in Acetone	132
30	Formation Constants and Limiting	
	Chemical shifts for the Complexation	
	of CsTPB by C222 in PC at Various	
	Temperatures	137
31	Formation Constants and Limiting Chemical	
	Shifts for the Complexation of CsTPB by	
	C222 in DMF at Various Temperatures	138
32	Formation Constants and Limiting	
	Chemical Shifts for the Complexation	
	of CsTPB [0.02 M] by C222 in	
	Acetone at Various Temperatures	139
33	Thermodynamic Parameters for the	
	Complexation of CsTPB by C222 in	
	Various Solvents	140
34	Temperature Dependence of the	
	Transverse Relaxation Times for	
	Free and Complexed Cesium Cations	
	in Propylene Carbonate	147

Page

Table

Reciproca

Time of C

B). . . .

37 Temperatu

Time in Po

the Corre

Relaxatic

(B) · · ·

38 Exchange

Parameter

Some Cesi

Propylene

Temperatu:
Relaxatic

Complexed

40 Temperatu:

Relaxatio

(C222) Ce

Tabl	le	Page
35	Temperature Dependence of the Transverse	
	Relaxation Times in Propylene Carbonate	
	in the Presence and Absence of C222	148
36	Temperature Dependence of the Exchange	
	Time τ , of Some CsC^+ Complexes in	
	Propylene Carbonate and Corresponding	
	Reciprocal Transverse Relaxation	
	Time of Cs ⁺ (Site A), and CsC ⁺ (Site	
	B)	161
37	Temperature Dependence of the Exchange	
	Time in PC in the Presence of C222 and	
	the Corresponding Reciprocal Transverse	
	Relaxation Times of Cs ⁺ (A) and Cs ⁺ C222	
	(B)	162
38	Exchange Rates and Thermodynamic	
	Parameters for Release of Cs ⁺ from	
	Some Cesium Macrocyclic Complexes in	
	Propylene Carbonate	166
39	Temperature Dependence of the Transverse	
	Relaxation Times of Free and 18C6-	
	Complexed Cesium Cation in Pyridine	172
40	Temperature Dependence of the Transverse	
	Relaxation Time of Free and Complexed	
	(C222) Cesium Cation in DMF	173

42 Temperatu Time in t and the (

> verse Re CsC⁺ (B)

43 Temperat Time in and the

verse F

CsC+ (I

44 Tempera

Time i the Co

Relaxa

45 Exchan eters

Propy1

46 Test o

on se

47 Estime the Ex

in Ace

41	Temperature Dependence of the Transverse	
	Relaxation Time of Free and Complexed (C222)	
	Cesium Cation in Acetone	174
42	Temperature Dependence of the Exchange	
	Time in the Presence of 18C6 in Pyridine	
	and the Corresponding Reciprocal Trans-	
	verse Relaxation Times of Cs ⁺ (A) and	
	CsC ⁺ (B)	176
43	Temperature Dependence of the Exchange	
	Time in the Presence of C222 in Acetone	
	and the Corresponding Reciprocal Trans-	
	verse Relaxation Times of Cs ⁺ (A) and	
	CsC ⁺ (B)	177
44	Temperature Dependence of the Exchange	
	Time in the Presence of C222 in DMF and	
	the Corresponding Reciprocal Transverse	
	Relaxation Times of Cs ⁺ (A) and CsC ⁺ (B)	178
45	Exchange Rates and Thermodynamic Param-	
	eters of 18C6 Complex Exchange in	
	Propylene Carbonate and Pyridine	184
46	Test of the Dependence of the AH2 Value	
	on $\delta_{\mathbf{e}}$	195
47	Estimated Enthalpies of Formation of	
	the Exclusive (ΔH_1) and Inclusive (ΔH_2)	
	in Acetone, PC and DMF	195

Release

Tab	ole	Page
48	Estimated Entropy Values for the	
	Complexation Reaction at 298°K	198
49	Activation Parameters for the	
	Release of Cs ⁺ from Cs ⁺ C222 in DMF	200

CsNCS

Crypt.

Newly

crypta

The F:

near ;

field

centr

133_{Cs} 7

to in

tempe:

(c) 3

paris

Appar

prepar

Vesse

Vesse

Block

magne couce:

chemi

variou

LIST OF FIGURES

Figure		Page
1	Dibenzo-18-Crown-6 (DBC)	4
2	NaBr-DBC-2H ₂ O Crystal Structure	6
3	CsNCS-tetramethyl-DBC (1:1)	7
4	Cryptand, C (k+1, m+1, n+1)	15
5	Newly Synthesized macrotricyclic	
	cryptand	19
6	The Frequency of the Cs resonance	
	near 28.013 MHz at fixed applied	
	field as a function of molar con-	
	centration in H_2^{16} 0, D_2^{16} 0, and H_2^{18} 0	41
7	133 _{Cs} Shift data (CsCl·MeOH) relative	
	to infinite dilution shifts at three	
	temperatures (a) 298°K; (b) 308.3°K;	
	(c) 326°K and (d) CsCl+H ₂ O for com-	
	parison	41
8	Apparatus for storing solvent in the	
	preparation of NMR sample	49
9	Vessel for solvent purification	50
10	Vessel for DMF purification	51
11	Block diagram of the multinuclear	
	magnetic resonance spectrometer	53
12	Concentration dependence of the Cs-133	
	chemical shifts of cesium salts in	
	various solvents	64

19

20

Nonlin

shifts

Nonlir

shifts

Figure		Page
13	Crowns and [2]-cryptands	71
14	Chemical shifts of Cesium-133 as a	
	function of mole ratio of [18C6]/[Cs+	
	TPB $]$ in various solvents. $[CsTPB]_{T} =$	
	0.01 M	83
15	Chemical shifts of Cesium-133 as a	
	function of mole ratio of [DBC]/[Cs ⁺ TPB ⁻]	
	in various solvents. $[CsTPB]_T = 0.01 M.$	84
16	Chemical shifts of cesium-133 as	
	a function of mole ratio of [DCC]/	
	[Cs ⁺ TPB ⁻] in various solvents.	
	$[CsTPB]_{T} = 0.01 M$	85
17	Chemical shifts of cesium-133 as	
	a function of mole ratio of [C222B]/	
	[Cs ⁺ TPB ⁻]in various solvents.	
	$[CsTPB]_{T} = 0.01 M$	86
18	Chemical shifts of cesium-133 as	
	a function of mole ratio of [C222B]/	
	[Cs ⁺ TPB ⁻] in various solvents	
	$[CsTPB]_T = 0.01 M$	87
19	Nonlinear curve fitting of chemical	
	shifts $\underline{\text{vs}}$ [18C6]/[Cs ⁺ TPB ⁻] in DMSO	91
20	Nonlinear curve fitting of chemical	
	shifts vs [18C6]/[Cs ⁺ TPB ⁻]in MeCN	92

Figure

21	A stu
	<u>vs</u> mo
	- 38°C
22	A typ
	react
23	The i
	with
24	Mole
	study
25	Cesiu
	With
	in py
26	Insul
27	Test
	tube
28	A thr
	133 c
	122
	133 c
	133 c
29	133 c tempe and 1

shift

235° K

in py

igure		Page
21	A study of cesium-133 chemical shift	
	vs mole ratio $[18C6/Cs^{+}]$ at 24° , -6° ,	
	-38°C in pyridine. $[CsTPB]_T = 0.01 M.$.	95
22	A typical fitting of a two step	
	reaction	96
23	The interaction of solvent molecules	
	with complexed cesium ion	102
24	Mole ratio - Cesium-133 chemical shift	
	study for various ligands in DMF	104
25	Cesium-133 chemical shift variation	
	with the concentration of cesium salts	
	in pyridine	112
26	Insulated NMR reference sample	116
27	Test of the insulated reference	
	tube	118
28	A three-dimensional plot of the cesium-	
	133 chemical shift vs mole ratio and	
	temperature (°C) for solutions of CsTPB	
	and 18C6 in pyridine. The concentration	
	of CsTPB was 0.01 M	122
29	A comparison of simulated data (•) with	
	experimental data (▲) for a chemical	
	shift-mole ratio study at 297°K and	
	235°K for solutions of CsTPB and 18C6	
	in pyridine	124

31 Cesiui

ratio

brobA

tempe

32 Cesiu

at va

A plo

33

tion

acet

34 A ty

133

0.0

-46

 s_{em}

35

133

0.0

90

pe:

pr.

Page

Figure

0.02

PC..

37 Spect

a sol

0.01

repre

(left

of ex

Spect

38

39

40

41

a 80]

and

Spec

a so

and

Spec

a sc

0.0

Com

Wit

 IP^{6}

 $m_{\mathcal{O}_{\mathcal{C}}}$ Ph:

qs

36	Semilog plots of $1/T_2^{\pi}$ for cesium-	
	133 nucleus reciprocal absolute	
	temperature for solutions containing	
	0.02 M CsTPB and 0.02 M Cs ⁺ C222 in	
	PC	150
37	Spectra at various temperatures for	
	a solution containing 0.02 M CsTPB and	
	0.01 M C222 in PC. The dotted lines	
	represent the chemical shifts of CsC+	
	(left) and Cs ⁺ (right) in the absence	
	of exchange	153
38	Spectra at various temperatures for	
	a solution containing 0.02 M CsTPB	
	and 0.01 M C222B in PC	154
39	Spectra at various temperatures for	
	a solution containing 0.02 M CsTPB	
	and 0.01 M DCC (A) in PC	155
40	Spectra at various temperatures for	
	a solution containing 0.02 M CsTPB and	
	0.01 M 18C6 in PC	156
41	Computer fit of the spectrum obtained	
	with 0.02 M CsTPB and 0.01 M C222 in PC.	
	The mixture of dispersion and absorption	
	modes occurs because the first-ordered	
	phase correction was not made with the	
	gnostromotor	150

rate

1/T

45 Arrh

prop

46 Spec

a so

18C6

coal

and

poor

chem

the

47 Speci

a so

0.01

show

in t

42	Computer fit of a spectrum obtained	
	with 0.02 M CsTPB and 0.01 M DCC	
	(A) in PC	59
43	Computer fit of a spectra obtained	
	with 0.02 M CsTPB and 0.01 M 18C6	
	in PC	60
44	Arrhenius of plots of τ (Exchange	
	rates of Cs ⁺ ion from ligands) vs	
	1/T for PC solution	63
45	Arrhenius plot of τ (exchange	
	time of Cs ⁺ ion from C222) for	
	propylene carbonate solutions 1	64
46	Spectra at various temperatures for	
	a solution of 0.01 M CsTPB and 0.005 M	
	18C6 in pyridine. The linewidth at	
	coalescence were ~400 Hz. This fact	
	and the low concentration lead to the	
	poor S/N. The dotted lines show the	
	chemical shifts of CsC ⁺ and Cs ⁺ in	
	the absence of exchange 10	69
47	Spectra at various temperatures for	
	a solution containing 0.02 M CsTPB and	
	0.01 M C222 in DMF. The dotted lines	
	show the chemical shifts of CsC ⁺ and Cs ⁺	
	in the absence of exchange 1	70

49 Semi

nucl

eith

in p

abou-

_

inho

Sem

50

133

tai

Cs(

in

Αr

51

Cs

 \mathcal{P}^{α}

52 A

£

D

48	Spectra at various temperatures for
	a solution containing 0.02 M CsTPB and
	0.01 M C222 in acetone. The dotted
	lines show the chemical shifts of
	CsC ⁺ and Cs ⁺ in the absence of
	exchange
49	Semilog plots of $1/T_2^*$ for cesium-133
	nucleus vs 1/T for solutions containing
	either 0.02 M CsTPB or 0.02 M Cs+.18C6
	in pyridine. Values of $1/T_2^*$ less than
	about 10 sec ⁻¹ represent the effects of
	inhomogeneous broadening 175
50	Semilog plots of $1/T_2^*$ for the cesium-
	133 nucleus vs 1/T for solutions con-
	taining either 0.02 M CsTPB or 0.02 M
	CsC222 in DMF and in acetone. Values of
	1/T [*] ₂ less than about 10 sec ⁻¹ represent
	inhomogeneous broadening 179
51	Arrhenius plots of τ (exchange time for
	Cs ⁺ ion from 18C6) in propylene car-
	bonate
52	Arrhenius plots of τ (exchange time
	for Cs ⁺ ion from the ligand C222) in
	DMF solution

(dott

conve

55 Spect

low

dott

of C

A cc

56

ing

vs

val

guq

Page

Figure

CHAPTER I

HISTORICAL

<u>1. I</u>

F

not c

becau

were

_

fact,

and c

tion

teres

devel

Point

in th

their

trans

more

ethe:

sess

alka

synt

liga

gand

tior

oue

Whic

rea

NMP.

1. INTRODUCTION

For many years, complexes of alkali metal ions were not considered an exciting area for chemical investigation, because it was assumed by most chemists that the complexes were neither stable nor important, and, as a matter of fact, alkali salts were frequently used to achieve high and constant ionic strength in solutions, when complexation with other metal ions was occurring. Recently, interest in these alkali metal coordination complexes has developed, both from the chemical and the biological points of view, the latter because of their importance in the metabolism of plants and liver mitochondria and their significance as models for investigation of active transport processes in general. The first synthetic ligand, more or less specific for alkali cations was a cyclic polyether obtained by Pedersen in 1967 (1). The ligand possesses a bidimensional cavity which can accommodate an alkali cation. Soon thereafter Lehn and coworkers (2) synthesized cryptands which are diazapolyoxamacrocyclic ligands with tridimensional cavities. Both types of ligand can form very stable alkali metal complexes in solution as well as in crystalline form. This fact enables one to more easily control and investigate the parameters which determine the characteristics of the complexation reaction.

During the past decade, it has been found that alkali

NMR spectra are very sensitive probes of the immediate

envir mainl

ion b

nonac

II.

Ι

1964, bioti

rat 1

and s

on mo induc

phore

the s

in ma

macro

prono chara

ing s

(A)

M

sized

environment of the alkali metal ion (3-7). This work mainly concerns some aspects of the complexation of cesium ion by crown and cryptand complexing agents in various nonaqueous solvents as studied by Cs-133 NMR.

II. HISTORICAL BACKGROUND

Interest in the polyether type ligands has grown since 1964, when Pressman and Moore discovered that the antibiotic valinomycin exhibits alkali cation specificity in rat liver mitochondria (8). Later, in 1966, Stefanač and Simon (9) showed by electromotive force measurements on model membranes that alkali ion selectivity is mainly induced through complex formation of the antibiotic ion-phore with the cation in question. This observation was the starting point which stimulated scientific interest in macrocyclic complexation of metal ions. Synthetic macrocyclic polyether-crowns and cryptand ligands have very pronounced complexation abilities. Their special physical characteristics will be reported separately in the following section.

(A) MACROCYCLIC POLYETHER-CROWN COMPLEXATION OF ALKALI METAL IONS

More than 50 macrocyclic "crown" ethers were synthesized by Pedersen, and many were found to solubilize

Was to

alka

of t

is s

numb

resp

the 1

comp:

(metal

larger

simulta

Tru of seve alkali metal salts in non-polar solvents. The structure of the first crown compound, dibenzo-18-crown-6 (DBC) is shown in Figure 1, where "18" and "6" indicate the total number of atoms and the number of oxygen atoms in the ring respectively. Ultraviolet and infrared measurements of the DBC-KSCN system indicated the formation of a 1:1 complex (10). It was further shown that when the cation

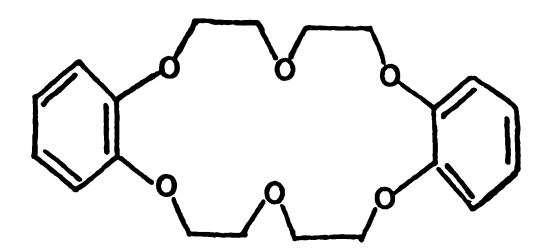


Figure 1. Dibenzo-18-crown-6 (DBC).

was too large to fit in the central hole of a cyclic polyether ligand, complexes with mole ratios of 1:2 or 2:3 (metal:ether) could also be obtained (11). Some of the larger ethers have been shown to complex two metal ions simultaneously (12).

Truter et al. (13) determined the crystal structures of several crown complexes. They showed that in the solid

S +1

fc

in

Ped

(ii)

state, the alkali metal ion is located in the middle of the polyether ring and the ligands are in a gauche conformation about the aliphatic carbon-carbon bonds. The interesting features revealed in their work and that of Pedersen are the following:

- (i) When the number of oxygen atoms is even and no larger than six, they are coplanar in the ring, and the apex of the C-O-C angle is centrally directed in the same plane. Symmetry is at a maximum when all the oxygen atoms are evenly spaced in a circle. When seven or more oxygen atoms are present in the polyether ring and the complexed cation is larger than the cavity diameter, the oxygen atoms cannot assume a coplanar configuration and, consequently, arrange themselves around the surface of a right circular cylinder with the apices of the C-O-C angles pointed toward the center of the cylinder.
- (ii) The second interesting feature revealed was that, even in the crystalline state, there are interactions between the cation, anion and solvent molecules, as shown in Figure 2 for the NaBr-DBC-2H₂O complex (14). In this case, one sodium ion in ring A, is in a hexagonal bipyramid of oxygen atoms, six from the ligand and two axial water molecules. The sodium ion in ring B is attached

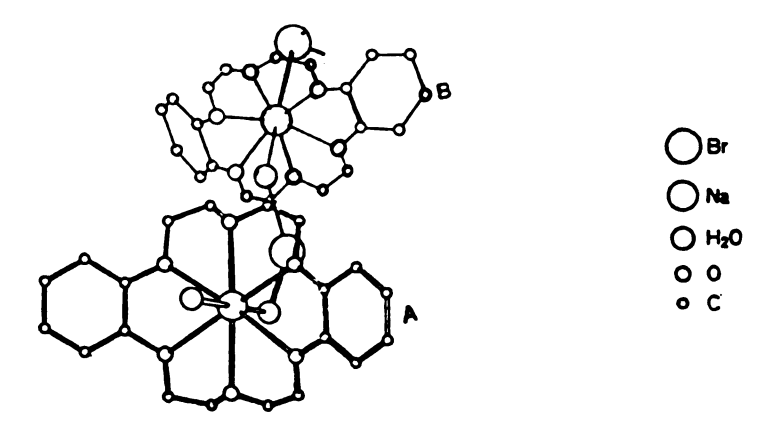


Figure 2. NaBr-DBC-2H₂O crystal structure.

to a bromide ion, at one apex of a hexagonal bipyramid, the ligand forming the equator and water the other apex. The structure is held in a chain by water-bromide and water-water hydrogen bonds. Another example is the structure of the 1:1 compound CsNCS-tetramethyl-dibenzo-18C6 as shown in Figure 3. The compound shows equal sharing of the two thiocyanate ions between the two metal ions and a somewhat unsymmetrical environment for cesium.

(iii) It was also found that the stoichiometry in a unit cell may not necessarily be the stoichiometry of the complex. For instance, the unit cell of

The

by

Where MC

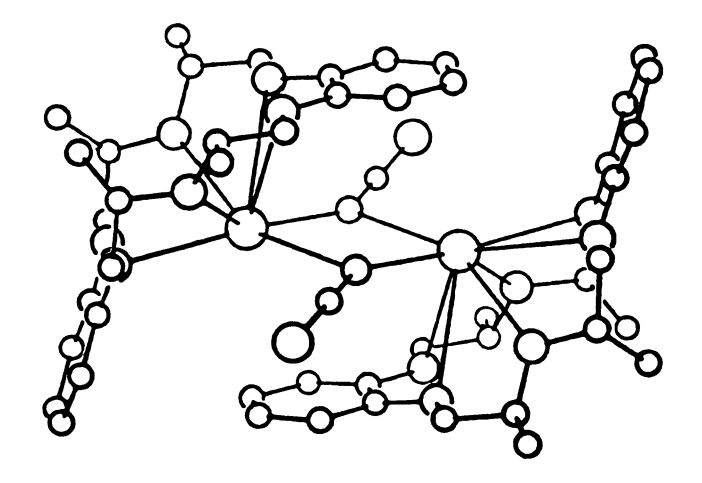


Figure 3. CsNCS-tetramethyl-DBC (1:1).

a 3:2 RbSCN complex (15) contains four molecules of a 1:1 RbSCN-DBC complex and two uncomplexed polyether molecules of crystallization.

The stability constant, K, of a complex is defined by

$$K = [MCr^{+}]/[M^{+}][Cr]$$

where MCr⁺ is the complexed ion formed from metal ion (M⁺)

Va

select

fluorer

(THF) a

Viscosi

in THF

and ligand (Cr) by the following reaction:

$$M^{+} + Cr \stackrel{K}{\stackrel{?}{=}} MCr^{+}$$
 (I.1)

Values of the stability constants (or formation constants) have been measured by a calorimetric titration technique (16), by potentiometric measurements with ion-selective electrodes (17) and by spectroscopic methods (18). These studies revealed that the stability constant goes through a maximum for each cation with increasing polyether ring size. The maximum for Na⁺ is between 15-crown-5 and 18-crown-6, for K⁺ is 18-crown-6; for Cs⁺ between 18-crown-6 and 21-crown-7. These optimum ring sizes are those which provide the closest fit between the cation and the "hole".

Pedersen and Frensdorff (19) noted that very few data are available on complexation reactions in solvents less polar than methanol. In solvents of lower polarity, ion-pair formation becomes significant so that the anion effects would be appreciable. Smid et al. (18,20-22) investigated the interactions of alkali metal ions and their fluorenyl ion pairs with crown ethers in tetrahydrofuran (THF) and tetrahydropyran (THP) by using optical spectroscopy, distribution equilibria, conductances, and viscosities. From their early conductance study (23,24) in THF, it is known that at room temperature, the salt

exi
a s
cro
solv
only
two

pair

sents
solver
ion pa
dipole
associ
consta

metal ;

^{detail.}

calorim

alkali

where

exists predominantly as a tight ion pair but changes into a solvent-separated ion pair at lower temperatures. When crown ethers are added to fluorenyl salts in ethereal solvents, complex formation occurs. In systems where only 1:1 crown-ion pair complexes are formed, at least two isomeric complexes can be found, i.e., a crown complexed tight ion pair $(F\bar{L},M^+Cr)$ and a crown separated ion pair $(F\bar{L},CrM^+)$ (25). The equilibria in the solution are,

$$Fl^-,M^+ + Cr \stackrel{+}{\downarrow} Fl^-,M^+Cr$$
 (I.2)

$$F\ell^-, M^+ + Cr \stackrel{?}{\downarrow} F\overline{\ell}, CrM^+$$
 (I.3)

$$ns + F\overline{\ell}, M^{\dagger}Cr \stackrel{?}{=} F\overline{\ell}, CrM^{\dagger}, ns$$
 (I.4)

where MCr⁺ denotes a complexed crown molecule, Fl⁻ represents the fluorenyl carbanion and ns is the number of solvent molecules interacting with the crown-separated ion pair. A semi-theoretical calculation of the electric dipole moment was used by Grunwald (26) to obtain the association constant for ion-pairing. From the formation constant, K, one can obtain the free energy of complexation, $\Delta G_{\rm C}$. However, the entropy and enthalpy of alkali metal ion complexation have not been studied in much detail. Simon et al. (27-29) used a computerized microcalorimeter to study the thermodynamic properties of alkali complexes of antibiotics, while Izatt et al. (30-32)

also to st synth

l rev cycli

tive.

ting

addi:

repla

is a

plexa

(DCC)

using of ex

that

equi

In bo

tion

to th

the al

also use a precision thermometric titration calorimeter to study the thermodynamics of formation of complexes of synthetic macrocyclic polyethers. The data shown in Table 1 reveal that, for the complexation reaction of macrocyclic ligands, usually ΔH_C and quite often, ΔS_C are negative. This is caused by the macrocyclic effect described by Margerum (37,38). He used this term in order to distinguish it from the chelate effect because there is an additional enhancement in stability beyond that expected from the gain in translational entropy when chelates replace coordinated solvent from metal ions.

Kinetics information about these complexation reactions is also very limited. Shchori et al. monitored the complexation of the sodium ion by DBC and dicyclo-hexyl-18C6 (DCC) in dimethylformamide and methanol solutions (4) by using ²³Na NMR measurements. From a study of the variation of exchange rates with concentration, they postulated that the exchange mechanism involved the complexation equilibrium,

$$Na^{+}(X^{-})$$
, Crown $^{+}_{-}Na^{+}(X^{-})$ + Crown (1.5)

In both solvents, the activation energy is 12.6±0.6 Kcal/mole for DBC and 8.3 Kcal/mole for DCC. The lower activation energy for releasing Na⁺ ion from DCC was attributed to the flexibility of the macrocyclic ring. Recently the above authors also studied the decomplexation kinetics

Thermodynamic Quantities for Complexation Reactions of Macrocyclic Polyethers. Table 1.

Macrocyclic Compound	Cation	Temp.	ΔH Kcal/mole	$^{\Lambda S}$ cal/mole deg			Ref.
1,2 Benzo-15C5	Na+	25	-1.77	-2.6	20/80	(MeOH/H ₂ 0)	33
		25	-2.63	-3.5	40/60	(MeOH/H ₂ O)	33
		25	-3.78	-5.2	60/40		33
		25	-3.82	-3.7	70/30		33
	+ ×	25	-8.32	-17.6	80/20	(MeOH/H ₂ O)	33
		25	-1.8	-0.5	20/80	(MeOH/H ₂ O)	33
		25	-2.51	1.4	40/60	(MeOH/H ₂ O)	33
		25	-3.52	-0.2	60/40	(MeOH/H ₂ O)	33
		25	-3.67	1.1	70/30	(MeOH/H ₂ O)	33
		25	-10.20	-21.3	80/20	(MeOH/H ₂ O)	33
1,2,4 Methyl- benzo-18C6	+	25	-3.0	-10.4	THF	1	33
1,2,5,6 Dibenzo- 18C6	+ 8 N	25	.9	-7	DMF		33
	+ ×	25	-5.5	6.9-	DMSO		33
1,2,5,6- Dihexylcyclic- 18C6 (isomer A)	+*	10	-4.14	.4. 8.	н		33
		25	-3.88	-3.8	н,0		33
		٦,	כר טו־		2004020	9	23

Macrocyca

Table 1. Continued

Macrocyclic Compound	Cation	Temp.	ΔH Kcal/mole	ΔS cal/mole deg		Ref.
		40	-3.58	-2.7	Н20	33
	4 22	10	-3.43	-4.8	н20	33
		25	-3,33	-4.2	H ₂ 0	33
		40	-3.29	-4.1	н,20	33
	cs+	10	-2.40	-3.9	H ₂ 0	33
		25	-2.41	-3.7	н_20	33
		40	-2.38	-3.2	н ₂ о	33
	NH ⁺	25	-2.16	-1.2	H ₂ 0	33
Isomer B	Na +	25	-2.5	9.0-	DMSO	33
		25	9-8-۰	!	Etoh	33
		25	-5.6	-1.9	МеОН	33
	+ ×	10	-5.78	-12.2	н ₂ 0	33
		25	-5.07	9.6-	H ₂ 0	33
		40	-4.19	-1.5	н_0	33
		25	-7.7	-13.5	DMSO	33
		25	∿-12.6	!	Etoh	33
	+ ×	25	-10.5	-10.5	МеОН	33
		25	-11.06	1 1	Acetone	33
	RD+	10	-4.6	-11.9	н ₂ о	33

Table 1. Continued.

Macrocyclic Compound	Cation	Temp.	ΔH Kcal/mole	ΔS cal/mole deg		Ref.
		25	-3.97	-9.3	н,о	33
		40	-3.30	9-9-	H ₂ 0	33
	NH ⁺	25	-3.41	-7.8	H ₂ 0	33
	Agt	25	-2.09	0.3	H ₂ O	33
1,2,3,4- Dibenzo-30C10	+ BN	25	4-	1 1	Меон	33
	+*	25	11.5	!!!	МеОН	33
	RP+	25	-12.7	1 1	МеОН	33
	Cs+	25	-11.2	!	Меон	33
	NH ⁺	25	-5.5	! ! !	МеОН	33
	T1+	25	-11.0	!	МеОН	33
Valinomysin	+*	25	-2.13	-5.16×10^{-1}	EtoH	34
Monactin	+ *	25	-10.42	-14.41	МеОН	35
	Na+	25	-2.63	+3.49	МеОН	36
Monactin	Na+	25	0.9-	-8.13	МеОН	36
Monensin	+	25	-3.87	+7.41	Меон	29

of the for still as - x-ra show

K⁺,

same

to p

less

is a

That symbo

open

ph a 1

the st

of DBC-K⁺ and DBC-Rb⁺ complexes in MeOH solutions by means of alkali metal NMR (5). The activation energy (E_a) for the decomplexation of the K⁺ ion is 12.6 Kcal/mole, while for Rb⁺, the exchange between free and complex sites was still indicated as being rapid even at temperatures as low as -50°. They interpreted these results as follows: The x-ray crystallograph study done by Truter et al. (15), shows that both Na⁺ and K⁺ can fit the cavity size of DBC very well, therefore for these two ions they obtained the same E_a value. However, Rb⁺, a larger cation, is forced to protrude from the cavity plane and, consequently, is less tightly bound to the DBC molecule.

The complexation reaction of dibenzo-30Cl0 with Na^+ , K^+ , Rb^+ , Cs^+ , NH_4^+ , Tl^+ in methanol solution was investigated by Chock (39). The reaction mechanism he postulated is as follows:

fast
$$Cr_1 \stackrel{?}{\downarrow} Cr_2$$
 (1.6)

$$Cr_2 + M^+ \stackrel{k_{12}}{\underset{k_{21}}{\downarrow}} MCr^+$$
 (I.7)

That is, a conformational transition was proposed. The symbol Cr₁ represents an unreactive species, Cr₂ is an open configuration which is ready to complex the cation, and MCr⁺ is a closed configuration which is stabilized by a monovalent cation. His results also emphasized that the stability of the complex is dependent on the ionic

radi

DBC

Cuss

Thei

thus

be o

(B)

With

gCCOI

selec

in ge

radius and the hydration energy of the cations under study. Cussler and coworkers (40) made conductance studies of DBC and DCC in acetonitrile (MeCN) and in methanol (MeOH). Their results indicated that the stability of the complex is affected by the solvation of the cation under study and thus solvent effects on the complexation reaction cannot be overlooked.

(B) COMPLEXATION OF METAL IONS BY MACROHETEROCYCLIC LIGANDS-CRYPTANDS.

Cryptands are polyaza and polyoxa macrocyclic compounds with tri-dimensional cavities (Figure 4). In order to

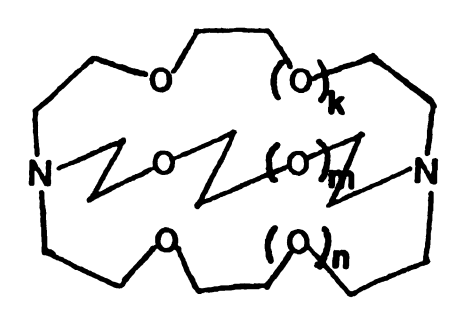


Figure 4. Cryptand, C (k+1,m+1,n+1).

accommodate different cations, the cavity size can be varied by changing the length of the ether bridge. The selectivity of complexation and stability of complexes, in general, are several orders of magnitude greater than

for in

fre not

tand For

has

firs

Na⁺

proc than

caus

is i

in e

they solut

(EA)

 pl_{exa}

disso (NaC2

they

With .

satura

for crown compounds with the same number of oxygen atoms in the ring.

In general, the term cryptand is ascribed to the free ligand and the term cryptate to the complex. The notation C(n+1,m+1,k+1) is an abbreviation for a cryptand with n+1,m+1,k+1 oxygen atoms in each branch. For instance, if a hexaoxadiamine macrocyclic compound has a value n=m=k=1, then it can be written as C222.

The kinetics of the complexation by cryptands was first studied by Lehn et al. (41) through a PMR temperature study on the complexation of C222 with K⁺, Tl⁺, and Na in D₂O. They concluded that the exchange mechanism proceeded by a dissociation-complexation process rather than a bimolecular process. The symmetrical splitting caused by Tl+-H spin-spin coupling indicated that the ion is in the center of the molecular cavity. Dye and coworkers (42) studied the exchange rate of sodium cryptate in ethylenediamine. The activation free energy value they obtained is similar to that of Lehn obtained in aqueous solution. They also dissolved pure sodium in ethylamine (EA) and in THF in the presence of C222. Due to the complexation of the cryptand with Na⁺, the concentration of dissolved metal was greatly enhanced and a gold-colored (NaC222) + Na salt was formed (43a). At low temperatures (43b) they observed two NMR resonances, i.e., (NaC222) and Na, with the Na peak shifted upfield about 63 ppm from saturated aqueous NaCl for both solvents, i.e., EA and THF.

Kint

1

by Ca

is re

This

et all studi

and i

the a

and n

ions

Lehn

noted

insid Obser

(1) C

Kintzinger and Lehn (44) also used ²³Na-NMR to study the complexation of Na⁺ ion with cryptands. They found that the ²³Na nuclear quadrupole coupling constant decreased with an increasing number of oxygen atoms in the ligand. The chemical shift (referred to a 0.25 M aqueous NaCl solution as external reference), had values of 11.15 ppm for Na⁺-C211,-4.25 ppm for Na⁺-C221, and -11.45 ppm for Na⁺-C222. The line widths at halfheight were 132±3, 46±2 and 29±1 Hz, respectively.

Lithium-7 NMR kinetics studies have also been performed by Cahen, et al. (6). They found that the activation energy for the decomplexation of the Li-cryptand complex is related to the Gutmann donor number of the solvent.

This result contrasts with the kinetics studies of Shchori et al. who used crown complexing agents. The latter authors studied the exchange rate of Na-DBC in DMF and methanol and noted that there seemed to be no solvent effect on the activation energy. However the donor number for DMF and methanol are very nearly same.

In addition to the study of the complexation of metal ions with macrobicyclic ligands (denoted as [2]-cryptands), Lehn et al. also synthesized macrotricyclic ligands (denoted as [3]-cryptands) (45,46). Later, they also studied the cation exchange rate between binding sites on two rings inside the cavity of a [3]-cryptate by ¹³C NMR. Their observation for this study is summarized as follows:

(1) Complexes display an intramolecular cation exchange

proces is loc shown

(2) 1 decrea

energy

(3) 2

preser of act

lar pr

exchar

alkali An

(47).

this r

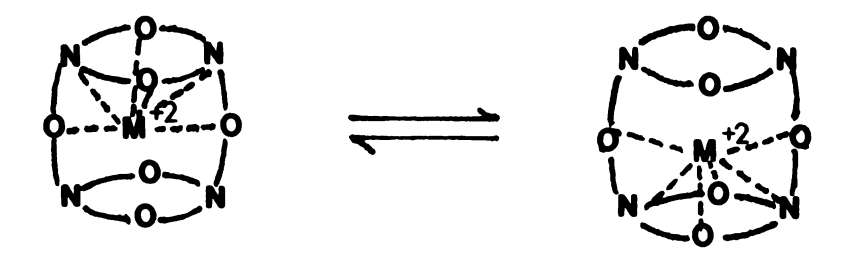
molect

Prelin

⁸tabil

in wat

process which interconverts two species in which the cation is located unsymmetrically in the molecular cavity, as shown below.



- (2) The free energies of activation, ΔG_C^{\dagger} for this process decrease with increasing size and decreasing hydration energy of the cations in the order $Ca^{+2} > Sr^{+2} > Ba^{+2}$.
- (3) An intermolecular cation exchange process is also present, but its rate is much slower and its free energy of activation is much higher than those of the intramolecular process. (4) Both intra and intermolecular cation exchange is fast for the weak complexes which form with alkali cations.

Another [3]-cryptand has been synethsized recently (47). As shown in Figure 5, the attractive feature of this molecule is that it possesses a spherical intramolecular cavity into which the cation may be placed. Preliminary measurements show that the logarithm of the stability constants for the K⁺, Rb⁺, and Cs⁺ complexes in water are about 3.4, 4.2 and 3.4, respectively; and

Fi

the :

pera K⁺,

(at

cryp

obta flow

kins

Mure

ca⁺²

and

figu

the :

has .

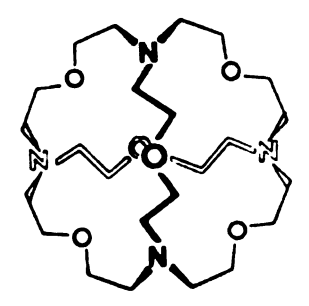


Figure 5. Newly synthesized macrotricyclic cryptand.

the PMR kinetic study obtained from the coalescence temperature showed that the free energies of activation for K^+ , Rb^+ and Cs^+ are 15.5 (at 28°), 16.7 (51°) and 16.1 (at 41°C) Kcal/mole.

Kinetics information about the complexation between cryptands and metal ions is scarce and has been mainly obtained by NMR techniques. Very recently, a stopped-flow technique (48) was used for a kinetics study by Wilkins et al. They followed the color variation of the murexide-Ca⁺² complexation reaction of murexide-Ca⁺² and Ca⁺²-cryptate. In this study, conformational changes, i.e., exo-exo endo-endo (41,49), were also considered. Endo and exo configurations are shown below. The endo configuration has the lone pair electrons directed toward the interior of the cavity while the exo configuration has the lone pair electrons turning outside.

Formation constants of alkali metal cryptates in

aque

sive niqu

tion

an a

COM

a po

rest

ing This

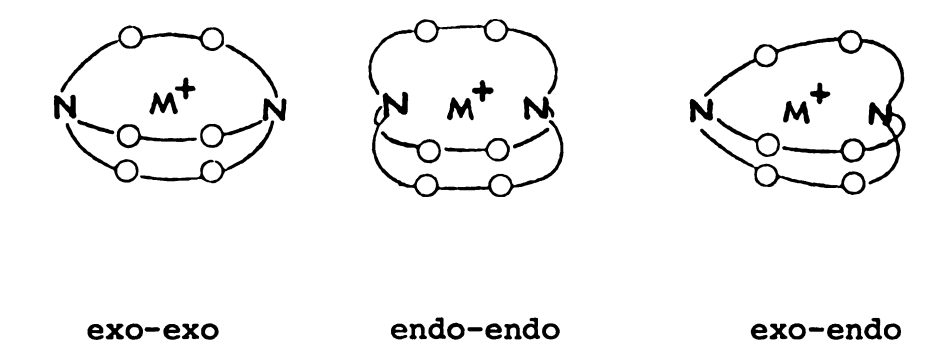
the

of p

the

from

stil



aqueous and methanolic solutions have been studied extensively by Lehn and coworkers who used potentiometric techniques. Recent reviews (50,33) contain extensive compilations of complexation constants. Cahen et al. (7) used an alkali NMR technique to study formation constants of complexation in several solvents. They found that, in a poor donor solvent such as nitromethane, the addition of C222 or C221 cryptand to a lithium perchlorate solution resulted in a drastic chemical shift which reached a limiting value at higher than 1:1 (ligand/metal) mole ratios. This phenomenon indicates that the formation constant of the resulting cryptate is large in contrast to the case of pyridine, a better donor solvent, in which the limiting value is not reached even at a 25:1 mole ratio because of the competitive action of the solvent.

The thermodynamic quantity ΔG^O can be obtained directly from the formation constant, but ΔH^O and ΔS^O values are still very limited in extent. Only very recently Lehn

and

cry

an a

Tab

comp

The

and cal

3.

Tab

Sr⁺

Ca+

In .

hea

[ca

havi

 $s\lambda w$

and coworkers (51) made calorimetric measurements under an argon atmosphere to avoid the problems caused when cryptand solutions absorb CO₂. Their data are listed in Table 2. In this work, they stressed explicitly that the complexation reactions to form cryptates have large negative changes in enthalpy, sometimes, negative entropy changes. These are important factors in determining the stability and selectivity of the complexation reaction. From their calorimetric study they observed the trends shown in Table 3.

Table 3. Trends in Thermodynamic Parameters with Cryptands.

Cation Complex With Cryptand	Dominant	Minor
Sr ⁺² ,Ba ⁺² (not with C ₂₂₂), Na ⁺ (C ₂₂₂)	ΔΗ<0	T ΔS>0
Na ⁺ ,K ⁺ ,Rb ⁺ ,Cs ⁺	ΔH<0	T ΔS<0
Ca ⁺²	ΤΔS>0	ΔH<0

In addition, they noted that $[Li^{\dagger} \subset C_{221}]$, $[Ca^{\dagger 2} \subset C_{211}]$, $[Ca^{\dagger 2} \subset C_{222}]$ are entirely entropy stabilized with about zero heat of reaction.

Crystal structures of a number of alkali cryptates
have been determined by Weiss and coworkers (52-55). For
[2]-cryptates it was observed that the metal ion is centrosymmetrically located in the cavity. In some cases, solvent

Thermodynamic Quantities of Alkali-Cryptate Complexation Reaction Measured by Calorimetry at 25°C in Water. Table 2.

Ligand	Thermoparameter (Kcal/mole)	Li ⁺ (0.78A)	Na ⁺ (0.98Å)	K ⁺ (1.33Å)	Na ⁺ (0.98Å) K ⁺ (1.33Å) Rb ⁺ (1.49Å)	Cs [†] (1.65Å)
211	ηН∇-	137.2	111.2	!	i	!
(1.6Å)	-ASg	25	28.3	1	1	!
211	-AH2	132.1	111.3	92.6	84.6	1 1
(2.2Å)	7S∇-	21.6	19.8	21.7	18.5	!!
222	- AH &	1 1 1	113	26	 	91
(2.8K)	7SV-	!	32	31	1	31
322	-AH2	!	! ! !	89.4	84.8	78.1
(3.6Å)	7S∇-	i ! !	1 1 1	19.5	21.7	26.2

 $\Delta H \ell = \Delta H_C + \Delta H_h$ $\Delta S \ell = \Delta S_C + \Delta S_h$ Where ℓ denotes "Ligation", i.e., transfer of the cation from the gas phase into NOTE:

the hydrated ligand with formation of the differently hydrated $\mathbf{M}^{+n}(\mathsf{gas})$

+ (L) aq + $[M^{+n}CL]$ aq.

c denotes transfer to complexed state.

h denotes hydration.

molecules are also linked to the complex, e.g., Rb⁺(C222) SCN⁻·H₂O, Ba⁺²(C222) (SCN)₂ H₂O (56) and Ba⁺² (C322) (SCN)₂· 2H₂O (57). The solvent molecule or anion can extend into the ligand cage and coordinate with the trapped metal ion in the center. It was also found that for [2]-cryptates the preferred configuration is endo-endo in the crystal. For [3]-cryptates (58,59) the metal ion is also located in the cavity. Monovalent ions usually form weaker complexes with [3]-cryptands but 1:2 (ligand/metal) complexes can be formed. The crystal structure of an Ag⁺-[3]-cryptate complex actually shows two silver ions located in the two rings and linked with a third Ag⁺ through the oxygen of the nitrate group of AgNO₃. This third Ag⁺ is outside of the cage.

In summary, the complexation reactions of metal ions with macrocyclic ligands depend on the following factors:

- (1) The type of binding site in the ring. For a ligand with a donor atom such as O, N or S, the stability usually follows the trend, O > N > S for small ions such as Li^+ , Na^+ . For a large ion such as NH_4^+ or a group B ion such as Ag^+ the same trend may not necessarily hold because of some covalency in the coordination.
- (2) The number of binding sites in the ring. Compare for example the log K value for the Na $^+$ and K $^+$ complexes of C222 (with Na $^+$ or K $^+$ in MeOH log K is larger than 8) and C22C $_8$ (with Na $^+$ in MeOH log K is 3.5 while for K $^+$

it cry

the

sit of

(3)

(60

sho

the

(4)

sul de

hic

ca.

OD

the

ef is

(5

li

so

Me re

(6

- it is 5.2). In this comparison, $C22C_8$ denotes a [2]-cryptand with one aliphatic branch. Both ligands have about the same cavity radius but $C22C_8$ contains two fewer oxygen sites. This results in a decrease in stability by a factor of 10^4-10^5 (50).
- (3) The relative sizes of the metal ions and the ligand (60). The K value as a function of the cation radius shows a maximum for any given ligand. This indicates that the ratio of cavity radius to the ionic radius contributes significantly to the selectivity of these ligands.
- (4) Steric hinderance and ligand thickness (61). The substituents on the ring will introduce rigidity and hinderance in the ligand. These can make the ligand have a higher selectivity and ability to discriminate against cations which are either smaller or larger than the preferred one.

The ligand interposes a layer between the cation and the outside medium. Therefore the thicker the ligand, the better the cation is shielded from the medium. This effect decreases long range ionic stabilization. The effect is larger the higher the dielectric constant of the solvent.

- (5) The solvent and extent of solvation of the ion and ligand. For example, Cahen's study illustrates that in solution the complexation reaction competes with solvation. Media which can solvate cations more strongly usually result in weaker complexes.
- (6) The electrical charge of the ion. Previous studies

have shown that, with a similar cation radius, a bivalent ion forms a stronger complex than a monovalent ion (61). However, in this case ligand thickness becomes very important because the long range interaction energy varies as the square of the ionic charge.

(7) Topology of the ligand. The dimensions and geometry of the ring can greatly affect the stability of the complex. This is most pronounced when the complexing groups are held in favorable positions by the ligand framework. The extent of ion-pairing also depends on the geometry of the ligand. In addition to the recent work of Smid et al., electron spin resonance studies (62,64) have been made of alkali metal hyperfine splittings in the presence of macrocyclic polyether ligands. These results illustrate that several types of ion-pairs are formed with crown complexes in low dielectric media. However this effect was not observed when cryptates were in the same media.

(C) NUCLEAR MAGNETIC RESONANCE

(i) INTRODUCTION

Electrolyte solutions are particularly suited to investigation by nuclear magnetic resonance techniques. The presence of extremely rapid and generally random molecular motions averages local magnetic and electric fields to very small values and can result in narrow resonance lines even for quadrupolar nuclei. This fact is important

bec and

In

che ef

fr

in

in

In

th

aŀ

of

ar

S

to

a:

IJΙ ħ

0

m.

i

Ŋ

0

£

because it enables small differences in magnetic shielding and/or fine structure of the resonance signal to be detected. In addition, broadening of the resonance line because of chemical exchange, hyperfine interaction or quadrupolar effects may be studied and chemical information derived from the observed behavior. Proton NMR is useful in the investigation of solvent or ligand behavior and can provide information about ion-solvent or ion-ligand interactions. In favorable cases, non-proton NMR can be used to study the ions themselves and thus provide direct information about such interactions. Although resonance frequencies of metal ions are sensitive to ion-solvent, ion-ligand, and inter-ionic interactions, the generally weak resonance signals and the special instrumentation required combined to make such studies rare prior to the last decade. All alkali metals possess at least one isotope with a magnetic nucleus; e.g., ⁷Li, ²³Na, ³⁹K, ⁸⁷Rb, and ¹³³Cs. herent intensity of the resonance is much lower than that of the proton. However, the sensitivity of the nuclear magnetic shielding constants to the nature of the surroundings is considerably larger and increases as the atomic number of the ion increases. This condition leads to a wide range of chemical shifts, from a few ppm to hundreds of ppm. Variations in the chemical shift result primarily from changes in the paramagnetic shielding constant, σ_n .

spi the

> in and

ter var

at

may

whe

(01

sion

full

appl

rect diff

divi

(ii) CHEMICAL SHIFT STUDIES OF ELECTROLYTE SOLUTIONS

For an assembly of identical but isolated nuclei of spin I and magnetic moment μ in a static magnetic field H_{O} , the simplest expression for the resonance condition is

$$v_{O} = \mu H_{O} / Ih = \gamma H_{O} / 2\pi \qquad (I.8)$$

in which ν_{0} is the frequency at which energy is absorbed and γ is the magnetogyric ratio. The latter has a characteristic value for each isotopic species. However, a variety of mechanisms may produce secondary magnetic fields at a nucleus. The actual field experienced by the nucleus may be written as

$$H = H_O (1-\sigma)$$
 (I.9)

where σ is a dimensionless quantity known as the shielding (or screening) constant.

Ramsey (65,66) has developed general theoretical expressions for chemical shifts caused by magnetic shielding of nuclei in molecules. This treatment has been applied succesfully to simple molecules but the approximations required to apply it to more complex systems yield only qualitatively correct results. Saika and Slichter (67) attempted to explain the difference in the shielding constants of F_2 and F. They divided the contributions into separate terms: (1) the

diam a pa

cont

expa envi

be I

have

ider Rams

nuc]

for

magr

103

inte

of (

orb:

give act

cova

ind

son

for pret

They

₫ue

Mutu

diamagnetic contribution for the atom in question. (2) a paramagnetic contribution for the same atom and (3) contribution from the electrons of other atoms.

When investigating an electrolyte solution, one can expand Ramsey's formulation as applied to a solid state environment. If alkali halide crystals are considered to be purely ionic in character, each constituent ion will have a spherical closed-shell electronic configuration identical to that expected for the isolated ion. In Ramsey's expression, the shielding constant of the ionic nucleus is determined only by the diamagnetic term, σ_{d} , for an isolated ion. Therefore, the observed large paramagnetic contributions found for crystals (usually 10²- 10^3 times larger than $\sigma_{\mbox{\scriptsize d}}$) indicate that there are additional interactions present which are able to distort the symmetry of the electron distribution and introduce some net orbital angular momentum into the ion. This perturbation gives rise to a paramagnetic chemical shift. Such interactions might be considered in terms of electrostatic, covalency or overlap effects. However, the calculations indicate (68) that neither electrostatic effects nor reasonable estimates of the degree of covalency can account for shifts of the magnitude observed. The best interpretation so far is that of Kondo and Yamashita (69). They suggested that the cause of the paramagnetic shift is due to the short range repulsive forces between ions. Mutual overlap of atomic wave functions of neighboring

io Pa

ra

to

eq

fo

(]

t)

ac

La

(

`

Ð

.

s

ĺ

_

C

W

,

Ŝ

е

ions produces a strong repulsive force mainly due to the Pauli exclusion principle. This force acts over a short range and competes with the electrostatic forces which tend to reduce the separation of oppositely charged ions. equilibrium in the crystal the attractive and repulsive forces are in balance. Kondo and Yamashita used Löwdin's (70) orthogonalized-atomic-orbital model and considered that the overlap integrals are significant only for interactions of orbitals which belong to nearest-neighbor ions. Later, both Ikenberry and Das (71) Hafemeister and Flygare (72) gave more exact derivations of the paramagnetic shift to be expected from overlap forces in alkali halide crystals. But at that time they ran into difficulty in comparing theoretical results with experiments because the experimental shielding data are usually referred to a reference sample in which the shielding constants are not known. Therefore it was thought that this problem could be solved by referring all experimental shielding constants to the infinite dilution chemical shift in water which, in principle, is supposed to be constant because of the strong hydration properties of water.

When the alkali salt is put into a solvent, the calculated paramagnetic shielding constant, σ_p , from the crystal state and the experimentally measured shift, δ , referred to the aqueous solution are related by the equation:

20

70 :q

is

CI

Da

r

0

t!

aı

Ot WC

> si re

va ir

fr

٩c

ci Di

sy

pa pa

co

$$\sigma_{aq}^{O} = \sigma_{p} - \delta \tag{I.10}$$

where $\sigma_{\mathbf{a}\sigma}^{\mathbf{O}}$ is the paramagnetic shift of the hydrated ion relative to the "free ion". Since $\sigma_{\mbox{\scriptsize aq}}^{\mbox{\scriptsize O}}$ should be independent of the partner ion in any alkali metal or halide series, the constancy of $\sigma_{a\sigma}^{O}$ obtained by a combination of theory and experiment, therefore, provides a test for the proposed overlap mechanism and the accuracy of the wave functions employed in the calculation. However, in reality, $\sigma_{a\sigma}^{O}$ is not constant. Attempts were made to explain the discrepancy by Hafemeister and Flygare (73), Ikenberry and Das (74) and Y. Yamagata (68) individually by using various models in the calculations. However, all of them could only illustrate that ion-solvent interactions can produce sizable paramagnetic shifts of the ionic nucleus, but their results were still not comparable with the experimental Therefore, it was suggested that chemical shifts in solutions may be caused not only by ion-solvent interactions in dilute solution, but also may have contributions from direct interionic effects.

By using the Kondo-Yamashita model one could in principle account for the chemical shifts in aqueous solutions. Direct collisions between ions will distort the spherical symmetry of the electron distribution and also can produce paramagnetic chemical shifts. In the solid state, the relative positions and distances of separation of the component ions are known, and, therefore, the theoretical

a[·]

u

se ma

sh

fo

bo wa

th se

ma:

the fir

the

Par

whe

<

10 1-1

attack is easier. In solution the environment of each ion varies randomly with time as the ion and solvent molecules undergo rotational and translational diffusion. served chemical shift is an average value resulting from many separate contributions corresponding to the various short-lived associations in solution. An exact expression for the shielding constant would require a knowledge of both the radial distribution function of other ions and water molecules about the central ion and the magnitude of the appropriate overlap integrals as a function of the separation. This information is difficult to obtain. make this problem tractible, Deverell et al. (75) modified the Kondo-Yamashita theory in the following way: At infinite dilution, the only interactions present are between the ion and the water molecules. This contribution to the paramagnetic chemical shift can be expressed by

$$\sigma_{\text{aq}}^{\text{o}} = \frac{-16\alpha^2}{\Delta} < r_i^{-3} >_{\text{p}} \Lambda_{i-H_2O}^{\text{o}}$$
 (I.11)

where Δ is the average excitation energy,

 α is the fine-structure constant,

- $\langle r^{-3} \rangle_p$ is the expectation value of r_i^{-3} for an outer pelectron of the central ion, i.
- is an appropriate sum of the squares of overlap integrals between the outer p-orbitals of the ions, i, and the outermost orbitals of neighboring water molecules. The superscript denotes zero

the

The

wher

tegr

ion

The and

solv

Prot

and

ther

shif

desc

stud

the

concentration of the counter ion.

As the concentration of the solution is increased, the presence of interionic processes has to be considered. The experimental shift, δ , can be expressed as

$$\delta = \sigma_{p} - \sigma_{aq}^{o} = \frac{-16\alpha^{2}}{\Delta} < r_{i}^{-3} >_{p} [\sum_{j} \Lambda_{i-j}^{c} + (\Lambda_{i-H_{2}O}^{c} - \Lambda_{i-H_{2}O}^{o})] \quad (I.12)$$

where $\Lambda_{\mathbf{i}-\mathbf{j}}^{\mathbf{C}}$ is the sum of the squares of the overlap integrals for the interionic contribution and is taken over all ions in solution other than the central ion, i. The ion j may be of like or unlike charge with respect to i. The superscript c denotes the concentration of the salt, and $(\Lambda_{\mathbf{i}-\mathbf{H}_2\mathbf{O}}^{\mathbf{C}} - \Lambda_{\mathbf{i}-\mathbf{H}_2\mathbf{O}}^{\mathbf{O}})$ represents changes in the effect of solvent-ion overlap integrals.

Both terms, Λ_{i-j}^{C} and $\Lambda_{i-H_{2}O}^{C}$, are dependent upon the probabilities of collision occurring between the central ion and other ions or water molecules in solution and are therefore concentration dependent. Also, from the factor $\langle r_{i}^{-3} \rangle / \Delta$, as shown in Table 4, it is possible to account for the observation that the magnitude of the chemical shift increases with the atomic number of the alkali ion.

The following is a recapitulation of the previously described development of alkali metal ion chemical shift studies:

Ramsey used standard perturbation theory to express the shielding constant as (67):

Tab:

a_{Re}

Table 4. Values of the Average Excitation Energy Δ , and the Expectation Value ${r_i^{-3}}_p$ for Alkali Metals.^a

Ion	<ri>-3> i p a.u.</ri>	Δ Rydbergs	$\frac{\langle r_i^{-3} \rangle_p}{\Delta}$	
Na ⁺	16	2.72	5.9	
K+	12.94	1.62	7.98	
Rb ⁺	20.22	1.47	13.8	
Cs ⁺	23.42	1.25	18.7	

aReference 76.

Si

no ti

ex

Th

t)

ir

to cı

t₁

$$\sigma = \sigma_{d} + \sigma_{p}$$

$$= \frac{e^{2}}{2mC^{2}} \{ \langle \psi_{o} | \sum_{k} \frac{r_{k}^{2} \hat{i} - \hat{r}_{k} \hat{r}_{k}}{r_{k}^{3}} | \psi_{o} \rangle + \sum_{m} (E_{o} - E_{m})^{-1} [\langle \psi_{o} | \sum_{k} \hat{i}_{k} | \psi_{m} \rangle \langle \psi_{m} | \sum_{k} \frac{\hat{i}_{k}}{r_{k}^{3}} | \psi_{o} \rangle + \text{etc} \}$$
 (I.13)

Since excited state wavefunctions and energies are usually not known, Ramsey introduced the average energy approximation and the paramagnetic shielding constant was then expressed as follows:

$$\sigma_{\rm p} = \left(-\frac{{\rm e}^2}{\Delta {\rm M}^2 {\rm c}^2}\right) < \psi_{\rm o} | \sum_{{\bf k} {\bf k}'} (\hat{\bf l}_{\bf k} \hat{\bf l}_{\bf k}' / {\bf r}_{\bf k}^3) | \psi_{\rm o} >$$
 (I.14)

∆ :average excitation energy.

e :electronic charge

M :electron mass.

C :velocity of light.

 $\hat{\ell}_{\mathbf{k}}$:angular momentum of the k'th electron, and

 r_k :radial distance of the k'th electron from the origin at the nucleus.

The subscript o refers to the ground state and m refers to the excited state.

For a crystal, an additional interaction force was introduced. Two models have been proposed in an attempt to rationalize the large paramagnetic shifts, σ_p , of ionic crystals. These are Yosida and Moriya's (77) chargetransfer covalency model (YM model), and Kondo and Yamashita's

(69) over of the qu halide md ${\tt plausible}$ derivation transfer lap betw∈ ion with $introduc \in$ in Ramsey integral i, and th Their cor pulsive f By combin more clos from alk also used the KY m atomic w but also Their ca can be n (next ne

Well as

relate w

For

(69) overlapping-ion model (KY model). Later, calculation of the quadrupole coupling constants in diatomic alkalihalide molecules (78) showed the KY model to be more plausible. However, Das et al. (71) gave a more exact derivation by including the effects of overlap and charge transfer covalency. For the KY model they considered overlap between the outmost s and p orbitals of the central ion with those of neighboring ions. Das et al. not only introduced $\langle r_i^{-3} \rangle_p$ for a p electron of the central ion, i, in Ramsey's expression, but also included the overlap integral between the outer p-orbitals of the central ion, i, and the outmost s and p orbitals of all other ions, j. Their conclusion was that the KY model (short-range repulsive force) is predominant over the YM model (covalency). By combining the two effects, the resultant calculation more closely approximates the experimental data obtained from alkali halide crystals. Hafemeister and Flygare (72) also used the symmetrical orthogonalization method as did the KY model, but they not only considered the overlap of atomic wavefunctions of nearest-neighbors in the lattice but also included the next nearest-neighbor's interaction. Their calculations indicate that alkali-alkali interactions can be neglected but for the halide ions, halide-halide (next nearest-neighbor interactions) should be included as well as halide-alkali interactions.

For the case of solutions, however, $\sigma_{\rm p}$ still does not relate well to the observed values. Yamagata (68) considered

the dipo molecul€ shifts (ions but computed approac! meantime Hartreegive the stantia] and cowo cept to expressi describe be madeabout th when Lut results optical obtained parison

shifts }

^{giv}en ir

the dipole polarization of the ion by adjacent water molecules. Calculations based on this mechanism predict shifts of the correct order of magnitude for the halide ions but not for alkali metal ions. Ikenberry and Das computed $\sigma_{a\sigma}^{Rb^+}$ for a model of $Rb^+(H_2O)_6$ by using the same approach as they did for alkali-halide crystals. meantime, Hafemeister and Flygare also used D. Mayer's Hartree-Fock wavefunction to calculate σ_{aq}^{Rb} . Both results give the right order of magnitude but still disagree substantially with the experimental observations. and coworkers applied a short-range repulsion force concept to solutions, as shown in Equation (I.12). With this expression, the concentration-dependent phenomena can be described but complete calculation of the shifts could not be made at the time because of the lack of information about the experimental value of σ_{aq}^{O} . This problem was solved when Lutz (79) determined $\sigma_{a\sigma}^{O}$ directly by combining the results obtained from precision NMR, atomic beam, and optical pumping experiments. A summary of $\sigma_{a\alpha}^{O}$ values obtained by different means is listed in Table 5. A comparison of experimental results with calculated chemical shifts in halide crystals and aqueous solution has been given in Ceraso's thesis (95), page 39.

+ Σ

Values of σ_{aq}^{O} Obtained by Various Techniques Table 5.

Author	Model	Mechanism	o ^{M+} aq vs Free Ion	Ref.
Ikenberry and Das	г ь ⁺ (н ₂ 0) 6	Overlap	-0.65 x 10 ⁻⁴	7.4
Hafemeister and Flygare	Rb ⁺ Solution	D. F. Mayer's Hartree-Fock Wavefunction	-0.2 × 10 ⁻⁴	72
Yukio Yamagata	Rb ⁺ (H ₂ O)	Dipole Polarization	-0.07×10^{-4}	89
Deverell and Richards	Rb ⁺ Solution	Overlap but consider ion-ion interactions	No value reported	75
Lutz	Rb ⁺ Solution	Experiment	-2.1 x 10 ⁻⁴	79

Table 6

The was fire

authors With con

large s:

cesium i

adding linearl;

the shif

(iii) CESIUM NUCLEAR MAGNETIC RESONANCE

The physical properties of the Cs-133 nucleus are shown in Table 6.

Table 6. The Physical Properties of the Cs-133 Nucleus.

Resonance frequence in MHz for a 1.4 T. field	7.87
Natural abundance, %	100
Relative sensitivity (vs. ¹ H) for an equal number of nuclei at constant field.	4.74×10^{-2}
Magnetic moment in multiples of the nuclear magneton (eh/4 π mc)	2.5642
Spin I, in multiples of $h/2\pi$	7/2
Electric quadrupole moment Q, in multiples of barns ²	0.003

The magnetic resonance of cesium ions in solutions was first studied by Gutowsky and McGarrey (80). The authors observed that the ¹³³Cs resonance frequency varied with concentration. Carrington et al. (81) also observed large shifts of the cesium resonance upon variation of the cesium halide concentration. They studied the effects of adding various salts to CsCl solutions. The shift varied linearly with the mole fraction of added salt and in general the shift was greater the larger the anion.

chemica] solution of the atomic : and lowetion we were obs the salt $\mathtt{definit}_{\boldsymbol{\varepsilon}}$ increasi The auth resonand actions ions. E Yamashit shift at The conc result f

ions may

rise to

the ions shift.

to the f

More

More recently Deverall and Richards (75) studied the chemical shifts of alkali halide and nitrate aqueous solutions by the alkali NMR technique. The magnitudes of the shifts increased considerably with increasing atomic number of the cation, and shifts to both higher and lower fields relative to the cation at infinite dilution were observed. The resonances of K⁺, Rb⁺ and Cs⁺ were observed to vary linearly with the mean activity of the salt and, for all alkali cations, anions showed a definite series of shielding effects, i.e., the order of increasing shielding was $I^- < Br^- < Cl^- < F^- < H_2O < NO_3$. The authors concluded that the chemical shifts of the cation resonances were not only caused by changes in the interactions with solvent molecules, but also with counterions. By a modification of the theory of Kondo and Yamashita, and the expression of Das et al., the chemical shift at infinite dilution was formulated as Eq. I.ll. The concentration dependence of the chemical shift may result from two processes. Firstly, the addition of other ions may modify the ion-solvent interactions which give rise to $\sigma_{\text{ag}}\text{,}$ and, secondly, direct interactions between the ions during collisions may also contribute to the shift. So the chemical shift at concentration C, relative to the free ion can be written as

$$\sigma = -16\alpha^2 < \frac{1}{r^3} >_{np} \frac{1}{\Delta} \left[\Lambda_{ion-ion}^{c} + \Lambda_{ion-water}^{C} \right] \quad (I.15)$$

where A concent:
that the be active equation solution by halications.
concent:
strong actions.
may be a

solvents
solution
applied
in H 16
Figure
indistir

and grea

cations

degree d

infinite tion in that the the mass where Λ^{C} is a sum of the squares of overlap integrals at concentration of salt C. Deverall et al. (77) also found that the approach of the two oppositely charged ions will be activity dependent, and the term $\Lambda_{\text{ion-ion}}^{\text{C}}$ in the above equation should increase linearly with the activity of the solution. The increased paramagnetic shielding caused by halide ions of high atomic number is mainly caused by the higher values of the overlap integrals for the larger anions. The small shifts observed for Li⁺ and Na⁺ with concentration in aqueous solution are probably caused by strong hydration which inhibits direct cation-anion inter-The increase in the interaction from K⁺ to Cs⁺ may be partly due to a decreasing strength of hydration and greater facility of approach of the anion to the larger cations, as well as to the increase in size and greater degree of overlap.

Halliday and coworkers (82) experimented with isotopic solvents and observed Cs⁺ resonance shifts in dilute salt solutions. They studied the Cs⁺ resonances, at fixed applied field and as a function of molar concentration, in H_2^{16} O, D_2^{16} O and H_2^{18} O. The results are shown in Figure 6. The shifts observed in H_2^{16} O and H_2^{18} O are indistinguishable and extrapolate to the same value at infinite dilution. However, the shift at infinite dilution in D_2^{16} O lies at a lower value. These results showed that the isotope effects cannot simply be a function of the masses of the molecules and suggest strongly that at

Pigure 6

Pigure 7

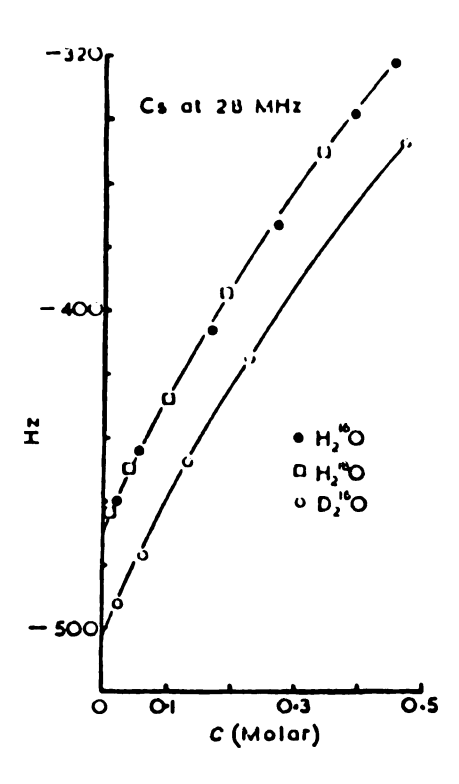


Figure 6. The frequency of the Cs resonance near 28.013 MHz at fixed applied field as a function of molar concentration in H₂¹⁶O, D₂¹⁶O, and H₂¹⁸O. (82)

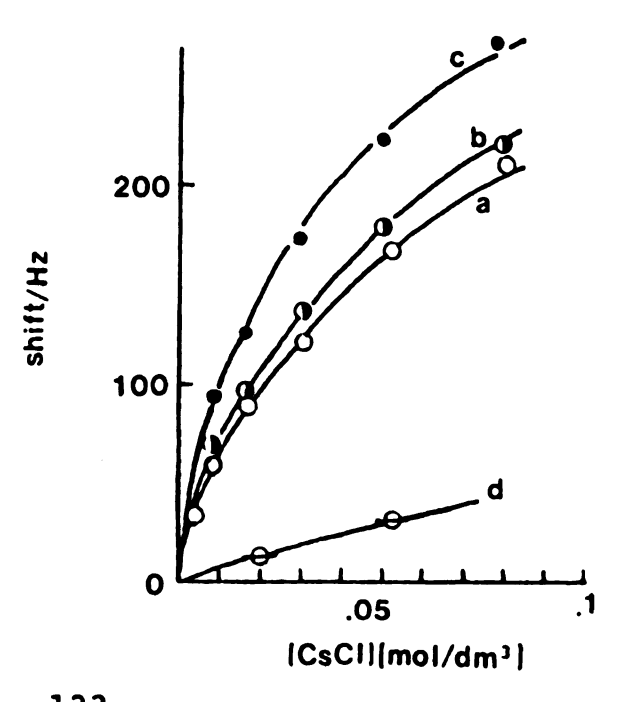


Figure 7. 133Cs shift data (CsCl·MeOH) relative to infinite dilute shifts at three temperatures (a) 298°K; (b) 308.3°K; (c) 326°K (84) and (d) CsCl + H₂O (83) for comparison.

infinite
in the s
from H₂(
ance cas
from "on
somewhat
with H₂(
to cause

published solvents. They first their or of 0.03 which a gives a the valueous For the Cs-133 and Csf. The shi in Figure

shift v

referri

referer

related

infinite dilution, the isotope effect is caused by a change in the strength of the solvent hydrogen bonds in passing from $\rm H_2O$ to $\rm D_2O$. The paramagnetic shift of the $\rm Cs^+$ resonance caused by adjacent water molecules arises mainly from "overlap" interaction of the water molecules. The somewhat stronger hydrogen bonds formed by $\rm D_2O$, compared with $\rm H_2O$, might easily modify the paramagnetic shift so as to cause the observed diamagnetic shift.

At about the same time, Sharp and coworkers (83,84) published an alkali metal NMR study of Cs⁺ in various solvents at lower concentrations and at various temperatures. They first studied cesium salts in aqueous solution and their observations indicated that in the concentration range of 0.03 to 2 M, the data follow an empirical relation in which a plot of log (shift) vs. log (molar concentration) gives a straight line with slope g. Later, they also tested the validity of this empirical logarithmic law for nonaqueous solutions and found it was much less satisfactory. For the investigation of the temperature dependence of the Cs-133 chemical shift, they studied the systems CsCl-MeOH and CsBr-H₂O at a series of different concentrations. The shifts varied only slightly with temperature as shown in Figure 7. It should be noted that the reported chemical shift value at various temperature was obtained by first referring to a 2 M CsCl aqueous solution as an external reference measured at the same temperature and then further related to the value at infinite dilution at that temperature.

III. g

of alkalinteres tions. tion renonaque is a sesolution study ovestigal

IV) of

tands i

III. CONCLUSIONS

From the above discussion, it is evident that a study of alkali complexes with macrocyclic ligands is chemically interesting. In addition, it should have many useful applications. Information on the thermodynamics of these complexation reactions is very sparse, especially for reactions in nonaqueous solvents. It is also evident that alkali NMR is a sensitive probe of the complexation of alkali ions in solution and therefore is a very useful technique for the study of cryptate complexes. This thesis reports an investigation by the Cs-133 NMR technique of the equilibrium properties (Chapter III) and dynamic properties (Chapter IV) of the complexation of cesium ion by crowns and cryptands in various nonaqueous solutions.

CHAPTER II EXPERIMENTAL PART

I. SYNTHESIS OF CESIUM TETRAPHENYLBORATE AND LIGAND PURI-FICATION.

Cesium tetraphenylborate (CsTPB) was made by mixing a tetrahydrofuran (THF) (Burdick and Jackson Laboratories Inc.) solution of sodium tetraphenylborate (NaTPB) with a concentrated aqueous solution of cesium chloride (Ventron Alfa Products, 99.9% pure). The fine white precipitate was washed continuously with conductance water; sodium contamination was checked with a flame emission spectrometer (EU-703) and was found to be less than 0.01%. Cesium triiodide solutions were made by mixing equimolar amounts of cesium iodide (Ventron Alfa Products, 99.9% pure) and iodine (Baker and Adamson) in an appropriate solvent.

Crown ligand 18C6 (PCR, Inc.) was purified by forming a complex with acetonitrile (Mallinckrodt A. R. grade). When about 50 grams of 18C6 was dissolved at ambient temperature, in 125 ml of acetonitrile (MeCN), fine white crystals of the 18C6·MeCN complex were formed. The flask was cooled in an ice-acetone bath to precipitate as much complex as possible and the solid was then collected by rapid filtration. The hygroscopic crystals were transferred to a round-bottom flask equipped with a magnetic stirring bar and a vacuum take-off. The weakly bound MeCN was removed from the complex by pumping under vacuum for a few hours. The m.p. of recrystallized 18C6 was 39°C, the same as that reported (85).

of the

Inc. an hexane

Cry

with a

Cry

was use chased and B). these t

used fo reports

(Fisher I.D.) w

process no air

the col

grams c solutio

With n-

diethyl elute t

ing so

Isomer

ph a t from e

ivory

Cryptand C222 was obtained from E. M. Laboratories,
Inc. and was purified by two recrystallizations from nhexane followed by vacuum sublimation. The melting point
of the snow-white sublimate was 68° (reported 68°C (86))
with a melting range of less than one degree.

Cryptand C222B was a gift from E. M. Laboratories and was used as received. Dicyclohexyl-18C6 (DCC) was purchased from duPont Co. as a mixing of the two isomers (A and B). For lineshape analysis purposes, a separation of these two isomers was carried out, and only isomer A was The method used was based on two used for the study. reports (87,88). Approximately 100 g of Alumina Absorption (Fisher) was weighed and packed slowly in a column (2 cm I.D.) which already contained n-hexane. During the packing process, the column was checked constantly to insure that no air bubbles were trapped. After packing was completed, the column was eluted several times with n-hexane. Five grams of DCC were dissolved into 10 ml n-hexane and the solution was poured into the column, which was then washed with n-hexane a few times. A mixture of n-hexane and diethyl ether (Mallinckrodt A.R. grade) was then used to elute the column. The mole fraction of ether in the eluting solvent was increased gradually for each addition. Isomer A was eluted first and then the solvent was removed by a flash-evaporator. Isomer A was recrystallized twice from ether and then the crystals were taken out with ivory forceps to avoid contamination by metal ions.

,

В

a: G:

IJ

Шe

we su

ac

an

sh

Then the crystals were pumped on in a container on a vacuum line overnight. The white crystals melted at 61-62°C.

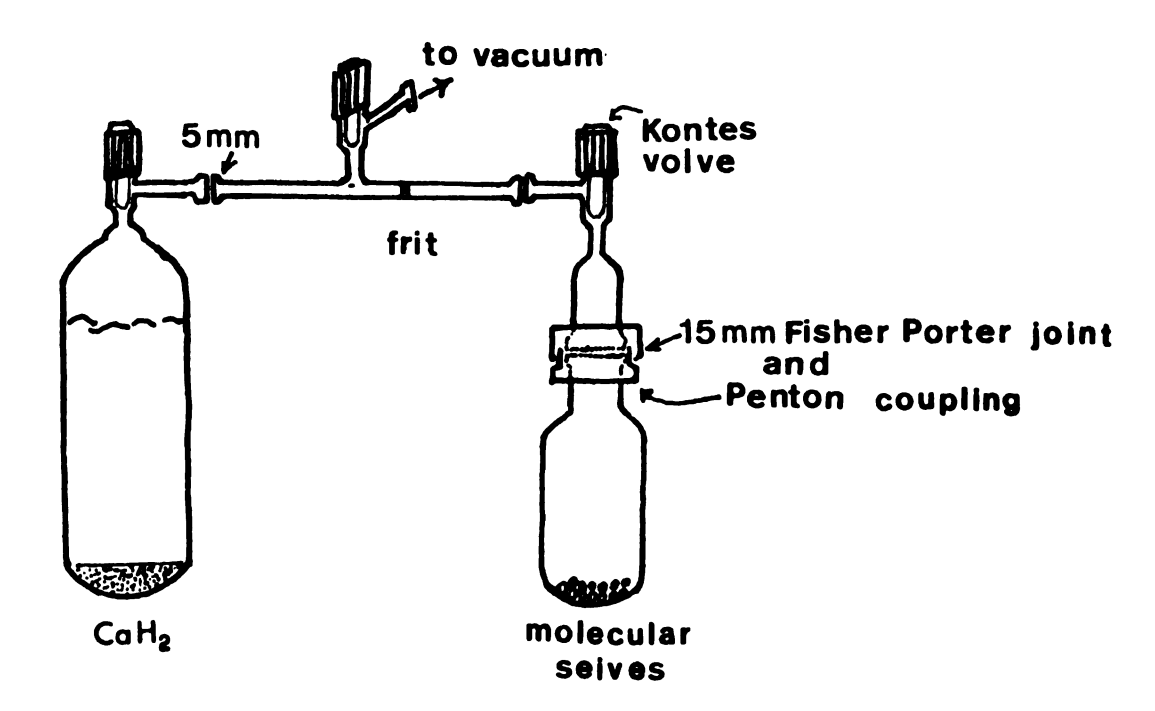
If the m.p. range was larger than 1½ degrees, the separation was repeated again using a newly-packed column. Isomer

B could be stripped off from the column by eluting with anhydrous methyl alcohol (Absolute, Mallinckrodt A. R.

Grade), then recrystallized from n-hexane (m.p. 69-70°C).

II. SOLVENT PURIFICATION AND SAMPLE PREPARATION.

Propylene carbonate (Aldrich), acetone (Fisher), dimethylsulfoxide (Baker, Reagent grade) and acetonitrile were first dried with calcium hydride under reduced pressure and then transferred by vacuum distillation to newly activated molecular seives (Linde Type-4A, (Matheson Coleman and Bell)) through a T-shaped joint with a coarse frit as shown below.



After 12 hours this solvent was vacuum distilled to another container (Figure 8). Before vacuum distillation, this bottle was pumped on the vacuum line for a few minutes through joint (1) and heated gently to get rid of adsorbed moisture on the surface. The distilled solvent was kept in the drying vessel and transferred to the sample tube when needed. The sample compartment was first pumped on line through joint (2) for a few minutes before transfer. After the desired volume of solvent had been transferred, the solution was cooled with dry ice and the sample tube was flame sealed off. During transfer, the pressure in the stock bottle must be higher than that in the sample tube; otherwise "bumping" of the solution can occur.

Pyridine (Fisher) was dried over CaH₂ under reduced pressure overnight and then further dried by the following method: Sodium and potassium (J. T. Baker Co. 99.99% pure) were packed into small ampoules as described in F. Tehan's thesis (89). A three-to-one ratio of potassium and sodium in the small ampoules was put into the sidearm of the bottle and sealed as shown in Figure 9. Benzo-phenenone (Matheson Coleman and Bell) was placed into the vessel in an amount slightly less than the stoichiometric amount of metals, then the vessel was vacuum-line pumped. When the pressure in the line went to 10⁻⁶ torr, the metal was heated by a gas flame until all metals left the first section and glass ampoules; leaving some impurities in

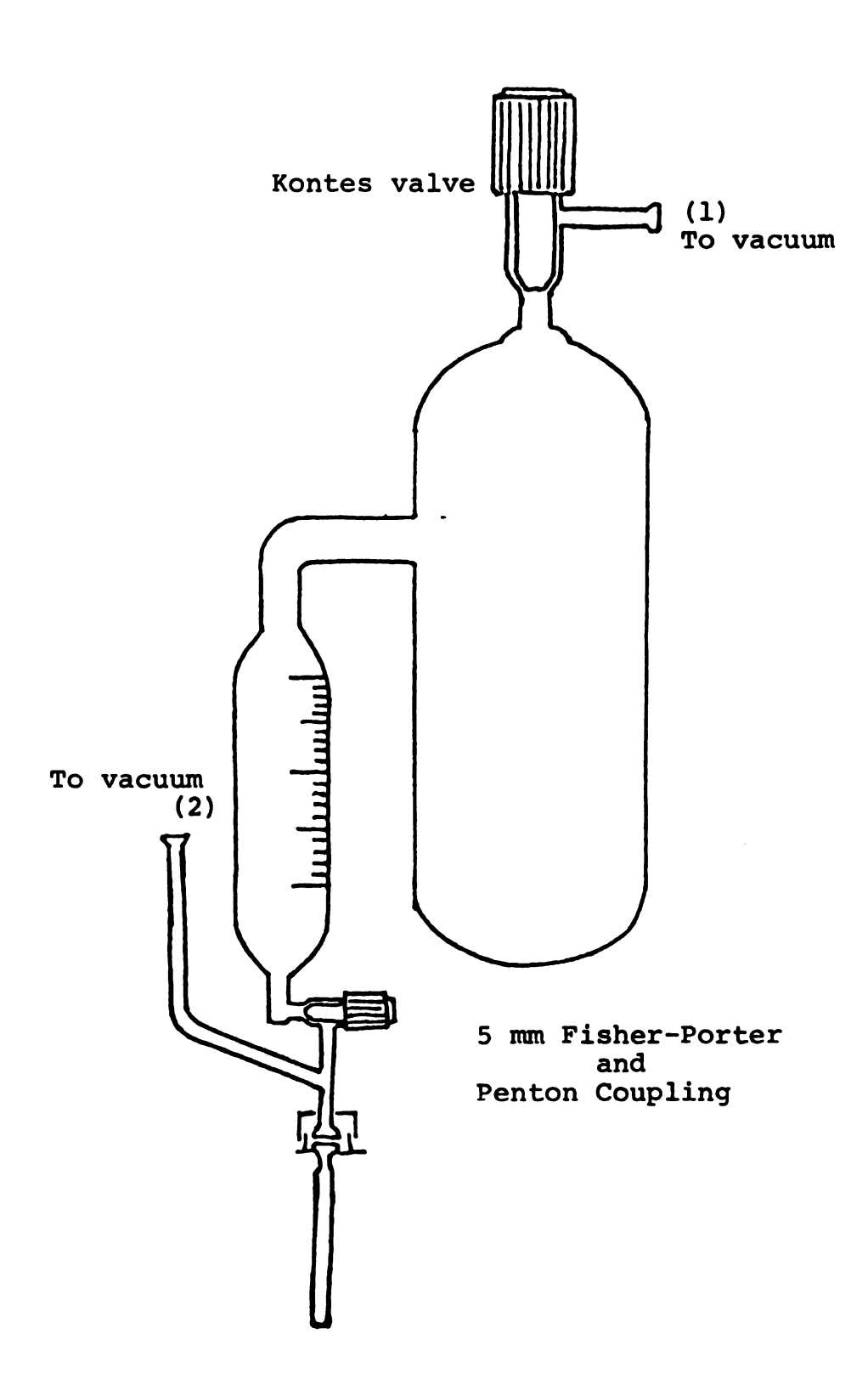


Figure 8. Apparatus for storing solvent in the preparation of NMR sample.

pur

(cau

india to be

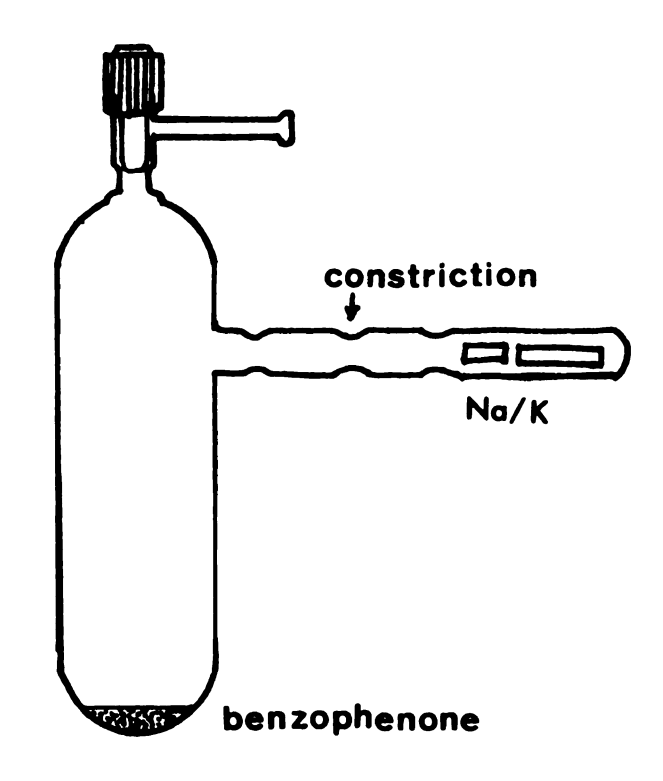


Figure 9. Vessel for Solvent Purification.

this section. The first constriction to isolate the impurities away from the Na/K alloy was made by flame seal-off. The sidearm was repeatedly heated and sealed off, in such a way the metal was finally distilled into the bottle. After the Na/K alloy was in the bottle, the last constriction was sealed-off and pumping was continued for awhile and then pyridine was distilled over. When pyridine was distilled through the vacuum line, a blue-colored solution (caused by the formation of benzophenone radical anions) indicated that the solvent was dried. The above method had to be modified for drying DMF, since it decomposes when

p] Ar

TH

pc

ir

po si

rem

pun

N,N

placed in contact with an alkali metal in basic solution.

An anthracenide radical anion was first formed by distilling THF into the bottle which contained freshly distilled potassium and anthracene. A blue solution formed indicating that the anthracenide radical anion was present. After pouring the blue solution into vessel B (Figure 10) the side bottle with metal was sealed-off. Then the THF was

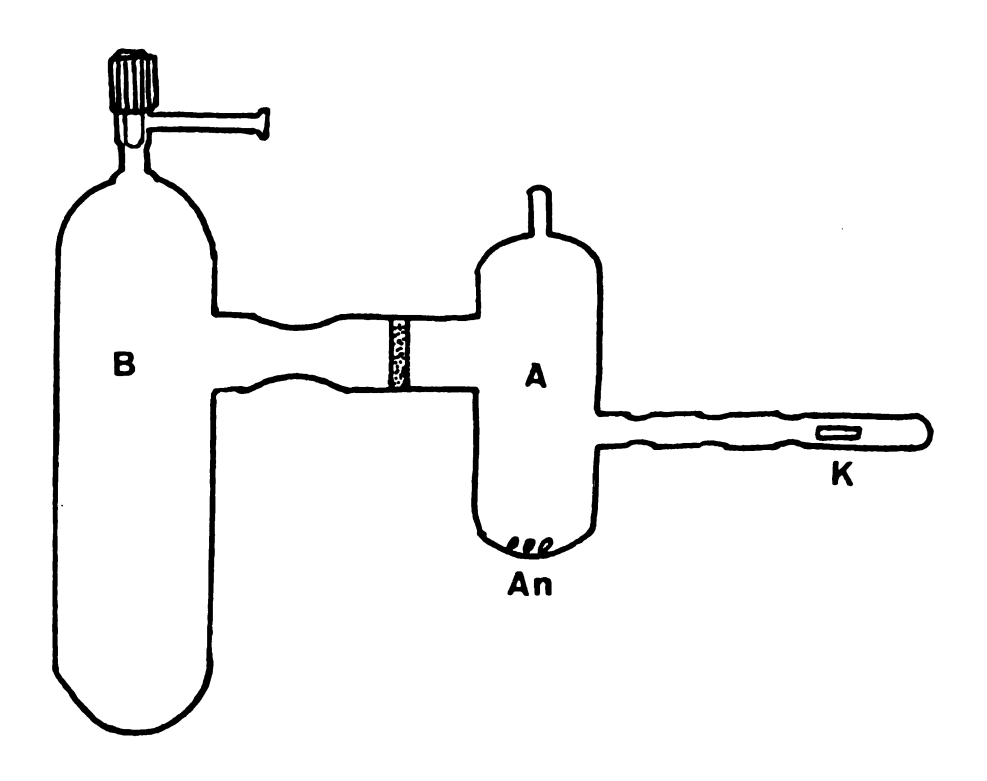


Figure 10. Vessel for DMF Purification.

removed by vacuum distillation and the blue salt was

Pumped overnight to make sure that all THF was removed.

N,N-dimethylformide (DMF) (Burdick and Jackson Laboratories,

Ph Pp

wi

I

aı

eı

b]

di

II

in an

100

60 of

et.

tra The

mix

is

sin wor

ete

35 1

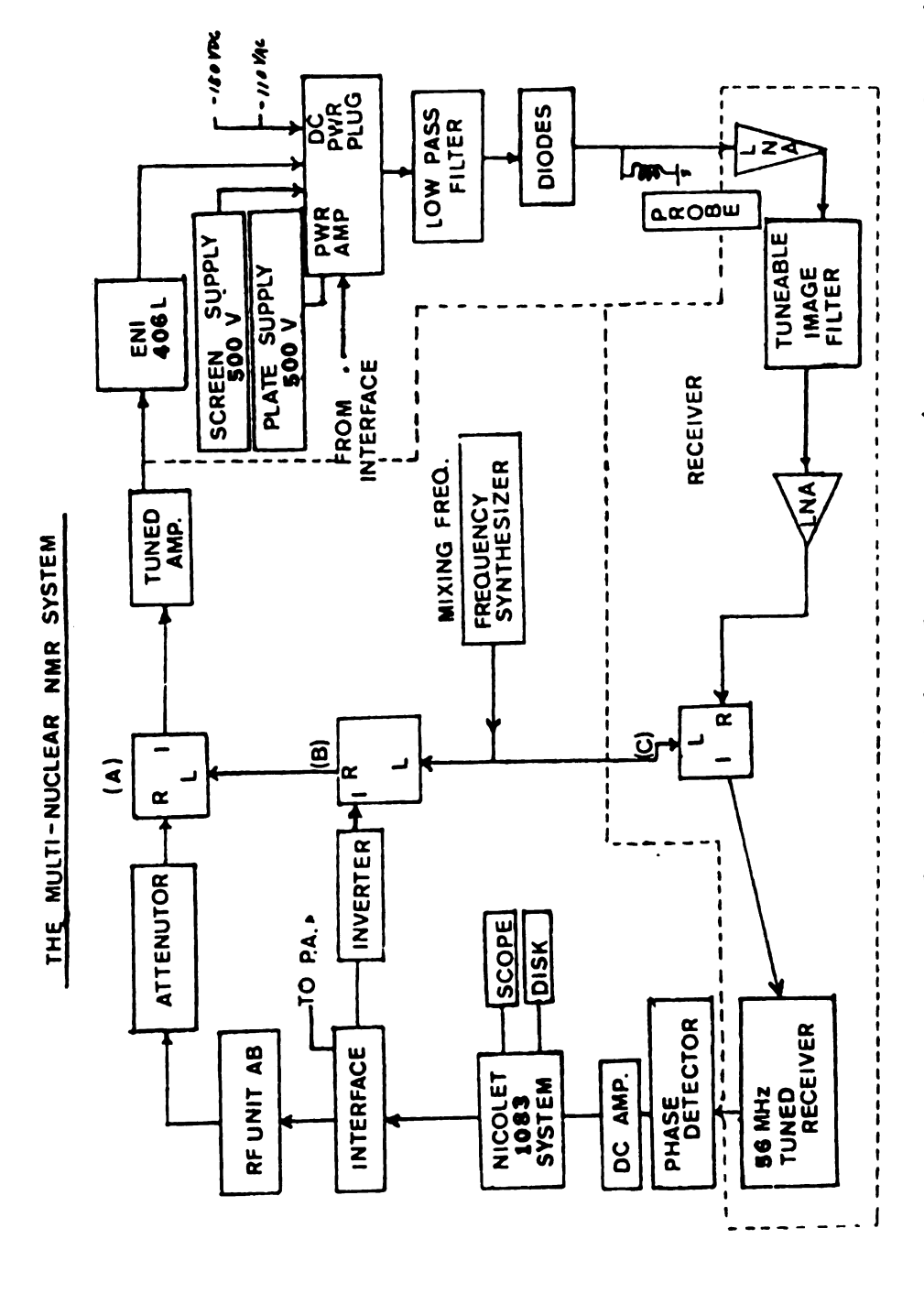
Inc.) was dried over CaH_2 under reduced pressure overnight and the dried DMF was distilled into the vessel after evacuation to 10^{-6} torr. If the solution was greenishblue, it indicated that the solvent was dry; if not, the distillation was repeated.

All solvents except acetone were analyzed for water with an automatic Karl Fisher Titrator (Aquatest II) from Photovolt Corp. The water content was always below 100 ppm.

III. THE NMR SPECTROMETER; MEASUREMENT AND DATA HANDLING.

A Varian DA-60 NMR spectrometer was modified to operate in the pulsed mode at a field of 1.409 T. The ¹³³Cs resonance frequency at this field is 7.8709 MHz. The field is locked by a home-built (90) lock probe which uses the DA-60 console to lock on the proton resonance. A Block diagram of the spectrometer is shown in Figure 11. The spectrometer consists of three main parts. The first is a tuned transmitter/receiver section which operates at 56.44 MHz. The second section consists of a network of double balanced mixers coupled to a frequency synthesizer. The third part is a wideband transmitter/receiver network coupled to a single coil tunable probe. By utilizing the mixing network, broad band amplifiers and tunable probe, this spectrometer can observe NMR signals in the range of about 2 to 35 MHz.

				1
11.				
_				



Block diagram of the multinuclear magnetic resonance spectrometer. Figure 11.

co li

Pe C:

01

me ma

in

2

r

0

t a

đ

The NMR spectrometer is interfaced to a Nicolet 1083 computer for time averaging of spectra and also for online Fourier transformation of data. Chemical shift readout was directly obtained from the spectra during the experiment, and all the shifts were calibrated with 0.5 M CsBr in water being an external reference during measurement. However, all data reported in this thesis are ultimately referenced to infinitely dilute Cs⁺ in water at 25°C. The reported data are also corrected for differences in bulk diamagnetic susceptibility between sample and reference according to the following equation:

$$\delta_{\text{corr}} = \delta_{\text{obs}} + \frac{2\pi}{3} \left(\chi_{\mathbf{v}}^{\text{ref}} - \chi_{\mathbf{v}}^{\text{sample}} \right) \tag{II.1}$$

where χ_{V}^{ref} and χ_{V}^{sample} are the volume susceptibility of the reference and sample solutions respectively and δ_{obs} and δ_{corr} are the observed and the corrected chemical shifts, respectively. Values of δ_{corr} were calculated on the basis of published magnetic susceptibilities of various solvents (91). It was assumed that the concentration of added salt was low enough that the magnetic susceptibilities of the solvent were not affected. The magnitude of the correction for various solvents is shown in Table 7. Lineshape analysis data were stored on magnetic disc in the form of free induction decay signals. Later these data in the time domain were Fourier-transformed without any smoothing or exponential multiplication. They were then transferred to

•

Pob1 2 .

Physical Properties of Solvents and Correction for Magnetic Susceptibility on DA-60. Table 7.

Solvent	Dielectric Constant	Gutmann's Donor Number	Volumetric Susceptibility	Correction on DA-60 (ppm)
Pyridine	12.40	33.1	0.612	-0.226
Dimethylsulfoxide (DMSO)	46.68	29.8	0.605	-0.241
Dimethylformamide (DMF)	36.71	26.6	0.573	-0.308
Acetone	20.7	17.0	0.460	-0.545
Propylene Carbonate (PC)	65.0	15.1	0.634	-0.180
Acetonitrile (MeCN)	37.5	14.1	0.534	-0.390

DN = -AHE.P.D.SbCl₅ ^aAn empirical parameter to express the nucleophilic properties of solvent, which is defined as the negative ΔH -value in Kcal/mole for the interaction of the electron pair donor with SbCl $_5$ in a highly diluted solution of dichloroethane. DN = $^{-\Delta H}_{\rm E.P.}$



paper tape as octal numbers. This paper tape was then read and punched onto computer cards in octal form. The CDC 6500 computer program CONVERT transferred the octal numbers to decimal numbers in a format which is compatible with the KINFIT program. The program CONVERT and its deck structure are listed in Appendix C.

The equilibrium and kinetics data were all fitted with the appropriate equations by using the least-squares curve fitting program, KINFIT. The related equations and deck structure are listed in the Appendices.

CHAPTER III

STUDY OF FORMATION CONSTANTS OF CESIUM TETRAPHENYLBORATE

ION PAIR AND OF COMPLEXES WITH

MACROCYCLIC LIGANDS IN VARIOUS SOLVENTS

I. INTRODUCTION

Previous studies in our laboratories (92-95) and elsewhere (75,83,96,97) have shown that alkali NMR offers a very sensitive probe of the environment of ions in electrolyte solutions; for example, sodium ions in various solvents, and solvent mixtures. The linear relationship between sodium-23 infinite dilution chemical shifts and solvent Gutmann donor numbers illustrates the capability of this technique (98) for predicting donor abilities of various solvents. Of all the alkali metal ions, cesium-133 has the widest range of chemical shifts and its shift is therefore most sensitive to variations in the immediate environment.

In 1975 Cahen et al. (93) showed that nuclear magnetic resonance of the lithium nucleus could be used to measure the stability constants studies of lithium complexes in solution. The purpose of the study described in this chapter was to extend the NMR investigation of alkali salt solutions to cesium salts and complexes in solutions.

It should be noted that in solvents of low dielectric constant and/or in concentrated solutions, cesium salts may form ion pairs or even higher ionic aggregates.

Naturally, it was important for us to determine the extent of ionic association of cesium salts in nonaqueous solvents prior to the study of the complexation reaction.

II. INVESTIGATION OF CESIUM SALTS IN NONAQUEOUS SOLVENTS.

The concentration dependence of 133 Cs chemical shifts as a function of the salt concentration was studied for CsTPB,CsI $_3$ and CsSCN in pyridine, acetone, MeCN, PC, DMF, and DMSO. The results are shown in Table 8 and Figure 12. It can be seen from Figure 12 that only in the case of solutions in pyridine, acetone and MeCN did we observe the variation of chemical shift with concentration, which is characteristic of contact ion pair formation. Of the solvents listed in Table 7, pyridine has the highest donor number (DN=33.1) and the lowest dielectric constant (ϵ = 12.40), yet the curvature of the plot indicates that in this solution there is relatively strong contact ion pairing.

Cesium triiodide is known to be a strong electrolyte (99) and the virtual absence of a concentration dependent chemical shift in pyridine solution indicates that the extent of ion pairing is very small in this case. Cesium thiocynate has a very low solubility in pyridine, so that chemical shifts were determined at only five points in the concentration range of 0.007 to 0.0005 M. The chemical shift becomes more diamagnetic as concentration is decreased. Although the change in chemical shift is small compared, for example, to that for CsTPB, the curvature indicates that both CsTPB and CsSCN form ion-pairs, since the curvature changes dramatically as the concentration decreases. It should be noted that it is the curvature of the chemical

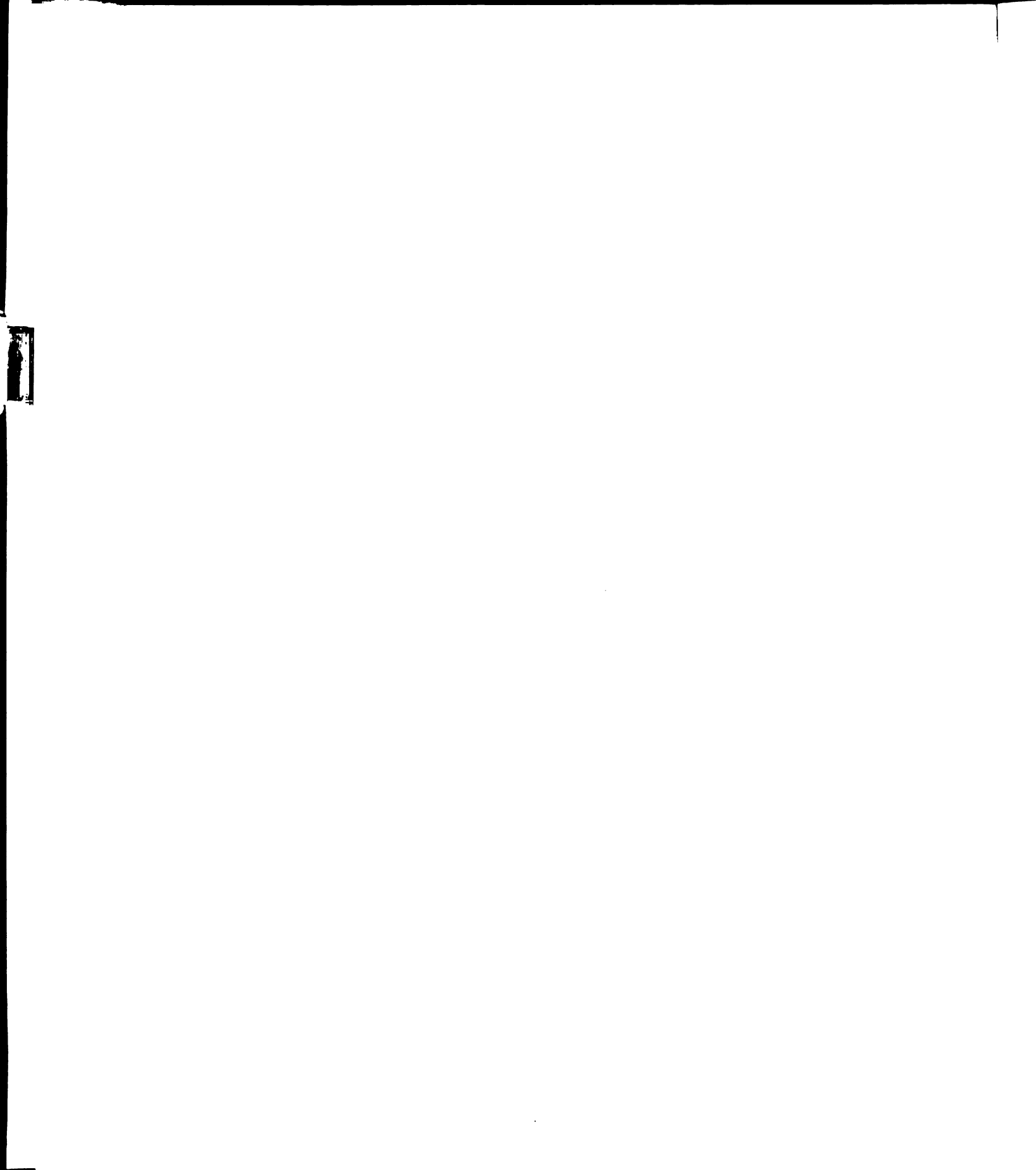


Table 8. Cesium-133 Chemical Shifts of Cesium Salt Solution at 25°C

Salt:Cs	TPB	CsSCN	I	CsI ₃	
Solvent:Py	ridine	Pyridi	ne	Pyridi	ne
Conc. (M)	ppm	Conc. (M)	ppm	Conc. (M)	ppm
0.015	37.81	0.007	-35.10	0.02	-32.93
0.0121	37.18	0.005	-34.94	0.019	-32.31
0.01	33.0	0.003	-34.32	0.013	-31.69
	33.15	0.001	-32.46	0.008	-30.76
0.009	31.29	0.005	-31.69	0.007	-30.45
0.008	29.12	0*	-30.76	0.002	-28.90
	29.13			0*	-29.41
0.007	26.94				
0.006	24.46				
	24.01				
0.005	22.29				
0.004	17.95				
	17.34				
0.003	14.23				
0.0025	11.74				
0.002	8.03				
0.001	1.27				
0.0005	-8.25				
0*	-15.64				

Table 8. Continued

Salt:Cs'		Cs	•	Cs	•
Solvent	:PC	Po	C	Acet	one
Conc. (M)	Δppm	Conc. (M)	Δppm	Conc. (M)	Δppm
0.02	36.63	0.02	34.43	0.05	20.73
0.01	35.89	0.01	34.43	0.03	21.81
0.008	35.89	0.008	34.74	0.01	22.90
0.006	35.52	0.006	34.74	0.008	23.21
0.005	35.27	0.004	35.05	0.006	23.52
0.003	35.27	0.002	35.05	0.004	23.83
0.001	35.02	0.001	35.21	0.002	23.83
0*	34.02	0*	34.45	0.001	24.30
				0*	23.96

Table 8. Continued

Salt:Calsider Solvent:	3	CsI ₃ MeCN		CsTP1 MeCN	
Conc. (M)	Δppm	Conc. (M)	Δppm	Conc. (M)	Δppm
0.3	-70.47	0.3	-41.31	0.015	-20.88
0.05	-69.23	0.1	-37.59	0.012	-22.74
0.03	-68.77	0.05	-35.42	0.009	-23.77
0.01	-68.46	0.03	-34.17	0.007	-25.44
0.008	-68.46	0.01	-34.01	0.005	-26.93
0.006	-68.15	0.008	-33.86	0.003	-27.59
0.004	-68.15	0.006	-33.24	0.002	-28.89
0.002	-68.15	0.004	-33.24	0.001	-30.38
0.001	-67.99	0.002	-33.24	0*	-34.03
0*	-67.96	0.001	-33.09		
		0*	-32.61		

Table

S

Conc

0.3

0.3

0.0

0.0

0.0

0.0

0.0

0.0

0*

* Data

NOTE:

Table 8. Continued

Salt:Ca Solvent	•	CsI ₃ MeOH		CsI Formic	•
Conc. (M)	Δppm	Conc. (M)	Δppm	Conc. (M)	Δppm
0.30	-3.38	0.05	37.43	0.3	12.34
0.10	-0.12	0.03	39.61	0.1	20.87
0.06	-0.12	0.01	42.25	0.05	23.51
0.04	0.34	0.008	42.35	0.03	25.06
0.02	0.34	0.006	43.64	0.01	26.45
0.01	0.34	0.004	43.64	0.008	27.07
0.008	0.49	0.002	44.42	0.006	27.23
0.006	0.49	0.001	44.88	0.004	27.54
0.004	0.65	0*	45.03	0.002	27.85
0.002	0.80			0.001	27.85
0*	0.9			0*	28.23

^{*}Data obtained by extrapolation.

NOTE: CsTPB in acetone, DMF, DMSO are collected by L. L. Liu.

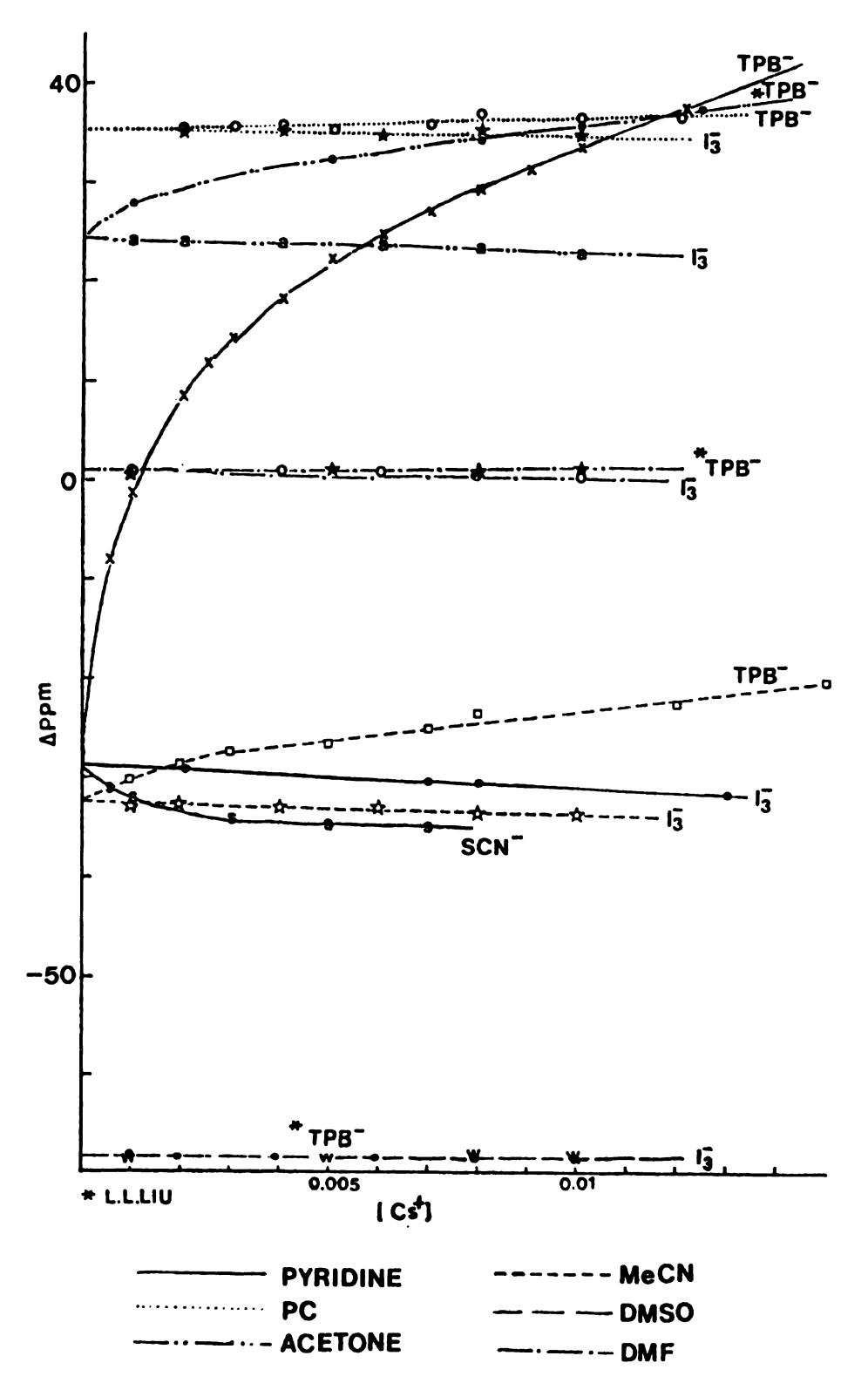


Figure 12. Concentration dependence of the Cs-133 chemical shifts of cesium salts in various solvents.

that
the (
shift
value
shows

shif

and :

pyri

in th

The :

ion p

giver

where

X_{f a}

the

shift <u>vs</u> concentration together with the limiting shift that determines the association constant. Thus even though the CsTPB curve shows a much larger change in chemical shift than does CsSCN, the latter reaches its limiting value at lower concentrations than does CsTPB. This clearly shows that the ion-pair association constant is larger for CsSCN. The infinite dilution chemical shifts of Cs⁺ in pyridine were -15.6, -30.8, and -29.4 ppm for TPB⁻, SCN⁻, and I₃, respectively. The value -29.4 ppm was chosen as the infinite dilution chemical shift of Cs⁺ in pyridine. The ion pairing constants of CsTPB and CsSCN were calculated in the following way.

The exchange between free solvated cesium ion and the ion pair is fast on the NMR time scale, consequently, only one resonance signal is observed and the chemical shift is given by the expression (97)

$$\delta_{\text{obs}} = X_f \delta_f + X_{ip} \delta_{ip} = X_f \delta_f + (1 - X_f) \delta_{ip}$$
 (III.1)

where δ_f and δ_{ip} are the chemical shifts characteristic of the free and ion paired cesium ion respectively, while X_f and X_{ip} are the corresponding relative mole fractions of the two cesium species.

Obviously,

$$X_{f} = \frac{C_{f}^{M}}{C_{+}^{M}}$$
 (III.2)

whe

The mat

Sul

re.

to

sŀ tŀ

e: Ţ

0 (

9

C

where C_f^{M} is the concentration of the free cesium ion and C_t^{M} is the total concentration of the cesium salt. Substitution of Equation (III.2) into (III.1) gives

$$\delta_{obs} = \frac{c_f^M}{c_t^M} (\delta_f - \delta_{ip}) + \delta_{ip}$$
 (III.3)

The concentration equilibrium constant for the ion pair formation is

$$K_{ip} = K_a = \frac{(Cs^+, X^-)}{(Cs^+)(X^-)\gamma_{\pm}^2} = \frac{C_t^M - C_f^M}{(C_f^M)^2} / \gamma_{\pm}^2 = K_c / \gamma_{\pm}^2$$
 (III.4)

Substituting Equation (III.4) into Equation (III.1) and rearranging gives

$$\delta_{\text{obs}} = \frac{\left[-1 + (1 + 4K_{\text{a}}\gamma_{\pm}^{2}C_{\text{t}}^{\text{M}})^{1/2}\right]}{2K_{\text{a}}\gamma_{\pm}^{2}C_{\text{t}}^{\text{M}}} (\delta_{\text{f}} - \delta_{\text{ip}}) + \delta_{\text{ip}} (\text{III.5})$$

Equation (III.5) relates the observed chemical shifts to the total concentration of the salt (C_t^M) , the chemical shift characteristic of the free Cs^+ ion (δ_f) and that of the Cs^+ ion in the ion pair (δ_{ip}) , the mean activity coefficient γ_\pm and the ion pair formation constant K_{ip} . The values of C_t^M and δ_f are obviously known and those of γ_\pm were calculated using Debye-Huckel Equation (III.6) $(\underline{a} = 5.3 \text{ Å } (100))$. Equation (III.5) cannot be solved directly since it has two unknowns δ_{ip} and K_{ip} . The values of δ_{ip} and of K_{ip} were obtained with the help of a non-linear

lea

The

tha

be

the

Tab

least squares curve-fitting program KINFIT (101).

$$-\log \gamma_{\pm} = \frac{\frac{1.823 \times 10^{6}}{(DT)^{3/2}} |z_{+} z_{-}| \sqrt{I}}{1 + \frac{5.029 \times 10^{9}}{(DT)^{1/2}} \underline{a} \sqrt{I}}$$
(III.6)

The results are shown in Table 9. The ion pairing constant (K_{ip}) for the thiocynate salt is over twice as large as that of the tetraphenylborate salt. This phenomenon may be caused by the different extents of polarization of the Cs⁺ ion by the two anions.

Table 9. Ion Pair Formation Constants of Cesium Salts in Various Nonaqueous Solvents.

Solvent	Salt	K _{ip}
Pyridine	CsTPB	$(3.7\pm0.3) \times 10^2$
	CsSCN	$(9.3\pm0.2) \times 10^2$
Acetone	CsTPB	$(2.1\pm0.3) \times 10$
MeCN	CsTPB	$(3.8\pm1.) \times 10$
PC	CsTPB	$(1.6\pm0.7) \times 10$
DMF	CsTPB	~0
DMSO	CsTPB	~0

Cs⁺ ic and ic and cc

a popu

have t

respect
complex
reactio

represe

shift a

ہے!

III. FORMATION CONSTANTS OF CESIUM TETRAPHENYLBORATE COMPLEXES WITH CROWNS AND CRYPTANDS IN VARIOUS SOLVENTS.

In a solution of a cesium salt and a ligand we may have the following solute species: ligand molecules, free Cs⁺ ions, ion-paired Cs⁺ ions, complexed Cs⁺ ions and, free and ion-paired anions. When the exchange between the free and complexed Cs⁺ ion is fast on the NMR time scale, only a population averaged chemical shift is observed.

$$\delta_{obs} = \delta_{\mathbf{F}} X_{\mathbf{F}} + \delta_{ip} X_{ip} + \delta_{c} X_{c}$$
 (III.7)

In the above equation $\delta_{\rm obs}$ is the observed chemical shift and $X_{\rm f}$, $X_{\rm ip}$, $X_{\rm c}$ are the relative mole fractions of free Cs⁺ ions, ion-paired Cs⁺ and complexed Cs⁺ ions respectively. The corresponding chemical shifts of free, complexed and ion paired Cs⁺ ions are $\delta_{\rm f}$, $\delta_{\rm c}$, $\delta_{\rm ip}$. The reactions which take place in a CsTPB solution may be represented by:

$$Cs^+ + TPB^- + Cs^+ \cdot TPB^-$$

Cesium ions are not as strongly solvated as smaller

ions

actio

that large

compe

be si

cause

we wr

where

were

as

٠,

 $\mathbf{E}_{\mathcal{C}}$

t:

C

ions and therefore, the ion pairing and complexation reaction may be more important. In this study it was found that the formation constants of the complexes were much larger than the ion-pairing constants; therefore, the competitive reactions of ion-pairing and complexation can be simplified by assuming that complexation is the major cause of the variation of the chemical shift. That, is we write

$$\delta_{\text{obs}} = \delta_{\mathbf{F}}^{\dagger} X_{\mathbf{F}}^{\dagger} + \delta_{\mathbf{C}} X_{\mathbf{C}}$$
 (III.8)

where

$$\delta_{\mathbf{F}}^{\prime} \mathbf{X}_{\mathbf{F}}^{\prime} = \delta_{\mathbf{F}} \mathbf{X}_{\mathbf{F}} + \delta_{\mathbf{ip}} \mathbf{X}_{\mathbf{ip}}$$

The formation constants of the complexation reactions were determined by measuring the cesium chemical shifts as a function of ligand/Cs⁺ mole ratio, then followed by a computer fit of the data with the equation

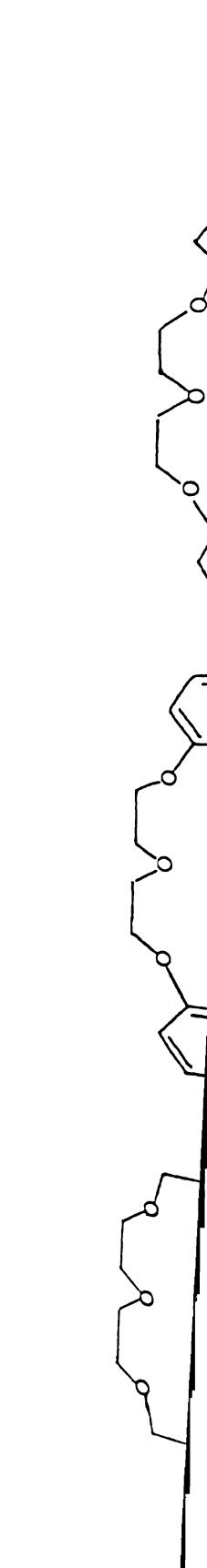
$$\delta_{\text{obs}} = \left[(K \ C_{\text{t}}^{M} - K \ C_{\text{t}}^{L} - 1) + (K^{2}C_{\text{t}}^{L2} + K^{2} \ C_{\text{t}}^{M2} - 2K^{2}C_{\text{t}}^{L}C_{\text{t}}^{M} \right]$$

$$+ 2K \ C_{\text{t}}^{L} + 2K \ C_{\text{t}}^{M} + 1)^{1/2} \left[\frac{\delta_{\text{f}} - \delta_{\text{c}}}{2K \ C_{\text{t}}^{M}} \right] + \delta_{\text{c}}$$
(III.9)

Equation (III.9) has two adjustable parameters, the formation constant K, and the limiting chemical shift of the complex δ_C (for details see Appendix B). In the above

equation C_{t}^{M} and C_{t}^{L} are the analytical concentrations of the metal ion and ligand respectively. Due to solubility limitations, the concentration of CsTPB was kept at 0.01 M for all complexation studies. The crowns used in this study were 18-Crown-6, dicyclohexyl-18C6 (DCC), and dibenzo-18C6 (DBC). Their cavity diameters are reported to be in the range of 2.6-3.2 Å (16). The cryptands used were C222 and C222B where B indicated the benzo group on the ther chain (Figure 13). The cavity diameters of the cryptands are about 2.8 \mathring{A} (102). All the results of this study are given in Tables 10-14 and shown in Figures 14-18. Cesium NMR resonance signals are usually very narrow (< 2Hz). Therefore no error bars are indicated in the chemical shift vs. mole ratio graphs. The corresponding K value from each mole ratio study was computed by using KINFIT and is listed in Table 15.

Two techniques were involved to compute K values with KINFIT: i.e., curvefitting and simulation. When the K value is about 10⁵ or larger, it is difficult to fit the region around the sharp break at the stoichiometric mole ratio. Usually the fitting process will either fail to converge or will give a very large standard deviation. The simulation technique uses KINFIT to imitate a system which is fully defined by a set of given conditions. For example, the initial estimate for a curvefitting process is the starting value which is varied by iteration. For



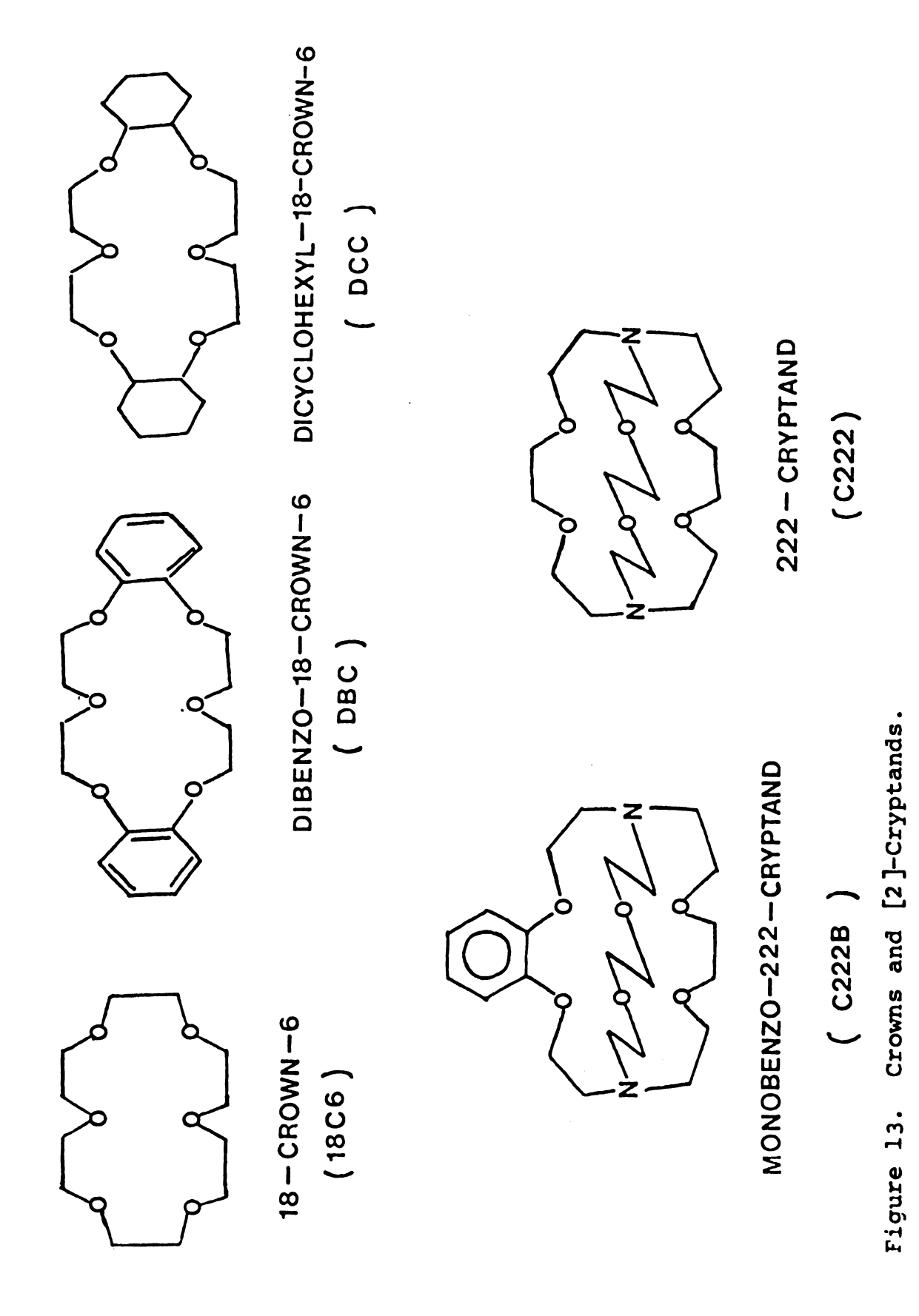


Table 10. Mole Ratio Study of 18C6 Complexes with Cesium Salts in Various Solvents by Cs-133 NMR at 25°C.

Salt:0	CsTPB				
Solvents	Pyradine	Acet	one	PC	
[18C6]		[18C6]		[18C6]	
[Cs ⁺]	Δ ppm	[Cs [†]]	Δppm	[Cs ⁺]	∆ppm
0	32.38	0	35.41	0	36.16
0.28	17.66	0.36	23.77	0.27	28.80
0.51	9.37	0.72	10.42	0.5	21.44
0.78	-3.48	0.90	7.19	0.77	14.73
1.0	-9.91	1.00	6.35	1.00	10.72
1.19	-6.56	1.46	9.89	1.28	9.79
1.46	-0.222	1.19	7.47	1.58	10.54
1.90	5.65	1.80	13.15	1.74	10.54
2.04	8.91	2.00	14.46	2.12	11.93
2.56	15.90	2.50	18.28	2.60	13.42
3.03	20.08	2.77	19.67	3.10	14.54
4.09	26.06	5.15	28.99	5.40	19.29
6.28	34.06	7.08	33.18	6.89	21.53
6.91	35.45	10.3	36.81	8.90	24.51
12.62	40.95	16.54	40.54	22.40	33.27
		18.95	41.38	31.3	35.88

Table 10. Continued.

DM	ıF	Me	CN	DM	so
[18C6] [Cs ⁺]	Δppm	[18C6] [Cs ⁺]	Δppm	[18C6] [Cs ⁺]	Δppm
0	0.81	0	-24.51	0	-67.96
0.33	-0.37	0.33	-21.16	0.23	-58.18
0.63	-1.98	0.62	-18.55	0.59	-44.76
0.90	-2.73	0.77	-17.15	0.90	-34.98
1.00	-2.82	1.00	-15.48	1.00	-33.40
1.35	-2.82	1.28	-14.45	1.24	-30.51
1.45	-2.63	1.40	-14.18	1.45	-29.21
1.69	-2.54	1.89	-12.96	1.80	-27.25
1.99	-2.17	2.06	-12.68	2.19	-25.95
2.72	-1.42	2.49	-11.75	2.33	-25.67
3.0	-0.96	3.23	-10.26	3.12	-24.08
5.19	1.37	4.85	-6.81	4.72	-22.22
7.60	3.70	7.26	-2.62	7.24	-20.08
10.23	5.94	11.05	2.78	9.85	-18.50
30.74	18.23			19.7	-12.81

Table 10. Continued.

	·				
Salt	:CsI	Cs	ı	Cs	C1
Solven	t:DMF	н ₂	o	H ₂	o
[18C6]		[18C6]		[18C6]	
[Cs ⁺]	Δppm	[Cs ⁺]	Δppm	[Cs ⁺]	Δppm
0	-1.89	0	-0.55	0	-0.19
0.32	-3.01	0.28	-0.65	0.5	-0.19
0.51	-3.10	0.51	-0.65	1.0	-0.19
0.82	-4.03	0.72	-0.74	1.5	-0.59
1.00	-4.31	1.00	-0.74	2.0	-0.59
1.55	-4.03	1.48	-0.74	2.5	-0.75
1.81	-3.75	1.26	-0.93	4.	-0.90
2.15	-3.47	1.82	-1.11	6.	-1.06
2.67	-3.01	2.05	-1.11		
3.15	-2.35	3.20	-1.38	8.	-1.37
5.08	-0.40	2.49	-1.30		
6.90	1.47	7.31	-1.86		
4.06	5.19	11.41	-2.16		
20.7	11.71				
24.35	13.67				

Table 11. Mole Ratio Study of DBC Complexes with CsTPB in Various Solvents by Cs-133 NMR at 25°C.

Solvent:					
Pyri	.dine	Acet	one	P	C
[DBC] [Cs ⁺]	Δppm	[DBC] [Cs ⁺]	Δppm	[DBC]	Δppm
0	32.23	0	35.52	0	36.01
0.15	28.77	0.06	34.90	0.19	34.28
0.46	20.46	0.32	30.19	0.46	30.55
0.65	17.48	0.63	26.72	0.685	28.82
0.99	13.88	1.00	25.10	1.00	27.08
1.29	15.62	1.38	26.96	1.20	26.71
1.50	17.97	1.49	27.58	1.39	26.71
1.92	24.92	1.79	29.69	1.40	26.71
1.98	25.30	2.00	30.81	1.55	27.20
2.18	33.49	*2.91	32.30	2.17	28.20
2.41	29.02			2.24	28.32
3.22	34.11			*3.0	29.69
6.17	39.57				
7.48	40.31				
9.81	40.68				

^{*}DBC not completely dissolved.

Table 11. Continued.

Solvent:					
DM	F	Me	CN	DM	SO
[DBC] [Cs ⁺]	Δppm	[DBC] [Cs ⁺]	Δppm	[DBC] [Cs ⁺]	Δppm
0	1.89	0	-24.41	0	-68.08
0.13	2.51	0.29	-20.07	0.13	-66.60
0.36	3.63	0.45	-16.84	0.32	-63.99
0.57	4.74	0.61	-15.23	0.55	-61.14
1.00	5.86	1.00	-8.90	1.00	-55.93
1.13	6.73	1.25	-5.18	1.14	-54.8
1.33	7.10	1.48	-2.57	1.20	-54.3
1.54	7.71	1.59	-1.33	1.69	-49.60
1.86	8.59	2.04	3.13	1.84	-47.74
2.06	8.96	2.27	5.62	2.14	-56.00
2.12	9.33	2.65	8.59	2.31	-44.76
2.61	10.82	2.95	10.95		
3.33	11.82	4.07	17.15		
3.74	12.44	5.82	23.36		

Table 12. Mole Ratio Study of DCC Complexes with CsTPB in Various Solvents by Cs-133 NMR at 25°C.

Solvent:					
Acet	one	PC		Pyri	dine
[DCC]	Δppm	[DCC] [cs ⁺]	Δppm	[DCC] [Cs ⁺]	Δppm
0	36.26	0	35.77	0	32.25
0.27	24.48	0.22	23.23	0.19	23.19
0.56	10.59	0.40	17.28	0.39	5.07
0.89	-6.29	0.75	-3.32	0.71	-13.41
1.00	-9.14	1.00	-13.00	1.00	-30.78
1.15	-14.97	1.10	-18.58	1.23	-33.76
1.44	-18.45	1.50	-21.06	1.52	-34.13
1.87	-18.82	1.70	-21.19	1.64	-34.13
1.99	-18.82	2.14	-21.56	2.09	-33.76
2.17	-18.82	2.49	-21.68	2.13	-33.89
2.42	-18.57	2.97	-21.43	2.76	-33.02
2.83	-18.32	3.09	-21.43	2.93	-32.77
3.07	-18.08	3.25	-21.31	2.99	-32.40
5.86	-15.35	4.45	-20.56	4.53	-30.04
7.79	-13.61	6.29	-19.32	6.11	-27.93
		8.74	-17.84	9.35	-23.96

Table 12. Continued.

Solvent:					
DM	F	MeC	N	DM	SO
[DCC] [Cs ⁺]	Δ ppm	[DCC] [Cs ⁺]	Δppm	[DCC] [Cs ⁺]	Δ ppm
0	1.15	0	-23.88	0	-68.27
0.17	-3.07	0.22	-26.36	0.25	-65.17
0.46	-9.77	0.55	-30.58	0.45	-62.44
0.73	-14.86	0.89	-34.67	0.72	-60.08
1.00	-20.32	1.00	-35.66	1.00	-57.60
1.25	-23.05	1.14	-36.41	1.26	-55.86
1.46	-24.66	1.65	-37.03	1.47	-55.24
1.60	-25.78	1.94	-37.03	1.89	-54.25
2.03	-27.39	2.02	-37.03	1.99	-53.51
2.19	-28.01	2.43	-36.66	2.6	-52.88
2.49	-28.63	2.75	-36.90	3.03	-51.77
2.91	-29.01	3.04	-36.78	3.37	-51.77
3.27	-29.25	3.71	-36.28	6.54	-49.78
5.06	-29.38	5.53	-35.29	8.52	-49.03
6.12	-29.50	6.74	-34.92		
9.81	-29.38	8.86	-33.68		

Table 13. Mole Ratio Study of C222B Complexes with CsTPB in Various Solvents by Cs-133 NMR At 25°C.

Solvent	:				
1	PC	Pyr	idine	Ace	tone
[C222B] [Cs ⁺]	Δρρπ	[C222B] [Cs ⁺]	Δppm	[C222B]	Δppm
0	36.34	0	32.25	0	34.90
0.21	22.74	0.32	15.37	0.36	14.38
0.52	-1.29	0.6	-3.61	0.5	-24.95
0.69	-14.71	0.83	-49.40	0.75	-39.47
1.04	-31.94	1.00	-66.89	1.00	-44.31
1.05	-35.11	1.16	-70.33	1.50	-50.14
1.16	-37.90	1.27	-74.83	1.70	-51.01
1.32	-39.67	1.36	-74.33	2.00	-51.75
1.49	-42.84	1.41	-75.33	2.50	-52.25
1.67	-44.87	1.64	77.56	3.53	-53.12
1.74	-46.06	1.77	-78.06	* ∞	-54.09±0.23
1.75	-45.73	1.99	-78.81		
1.92	-46.75	2.52	-79.55		
2.2	-48.05	3.20	-79.67		
2.7	-49.45	* œ	-80.60±0.15		
3.34	-50.2				
# ∞	-52.55±0.14				

^{*}Obtained by the curve-fitting program.

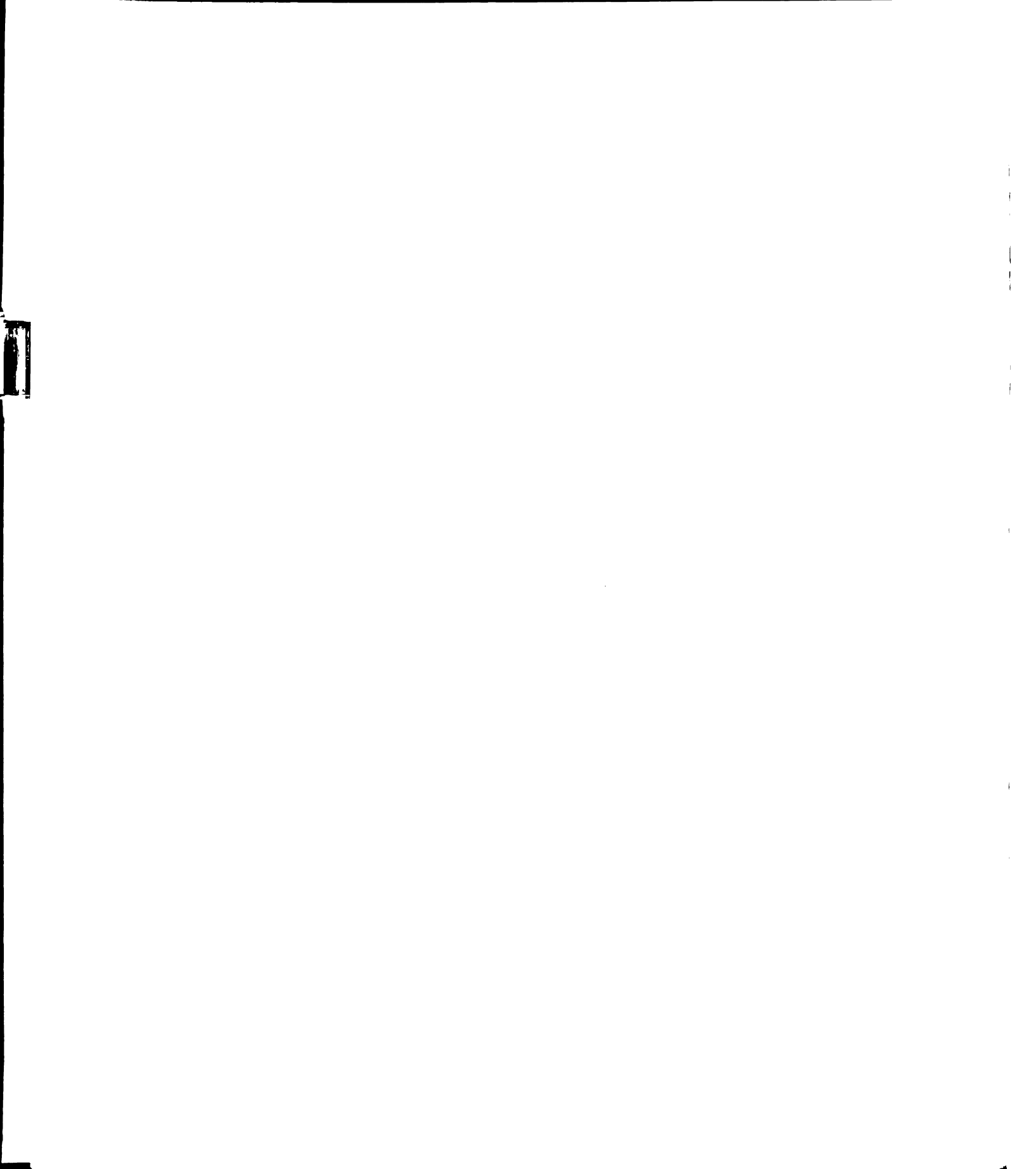


Table 13. Continued.

Solvent	:				
D	MF	Me	:CN	DMS	0
[C222B]	· Δppm	[C222B] [Cs ⁺]	Δppm	[C222B] [Cs ⁺]	Δppm
0	1.17	0	-24.09	0	-68.31
0.28	-4.12	0.35	-40.07	0.21	-68.46
0.41	-5.80	0.54	-50.62	0.53	-68.46
0.82	-11.20	0.68	-54.19	0.83	-68.46
1.00	-12.51	1.00	-65.51	1.00	-68.77
1.39	-17.07	1.32	-70.63	1.23	-68.46
1.53	-18.19	1.61	-72.33	1.42	-68.93
1.67	-19.77	1.98	-73.26	1.76	-68.93
2.0	-22.01	2.04	-73.26	2.18	-68.46
2.47	-24.99	2.41	-73.58	2.46	-68.46
2.90	-27.60	3.13	-73.89	3.07	-68.46
* _∞	-51.82±1.61	* ∞	-744±0.04		

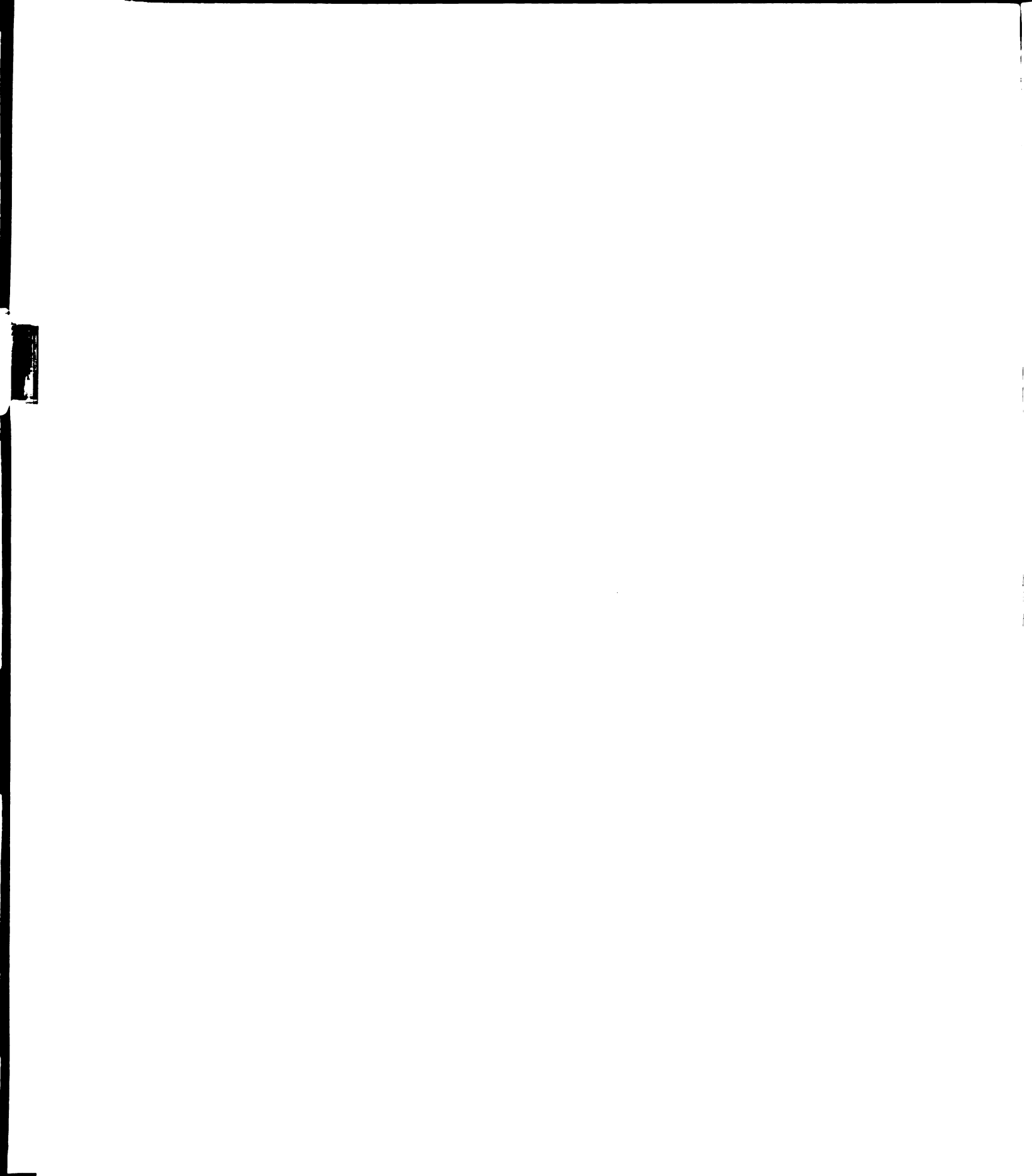


Table 14. Mole Ratio Study of C222 Complexes with CsTPB in Various Solvents by Cs-133 NMR at 25°C.

Solven	nt:				
	PC	Ace	tone		MeCN
[C222] [Cs ⁺]		[C222] [Cs ⁺]	Δppm	[C222] [Cs ⁺]	Δppm
0	36.45	0	35.83	0	-24.40
0.13	17.37	0.30	-17.17	0.26	-97.14
0.48	-56.72	0.58	-102.26	0.51	-132.97
0.72	-113.68	0.89	-165.60	0.72	-166.31
1.00	-175.56	1.00	-182.52	1.00	-206.17
1.19	-184.87	1.18	-192.51	1.37	-208.81
1.45	-189.21	1.58	-199.42	1.55	-209.58
1.93	-191.38	1.86	-200.36	1.72	-209.74
2.08	-191.69	1.97	-200.92	2.27	-210.20
2.23	-191.54	2.42	-201.29	2.36	-209.89
2.93	-192.62	2.89	-201.85	2.87	-210.05
3.17	-192.62	3.03	-201.85	3.11	-210.20
* co	-193.75±0.16	# co	-202.96±9.19	Ħœ	-210.39±0.

Table 14. Continued.

Solve	nt:				
	DMF	D	MSO	Pyri	dine
[C222]	- //00///	[C222] [Cs ⁺]	Δppm	[C222] [Cs ⁺]	Δppm
0	0.80	0	-67.01	0	30.81
0.19	-13.31	0.25	-70.56	0.25	
0.45	-35.02	0.57	-74.67	0.45	
0.60	-41.85	0.92	-79.90	0.72	
1.04	-63.30	1.00	-81.21	0.96	-217.33
1.20	-78.60	1.12	-82.52	1.28	-223.85
1.40	-87.60	1.46	-86.07	1.46	-224.47
1.70	-95.51	1.82	-89.99	1.81	-224.18
2.13	-105.90	2.12	-92.61	1.97	-224.18
2.40	-111.95	2.57	-95.97	3.05	-224.25
3.18	-121.25	2.75	-96.72		
3.56	-124.51	3.26	-100.64		
*œ	-155.80±2.30	* œ	-144.34±3.52		

[†]Data collected by L. L. Liu.

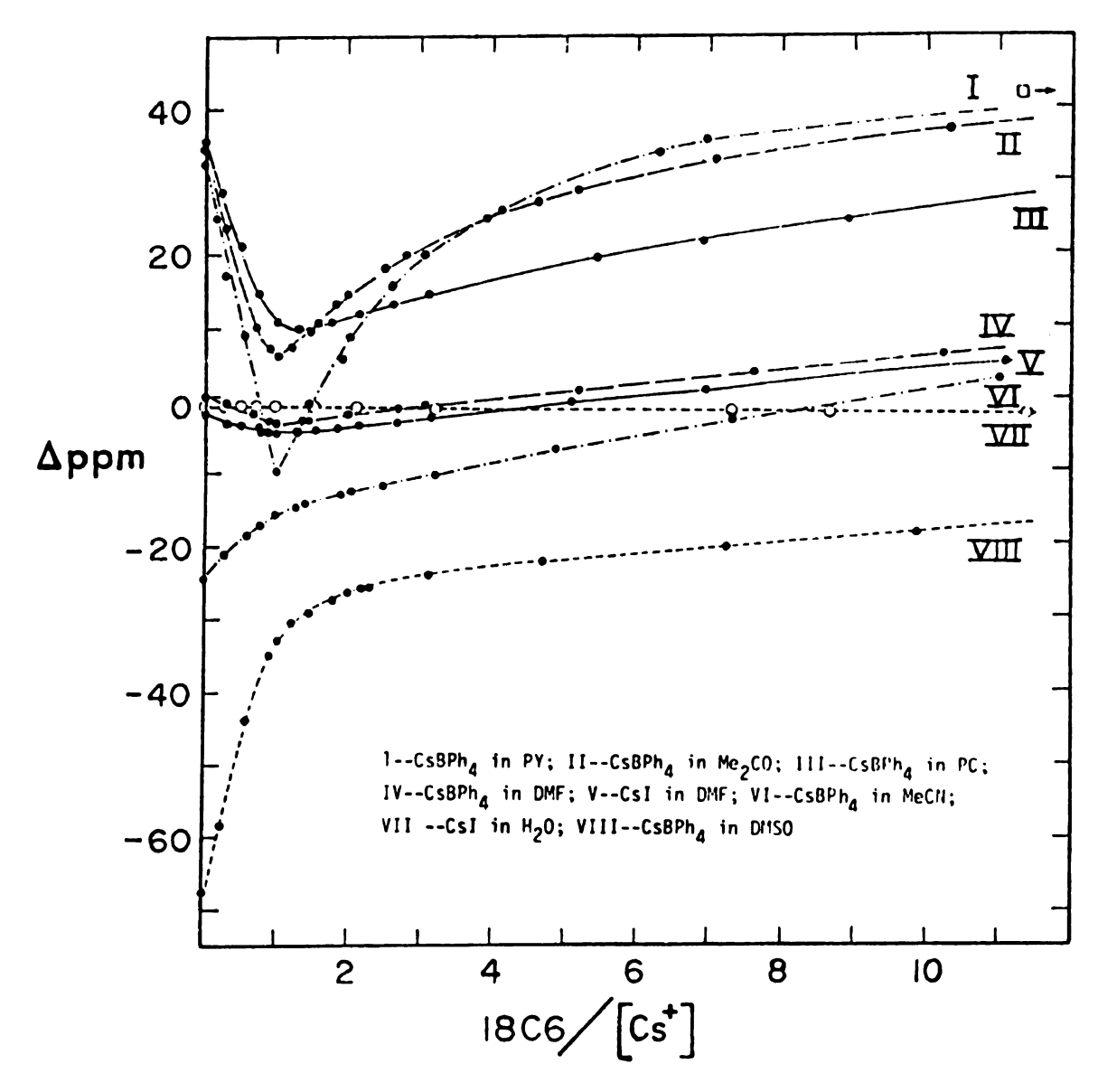


Figure 14. Chemical shifts of cesium-133 as a function of mole ratio of [18C6]/[Cs+TPB-] in various solvents. [CsTPB] $_{\rm T}$ = 0.01M.

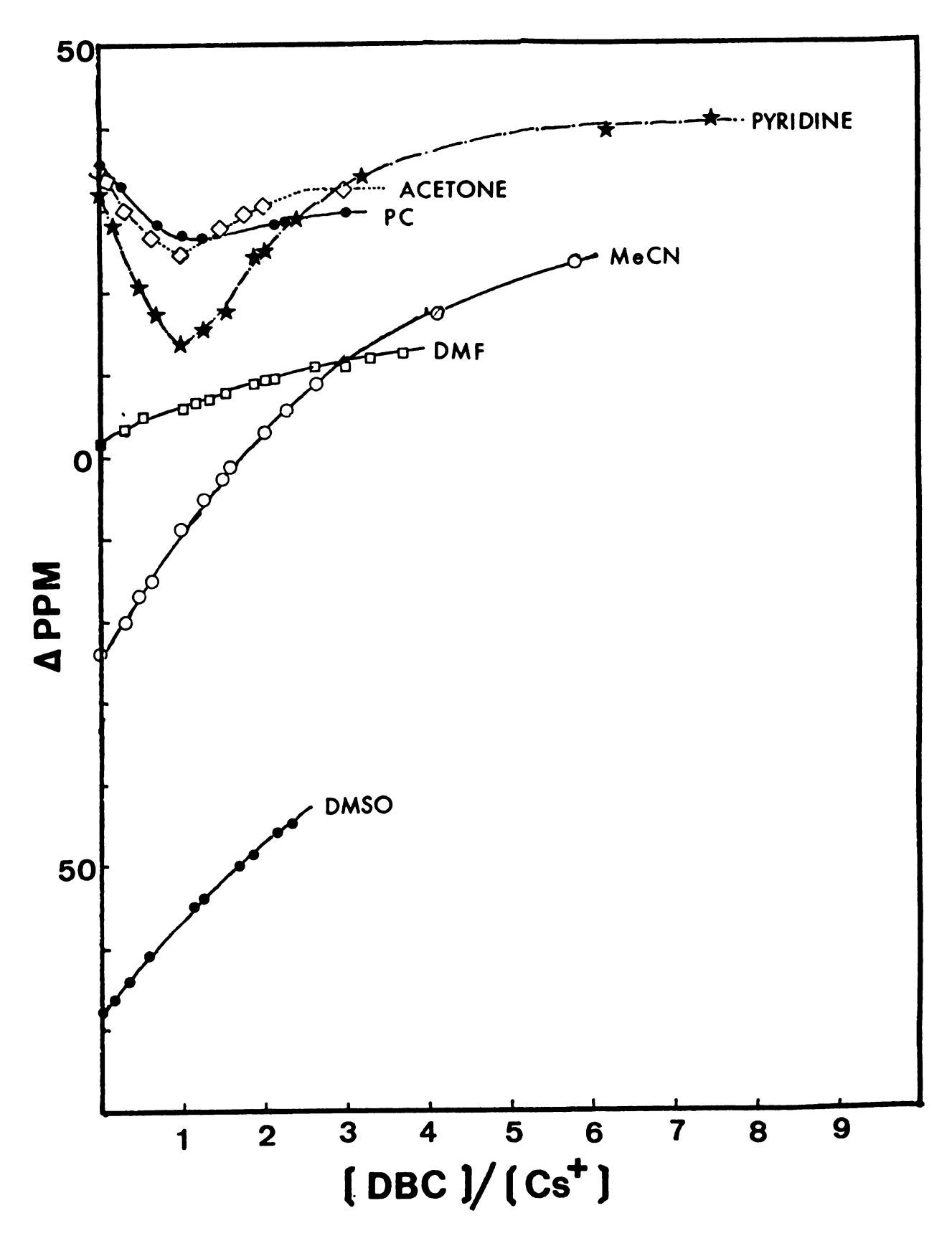


Figure 15. Chemical shifts of cesium-133 as a function of mole ratio of [DBC]/[Cs $^+$ TPB $^-$] in various solvents. [CsTPB] $_{\rm T}$ = 0.01 M.

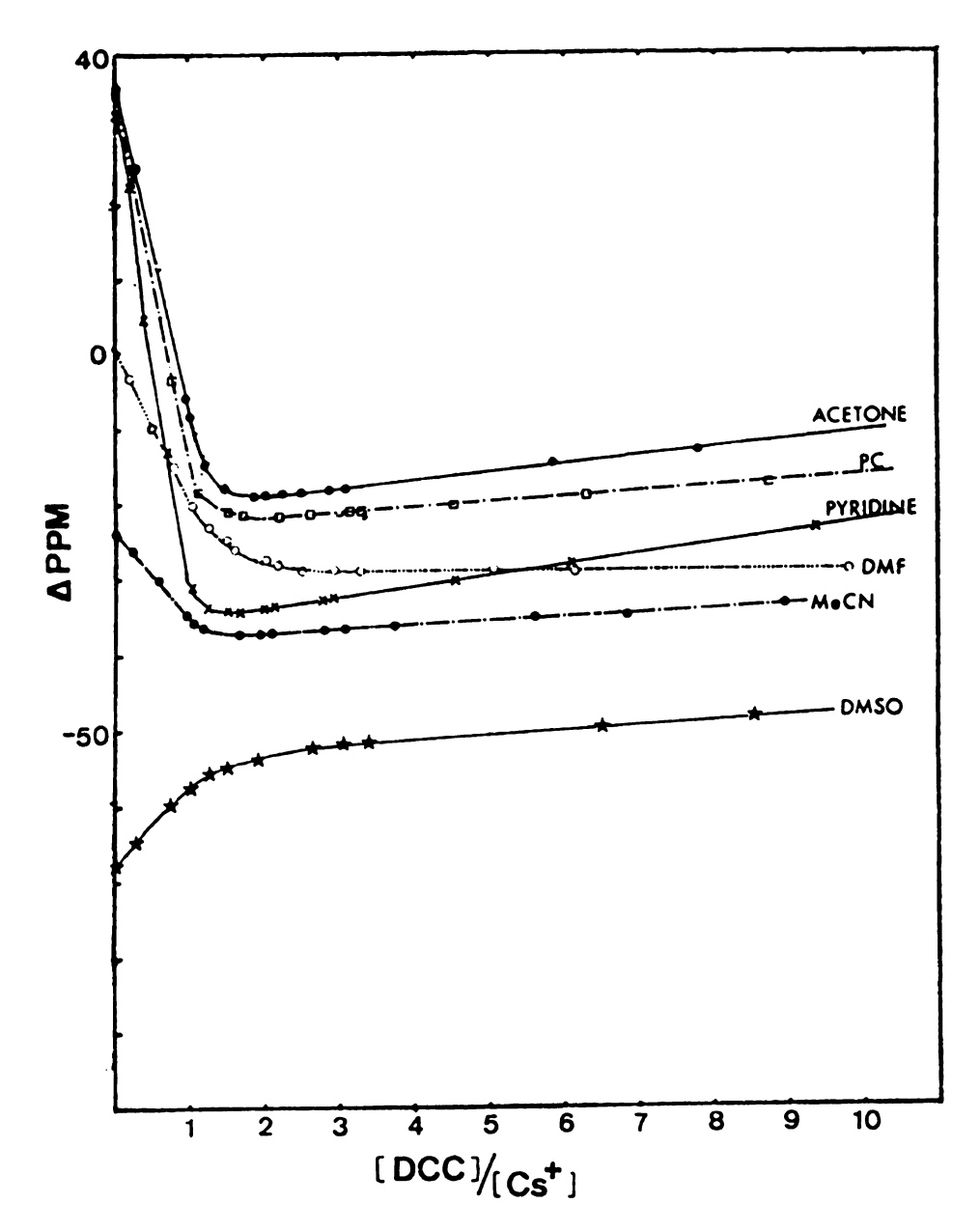


Figure 16. Chemical shifts of cesium-133 as a function of mole ratio of [DCC]/[Cs $^+$ TPB $^-$] in various solvents. [CsTPB] $_{\rm T}$ = 0.01M.

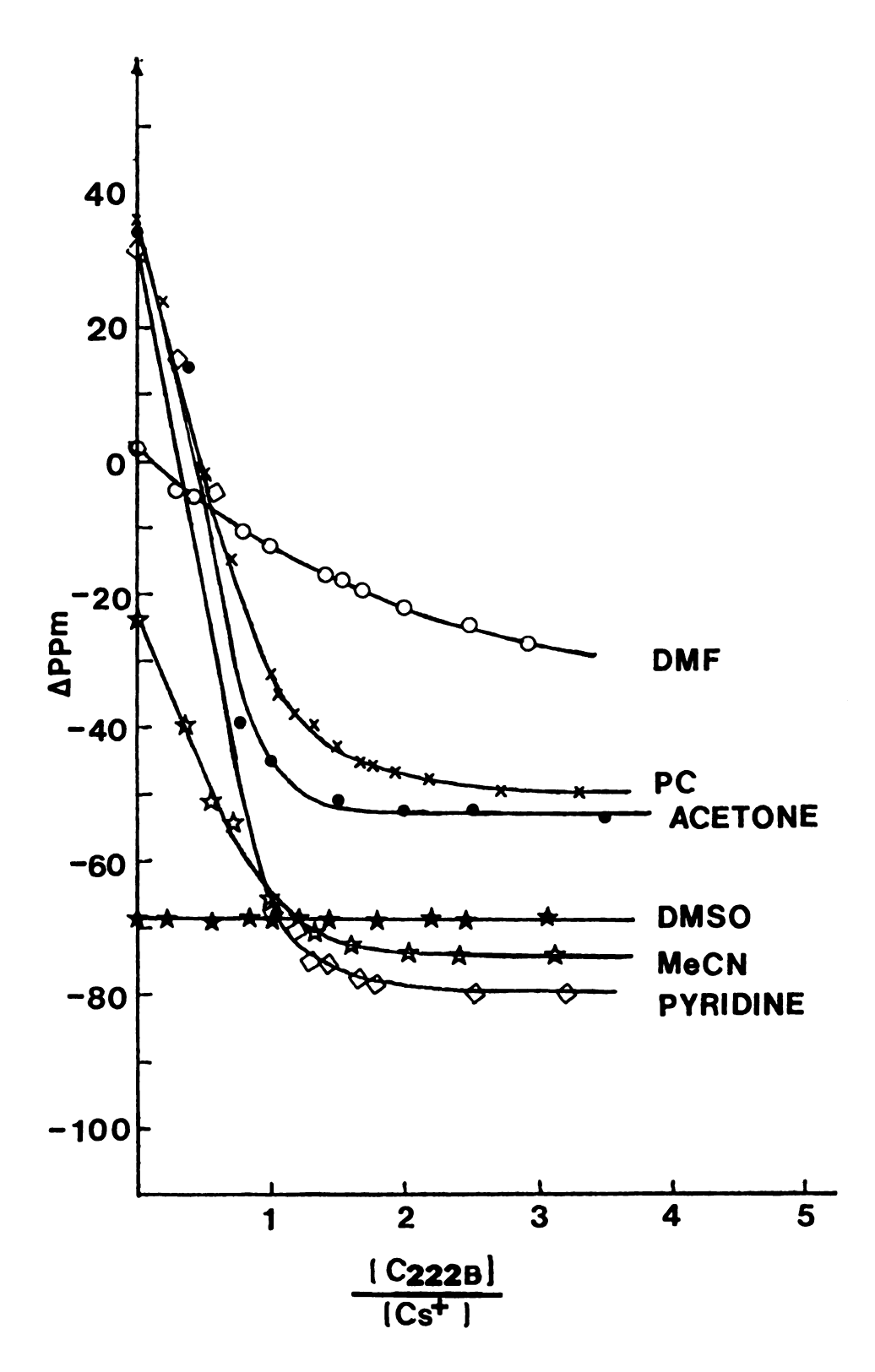


Figure 17. Chemical shifts of cesium-133 as a function of mole ratio of [C222B]/[Cs+TPB-] in various solvents. [CsTPB] $_{\rm T}$ = 0.01M.

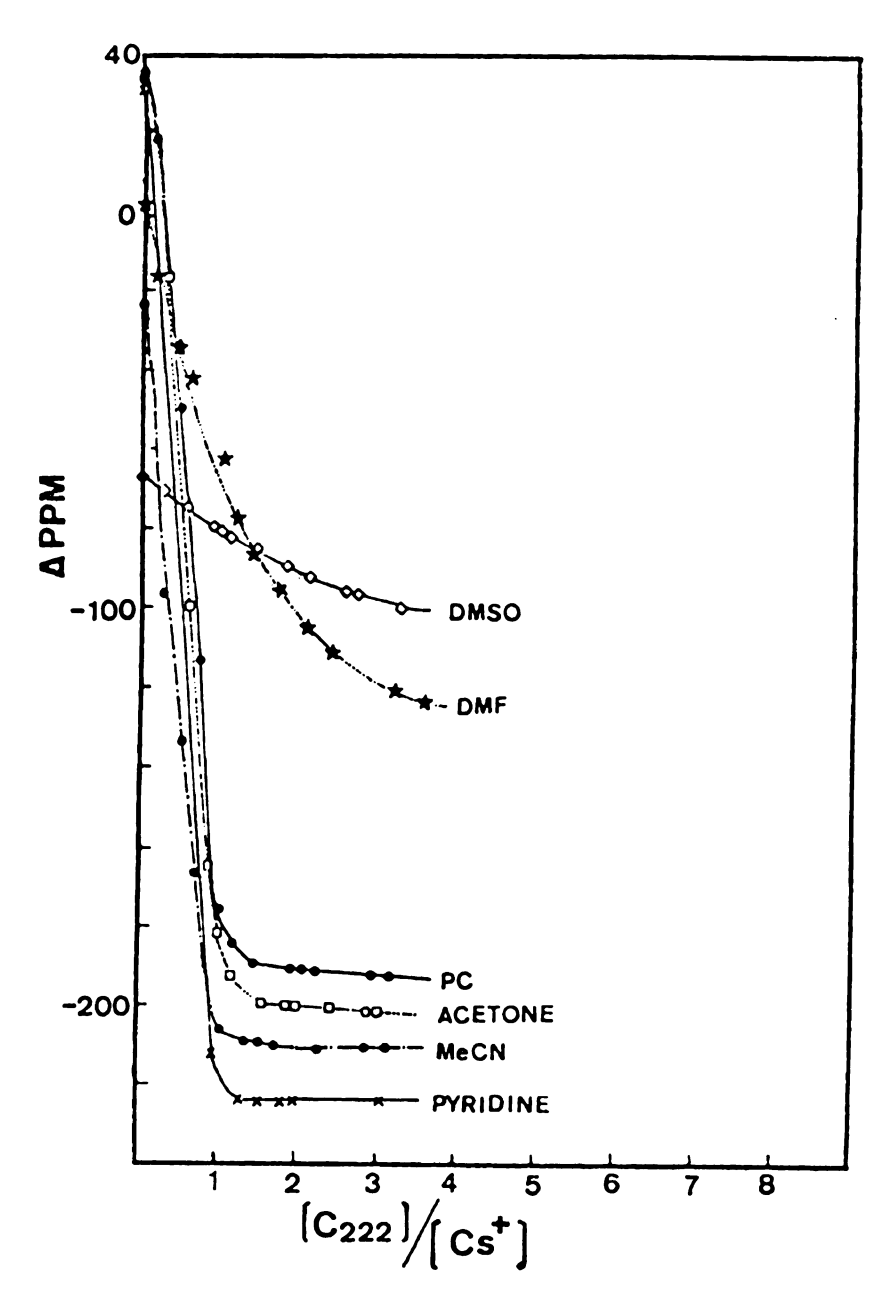


Figure 18. Chemical shifts of cesium-133 as a function of mole ratio of [C222B]/[Cs $^+$ TPB $^-$] in various solvents. [CsTPB] $_T$ = 0.01M.

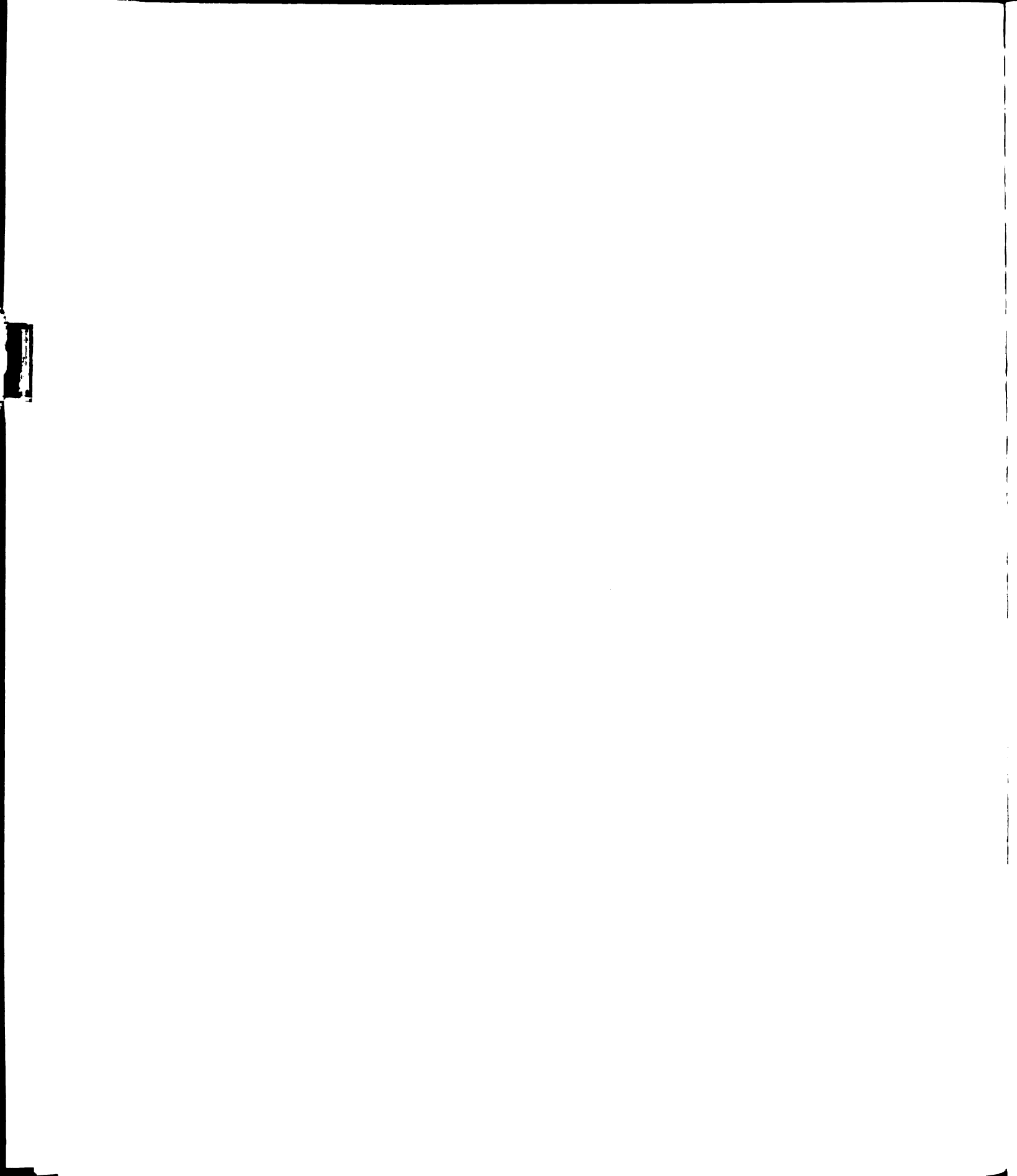


Table 15. Formation Constants of CsTPB [0.01 M] with Ligands in Various Solvents (25°C).

	18C6	рвс	DCC (Mixture)	C222	C222B
Pyridine	$K_1 > 10^7$ $K_2 = 71\pm 1$	(7.±2)×10 ³ (2.3±0.2)×10 ²	>10 ⁵ (a)	>105	(5.7±0.8)×10 ³
Propylene Carbonate	$K_1 = (1.5 \pm 0.6) \times 10^5$ $K_2 = 8 \pm 2$	~10 ³ (a)	~10 ⁴ (a)	(10±1)×10 ³	(14.8±0.6)×10 ²
Acetone	$K_1 > 10^5$ $K_2 = 34.0 \pm 0.5$	>10 ³ (a)	>104 (a)	(10.8±0.8)×10 ³	(3.5±0.7)×10 ³
DMF	$K_1 = (9 \pm 3) \times 10^3$ $K_2 = 2.44 \pm 0.05$	30±3 (b)	(2.4±0.9)×10 ³	(1.5±0.1)×10 ²	50±3
DMSO	$K_1 = (1.1\pm0.1)\times10^3$ $K_2 = 1\pm0.4$	22±3(b)	(1.6±0.1)×10 ²	27±3	0
MeCN	$K_1 > 10^5$ $K_2 = 4.4 \pm 0.3$	35±2 (b)	>10 ⁴ (a)	(4±1)×10 ⁴	(3.6±0.2)×10 ³

Complexation is observed but not enough data are available to determine K_2 . 3

It is probable that both 1:1 and 2:1 complexes form with DBC in these solvents. However, the shapes of the curves do not permit separation into two steps and the value given is calculated as if only the 1:1 complex formed. **Q**

simulation the initial estimate may be used to mimic the behavior of the system. For this reason, whenever the K value was too high to fit an experimental curve, the simulation technique was used to get a rough estimate of the association constant. However, such estimate cannot be taken very seriously.

(i) COMPLEXATION REACTIONS WITH CROWNS

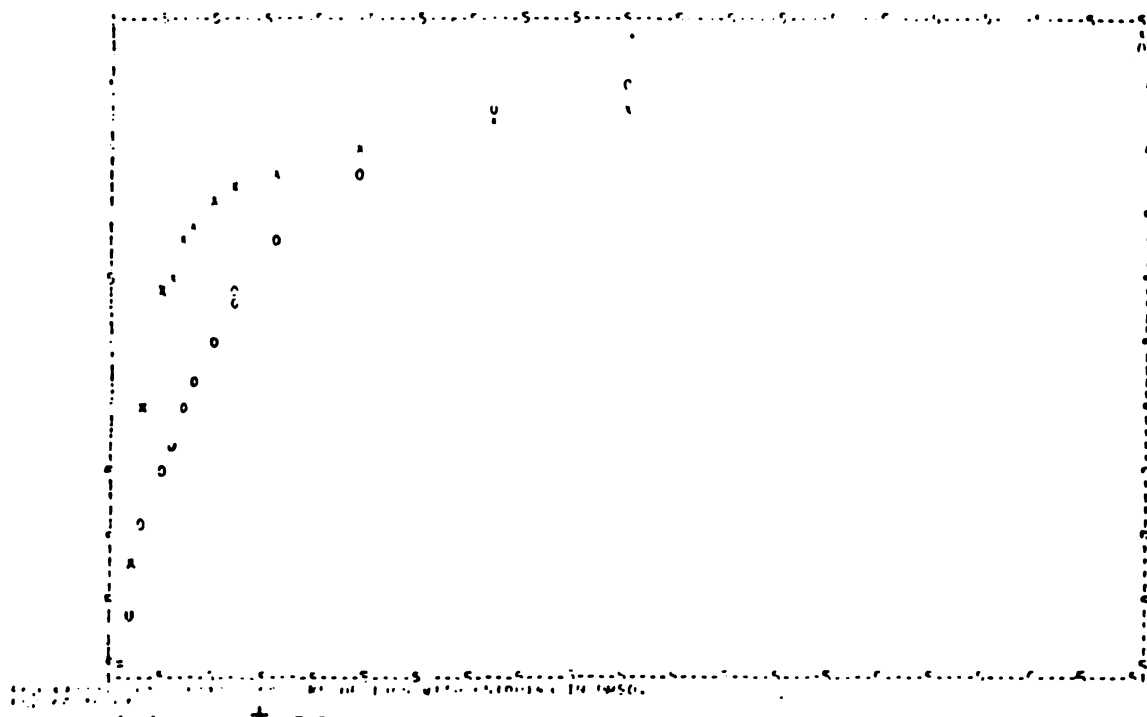
The variation of the Cs-133 chemical shift as a function of the 18C6/Cs⁺ mole ratio in different solvents is shown in Figure 14. It is immediately obvious that the solvent plays an extremely important role in the complexation process. The behavior in pyridine, acetone, and propylene carbonate solutions is especially interesting in that the Cs-133 resonance shifts linearly downfield until a 1:1 ligand/Cs⁺ mole ratio is reached and then shifts upfield as the concentration of ligand is further increased. The data seem to indicate a two-step reaction. First the formation of a stable 1:1 complex and then the addition of a second molecule of the ligand to form a "sandwich" complex (13).

In DMSO and MeCN solutions the Cs-133 resonance shifts only upfield with some indication of a weak "break" at the 1:1 mole ratio. The resonance continues to shift upfield even after the formation of a 1:1 complex but

there is no clear-cut evidence of a 2:1 complex. However, least-squares fitting of the data (Figure 19,20) based on the formation of only the one-to-one complex gave a large standard deviation and the fit was poor especially at lower concentrations of ligand. Therefore, a model was used which assumed that both one-to-one and two-to-one complexes are formed. The fit was much better as shown in Figure 19.

Cesium tetraphenylborate complexes with 18C6 in MeCN showed similar features to those in DMSO. Once again, attempts to fit the data, as shown in Figure 20 by assuming formation of only the 1:1 complex gives large deviations of the calculated curve from the experimental one. An attempt was made to include the 2:1 complex in the calculation. This resulted in a reasonably good fit of the data but a big standard deviation for the first formation constants (K_1) . This big standard deviation is mainly caused by the large value of K_1 .

When 18C6 forms a complex with CsTPB in pyridine solution, the change in direction at 1:1 mole ratio clearly indicates the formation of a second complex. However, the variation of the chemical shift with mole ratio does not clearly indicate the stoichiometry of the subsequent complexation. In order to discriminate a sandwich complex (2:1) from a club sandwich complex (3:2), a study of the temperature dependence of the chemical shift was carried out. From the data listed in Table 16 and plotted in



(a) Cs⁺·18C6 Model.

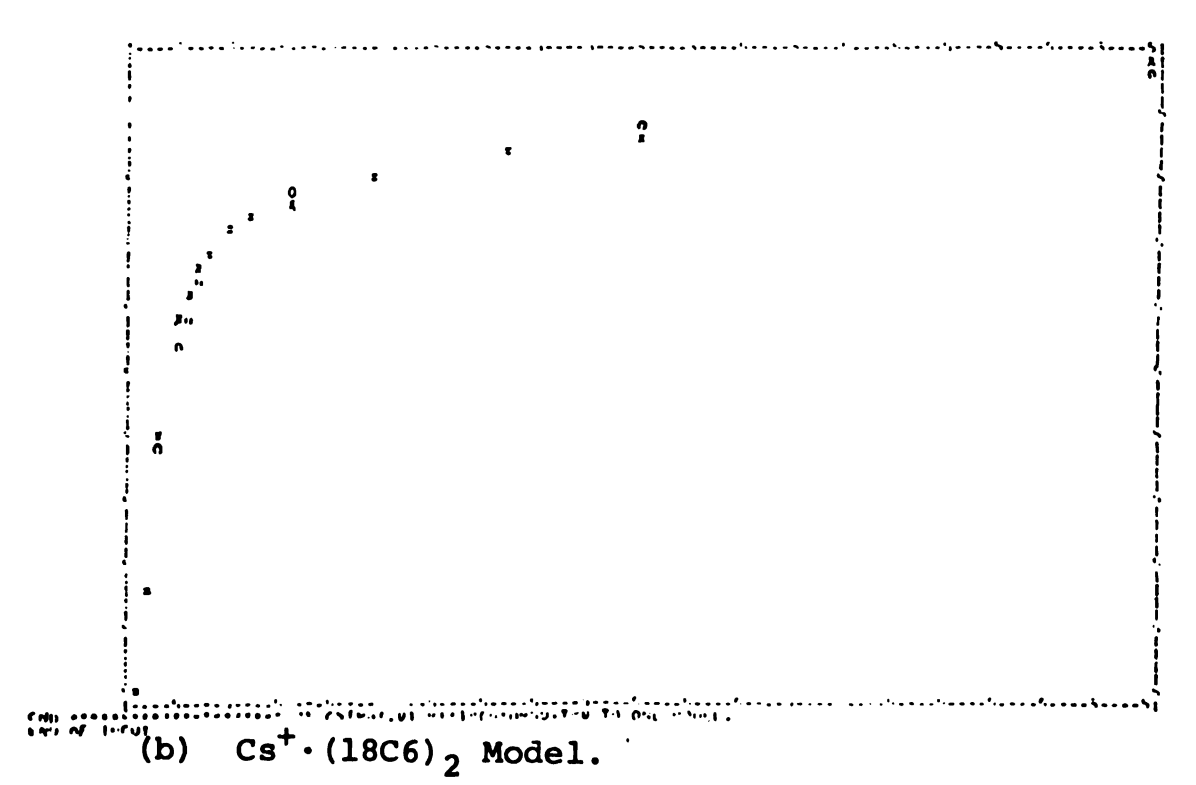
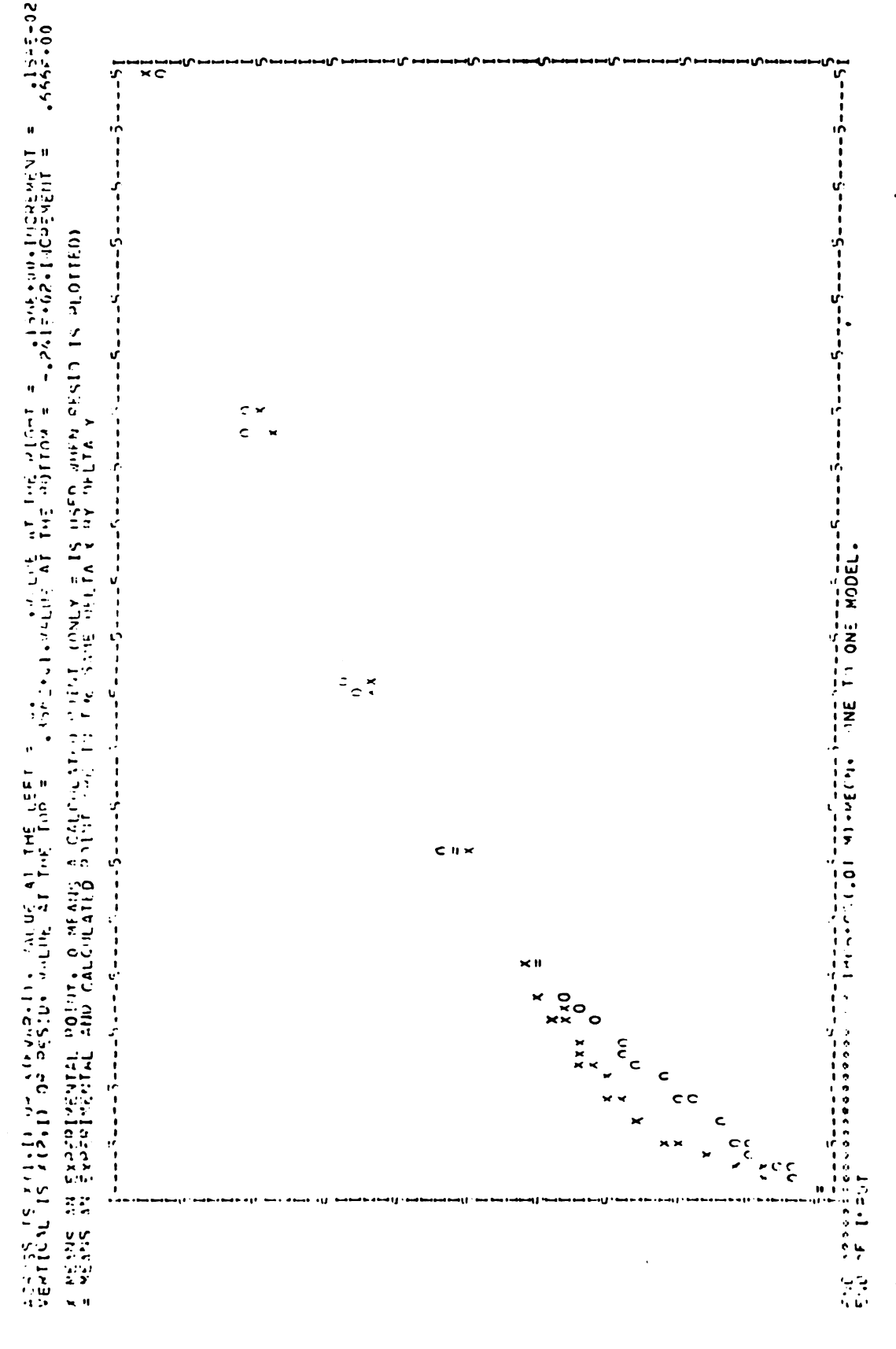


Figure 19. Nonlinear curve fitting of chemical shifts vs. [18C6]/[Cs+TPB-] in DMSO.



Nonlinear curve fitting of chemical shifts vs. [18C6]/[Cs⁺TPB⁻] in MeCN. Figure 20.

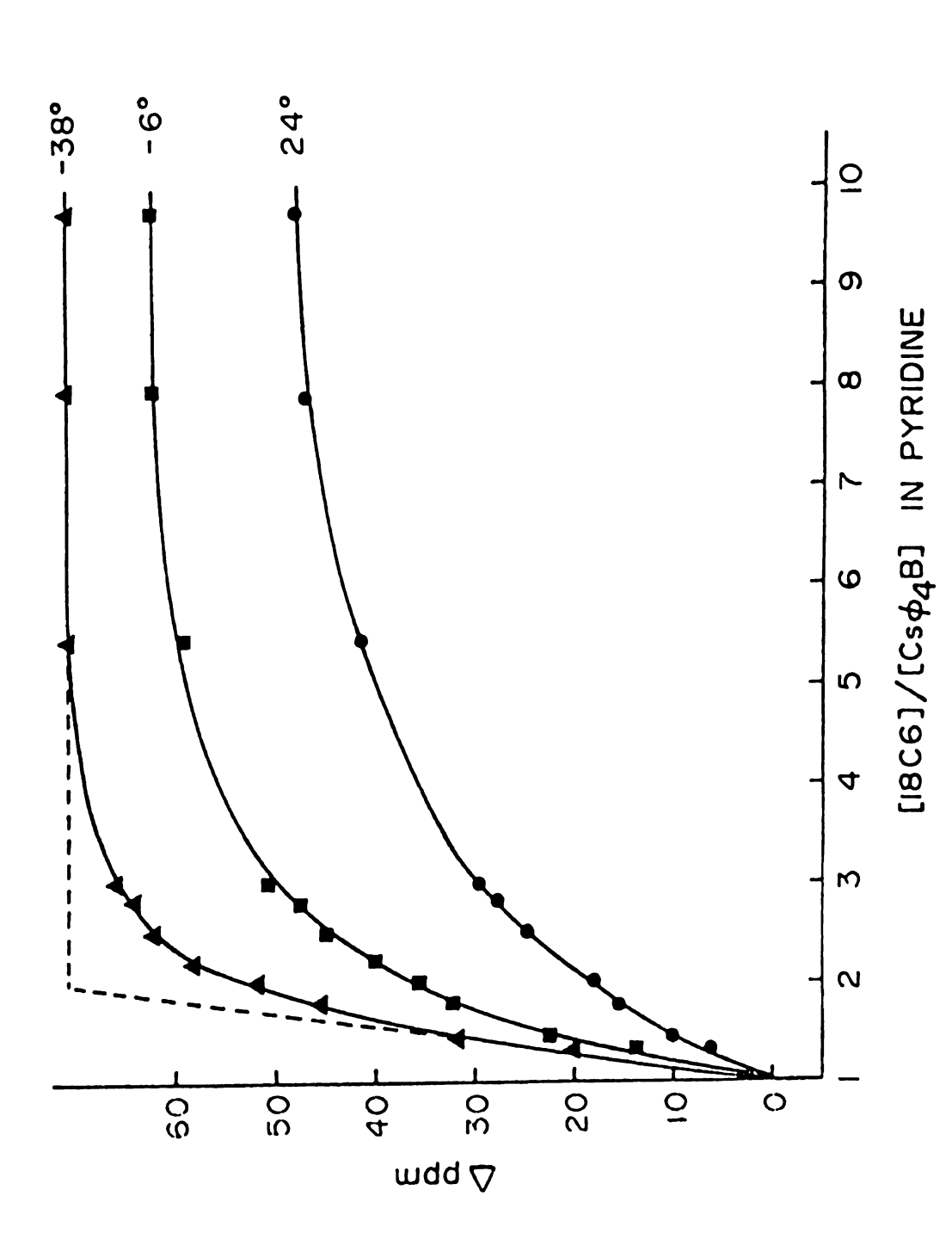
Table 16. Mole Ratio Study of 18C6 Complexes with CsTPB in Pyridine at 24°C, -6°C, -38°C.

	Δ ppm (<u>v</u>	s. 1:1 Complex)	
[18C6] [Cs ⁺]	24°C	-6°C	-38°C
1.00	0	0	0
1.34	6.36	13.80	20.01
1.45	10.24	22.49	31.95
1.77	15.51	32.41	45.78
2.00	18.15	35.52	51.83
2.20	21.71	40.01	58.19
2.50	24.66	29.77	61.91
2.83	27.61	32.25	64.24
3.00	29.62	34.88	65.94
5.44	41.41	44.33	69.98
7.90	46.99	47.29	71.06
9.75	48.85	47.60	71.22

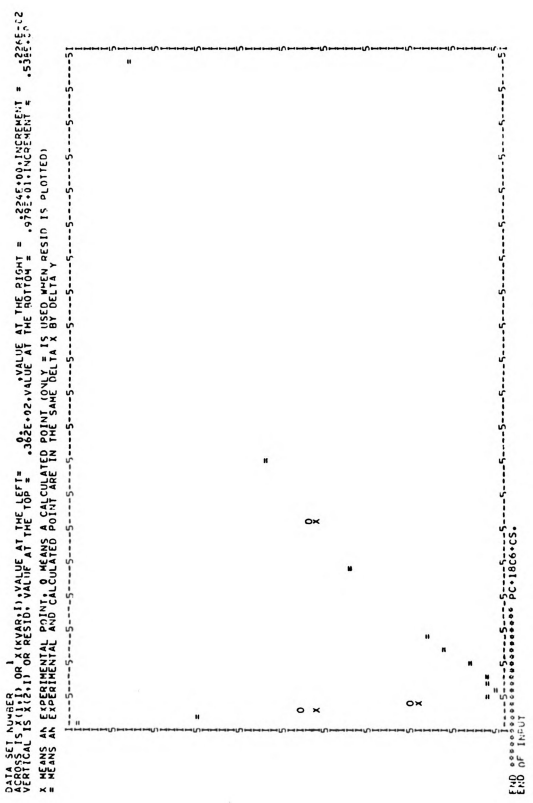
Figure 21, it is clear that the subsequent reaction forms a sandwich complex. The mole ratio plots in acetone, PC and DMF also exhibit a dip at a mole ratio of one. fore, by analogy, sandwich complex formation is postulated. However, one interesting feature in the mole ratio-chemical shift plots is different. In pyridine solutions the plot exhibits a sharp change in direction and a discontinuous The other three solvents give a somewhat different shape. These differences reflect different values of K1 and K_2 . In pyridine, K_1 is much larger than K_2 but the latter is also large. Therefore, a sandwich complex starts to form only when most of the Cs + ions have already formed the Cs⁺·18C6 complex. This condition gives a sharp discontinuity in the mole ratio-chemical shift plot at the 1:1 ligand/Cs $^+$ mole ratio. For the other solvents, K_1 is not as large as in pyridine and K_2 is also smaller. Therefore, a "rounded-off" dip is produced, because at mole ratios around unity both complexation reactions (<u>i.e.</u>, formation of $Cs^+ \cdot 18C6$ and $Cs^+ \cdot (18C6)_2$) are taking place. A typical fit of the data obtained in PC at 25°C with an equation which assumes a two step reaction with shifts in the opposite direction is shown in Figure 22.

It is also important that, in spite of the great differences in the shape of the curves, the limiting chemical shift of Cs⁺·(18C6)₂ complexes as determined by the KINFIT program (Table 17) seem to be independent of solvent.

This contrasts with the large solvent dependence of the



A study of cesium-133 chemical shift vs. mole ratio ([18C6]/Cs⁺TPB at 24°, -6°, -38°C in pyridine. [CsTPB]_T = 0.01 M. Figure 21.



A typical fitting of a two-step reaction. Figure 22.

Table 17. Limiting Chemical Shifts in Various Solvents.

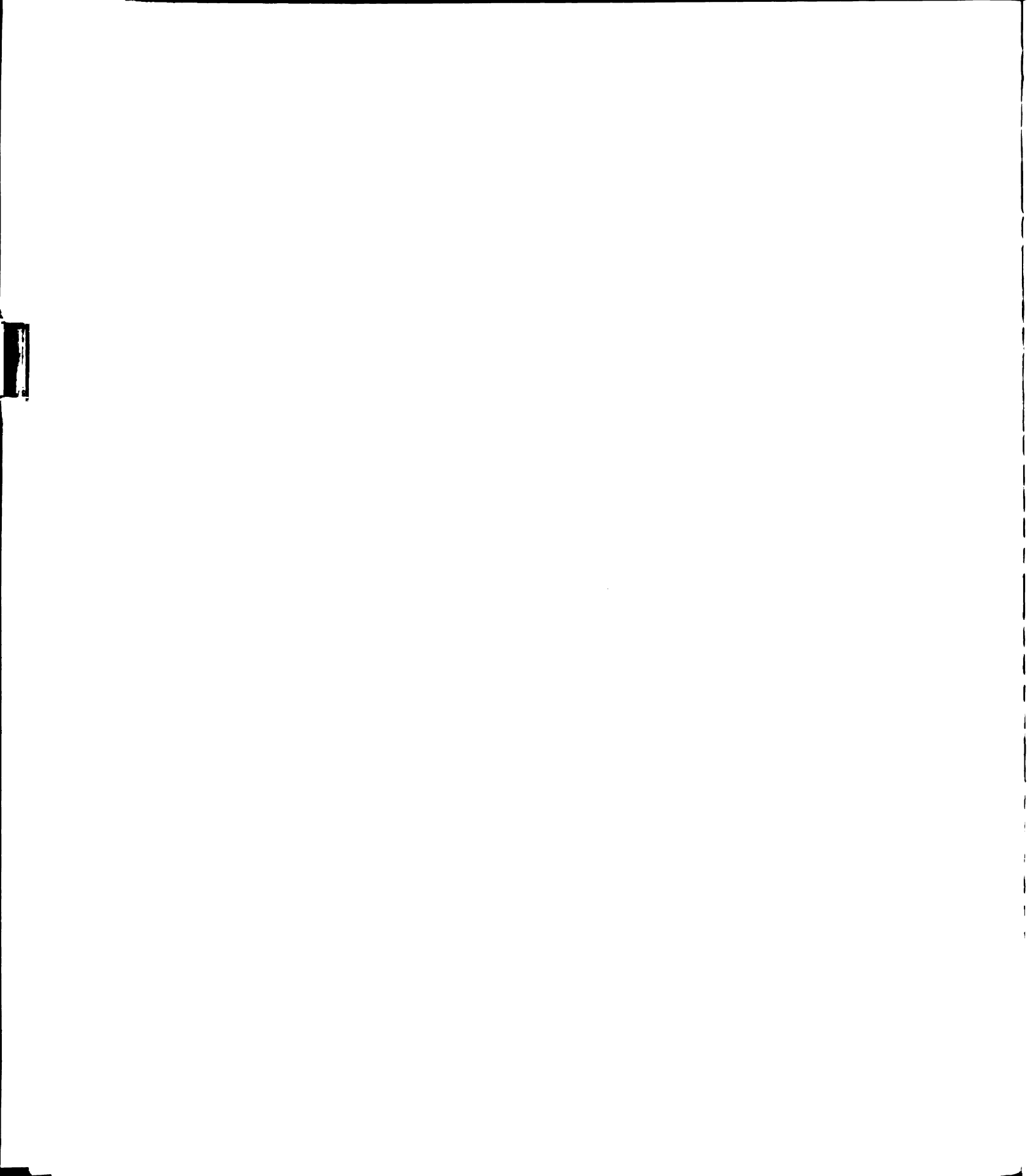
Solvent	Cs ⁺	Cs ⁺ • (18C6)	Cs ⁺ (18C6) ₂
PC	36.45	8.1±0.2	46.5±0.9
Acetone	35.83	6.35	47. ±9.
Pyridine	32.38	-9.35	48.2±0.2
DMSO	-67.96	-23.7±0.4	49. ±24.
DMF	0.81	-3.37±0.05	48.2±0.7

chemical shifts of the free cations and of the one-to-one complexes. This observation indicates that the primary solvation shell of the Cs⁺ ion is more or less completely displaced by the ligand when the two-to-one complex is formed.

The attachment of two benzo groups on 18C6 to form DBC, was expected to result in weaker complexes. This aromatic group decreases the basicity of the oxygen atoms (10) and also decreases the 0...0 distance which causes a decrease in cavity size (50). A mole-ratio study of DBC complexes with CsTPB in six solvents was made. The results showed some similarity to the case of 18C6; i.e., in pyridine, propylene carbonate and acetone we also observed 2:1 complex formation, while in DMF there was no change of direction, but only a continuous shift to higher fields which continued up to the solubility limit of DBC. In

MeCN and DMSO solutions, although the shift is in the same direction as in the case of 18C6, the curvature of the plot is much smaller. This shows that the complexation is weaker. An investigation of the half-height linewidth (Δν₁) at room temperature shows that DBC also forms more labile complexes with Cs⁺ than does 18C6. In the exchange region, i.e., when the mole ratio of ligand to total Cs⁺ is approximately 0.5, the half-height linewidth for 18C6 in pyridine (36.59 Hz) is much larger than it is with DBC (<1Hz). This phenomenon indicates that the 18C6 complex is less labile than the DBC complex and has a slower exchange rate at a given temperature. Even though it is hazardous to draw conclusions about thermodynamics from rate phenomena, we expect the more labile complex in these systems to be also the more weakly bound.

It was of interest to test the effect of a complexing agent which does not have aromaticity; therefore, dicyclohexyl-18C6 (DCC) was used. This ligand has five isomers of which only two have been isolated (termed isomers A and B). A mixture of these two isomers was used in this study. Figure 16 shows that some features of the plot of chemical shift vs. the mole ratio (DCC)/(Cs⁺) are different from those with 18C6 and DBC. There is no clear-cut change in direction (or reflection point) at a mole ratio of one-to-one as found for 18C6 and DBC in pyridine, propylene carbonate, and acetone solutions. The extent of the downfield (paramagnetic) shift is much greater for DCC in DMF



and the direction of the shift in the case of MeCN is also changed. This phenomenon may be caused by the higher rigidity of the DCC framework which results in a larger overlap of the lone pair electrons of oxygen with the cesium ion. This will introduce more orbital angular momentum, and thus more paramagnetic shift.

All three crown complexing agents form 2:1 complexes in PC, acetone and pyridine. Formation constants were obtained by fitting the appropriate equation to the data with the KINFIT program. The results are listed in Table 15. When the formation constants were too large, lower limits were estimated by simulating the data with KINFIT.

(ii) COMPLEXATION REACTIONS WITH CRYPTANDS.

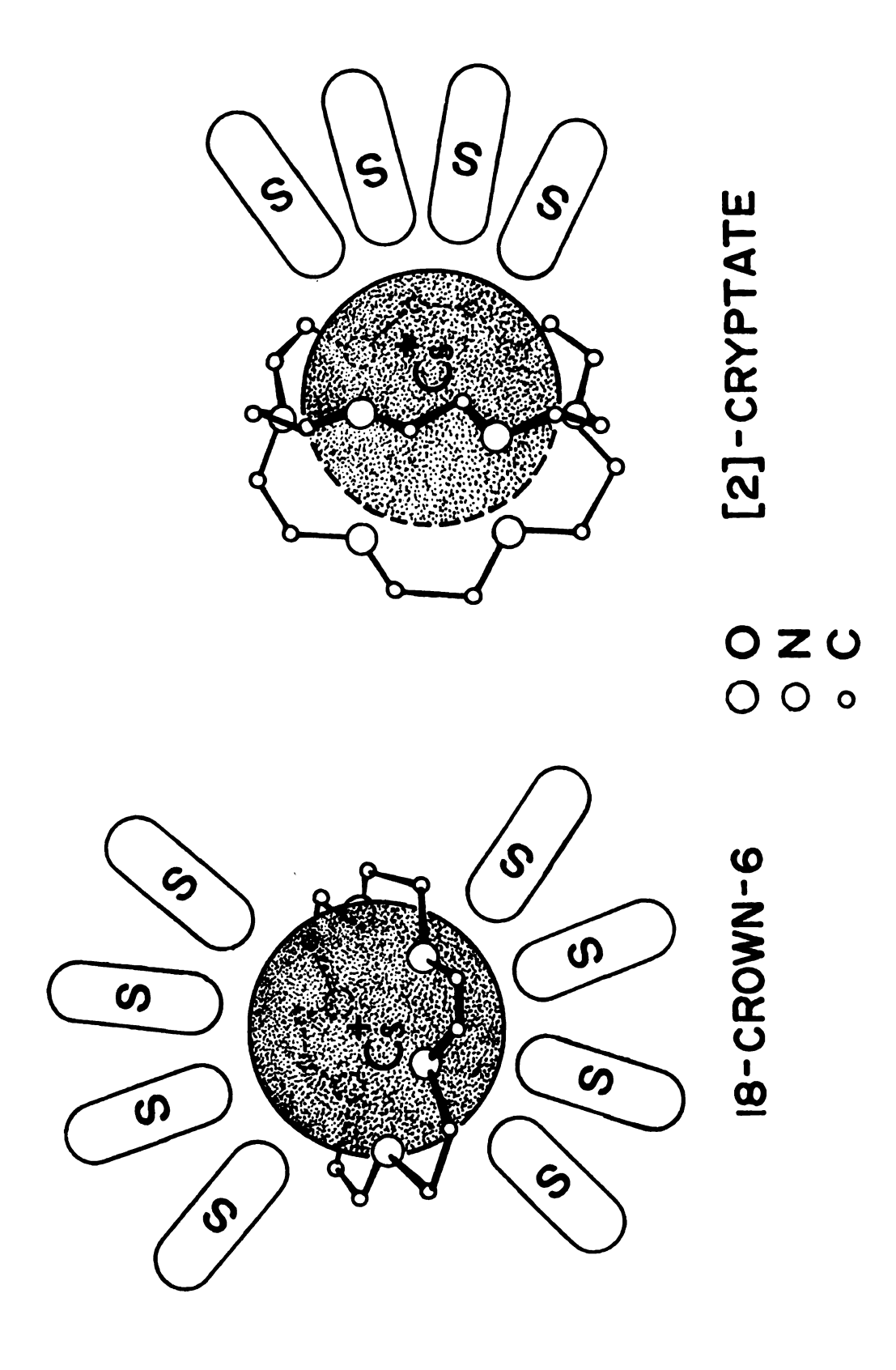
Cryptands are tridimensional ligands which can completely enclose a metal ion within the cavity. This property would make the complexation of cesium ion by cryptands stronger than that with crowns, except that the cation may be too large to fit into the cavity easily. The change of the chemical shift of Cs⁺ with the concentration of cryptand is in the paramagnetic direction. The magnitude of the shift for Cs⁺ complexes with cryptands is much larger than with crowns. This phenomenon, which is especially pronounced with C222, indicates that cryptands can perturb the Cs⁺ ion more; probably by increasing the overlap because of short range repulsions and introduce a larger orbital

angular momentum. With an ortho-benzo group in place of a -CH₂-CH₂- group in one of the ether chains, C222B not only has a decrease in the $0 \cdots 0$ distance, and more rigidity of the ligand but also a decrease in the basicity of the oxygen atoms on that branch. Therefore C222B should have less ability to "swallow" the cesium ion into its cavity which should lead to a (thermodynamically) weaker complex than with C222. This speculation is confirmed by the thermodynamics of complexation. The kinetics of exchange also indicates a more labile complex. At room temperature and (ligand)/(Cs⁺)=0.5, the resonance line of Cs⁺ with C222 in pyridine was so broad that the signal is barely observable ($\Delta v_{\text{L}} > 400 \text{ Hz}$), while for C222B, Δv_{L} in this region is approximately 15 Hz (Table 18). Another interesting fact is that in DMSO with C222B, there is no chemical shift variation as more ligand is added, while with C222, weak complexation is observed. On the other hand, all crown ligands form relatively strong complexes in DMSO. Perhaps this is because the solvent can still play an important role when crown complexes are formed. When Cs + is complexed by cryptand but before it has been completely surrounded by the cage, a strong competition between ligand complexation and solvation may be taking place as illustrated in Figure 23. Dimethylsulfoxide is a good donor solvent, so that a weaker complexing agent such as C222B cannot compete for Cs⁺ and no chemical shift variation results as the mole ratio is increased. However, in the

Table 18. Half-height Linewidth $(\Delta v_{\frac{1}{2}} \text{ Hz})^*$ of Cs^+ -Ligand Complexes at 24°C.

Ligand	Ligand/Cs ⁺	Δν _λ (Hz)
DCC	≈ 0. 5	69.65
DBC	≈ 0. 5	1
C222	≈0.5	>400 Hz
C222B	≈ 0. 5	14.47
18C6	≈0 . 5	36.59
	0	1.00
	0.39	16.17
	1.00	2.22
	1.5	≲1.00
	2.0	<1.00
	2.5	<1.00

^{*} $\Delta v_{\frac{1}{2}} = (v_{\frac{1}{2}})_{\text{sample}} - (v_{\frac{1}{2}})_{\text{ref}}.$



The interaction of Solvent Molecules With Complexed Cesium Ion. Figure 23.

case of C222, a stronger complexing agent, the Cs⁺ can be complexed more readily so that there is some chemical shift variation with ligand concentration. Because of the delicate balance between solvation and complexation, it seems that cryptands can serve as good ligands for the investigation of solvent effects and ligand effects on the complexation reaction.

The expression of Das (Equation I.15) for the chemical shift in an electrolyte solution, indicates that the extent of the paramagnetic shift is determined by the overlap integrals of ion-solvent and ion-ion interactions. idea, together with considerations of size and complexing ability can be used to explain the direction and magnitude of the shift which occurs upon complexation as well as solvent effects in electrolytic solutions. When a complexation reaction occurs in an electrolyte solution, there is competition between the donating ability of the solvent molecules, the counterions, and the donating sites of the complexing agent. This competition will have two effects on the variation of the chemical shift with the concentration of the complexing agent. For example, Figure 24 shows graphs of the chemical shift (in ppm) vs the mole ratio in DMF for all five ligands. This example clearly shows the two features referred to above. The "sharpness" of the curvature tells how easily the complexing agent can compete with the solvent, leading to displacement of the solvent

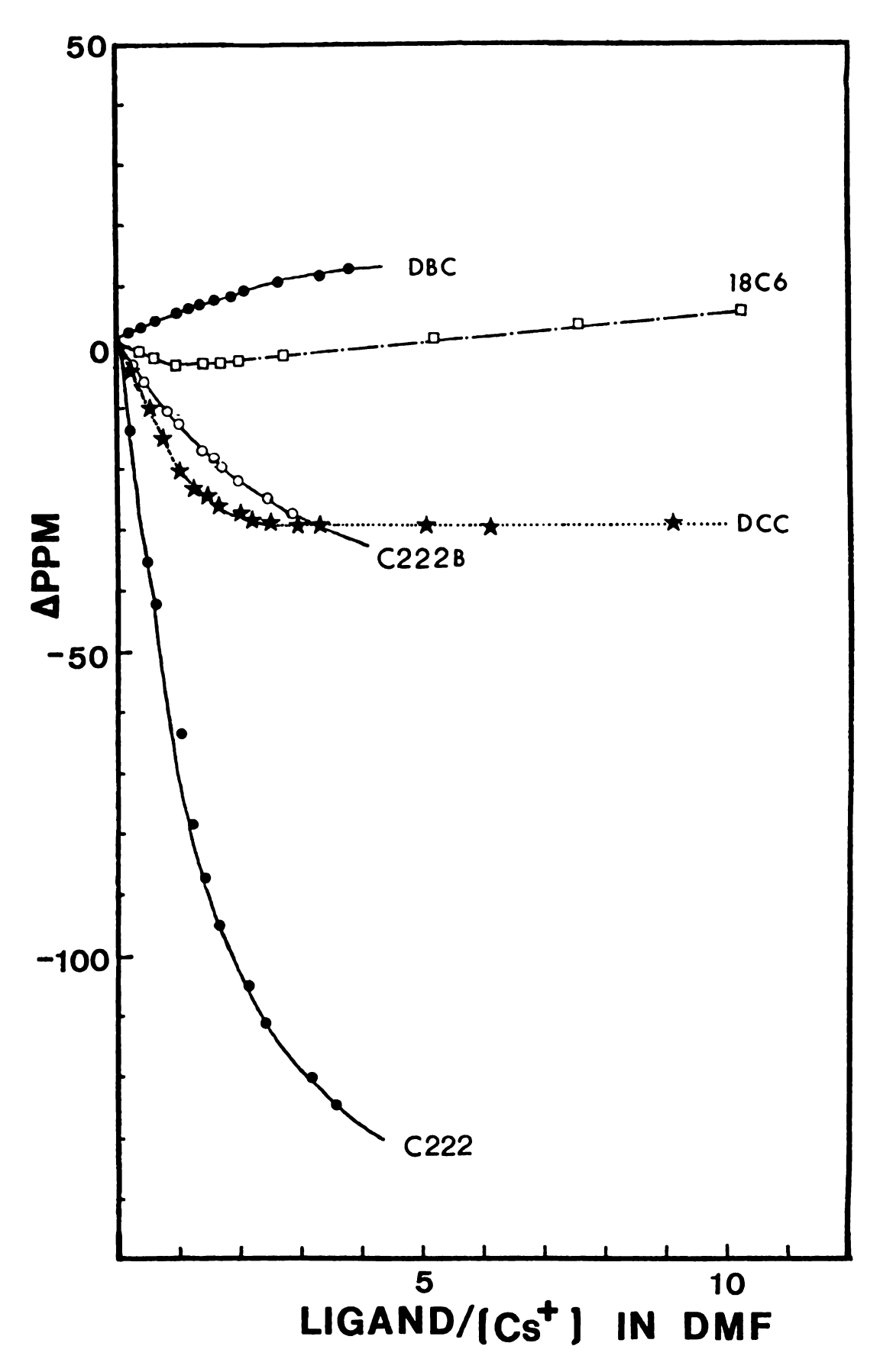


Figure 24, Mole ratio-cesium-133 Chemical Shift Study for Various Ligands in DMF.

shell and the counter ion. That is, the curvature gives us thermodynamic information. However, the direction of the chemical shift variation and the ultimate extent of the shift depends upon how much the donating electron pairs of the complexing agent can perturb the electron cloud of the cation. This perturbation, when greater than that of the solvent, leads to a paramagnetic shift. Dibenzo-18C6 appears to have weaker interaction of the lone pairs with the cesium ion than is the case for the other crowns, probably because of its rigidity and lower basicity of the oxygen atoms. In DMF solution, the chemical shift moves upfield with an increase in the mole ratio (that is, as the concentration of DBC increases). This phenomenon implies that the donating ability of the lone-pairs on oxygen in DBC is weaker than those of DMF. However it should be noted that repulsive interactions at short range contribute to the shift so that one cannot equate the magnitude of the shift only with an attractive interaction. Indeed, when the interaction is "forced" as when Cs is inside of a cavity which is too small, the repulsive interactions can lead to large paramagnetic shifts. event, the chemical shift variation indicates that complexation is taking place.

In the case of 18C6 which shows a change in direction of the shift at the 1:1 mole ratio, the upfield shift shows that the net contribution of the lone pair electrons of the 12 binding sites in a 2:1 complex is smaller than

that of the 6 binding sites of the 1:1 complex. This observation probably results from a large decrease in the individual overlap integrals in the 2:1 complex as the short-range repulsions are relaxed. The half height linewidth (Table 18) also decreases when the sandwich complex is formed. This phenomenon would be expected if the 12 oxygen atoms were symmetrically distributed around the cesium ion.

For DCC, the aliphatic cyclic substituent results in a better donating environment (i.e., closer oxygen-Cs⁺ contacts) as manifested by the chemical shift-mole ratio plot. Among all three crowns, DCC has the largest paramagnetic shift even though it does not form the strongest complex. The second formation constant of DCC complexes with Cs⁺ is the smallest of all three crowns in a given solvent. Both cryptands, with two more binding sites, and probably much closer oxygen-Cs⁺ contacts because of steric limitations can perturb the Cs⁺ electron cloud more and, therefore, introduce a larger paramagnetic shift than any of the crown ligands. However, probably because of the rigidity and size of the tridimensional ligands the stoichiometry of the complexes stops at 1:1.

A close examination of the K values for a given ligand shows clearly that the solvent plays an important role in the complexation. With crown type ligands, probably because the complexed (in 1:1 complexes) and the free cation both interact with the solvent appreciably, the

complexation constant is not as sensitive to solvent as with the cryptands. Figure 23 shows schematically how complexation and solvation might take place on opposite sides of the cation which could make this complexation system more affected by the solvent. Therefore, C222 was chosen to examine the relationship between solvent properties and the complexation equilibrium. The values of log K for C222 obtained in six solvents and in H20 and MeOH from another source (50) are listed in Table 19. Pyridine has the highest donor number but the lowest dielectric constant of all the solvents listed and it forms the strongest complexes. In PC, a solvent with the highest dielectric constant and the next to lowest donor number, an intermediate value log K is obtained. When water, DMF and DMSO are all solvents of high donor ability and high dielectric constant and all have small values of log These phenomena follow exactly the behavior found for ion pair formation. This fact may indicate that for a weakly solvated cation such as Cs⁺, the interactions between cations, anions, ligand molecules and solvent molecules depend on both the donor ability and the bulk dielectric constant of the solvent. The size and geometry of the solvent molecules may, of course, also play a role.

Log K Values of Cesium Salts with Ligands in Various Solvents (25°C). Table 19.

			Joq		
	1806	DBC	(Mixture)	C222	C222B
Pyridine	(1) > 7	(1) 3.85	(1) > 5	>4.6	3.76
	(2) 1.853	(2) 2.35	(2)*1~2		
Propylene	(1) 4.18	(1) ~3	(1) ~4	3.97	3.17
Carbonate	(2) 0.91	(2) *<1	(2) * 1		
Acetone	(1) > 5	(1) > 3	(1) > 4	,	,
	(2) 1.53	(2) *1~2	(2) ~1	4.03	3.54
DMF	(1) 3.97	(+) **,	•	;	
	(2) 0.39	T.48	3.38	2.16	1.70
DMSO	(1) 3.04	1.34(+)	2.20	1.43	N.A.
	(2) -0.004				
MeC::	(1) >5	1.54(+)	(1) *>4	4.57	3.55
	(2) >0.47		4.26 (40) (2) *<1		
Меон	4.62(17)	(1) 3.55 ⁽¹⁷⁾ (2) 2.92 ⁽¹⁷⁾	3.85 (40)	4.4 (50)	3.2 (50)
н ₂ о	0.8(17)	;	;	-0.7 (50)	-
	0.86				

Estimate values.

[†]It is probable that both 1:1 and 2:1 complexes form with DBC in these solvents. However, the shapes of the curves do not permit separation into two steps and the value given is calculated as if only the 1:1 complex formed.

- IV. TEMPERATURE DEPENDENCE OF THE CHEMICAL SHIFT AND ITS
 RELATIONSHIP TO THE THERMODYNAMICS OF COMPLEXATION
 REACTIONS.
 - (A) CESIUM TETRAPHENYLBORATE COMPLEXES WITH 18C6 IN PYRIDINE.

In this section, a detailed study of the two step reaction of the 18C6 complexed with Cs⁺ ion in pyridine will be considered. The possible equilibria for this system were first proposed as follows:

When the mole ratio of (18C6) to (Cs⁺) is zero, ion pair formation can occur:

$$Cs^{+} + TPB^{-} \stackrel{K_{ip}}{\neq} Cs^{+} \cdot TPB^{-}$$
 (III.3)

The observed chemical shift can be expressed as

$$\delta_{\text{obs}} = \delta_{\text{ip}} X_{\text{ip}} + \delta_{\text{F}} X_{\text{F}}$$
 (III.4)

When 18C6 is added to the cesium tetraphenylborate solution the possible reactions may be expressed as

In order to see if the above reaction scheme can be simplified, two studies of the concentration dependence of the chemical shift were carried out. The data obtained for reactions III.3 and III.5 are shown in Table 20 and Figure 25. It can be seen that the salt solution shows substantial ion-pairing ($K_{ip} = (3.7 \pm 0.3) \times 10^2$ as mentioned in Section III.I) while the 1-to-1 complex of 18C6 with Cs⁺ gives no evidence for contact ion pair formation. That is, $K_{ip}^* \approx 0$, and the above scheme can be reduced to three reactions, i.e.

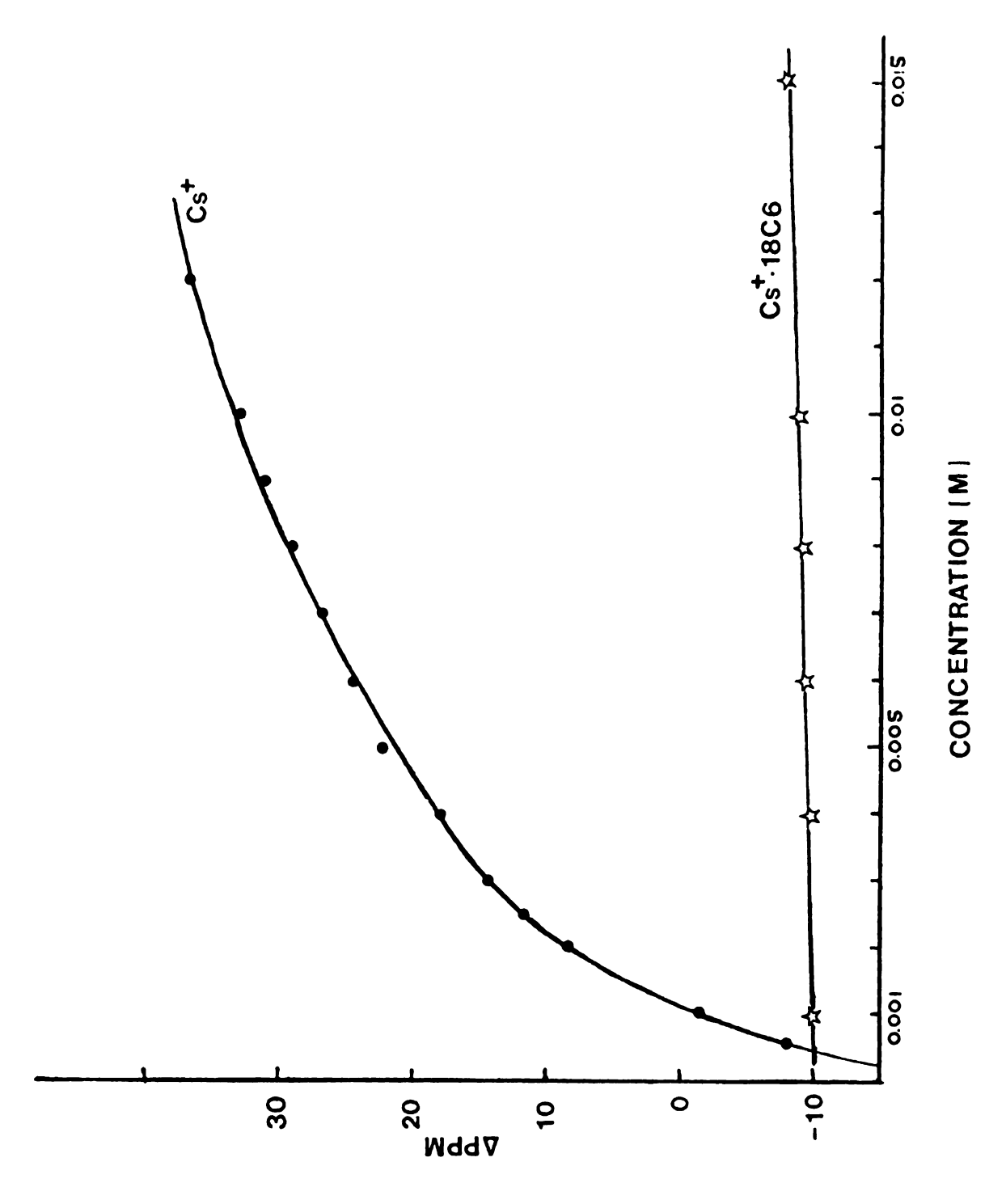
Cs⁺ · (18C6)₂

$$Cs^{+} + TPB^{-} \stackrel{K_{ip}}{\stackrel{?}{\xrightarrow}} Cs^{+} \cdot TPB^{-}$$
 (III.3)

Cs⁺ · (18C6)₂ + TPB⁻

Table 20. Concentration Dependence of the Chemical Shift at 25°C for CsTPB and its 1:1 Complex With 18C6 in Pyridine

Сsф	₽ B	Cso ₄ B +	18C6 (1:1)
Conc.	δconc.	Conc.	δconc.
0.015	37.81		
0.121	37.18	0.020	-7.25
0.010	33.15	0.015	-8.49
0.009	31.29	0.010	-9.58
0.008	29.12	0.008	-9.73
0.007	26.94	0.006	-10.35
0.006	24.46	0.004	-10.97
0.005	22.29	0.001	-10.66
0.004	17.95		
0.003	14.23		
0.0025	11.74		
1.002	8.03		
0.001	1.27		
0.005	-8.25		



Cesium-133 chemical shift variation with the concentration of cesium salts in pyridine. Figure 25.

$$Cs^{+} + 18C6 \stackrel{K}{\leftarrow} Cs^{+} \cdot 18C6$$
 (III.6)

$$Cs^{+} \cdot 18C6 + 18C6 \stackrel{K_{2}}{\leftarrow} Cs^{+} \cdot (18C6)_{2}$$
 (III.7)

The observed chemical shift can be expressed as

$$\delta_{\text{obs}} = \delta_{\text{F}} X_{\text{F}} + \delta_{\text{ip}} X_{\text{ip}} + \delta_{\text{c}_{1}} X_{\text{c}_{1}} + \delta_{\text{c}_{2}} X_{\text{c}_{2}} \qquad (III.8)$$

Where F, ip, c_1 , c_2 denote uncomplexed Cs^+ , ion-paired Cs^+ , $Cs^+ \cdot 18C6$ and $Cs^+ \cdot (18C6)_2$ respectively. By convention, δ_i and X_i denote the chemical shift and the relative mole fraction of Cs^+ in state i respectively.

In order to express the relative mole fractions in terms of overall concentrations the equilibrium constants are used as follows:

Let C denote 18C6, then

$$K_{ip} = [Cs^{+} \cdot TPB^{-}]/[Cs^{+}][TPB^{-}] \qquad (III.9)$$

$$K_1 = [Cs^+ \cdot C]/[Cs^+][C]$$
 (III.10)

$$K_2 = [cs^+ \cdot c_2]/[cs^+ c][c]$$
 (III.11)

Let C_{M}^{T} = total concentration of cesium salt. C_{L}^{T} = total concentration of 18C6.

then

$$C_{M}^{T} = [Cs^{+}] + [Cs^{+} \cdot TPB^{-}] + [CsC_{1}^{+}] + [CsC_{2}^{+}]$$
 (III.12)

$$C_{I_i}^T = [C] + [CsC^+] + 2[CsC_2^+]$$
 (III.13)

Equation III.12 can be further expressed in terms of [Cs⁺] through

$$c_{M}^{T} = [cs^{+}] + \kappa_{ip}[cs^{+}][TPB^{-}] + \kappa_{1}[cs^{+}][c] + \kappa_{1}\kappa_{2}[cs^{+}][c]^{2}$$

$$[cs^{+}] = c_{M}^{T}/\{1 + \kappa_{ip}[TPB^{-}] + \kappa_{1}[c] + \kappa_{1}\kappa_{2}[c]^{2}\} \quad (III.14)$$

Equation III.13 can be rewritten as

$$C_{L}^{T} = [C] + \kappa_{1}[Cs^{+}][C] + 2\kappa_{1}\kappa_{2}[Cs^{+}][C]^{2}$$

$$[C]^{2}\{2\kappa_{1}\kappa_{2}[Cs^{+}]\} + [C]\{1 + \kappa_{1}[Cs^{+}]\} - C_{L}^{T} = 0$$

therefore

$$[C] = \frac{-\{1+K_1[Cs^+]\} + \sqrt{(1+K_1[Cs^+])^2 + 8K_1K_2C_L^T[Cs^+]}}{4K_1K_2[Cs^+]}$$
(III.16)

The negative root was discarded because a negative [C] value has no physical meaning. If [Cs⁺] and [C] can be obtained then

$$X_{c_1} = K_1[Cs^+][C]/C_M^T$$
 $X_{c_2} = K_1K_2[Cs^+][C]^2/C_M^T$
 $X_f = [Cs^+]/C_M^T$
 $X_{ip} = [Cs^+ \cdot TPB^-]/C_M^T = K_{ip}[Cs^+][TPB^-]/C_M^T$

Thus, δ_{obs} could be easily calculated with information about δ_{f} , δ_{ip} , δ_{Cl} and δ_{C2} . However, the expression for $[Cs^{\dagger}]$ contains [C], while that for [C] also contains [Cs+]. In order to solve for [C] and [Cs+] without solving a cubic equation, an iteration technique was used to obtain both the concentration of Cs + and that of 18C6. An initial estimate of $[Cs^{+}]$ was made which depended upon the ratio of C_{τ}^{T} to C_{M}^{T} . When $C_{L}^{T} < C_{M}^{T}$, then $[Cs^{+}] \approx C_{M}^{T} - C_{L}^{T}$ because K_{1} is large. When $C_{T}^{T} \approx C_{M}^{T}$; $[Cs^{+}] \approx ((-1 + \sqrt{1 + 4K_{1}C_{M}^{T}})/2K_{1}$ and when $C_{T.}^{T} > C_{M}^{T}$, [Cs⁺] is very low. For the third case, an arbitrary small number was chosen, $[Cs^{+}] \approx 10^{-7}$, as an Starting with an initial estimate, the initial estimate. first value of [C] was obtained and used to calculate a more accurate estimate of [Cs+]. This procedure was repeated until the ratio of the "current" value of [C] to the previous value of [C] was close to unity. Then the final values of [C] and [Cs+] were used to calculate relative mole fractions and thus δ_{obs} . The Fortran expression and EQN subroutine deck structure which were used are listed in Appendix B-II.

As the data listed in Table 1 indicate, most macrocyclic complexation reactions are exothermic. It was therefore of interest to investigate the temperature dependence of the complexation of Cs⁺ by 18C6 in pyridine. In previous work, Lehn and coworkers (41) and Cahen et al. (93) both noted that the apparent chemical shift of the complexed metal ion varied with temperature. However no detailed study was made, probably because of difficulty in finding a proper absolute reference. For the present temperature study, an absolute reference was designed which was suitable for all temperatures (Figure 26).

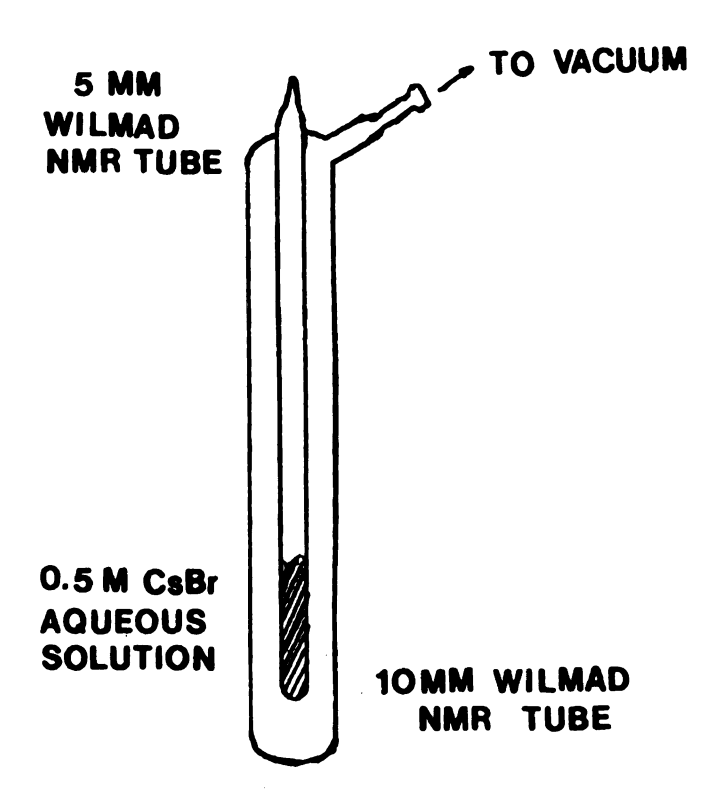


Figure 26. Insulated NMR Reference Sample.

A 0.5 M CsBr aqueous solution was sealed into a 5 mm precision Wilmad NMR tube which was concentrically sealed in a 10 mm precision Wilmad NMR tube. The space between the tubes was evacuated to 10^{-6} torr and then sealed.

The validity of this reference was tested and the results are shown in Figure 27 and are given in Table 21. The chemical shift of a 0.5 M CsBr aqueous solution in a 10 mm NMR tube was recorded as a function of temperature from the readout of the spectrometer. It was measured at the same temperature as the probe. The chemical shift of the absolute reference in the insulated tube was also recorded from the readout of the spectrometer. The measurement was made under exactly the same conditions as with the 10 mm NMR reference tube, but the insulated reference was left in the probe only during the time of data collection (i.e., less than one minute). In this way, the temperature of the solution in the insulated tube is at or near room temperature. The constancy of the chemical shift for the sample in the insulated tube demonstrates the validity of this technique in providing an absolute reference. Of course, the results also indicate that the interaction of the solute with the solvent changes with the temperature to give a temperature-dependent chemical shift.

Sharp and coworkers (83,84) also observed this phenomenon, but they compared their chemical shift to an external reference which was measured at the same temperature as sample. Their major interest was to measure the variation

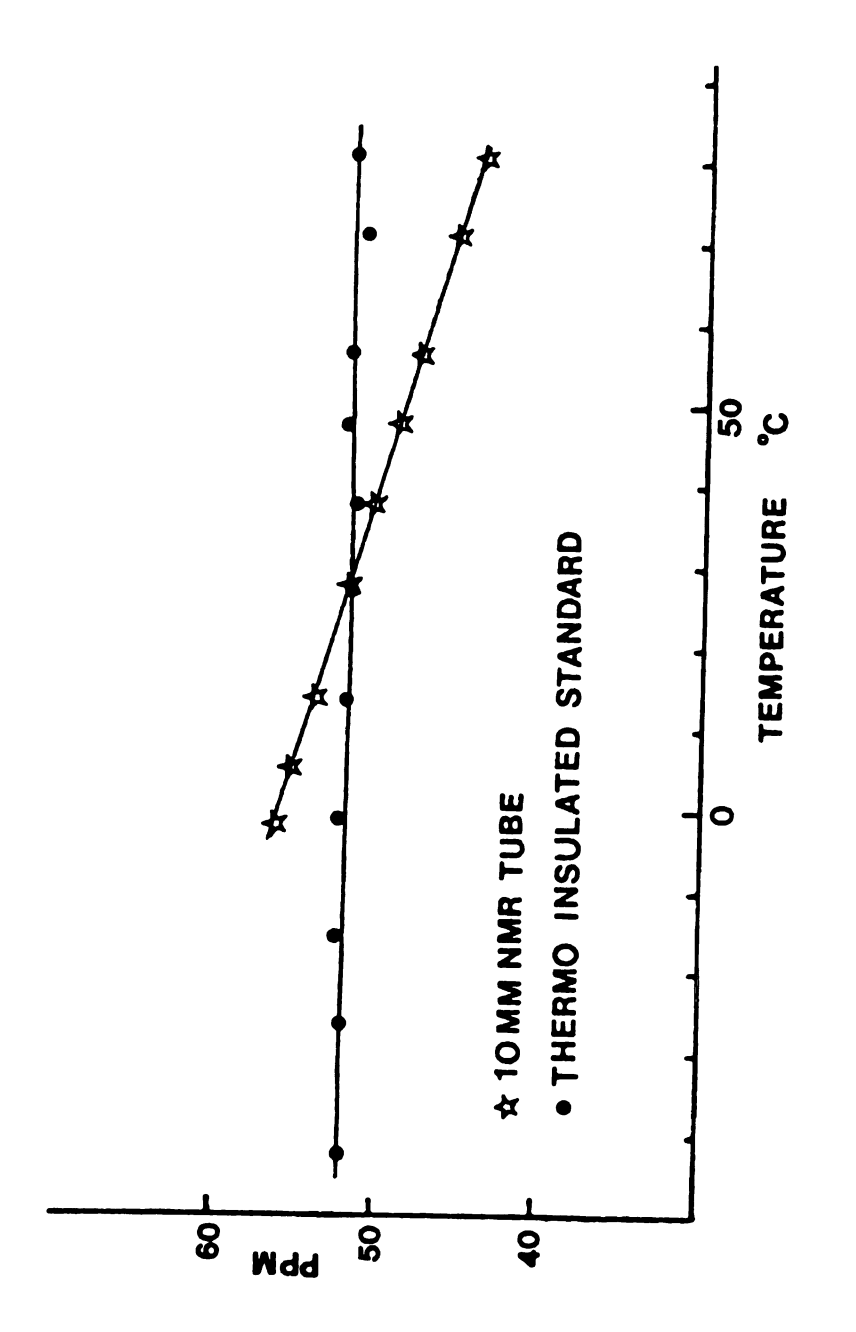


Figure 27. Test of the insulated reference tube.

Table 21. Data from the Test of the Insulated Reference Tube.

Varian DA-60 1.4T Mixing Frequency 48.585800 MHz Sweep width = 1000 Hz Dewell time = 500 μ s Delay time = 200 ns.

Temperature (°C)	10 mm NMR Tube	Insulated Standard
81.0	44.17	52.17
71.5	45.54	51.06
57.0	47.83	52.17
48.0	49.13	52.11
38.0	50.56	51.80
27.6	51.99	51.99
14.0	53.91	52.30
5.8	55.15	52.55
-0.6	56.39	52.48
-15		52.67
-26		52.42
-42		52.24

of the chemical shift with concentration at various temperatures and they did not emphasize the temperature dependence of the shifts.

With the aid of this new reference, a series of measurements were made of the temperature dependence of the chemical shift for the 18C6 complexes with CsTPB and for CsTPB itself. The results are listed in Table 22 and shown in Figure 28. The figure shows not only the marked change in chemical shift which occurs when 1:1 and 2:1 complexes form, but also how the chemical shifts of free and complexed cesium ions respond to variations in temperature. As the temperature decreases, the difference between the chemical shifts at mole ratios of zero and one gets smaller because the chemical shift of the 1:1 complex is less sensitive to temperature. As shown for the region of mole ratio larger than one, the second formation constant increases as the temperature decreases and eventually the "break" in the curve is sharp enough to show clearly that the stoichiometry of the second complex is 2:1. also be seen that the limiting chemical shift for the 2:1 complex is not very sensitive to temperature. All of the chemical shift-mole ratio curves at different temperatures show very sharp changes in direction at a mole ratio equal to one. This condition makes it impossible to extract a complexation constant from the data between mole ratios of zero and one by the nonlinear least-squares technique. However, it is possible to obtain an order of magnitude

Mole-Ratio-Temperature Data for the Chemical Shift of CsTPB in the Presence of 18C6 in Pyridine Table 22.

Temp.							[18C6] [CSTPB]							
707	0	0.23 0.3	0.39	0.68	1.00	1.33	1.00 1.33 1.77	2.0	2.2	2.5	3.0	2.2 2.5 3.0 5.44 7.90 9.75	7.90	9.75
3	32.52	21.35 14.0	14.06	3.36	-9.35	3.36 -9.35 -1.60 6.15	6.15	8.79	12,36	15.31	20.27	8,79 12,36 15.31 20.27 32.06 37.64 39.50	37.64	39.50
	0	0.25	0.5	1.0	1.33	1.53	1.73	2.0	2.34	2.63	3.28	1.33 1.53 1.73 2.0 2.34 2.63 3.28 4.08	8.22	9.20
285	29.26	11.58 4.45	4.45	-10.44		4.76	11.27	13.13	19.03	22.75	28.95	0.20 4.76 11.27 13.13 19.03 22.75 28.95 33.61 42.29	42.29	43.22
272	26.78	10.96	1.04	-12.61	1.66	7.86	7.86 15.62 18.10 24.61 28.33	18.10	24.61		35.26	35.26 38.57	45.70	46.01
255	21.82	•	*	-16.02	3.52		11.58 21.51 23.68 33.30 35.47	23.68	33.30		41.05 44.15	44.15	49.11	49.11
244	17.17	•	•	-17.58	4.76	14.37	14.37 25.23 28.64 36.09 40.43	28.64	36.09		44.77	46.94	50.05	50.36
235	235 15.00	•	*	-18.82		15.24	6.00 15.24 28.33 31.12 39.19 42.60 46.94 48.18	31.12	39.19	42.60	46.94	48.18	50.29	50.29
229	229 ⁺ 12.20	*	*	-19.75	5.07	16.55	29.26	32.99	40.12	43.84	47.56	-19.75 5.07 16.55 29.26 32.99 40.12 43.84 47.56 49.43 51.29	51.29	51.60

* Very broad resonance line.

⁺Samples sometimes were partially frozen.

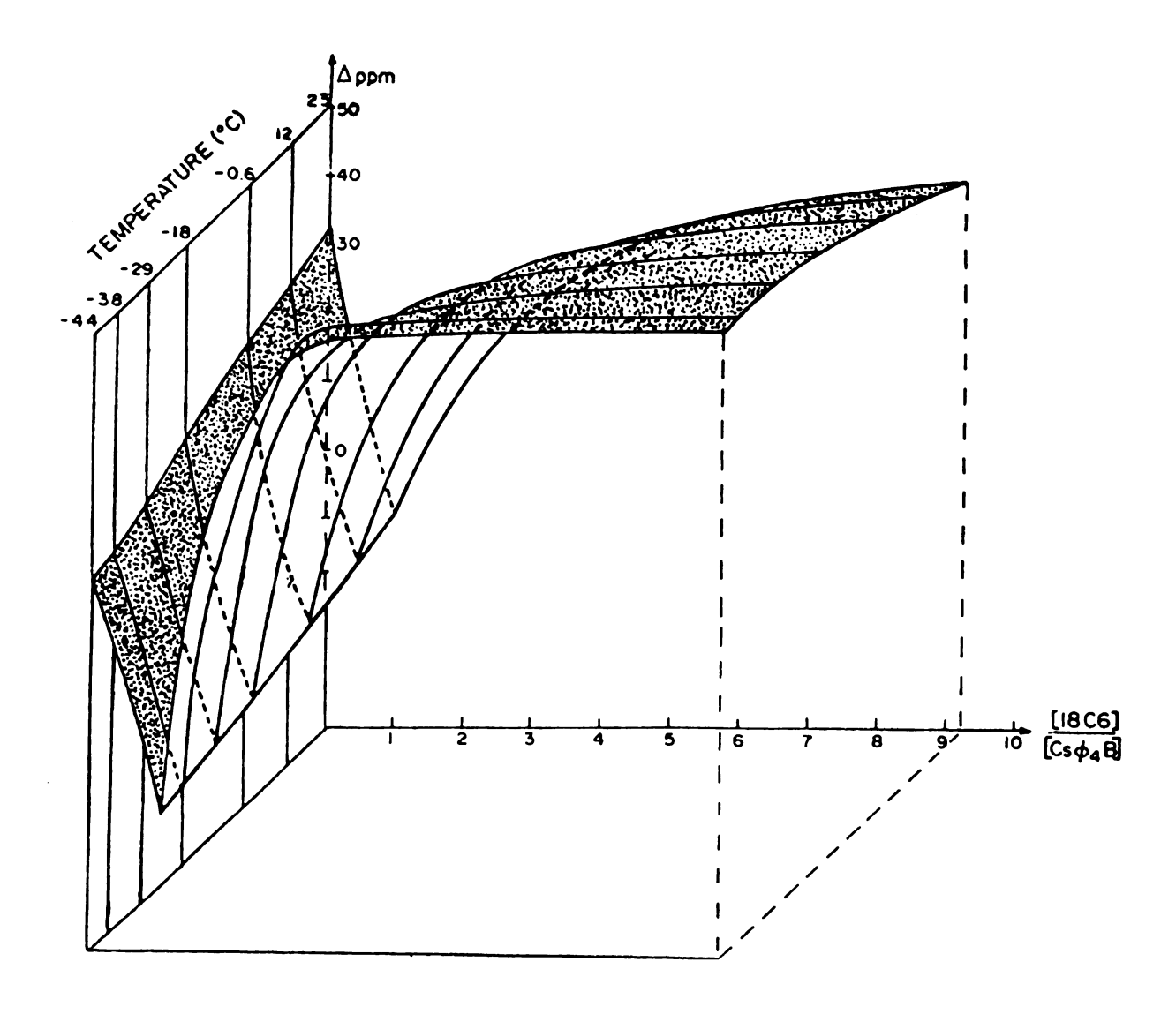
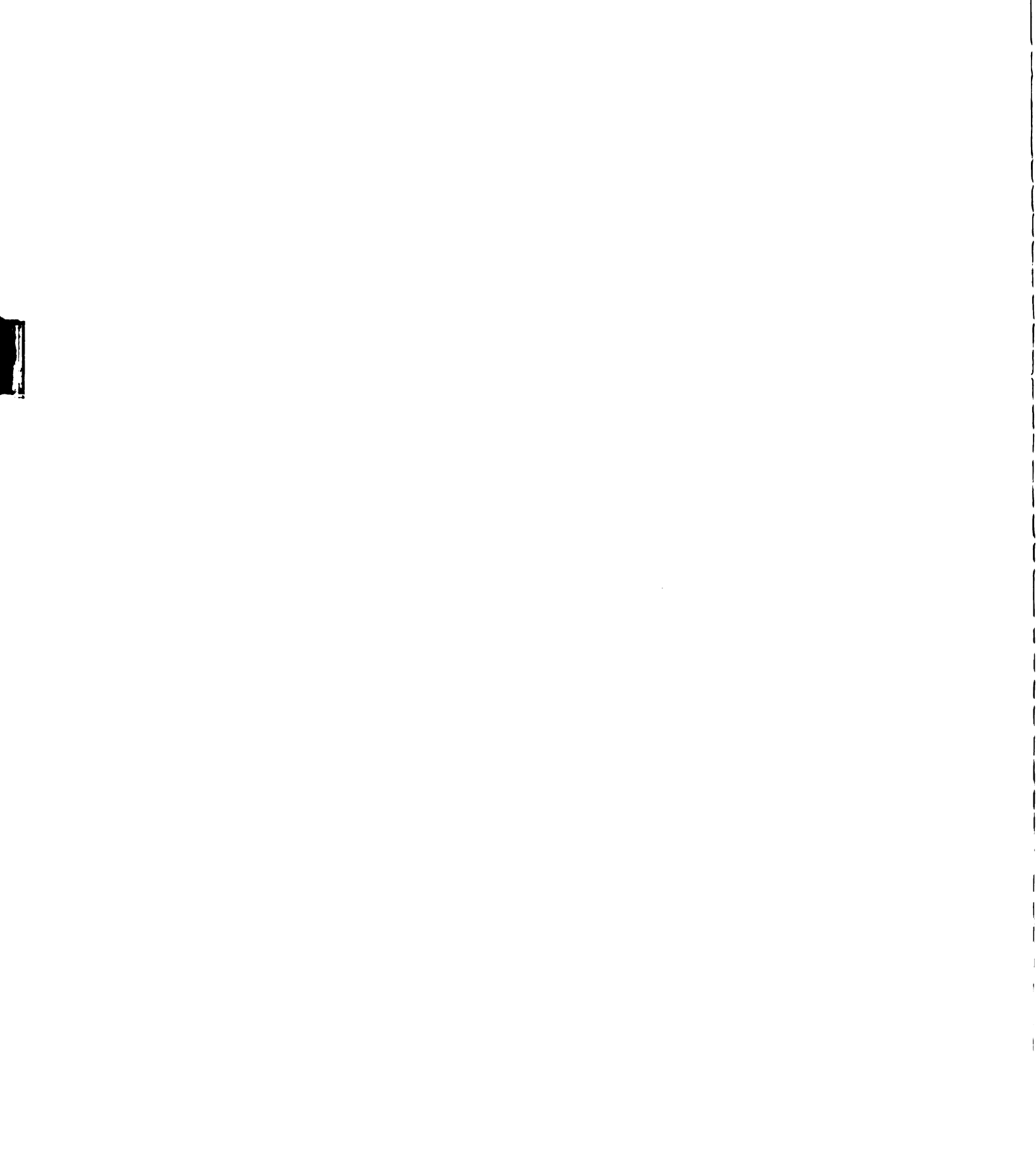


Figure 28. A three-dimensional plot of the cesium-133 chemical shift vs mole ratio and temperature (°C) for solutions of CsTPB and 18C6 in pyridine. The concentration of CsTPB was 0.01 M.



estimate of K₁ through simulation of the data by the iteration technique previously described. All such simulated "data" were compared with experimental results and adjustments in K₁ were made as needed. The values used for K₂ were obtained by a least-square fit of the data obtained at mole ratios higher than one. Two representative results are shown in Figure 29. The corresponding K₁ and K₂ values are listed in Table 23.

Table 23. The Simulated Formation Constants (K₁) and Least-squares Adjusted Constant (K₂) for the Complexation of Cesium Tetraphenylborate by 18C6 in Pyridine at Various Temperatures.

Temperature °K	ĸ ₁	к ₂	
297	5 x 10 ⁸	71.3	
285	5 x 10 ⁸	116.6	
272	5 x 10 ⁸	209	
255	109	414	
244	3 x 10 ⁹	605	
235	6 x 10 ⁹	1140	
229	3 x 10 ¹¹	3440	

Since the K_1 values are much larger than K_2 , at mole ratio equal to one, most Cs^+ can be considered to have been converted to $Cs^+ \cdot 18C6$. Therefore, it is possible to obtain K_2 values by fitting the data beyond a mole ratio of 1:1 with

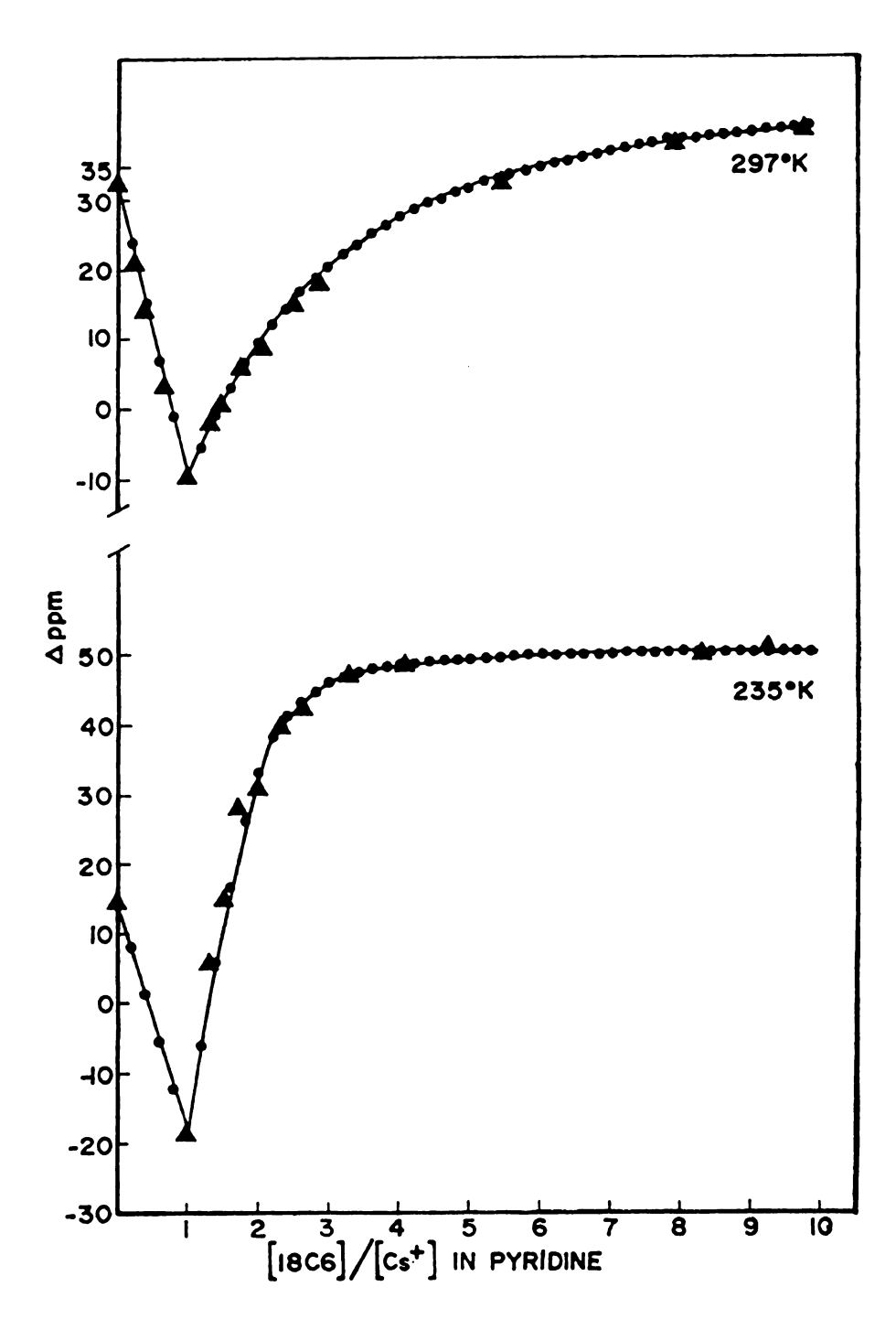


Figure 29. A Comparison of simulated data (●) with experimental data (▲) for a chemical shift - mole ratio study at 290°K and 235°K for solutions of CsTPB and 18C6 in pyridine.

the KINFIT program (Table 24) and thus obtain the enthalpy of the second complexation reaction. This procedure gives H_2 =-6.16±0.09 Kcal/mole. The relevant thermodynamic parameters are calculated by the following relationships:

$$\frac{d \ln K}{d (1/T)} = \frac{-\Delta H}{R}$$
 (III.17)

$$\Delta G = - RT lnK \qquad (III.18)$$

$$\Delta S = \frac{\Delta H - \Delta G}{T}$$
 (III.19)

and the resultant values are $(\Delta G_2)_{298} = -2.83\pm0.004$ Kcal/mole, $\Delta S_2 = -11.18\pm0.31$ cal/(mole K°). Again, it is worthwhile to note that the limiting chemical shifts of $Cs^+\cdot(18C6)_2$ are nearly temperature independent. This phenomenon may imply that the first solvation shell has been completely displaced by the ligand and also that there is no pronounced conformational change between 24° and -44°C.

(B) CESIUM TETRAPHENYLBORATE COMPLEXES WITH C222 IN VARIOUS SOLVENTS

The variation of chemical shift with temperature was also studied for the cryptand-Cs⁺ complexation reaction. The implications of these variations will be discussed later but in this section the overall formation constants of C222 complexes with CsTPB in DMF, PC and acetone

Limiting Chemical Shift of the $Cs^+(18C6)_2$ Complex and the Thermodynamic Parameters for the Reaction of $Cs^+\cdot 18C6+18C6$ \ddagger $Cs^+\cdot (18C6)_2$ in Pyridine at Various Temperatures. Table 24.

Temperature (°K)	$10^3 x (Temperature)^{-1}$	K ₂	lnK2	(Appm)
297	3.367	71.±1	4.27±0.02	48.23
285	3.509	117.±3	4.76±0.02	49.49
272	3.677	$(2.1\pm1)\times10^{2}$	5.34±0.06	49.95
255	3.922	$(4.1\pm0.6)\times10^{2}$	6.0 ±0.2	51.36
244	4.098	$(6.0\pm0.3)\times10^{2}$	6.41±0.05	51.89
235	4.255	$(1.1\pm1)\times10^{3}$	7.0 ±0.12	51.18

 $\Delta S_2 = -11.2 \pm 0.3 \text{ cal·mole}^{-1.K^{-1}}$

 $(\Delta G_2)_{298} = -2.830 \pm 0.004 \text{ Kcal/mole}$

 $\Delta H_2 = -6.2 \pm 0.1$ Kcal/mole

 $(\ln K_2)_{298} = 4.28\pm0.03$

will be considered. The relevant thermodynamic parameters of the complexation reaction can be calculated from the temperature and concentration dependence of the chemical shift, just as was done for complexation by crowns.

For this study two concentrations of CsTPB were used, 0.02 M and 0.01 M. The external reference was 0.5 M CsBr aqueous solution in a vacuum-jacketed tube. All of the chemical shifts measured at various temperatures are listed in Tables 25-29 and shown in Figures 30-32. The formation constants and limiting chemical shifts were computed by the KINFIT program and the results are listed in Tables 30-32. The corresponding thermodynamic parameters are listed in Table 33 and plots of ln K vs 1/T are shown in Figure 33. An interesting observation, which has consequence to be discussed in Chapter V is that the limiting chemical shift varies with temperature and as the temperature gets lower, this variation becomes smaller. In addition, the chemical shifts at low temperatures approach a value which is independent of the solvent used. These data indicate that the C222 complexation reaction with Cs⁺ is not validly described by a simple complexation reaction, such as

$$Cs^+ + C222 \stackrel{\rightarrow}{\leftarrow} Cs^+ \subset C222$$

in which Cstac222 denotes a complex with a Cs⁺ ion in the center of the cavity. More discussion of this anomaly will be given in Chapter V.

Mole Ratio-temperature Data for the Chemical Shift of CsTPB (0.02 M) in the Presence of C222 in PC. Table 25.

Mole Ratio				Temperature	ire °C			
	105°	°96	72°	46°	29°	-2°	-21°	-40°
0	49.16	49.48	43.89	39.86	42.46	33.66	31.48	28.38
0.20	30.59	19.07	10.39	3.24	-3.22	1 1 1	; 	!
0.51	0.16	-10.39	-27.14	-42.03	-50.71	; ; ;	1 1	i i i
0.63	-15.66	-33.34	-53.82	-73.05	-82.97	1 1	1 1	1
1.00	-57.23	-79.25	-118.95	-154.32	-176.96	-204.87	-216.97	-220.07
1.30	-75.53	-98.48	-136.01	-166.68	-186.57	-209.53	-217.90	-220.69
1.50	-82.66	-106.86	-141.91	-171.79	-188.43	-208.49	-217.90	-221.00
1.70	-86.69	-110.89	-145.63	-171.24	-189.06	-208.80	-216.59	-220.69
2.01	-94.14	-115.85	-147.49	-173.86	-189.37	-208.60	-217.38	-221.00
2.50	-103.13	-125.16	-150.45	-176.03	-189.99	-208.80	-217.59	!!!!!!!!!!!!!!!!!!!!!!!!!!!!!!!!!!!!!!!
3.00	-106.86	-126.71	-150.14	-175.41	-190.30	-208.60	-217.59	1
4.00	-113.99	-130.43	-152.94	-176.03	-190.61	-208.80	-216.35	-221.00

Mole Ratio - Temperature Data for the Chemical Shift of CsTPB (0.01 M) in the Presence of C222 in PC. Table 26.

Mole Ratio		Temperature	ູບ	Mole Ratio	Temperature	ture °C
	100°	70°	40°		25°	20°
0	46.22	46.06	45.60	0	46.22	45.91
0.186	34.43	25.35	19.39	0.13	27.14	
0.38	07.98	-30.40	-47.25	0.48	-8.69	
0.46	-10.55	-31.79	-47.92	0.72	-113.68	-110.74
0.72	-27.45	-61.88	-91.97	1.19	-175.10	-178.51
1.0	-54.90	-100.96	-144.86	1.45	-179.44	-182.85
1.19	-63.84	-124.54	-155.87	1.93	-181.61	-184.25
1.45	-77.08	-112.13	-164.24	2.08	-181.92	-184.87
2.08	-94.76	-138.03	-169.82	2.23	-181.77	-184.87
2.23	-98.17	-140.67	-170.76	2.93	-182.85	-185.33
2.93	-108.87	-145.48	-172.46	3.17	-182.85	-184.87
3.17	-110.74	-146.72	-172.31			

Mole Ratio - Temperature Data for the Chemical Shift of CsTPB (0.02 M) in the Presence of C222 in DMF. Table 27.

Mole Ratio				Ĥ	Temperature	၁ ့ မ			
	54°C	46°C	24°	-2°	-21°	-36.5°	-40°	-51°	-73°
0	6.85	5.92	1.89	3.23	-7.11	06.6-	-10.83	-13.01	-16.10
0.18	-4.93	-8.35	-17.03	-32.85	-40.30	-17.34	 	! ! !	1 1
0.5	-21.07	-28.51	-48.36	-77.52	-94.28	-99.23			1
0.75	-33.78	-42.78	-70.70	-110.71	-137.07	-157.55	 	1	1 1 1
1.0	-43.71	-53.33	-86.83	-131.49	-162.82	-186.08	-194.15	-214.0	-229.20
1.21	-51.46	-62.01	-98.32	-144.52	-174.30	-196.32	-201.90	1 1 1	! ! !
1.48	-60.15	-72.25	-109.47	-155.38	-181.74	-201.28	-206.25	!!!!!!!!!!!!!!!!!!!!!!!!!!!!!!!!!!!!!!!	
1.7	-65.42	-80.62	-115.05	-158.79	-183.91	-201.07	-206.25	1 1	
1.97	-71.94	-84.75	-121.57	-163.44	-186.39	-202.52	-207.49	-217.72	-228.27
2.3	-77.83	-90.86	-126.84	-166.54	-187.63	-204.07	-208.42	1 1 1	
3.3	-91.79	-106.68	-137.07	-171.19	-189.81	-204.69	-208.73	-219.58	-231.06
4.38	-100.78	-111.33	-142.35	-173.37	-191.36	-205.31	-208.73	-219.58	-231.47

Mole Ratio - Temperature Data for the Chemical Shift of CsTPB (0.01 M) in the Presence of C222 in DMF. Table 28.

0.0 15° -2° 15° -38° 0 0.80 0.34 -3.6 -4.4 -10.4 0.19 -13.31 -16.26 -25.78 -30.3 0.45 -35.03 -41.54 -63.0 -70.78 0.6 -41.85 -51.93 -75.56 -85.82 -183.67 -183.64 1.04 -71.94 -88.22 -124.26 -143.67 -183.67 -183.64 1.4 -87.60 -105.59 -142.56 -166.32 -191.7 1.7 -95.51 -113.19 -149.54 -166.32 -196.51 2.13 -105.9 -124.2 -158.38 -175.47 -202.87 2.4 -111.95 -129.01 -160.24 -177.33 -204.57 3.18 -121.26 -139.56 -166.45 -180.43 -206.88 3.56 -124.51 -166.45 -166.45 -180.45 -206.88	Mole Ratio		Temp	Temperature °C		
0.80 0.34 -3.6 -4.4 -13.31 -16.26 -25.78 -30.3 -35.03 -41.54 -63.0 -70.78 -41.85 -51.93 -75.56 -85.82 -71.94 -88.22 -124.26 -143.67 -78.61 -95.05 -130.77 -152.05 -87.60 -105.59 -142.56 -166.28 -95.51 -113.19 -149.54 -166.32 -105.9 -124.2 -158.38 -175.47 -111.95 -129.01 -160.24 -177.33 -124.51 -139.56 -166.45 -182.75		25°	15°	-2°	15°	-38°
-13.31 -16.26 -25.78 -30.3 -35.03 -41.54 -63.0 -70.78 -41.85 -51.93 -75.56 -85.82 -71.94 -88.22 -124.26 -143.67 -78.61 -95.05 -130.77 -152.05 -87.60 -105.59 -142.56 -162.28 -95.51 -113.19 -149.54 -166.32 -105.9 -124.2 -158.38 -175.47 -111.95 -129.01 -160.24 -177.33 -121.26 -136.76 -166.45 -180.43	0	0.80	0.34	-3.6	-4.4	-10.4
-35.03 -41.54 -63.0 -70.78 -41.85 -51.93 -75.56 -85.82 -71.94 -88.22 -124.26 -143.67 -78.61 -95.05 -130.77 -152.05 -87.60 -105.59 -142.56 -166.28 -95.51 -113.19 -124.2 -158.38 -175.47 -111.95 -129.01 -160.24 -177.33 -121.26 -136.76 -166.45 -180.43	0.19	-13.31	-16.26	-25.78	-30.3	1
-41.85 -51.93 -75.56 -85.82 -71.94 -88.22 -124.26 -143.67 -78.61 -95.05 -130.77 -152.05 -87.60 -105.59 -142.56 -166.28 -95.51 -113.19 -149.54 -166.32 -105.9 -124.2 -158.38 -175.47 -111.95 -129.01 -166.24 -180.43 -124.51 -139.56 -166.45 -182.75	0.45	-35.03	-41.54	-63.0	-70.78	
-71.94 -88.22 -124.26 -143.67 -78.61 -95.05 -130.77 -152.05 -87.60 -105.59 -142.56 -162.28 -95.51 -113.19 -149.54 -166.32 -105.9 -124.2 -158.38 -175.47 -111.95 -129.01 -160.24 -177.33 -121.26 -136.76 -165.36 -180.43 -124.51 -139.56 -166.45 -182.75	9.0	-41.85	-51.93	-75.56	-85.82	1 1 1
-78.61 -95.05 -130.77 -152.05 -87.60 -105.59 -142.56 -162.28 -95.51 -113.19 -149.54 -166.32 -105.9 -124.2 -158.38 -175.47 -111.95 -129.01 -160.24 -177.33 -121.26 -136.76 -165.36 -180.43 -124.51 -139.56 -166.45 -182.75	1.04	-71.94	-88.22	-124.26	-143.67	-183.64
-87.60 -105.59 -142.56 -162.28 -95.51 -113.19 -124.2 -158.38 -166.32 -105.9 -124.2 -158.38 -175.47 -111.95 -129.01 -160.24 -177.33 -121.26 -136.76 -165.36 -180.43 -124.51 -139.56 -166.45 -182.75	1.2	-78.61	-95.05	-130.77	-152.05	-191.7
-95.51-113.19-149.54-166.32-105.9-124.2-158.38-175.47-111.95-129.01-160.24-177.33-121.26-136.76-165.36-180.43-124.51-139.56-166.45-182.75	1.4	-87.60	-105.59	-142.56	-162.28	-196.51
-105.9 -124.2 -158.38 -175.47 -111.95 -129.01 -160.24 -177.33 -121.26 -136.76 -165.36 -180.43 -124.51 -139.56 -166.45 -182.75	1.7	-95.51	-113.19	-149.54	-166.32	-201.32
-111.95 -129.01 -160.24 -177.33 -121.26 -136.76 -165.36 -180.43 -124.51 -139.56 -166.45 -182.75	2.13	-105.9	-124.2	-158.38	-175.47	-202.87
-121.26 -136.76 -165.36 -180.43 -124.51 -139.56 -166.45 -182.75	2.4	-111.95	-129.01	-160.24	-177.33	-203.33
-124.51 -139.56 -166.45 -182.75	3.18	-121.26	-136.76	-165.36	-180.43	-204.57
	3.56	-124.51	-139.56	-166.45	-182.75	-206.80

Mole Ratio - Temperature Data for the Chemical Shift of CsTPB (0.02 M) in the Presence of C222 in Acetone. Table 29.

Mole 54° 46° 29° 24° -2° 0 46.94 45.66 41.62 41.05 43.6 0.29 -11.07 -12.36 -20.11 -17.27 0.48 -60.70 -66.34 -74.70 -77.44 1.00 -143.82 -154.11 -171.17 -175.77 -194.4 1.30 -169.57 -179.23 -195.05 -199.04 -215.25 1.50 -173.91 -182.34 -196.91 -200.28 -215.55 1.70 -176.08 -184.51 -198.16 -201.21 -215.88 2.50 -180.43 -187.30 -199.40 -202.45 -216.13 3.01 -181.46 -187.92 -199.71 -202.45 -216.13	29° 24 41.62 41 -20.11 -17 -74.70 -77 -118.75 -121	43.60	-21° 32.31	30.19	28.33	24.92
46.94 45.66 41.62 41.05 -11.07 -12.36 -20.11 -17.27 -60.70 -66.34 -74.70 -77.44 -100.40 -107.58 -118.75 -121.80 -143.82 -154.11 -171.17 -175.77 -1 -169.57 -179.23 -195.05 -199.04 -2 -173.91 -182.34 -196.91 -200.28 -2 -176.08 -184.51 -198.16 -201.21 -2 -178.25 -185.75 -198.47 -201.83 -2 -180.43 -187.30 -199.40 -202.45 -2 -181.46 -187.92 -199.71 -202.45 -2	29° 41.62 -20.11 -74.70 -118.75 -	43.60	1 1 10 1 1 1	30.19	-44° 28.33 	6 1
46.94 45.66 41.62 41.05 -11.07 -12.36 -20.11 -17.27 -60.70 -66.34 -74.70 -77.44 -100.40 -107.58 -118.75 -121.80 -143.82 -154.11 -171.17 -175.77 -1 -169.57 -179.23 -195.05 -199.04 -2 -173.91 -182.34 -196.91 -200.28 -2 -176.08 -184.51 -198.16 -201.21 -2 -178.25 -185.75 -198.16 -201.21 -2 -180.43 -187.30 -199.40 -202.45 -2 -181.46 -187.92 -199.71 -202.45 -2	41.62 -20.11 -74.70 -118.75 -	43.60	32.31	30.19	28.33	24.92
-11.07 -12.36 -20.11 -17.27 -60.70 -66.34 -74.70 -77.44 -100.40 -107.58 -118.75 -121.80 -143.82 -154.11 -171.17 -175.77 -1 -169.57 -179.23 -195.05 -199.04 -2 -173.91 -182.34 -196.91 -200.28 -2 -176.08 -184.51 -198.16 -201.21 -2 -178.25 -185.75 -198.47 -201.83 -2 -180.43 -187.30 -199.40 -202.45 -2 -181.46 -187.92 -199.71 -202.45 -2	-20.11 -74.70 -118.75 -		1 1 1	 		
-60.70 -66.34 -74.70 -77.44 -100.40 -107.58 -118.75 -121.80 -143.82 -154.11 -171.17 -175.77 -1 -169.57 -179.23 -195.05 -199.04 -2 -173.91 -182.34 -196.91 -200.28 -2 -176.08 -184.51 -198.16 -201.21 -2 -178.25 -185.75 -198.47 -201.83 -2 -180.43 -187.30 -199.40 -202.45 -2 -181.46 -187.92 -199.71 -202.45 -2	-74.70		1 1		1 1 1	
-100.40 -107.58 -118.75 -121.80 -143.82 -154.11 -171.17 -175.77 -1 -169.57 -179.23 -195.05 -199.04 -2 -173.91 -182.34 -196.91 -200.28 -2 -176.08 -184.51 -198.16 -201.21 -2 -178.25 -185.75 -198.47 -201.83 -2 -180.43 -187.30 -199.40 -202.45 -2 -181.46 -187.92 -199.71 -202.45 -2	-118.75 -	1 1 1	- 1	; ; ;		
-143.82 -154.11 -171.17 -175.77 -1 -169.57 -179.23 -195.05 -199.04 -2 -173.91 -182.34 -196.91 -200.28 -2 -176.08 -184.51 -198.16 -201.21 -2 -178.25 -185.75 -198.47 -201.83 -2 -180.43 -187.30 -199.40 -202.45 -2 -181.46 -187.92 -199.71 -202.45 -2				 	1 1 1 1	1 1 1
-169.57 -179.23 -195.05 -199.04 -2 -173.91 -182.34 -196.91 -200.28 -2 -176.08 -184.51 -198.16 -201.21 -2 -178.25 -185.75 -198.47 -201.83 -2 -180.43 -187.30 -199.40 -202.45 -2 -181.46 -187.92 -199.71 -202.45 -2	- /1:1/1-	-194.43	-217.46	-224.16	-229.74	-236.57
-173.91 -182.34 -196.91 -200.28 -2 -176.08 -184.51 -198.16 -201.21 -2 -178.25 -185.75 -198.47 -201.83 -2 -180.43 -187.30 -199.40 -202.45 -2 -181.46 -187.92 -199.71 -202.45 -2	-195.05	-215.22	-222.97	-226.64	-229.74	-236.88
-176.08 -184.51 -198.16 -201.21 -2 -178.25 -185.75 -198.47 -201.83 -2 -180.43 -187.30 -199.40 -202.45 -2 -181.46 -187.92 -199.71 -202.45 -2	-196.91 -200.	-215.53	-222.97	 	 	-236.57
-178.25 -185.75 -198.47 -201.83 -2 -180.43 -187.30 -199.40 -202.45 -2 -181.46 -187.92 -199.71 -202.45 -2	1 -198.16 -	-215.84	-223.28	 	 	-236.57
-180.43 -187.30 -199.40 -202.45 -2 -181.46 -187.92 -199.71 -202.45 -2	-198.47 -	-215.84	-223.28	-226.02	-230.15	-236.88
-181.46 -187.92 -199.71 -202.45 -	-199.40 -202.4		-223.28		1	-236.26
	-199.71 -	-216.15	-223.28	-226.33	-230.15	-236.57
4.02 -181.98 -188.23 -199.40 -2-2.45 -216.	-199.40 -	-216.15	-223.28	-226.64	-230.15	-236.57

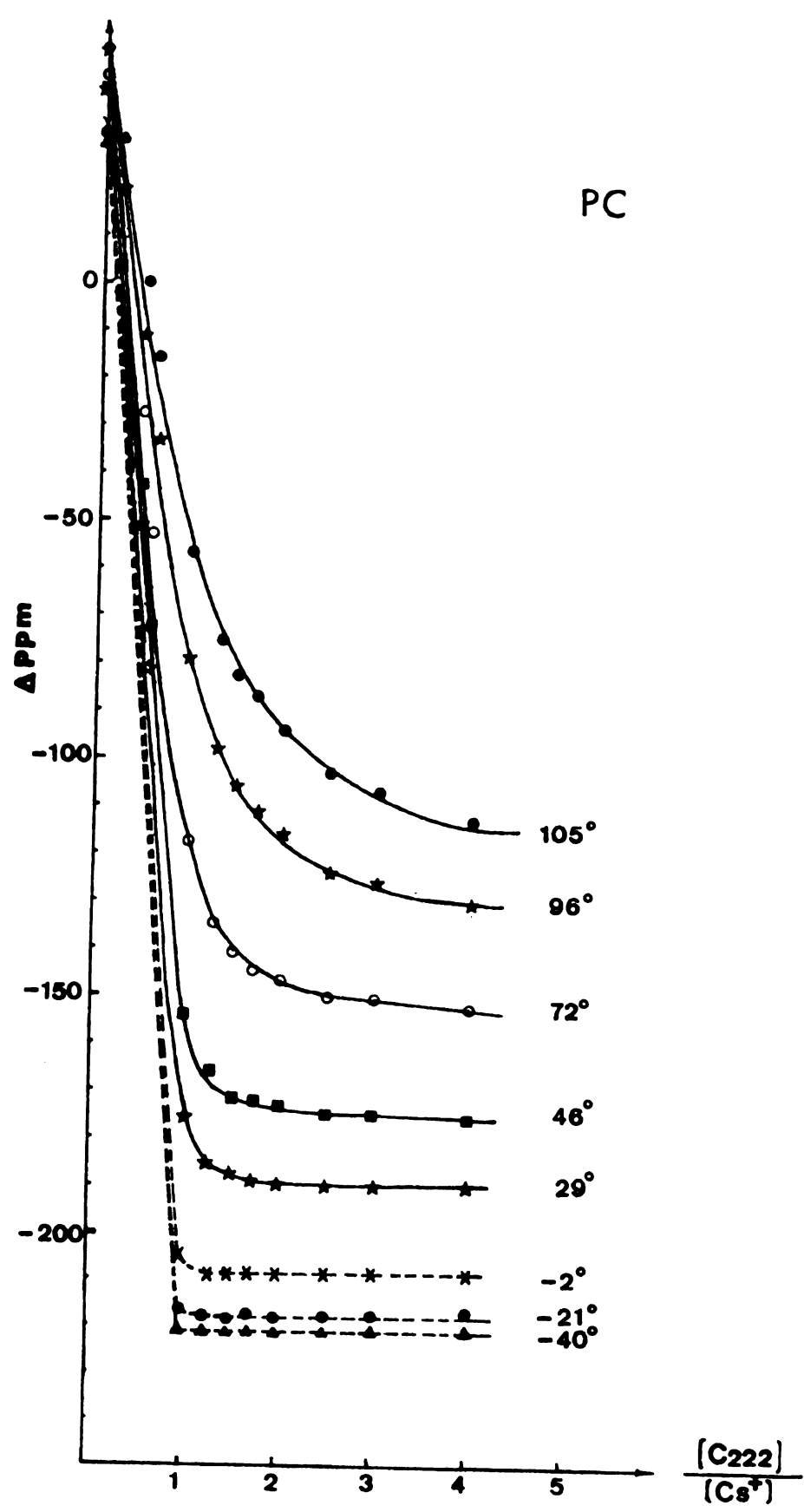


Figure 30. Cesium-133 Chemical Shift vs Mole Ratio of C222 to Cs⁺ in Propylene Carbonate at Various Temperatures.

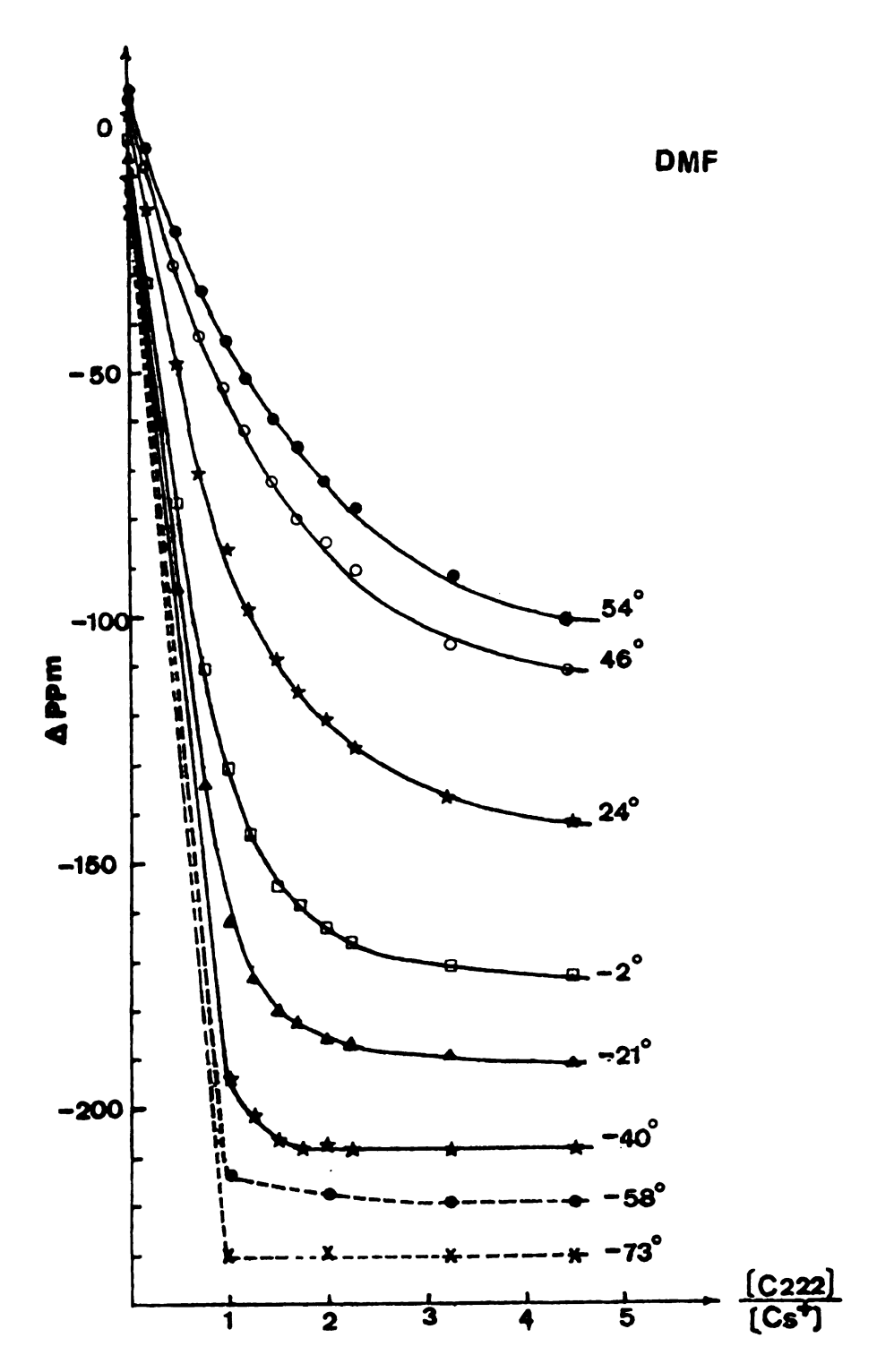


Figure 31. Cesium-133 chemical shift vs mole ratio of [C222]/ [Cs+TPB-] in DMF at various temperatures.

Figure 32. Cesium-133 chemical shift \underline{vs} mole ratio of C222 to Cs⁺ in acetone \overline{at} various temperatures.

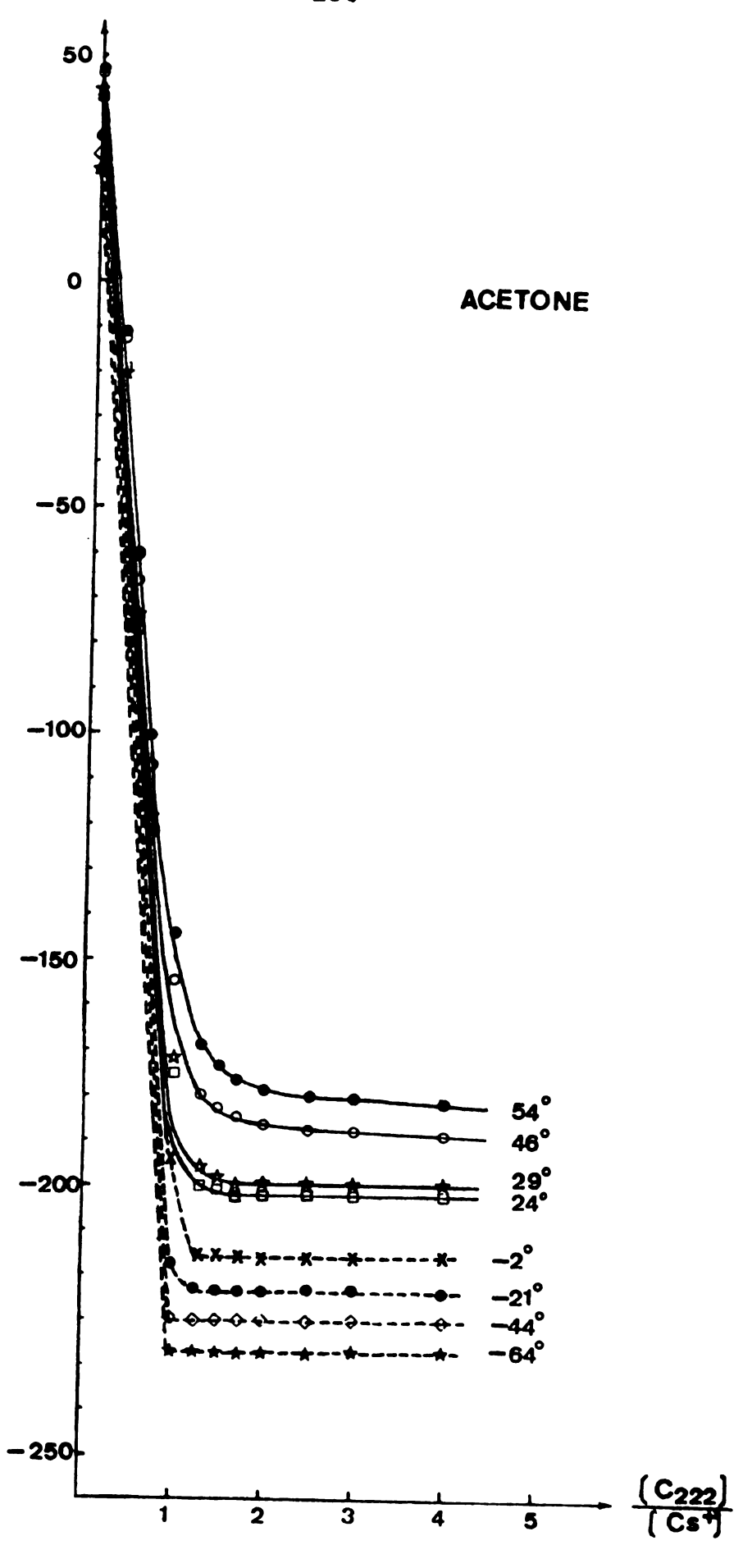


Figure 32.

Table 30. Formation Constants and Limiting Chemical Shift for the Complexation of CsTPB by C222 in PC at Various Temperatures.

Temperature	$(\Delta ppm)_{lim}$	K
Cs ⁺]= 0.02 M		
378	-129 ±1	$(1.7 \pm .1) \times 10^2$
369	-138.7±0.7	$(3.6\pm0.3)\times10^2$
345	-156.1±0.6	$(10\pm1)\times10^{3}$
319	-176.9±0.3	$(4.0\pm0.9)\times10^3$
302	-191.18±0.04	$(6.7\pm0.4)\times10^3$
271	-208.80	
252	-216.35	
s ⁺] = 0.01 M		
373	-184 ±2.0	$(2.6\pm0.2)\times10^2$
343	-202.9±0.5	$(8.6\pm0.4)\times10^{2}$
313	-220.5±0.2	$(4.1\pm0.3)\times10^3$
298	-230.2±0.2	$(10.\pm1) \times 10^4$

Table 31. Formation Constants and Limiting Chemical Shift for the Complexation of CsTPB by C222 in DMF at Various Temperatures.

Temperature °K	(∆ppm) _{lim}	K
Cs^{\dagger} = 0.02 M		
327	-134.4±0.4	44.3±0.5
319	-136 ±2	70 ±6.
297	-156.4±0.2	148.± 2.
271	-178.24±0.07	512.± 6.
252	-193.8±0.2	(11.1±0.8)x10 ²
233	-209. ±1.	$(6.\pm 2) \times 10^3$
215	-219.5	
200	-231.	
Cs^{\dagger} = 0.01 M		
298	-155 ±1	156 6
288	-159 ±3	$(2.6\pm0.3)\times10^{2}$
271	-172.0±0.5	$(6.9\pm0.3)\times10^{2}$
258	-185.5±0.8	$(9.2\pm0.9)\times10^{2}$

Table 32. Formation Constants and Limiting Chemical Shift for the Complexation of CsTPB (0.02 M) by C222 in Acetone at Various Temperatures.

Temperature °K	(∆ppm) _{lim}	к
327	-183.9±0.2	(1.9±0.2)×10 ³
319	-189.3±0.8	$(3.8\pm0.3)\times10^3$
302	-199.7±0.2	(1.8±1.1)×10 ⁴
297	-202.7±0.9	$(1.8\pm0.5)\times10^{4}$
271	-216.15	
252	-223.28	
229	-230.02	
209	-236.57	

Table 33. Thermodynamic Parameters for the Complexation of CsTPB by C222 in Various Solvents

Solvent	ΔH (Kcal/mole)	ΔG (Kcal/mole)	lnK (298°K)	ΔS (cal/mole.°K)
DMF	-7.5±0.3	-2.94±0.01	4.97±0.08	-15±1
	*-7. ±1	-3.08±0.02	5.2±0.2	-13±3
PC	-10.9±0.9	-5.50±0.01	0 2+0 2	10+4
PC		-5.30 ± 0.01 -5.4 ± 0.001		
Acetone	-15 ±2	-5.9±0.2	9.9 ±0.2	-31±7

 $^{*[}Cs^{+}] = 0.01 \text{ M.}$ All other cases $[Cs^{+}] = 0.02 \text{ M.}$

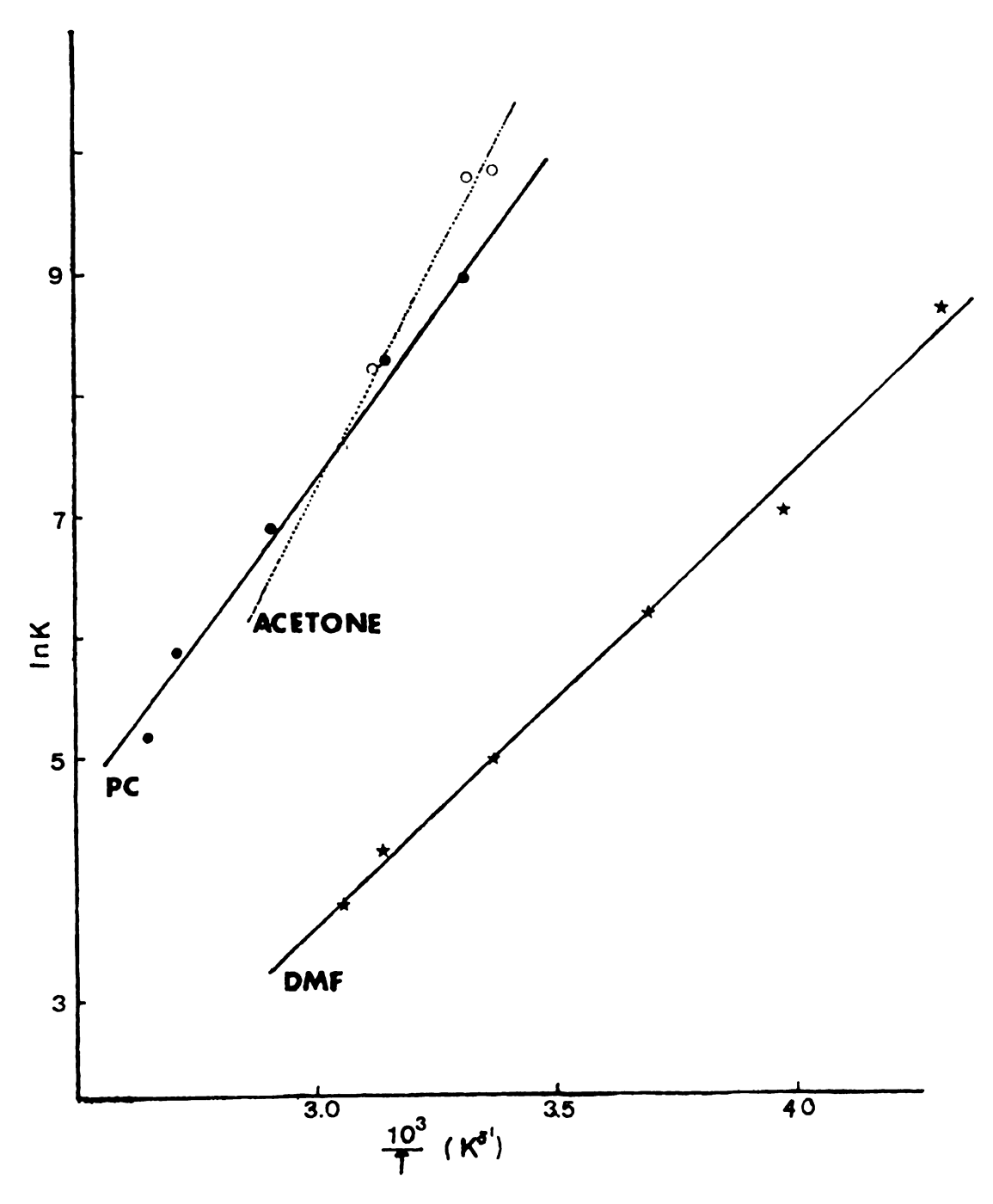


Figure 33. A plot of $lnK ext{ vs } 1/T$ for the complexation reactions of $Cs^+ ext{ with } C222$ in acetone, PC and DMF.

CHAPTER IV

A STUDY OF THE DYNAMICS OF
CESIUM TETRAPHENYLBORATE COMPLEXES
WITH CROWNS AND CRYPTANDS

INTRODUCTION

The complexation studies described above showed that the stabilities of crown and cryptate complexes strongly depend on the nature of the solution and that the topology of the ligand dramatically affects the extent of the complexation reaction in a given solvent. Therefore, NMR lineshape analysis at various temperatures was used to study the kinetics of the complexation reaction. The rates of cesium ion exchange in the presence of the macrocyclic ligands in PC, pyridine, acetone and DMF were calculated from the exact expression for a general two site exchange of uncoupled spins. The equations were fitted to the experimentally observed lineshape with the aid of the generalized weighted non-linear least squares program KINFIT. It was suspected that the activation parameters obtained from lineshape analysis at various temperatures might help to further investigate how the topology of the ligand and the nature of the solvent affect the complexation process.

II. DETERMINATION AND INTERPRETATION OF THE LINESHAPES

The modified Bloch equations (103,104) which describe the motion of the X and Y components of magnetization in the rotating frame, are expressed as follows:

$$\frac{dG_{A}}{dt} + \alpha_{A}G_{A} = -i\gamma H_{1}MO_{A} + \tau_{B}^{-1}G_{B} - \tau_{A}^{-1}G_{A} \qquad (IV.1)$$

$$\frac{dG_{B}}{dt} + \alpha_{B}G_{B} = -i\gamma H_{1}Mo_{B} + \tau_{A}^{-1}G_{A} - \tau_{B}^{-1}G_{B}$$
 (IV.2)

with

$$G_{A} = u_{A} + iv_{A}$$
 (IV.3)

where v represents the absorption mode lineshape and u represents the dispersion mode lineshape. Then $G(\omega)$ is a general expression for the lineshape which can predict the entire range of exchange from the extreme slow limit to the extreme fast limit. At the fast exchange limit $\tau << \frac{1}{(\omega_A^{-\omega_B})}$, and only one signal is observed, while at the slow exchange limit, $\tau >> \frac{1}{(\omega_A^{-\omega_B})}$, one can distinguish separate signals from the two sites. The exchange times, τ , at different temperatures supply—all of the kinetics information.

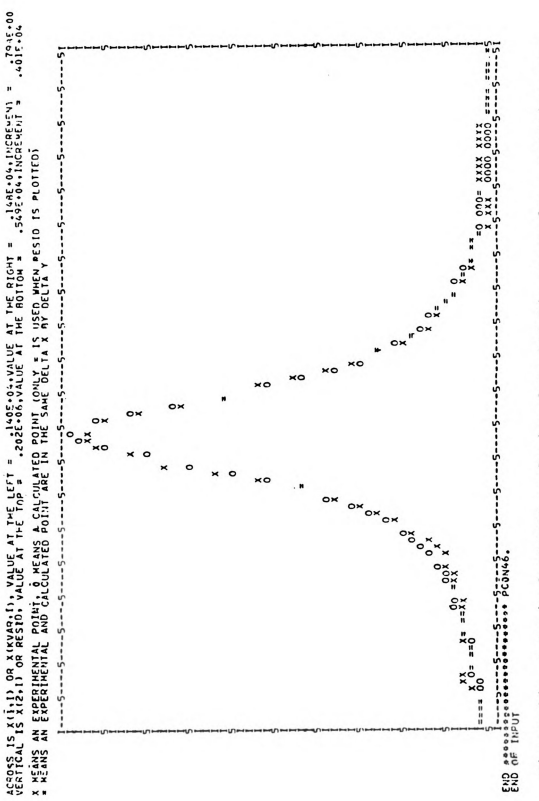
(A) MEASUREMENTS IN THE ABSENCE OF EXCHANGE

In order to determine the linewidth of the two distinguishable sites at various temperatures in the absence of exchange, separate lineshape analyses were made of the salt (site A) and the completely complexed Cs^+ ion (site B) at various temperatures. The values of T_{2B} were studied over the temperature range where the formation constant is larger than 10^3 . Therefore, the populations P_A and P_B can be determined directly from the mole ratios of ligands and cesium salt added to the solution. All experimental

lineshapes in the absence of exchange were found to be Lorentzian.

The values of ω and T_2 for the free and the complexed ion were determined by fitting a Lorentzian line to the observed signal. A typical example for a fit of 0.01 M CsTPB in PC is shown in Figure 34. The five adjustable parameters were the amplitude, K, the Larmor frequency, ω , the linewidth parameter, T_2 , the height of the baseline, c, and the zero-order phase correction, θ . The first-order phase correction, θ_1 , can be determined experimentally by following the procedure in the NMR Manual from the Nicolet Instrument Corp. (105). Therefore, the first-order phase correction is introduced as an externally determined quantity while all of the other five parameters were adjusted by KIN-FIT. The factors which can affect these parameters are described in detail in reference 95.

The variations in linewidths with temperature for the free and complexed cesium ion, in the presence of 18C6, DCC(A), C222B and C222 in PC solution are listed in Tables 34 and 35 and the data are plotted in Figures 35 and 36. The natural linewidth of the cesium ion is very narrow (since the quadrupole moment, Q = 0.003 barns, is small) and the linewidth is predominantly determined by the inhomogeneity of the field. Therefore, only T_2^* values are reported. The quantity T_2^* is defined by $(T_2^*)^{-1} = (T_{2inh})^{-1} + (T_{2nat})^{-1}$ where T_{2inh} is caused by inhomogeneous broadening and T_{2nat} is the natural linewidth of the species under



A typical KINFIT analysis of Cs-133 lineshape for a solution containing 0.01 M CsTPB in propylene carbonate at -46°C. Figure 34.

Relaxation Times for Free and Com-

Temperature	Cs ϕ_A B	Temperature	cs ⁺ .18C6
¥°	$\mathtt{T}_2^*(\mathtt{sec})$	Χο	$\mathbf{T_2}^*(\mathbf{sec})$
298.0	0.081 (0.008)	303.0	0.10 (0.01)
284.8	0.082 (0.0071)	284.8	0.093 (0.007)
266.0	0.065 (0.005)	253.8	0.068 (0.004)
253.8	0.053 (0.003)	245.0	0.048 (0.004)
245.0	0.046 (0.004)	266.0	0.083 (0.01)
225.0	0.028 (0.004)	225.0	0.028 (0.004)
Temperature	Cs+DCC	Temperature	Cs+.C222B
M °	$T_2^*(sec)$	Ж°	$\mathtt{T}_2^*(\mathtt{sec})$
302.0	0.078 (0.004)	303.0	0.037 (0.004)
297.0	0.072 (0.008)	289.0	0.022 (0.003)
284.0	0.072 (0.005)	280.0	0.020 (0.005)
259.0	0.043 (0.004)	262.0	0.005 (0.001)
248.0	0.030 (0.004)	254.0	0.004 (0.002)
234.5	0.008 (0.001)	239.0	0.0014 (0.0006)
208.5	0.0044 (0.005)		

NOTE: $T_2(REF) = T_2(lmh) = 0.087 sec$

Table 35. Temperature Dependence of the Transverse Relaxation Times in Propylene Carbonate in the Presence and Absence of C222.

CsTPB

Temperature °K	T ₂ (sec)	
284	0.08 (0.01)	
273	0.07 (0.01)	
252	0.06 (0.01)	
227	0.037 (0.007)	

Cs⁺•C222

Temperature °K	T ₂ *(sec)	
298	0.015 (0.003)	
286	0.012 (0.0007)	
273	0.006 (0.002)	
258	0.0050 (0.0003)	
241	0.0028 (0.0002)	
230	0.0013 (0.0002)	

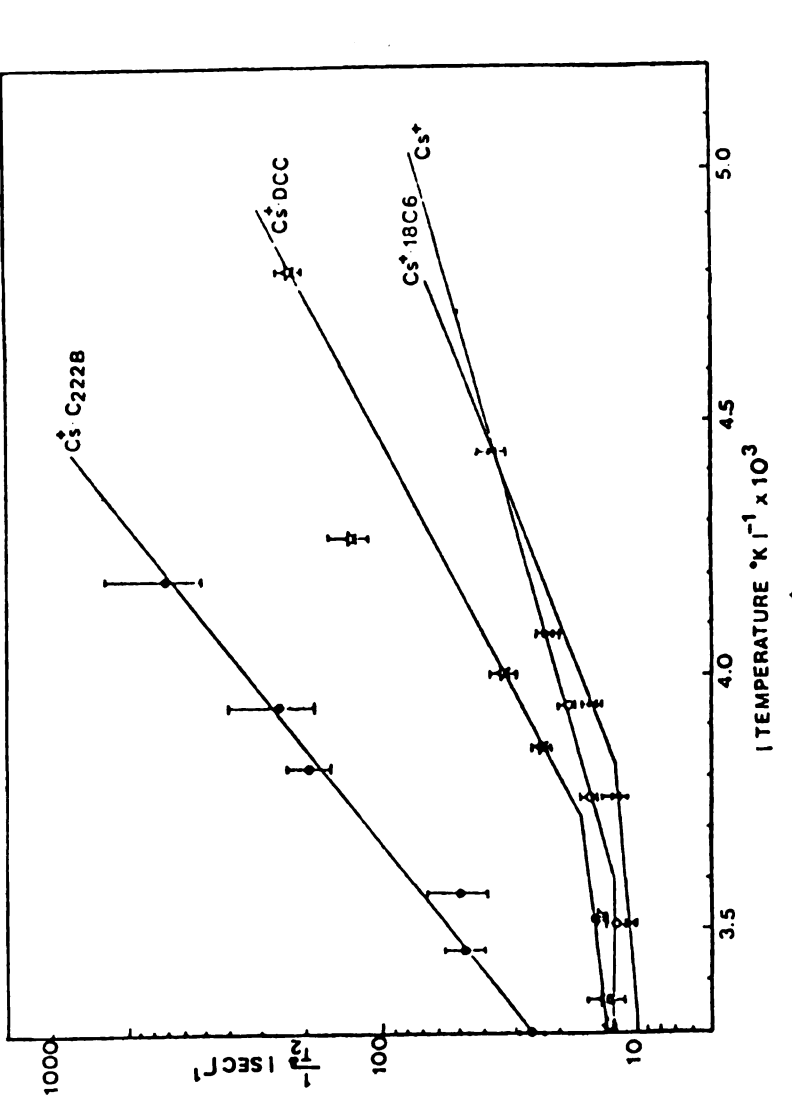


Figure 35. Semilog plots of $1/T_2$ for the Cs-133 nucleus $\frac{vs}{s}$ 1/T for solutions containing 0.02 M total Cs⁺ concentration in the presence and abababeace of various complexing agents. $1/T_2$ values below about 15 sec-1 represent inhomogeneous broadening.

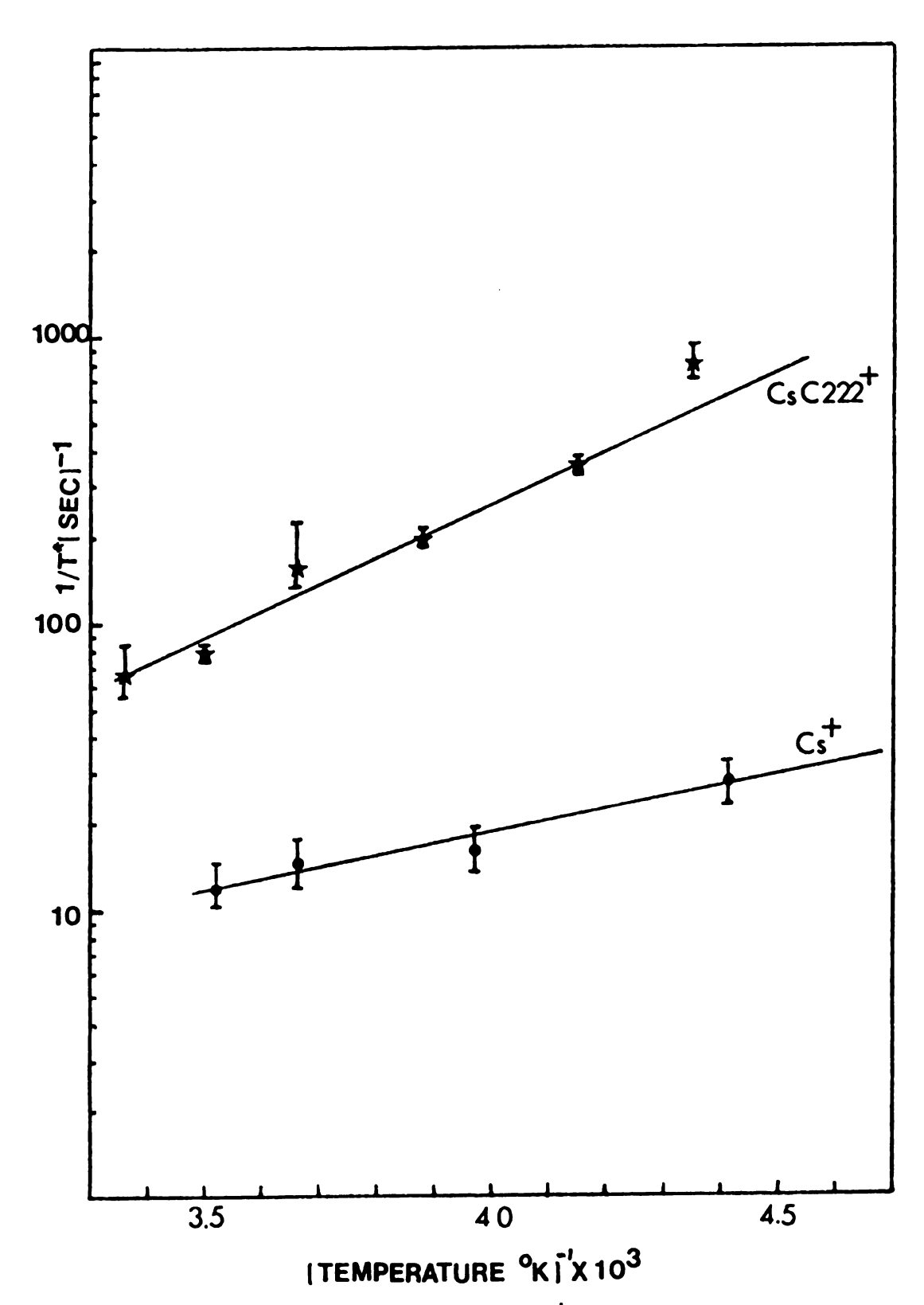


Figure 36. Semilog plots of 1/T₂ for Cs-133 nucleus reciprocal absolute temperature for solutions containing 0.02 M CsTPB and 0.02 M Cs+·C222 in PC.

study. As Figure 35 shows, the broadening of the lines by increased viscosity occurs only at very low temperatures.

The exchange study was carried out under exactly the same field conditions as the nonexchange case to avoid systematic errors. In order to insure that saturation effects were absent, a smaller than 90° pulse (usually 20°) was used. In addition, tests were made to be sure that the S/N ratio of the FID (Free Induction Decay) was not decreased by a slight increase of the pulse power or repetition rate. The spectra were also collected within the first 3/5 of the sweep width used. This procedure was followed to insure that the signal intensity was not attenuated by the filter.

(B) EVALUATION OF EXCHANGE TIMES

To evaluate the exchange time, τ , Equation IV.7 can be rewritten to include the baseline correction.

$$G(\omega) = K(v\cos\theta - iu\sin\theta) + C$$
 (IV.17)

where
$$\theta = \theta_0 + \theta_1$$
 and $u = \frac{QT-SV}{S^2+T^2}$ $v = \frac{QS+VT}{S^2+T^2}$

$$S = \frac{P_A}{T_{2A}} + \frac{P_B}{T_{2B}} + \frac{\tau}{T_{2A}T_{2B}} - (\omega_A + \Delta - \omega) \cdot (\omega_B + \Delta - \omega) \qquad (IV.18)$$

$$T = P_{A}\omega_{A} + P_{B}\omega_{B} + \Delta - \omega + \tau \left[\frac{\omega_{A} + \Delta - \omega}{T_{2B}}\right] \cdot \left[\frac{\omega_{B} + \Delta - \omega}{T_{2A}}\right] \qquad (IV.19)$$

$$V = (P_B \omega_A + P_A \omega_B - \Delta - \omega) \tau \qquad (IV.20)$$

The frequency shift parameter, Δ , was introduced because of field drift of the NMR spectrometer (~ 2 Hz per day). The values of ω_A and ω_B were determined separately but under exactly the same experimental conditions as those used to collect exchange data.

All the data were stored on a magnetic disc and punched out on paper tape when needed. Up to this step in the process, neither data smoothing nor parameter adjusting were used except that an approximate zero-order phase correction was made. This correction had no effect on the fit of the data since θ_0 was re-adjusted by the KINFIT program.

III. RESULTS AND DISCUSSION

(A) LIGAND EFFECT ON EXCHANGE RATE

Except for DBC, all the complexes which were used in the equilibrium study were also used for the exchange study in PC solution. Their spectra, collected at various temperatures are shown in Figures 37-40. Figure 37 shows that the resonance at the fast exchange limit is not half-way between the two peaks of the slow exchange limit. However, this is not unexpected because the chemical shift-

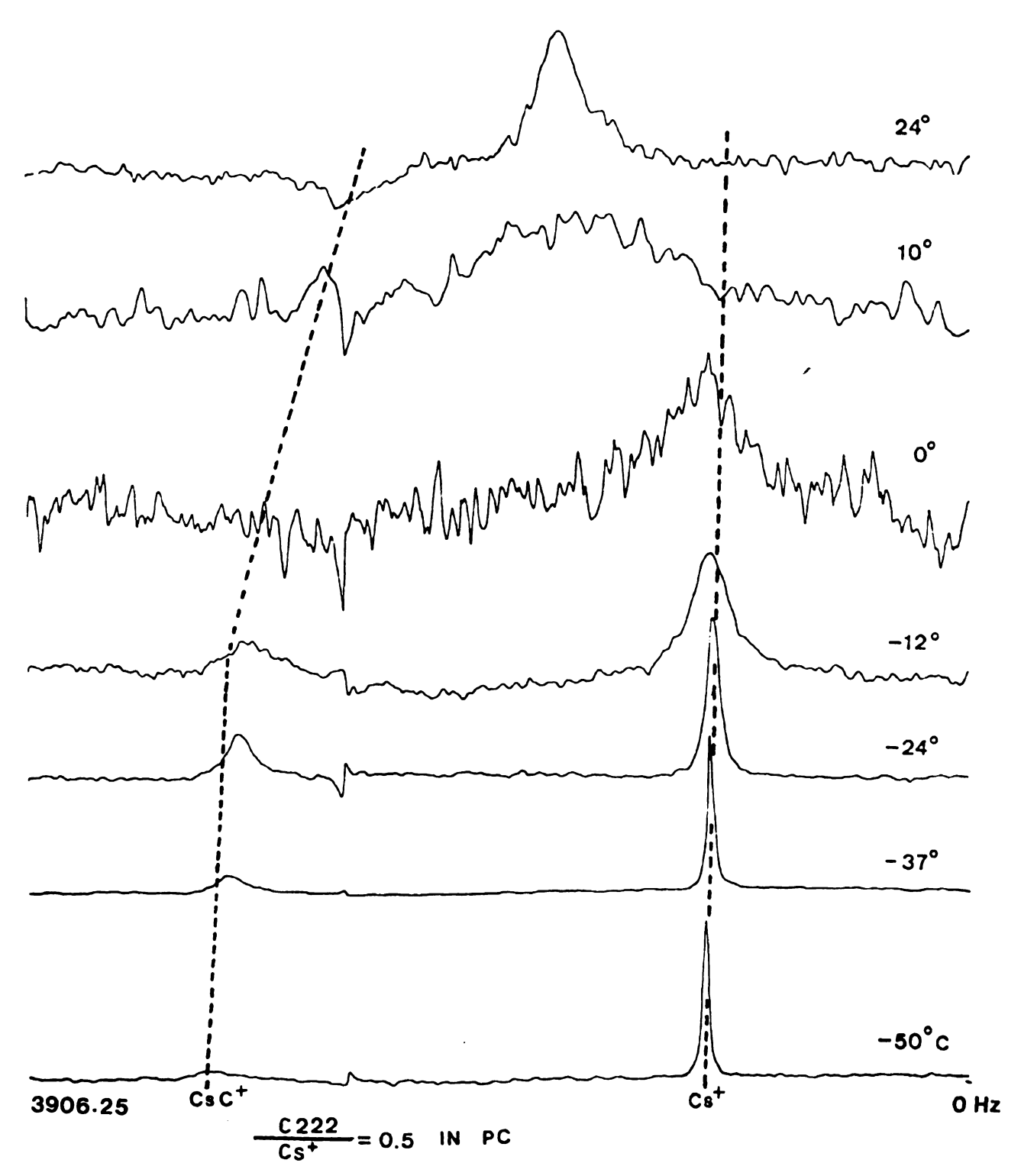


Figure 37. Spectra at various temperatures for a solution containing 0.02 M CsTPB and 0.01 M C222 in PC. Dotted lines represent the chemical shifts of CsC+ (left) and Cs+ (right) in the absence of exchange.

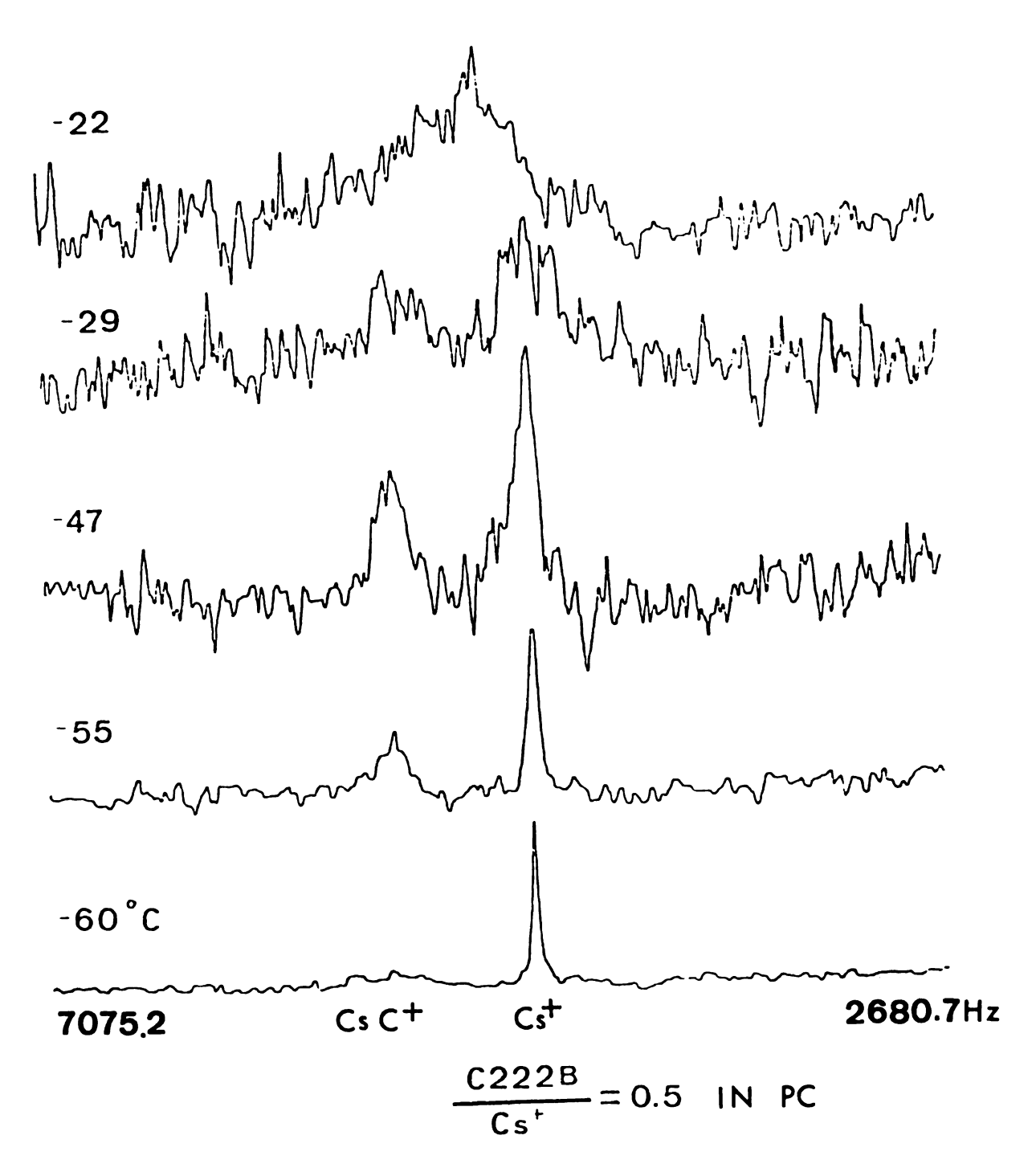


Figure 38. Spectra at various temperatures for a solution containing 0.02 M Cs ϕ_4 B and 0.01 M C222B in PC.

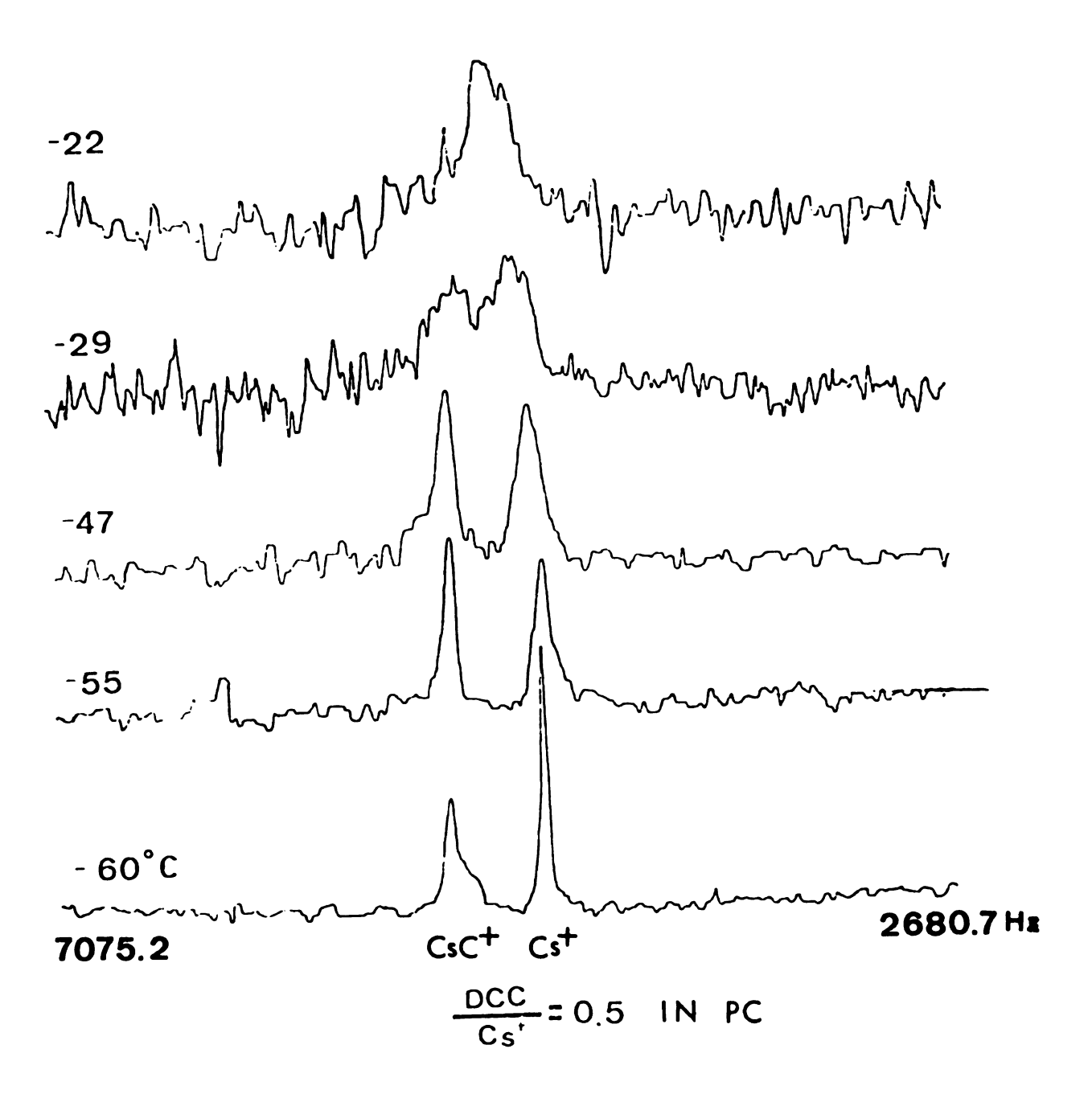


Figure 39. Spectra at various temperatures for a solution containing 0.02 M Cs ϕ_4 B and 0.01 M DCC (A) in PC.

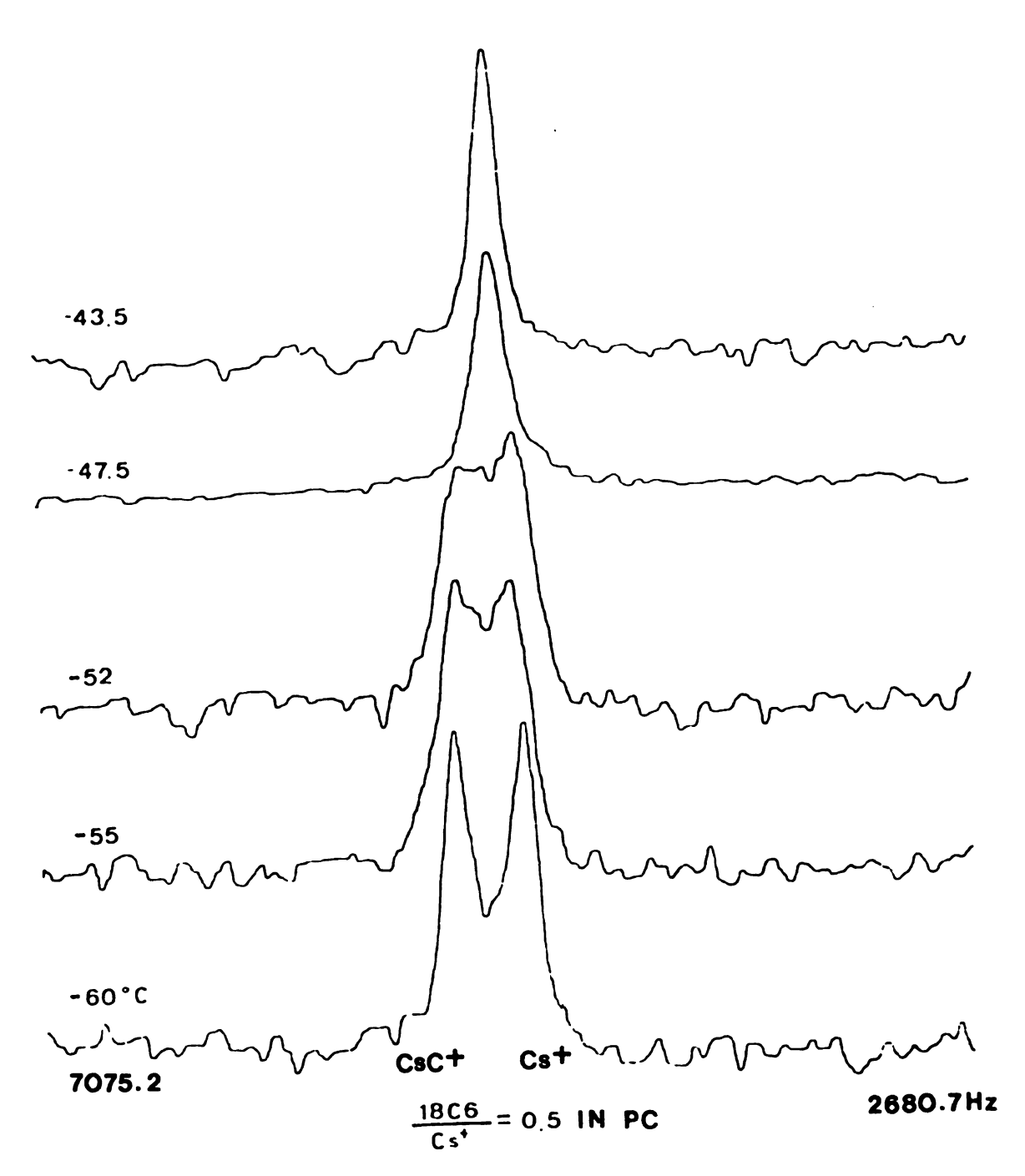
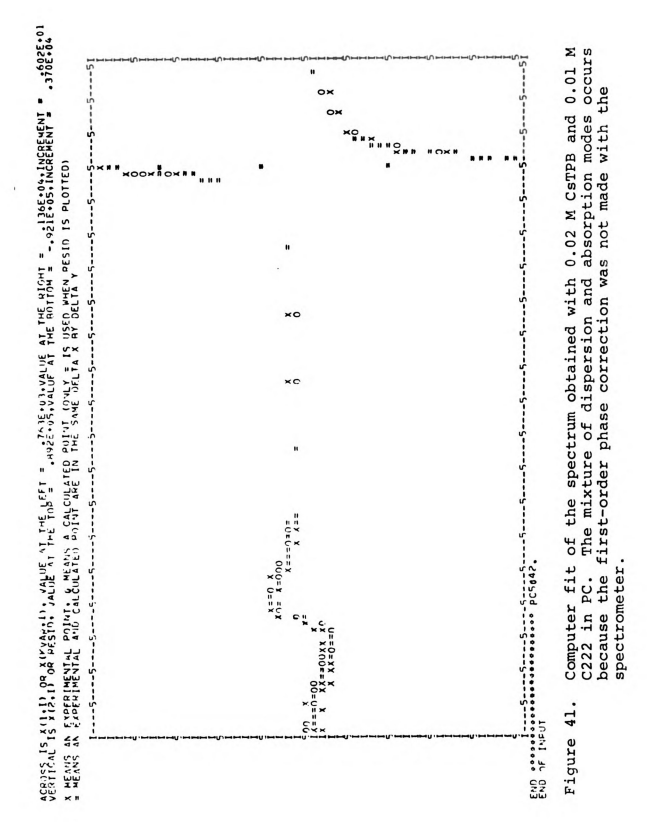
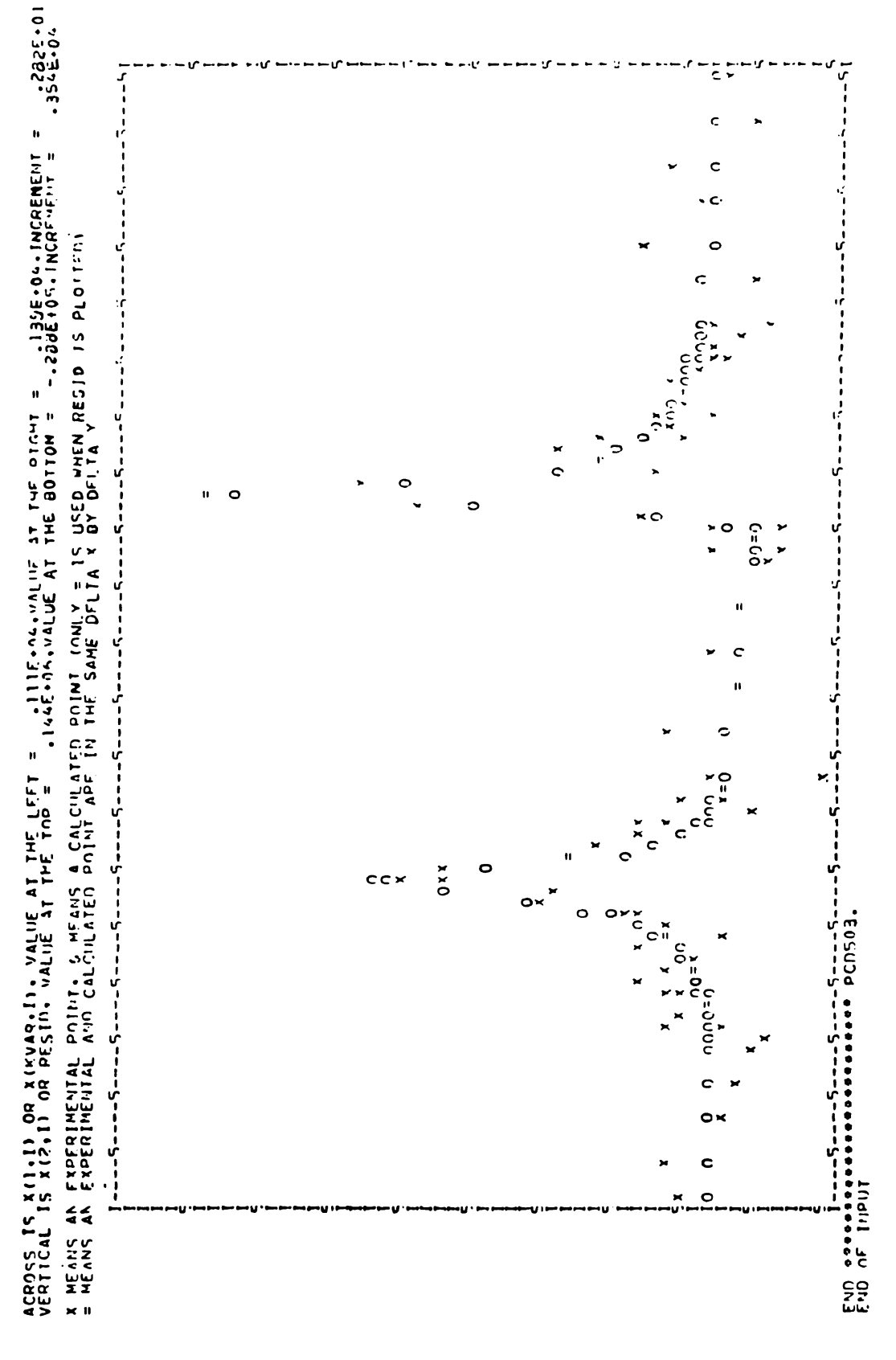


Figure 40. Spectra at various temperatures for a solution containing 0.02 M $Cs\phi_4B$ and 0.01 M 18C6 in PC.

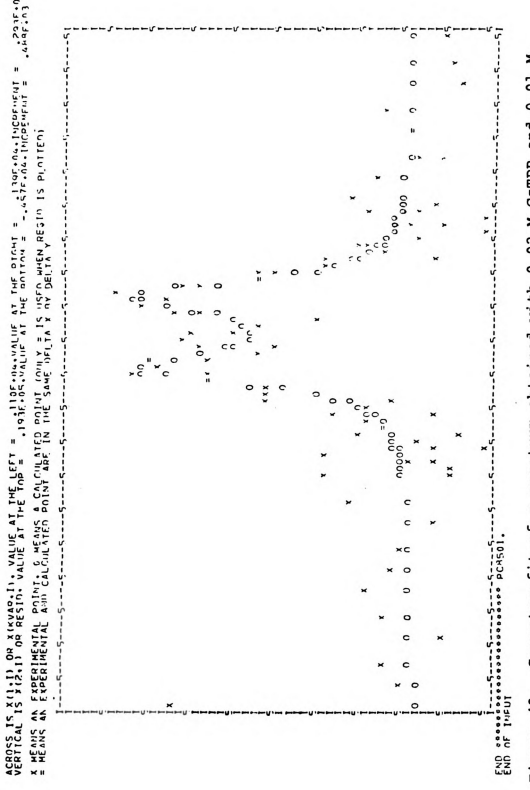
temperature dependence study showed that the limiting chemical shift of the complexed Cs⁺ is very temperature dependent.

Examples of the computer fitting are shown in Figures 41-43. Figure 41 illustrates how the absence of spectrometer first and zero order phase corrections affects the shape of the peak. In Figures 37-40, by contrast, the spectra were plotted after both phase corrections had been instrumentally made. For the computer fitting process only an approximate zero order phase correction was made on the raw data. The first order phase correction was not made by the spectrometer in order to avoid distortion of the baseline. Therefore, for example, the spectra shown in Figure 41, have two peaks which are 180° out of phase. Figures 41-43 also illustrate how the first order phase correction depends on frequency. In Figure 41 the two peaks are approximately 2000 Hz apart and the two resonance lines are 180° out of phase, while in Figure 42, the two peaks are only about 300 Hz apart; therefore, the phase difference of the peaks is very small. The exchange times (τ) obtained by fitting the data are listed in Tables 36 and 37 the Arrhenius plots of exchange times (semi-log scale) vs. the reciprocal of the absolute temperature are shown in Figures 44 and 45. Of the four complexes, the one with C222, at room temperature, has the slowest exchange rate in PC. This fact suggests that the process has the highest





a spectrum obtained with 0.02 M CsTPB and 0.01 M Computer fit of DCC (A) in PC. Figure 42.



Computer fit of a spectrum obtained with 0.02 M CsTPB and 0.01 M 18C6 in PC. Figure 43.

Table 36. Temperature Dependence of the Exchange Time τ , of some CsC⁺ complexes in propylene Carbonate and the Corresponding Reciprocal Transverse Relaxation Time of Cs⁺ (Site A), and CsC⁺ (Site B).

	Temperature °C	τ (msec)	$\frac{1}{T_{2A}}$ (sec)	$\frac{1}{T_{2B}}(sec)$
(A) 18C6	-60.0	3.3 (0.3) ^b	50.00	58.00
	-55.0	2.2 (0.2)	41.00	48.01
	-52.0	1.8 (0.1)	40.49	42.99
	-44.0	0.59(0.03)	33.00	32.00
(B) DCC	-55.0	20. (7.)	43.50	130.55
	-47.5	8. (1.)	34.97	92.00
	-36.0	3.4 (0.7)	26.50	54.00
	-23.0	1.4 (0.2)	20.49	33.00
	-10.5	0.73 (0.06)	16.00	20.49
	-4.7	0.33 (0.06)	13.70	16.21
(C) C222B	-42.0	13.3 (0.70)	30.00	73.00
	-36.0	1.8 (0.4)	27.00	55.87
	-29.0	0.8 (0.2)	22.99	42.02
	-22.7	0.40 (0.06)	20.28	32.47
	-10.5	0.08 (0.01)	16.00	20.49
	-32.0	1.0 (0.2)	24.51	46.95

a_{0.02} M CsTPB + 0.01 M ligand.

bStandard deviation.

Table 37. Temperature Dependence of the Exchange Time in PC in the Presence of C222 and the Corresponding Reciprocal Transverse Relaxation Times of Cs⁺ (A) and Cs⁺ C222 (B).a

remperature °C	τ (ms	ec)x10 ²	$\frac{1}{T_{2A}}(sec)^{-1}$	$\frac{1}{T_{2B}}(sec)^{-1}$
24	1.6	(0.2) ^b	10.53	68.03
10	4.6	(0.8)	6.08	144.93
0	56.	(29.)	13.50	172.41
-12	119.	(19)	16.00	178.57
-25	314.	(16)	19.01	270.27
-35	523.	(19)	21.98	384.62
-37	538.	(97)	22.99	429.19
-41	688.	(14)	24.51	500.00

 $^{^{\}rm a}$ 0.02 M CsTPB + 0.01 M C222

b_{Standard deviation.}

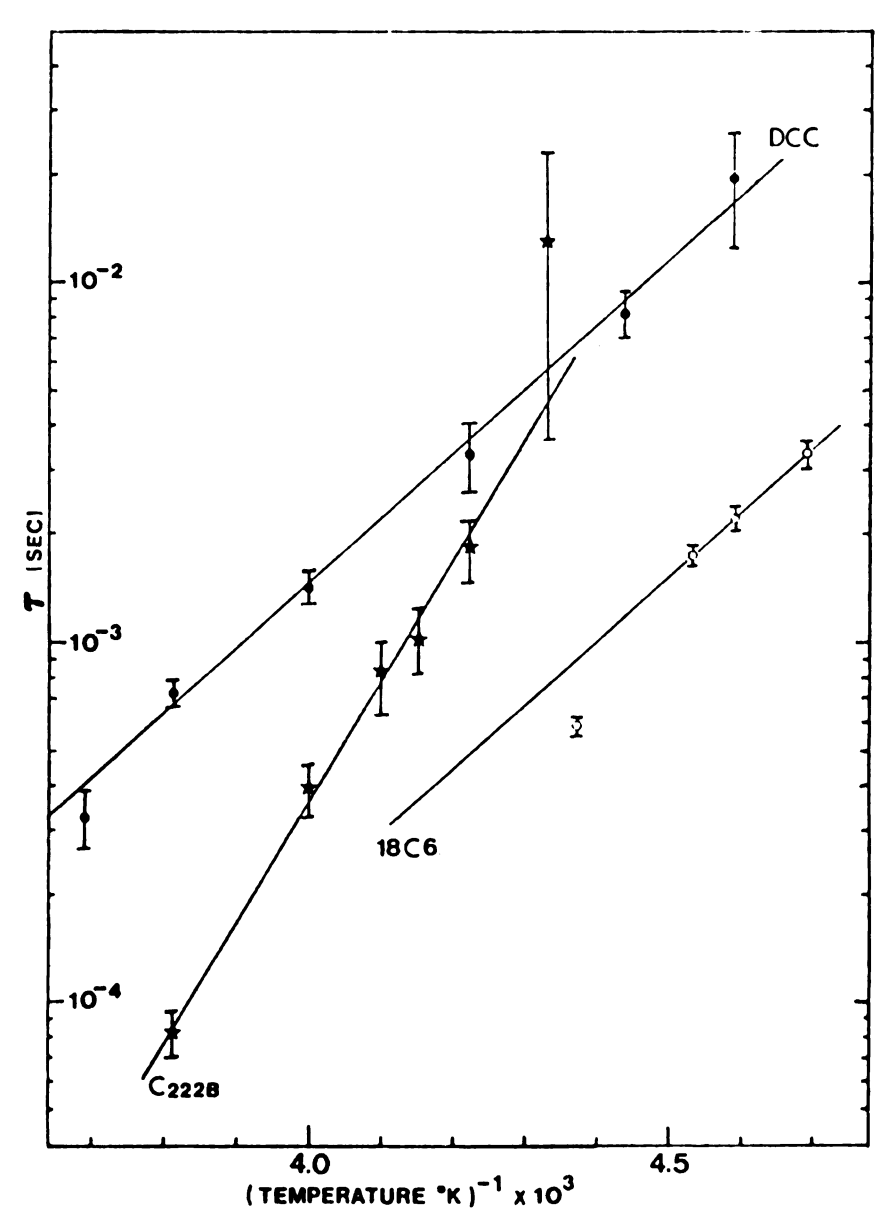


Figure 44. Arrhenius of plots of τ (exchange rates of Cs⁺ from ligands) vs τ^{-1} for propylene carbonate solutions.

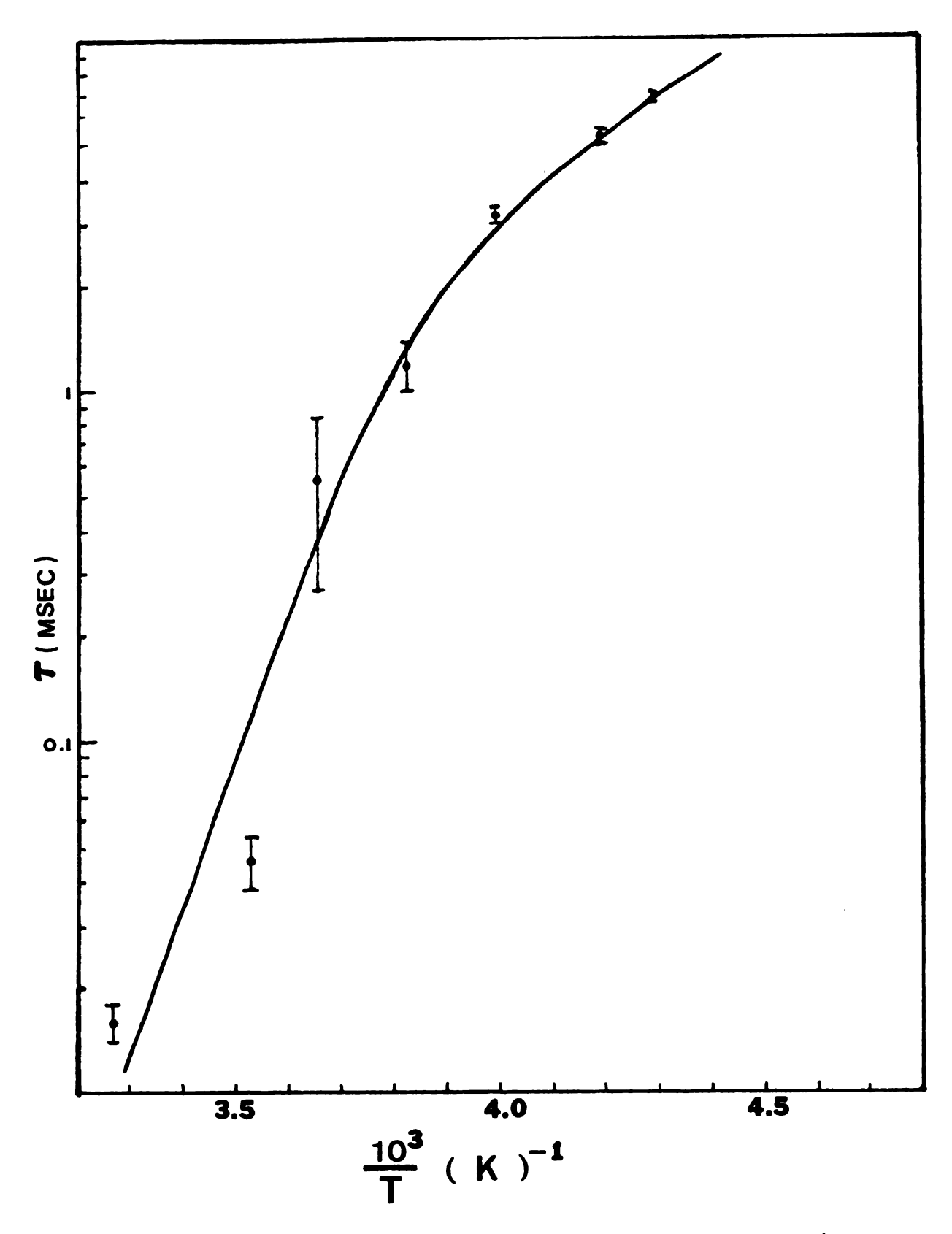


Figure 45. Arrhenius plot of τ (exchange time of Cs from C222) for propylene carbonate solutions.

steric hindrance. The broad temperature range from coalescence to the slow limit indicates that C222 processes the highest activation energy, but because of the complexity of the plot of τ vs (temperature)⁻¹ as shown in Figure 45, the interpretation will be deferred until the next chapter.

The activation energies and the exchange times at 298° for the other three ligands were obtained from the Arrhenius equation. Then by using the following relationships:

$$\tau = \frac{1}{2k_b}$$
 (IV.21)

$$\Delta H_{O}^{\neq} = E_{a} - RT \qquad (IV.22)$$

$$\Delta S_{o}^{\neq} = R \ln k_{b} - R \ln \frac{kT}{h} + \frac{\Delta H_{o}^{\neq}}{T}$$
 (IV.23)

$$\Delta G_{O}^{\neq} = \Delta H_{O}^{\neq} - T \Delta S_{O}^{\neq}$$
 (IV.24)

all related activation parameters could be calculated (Table 38). In the above equations, ΔG_{0}^{\neq} , ΔH_{0}^{\neq} and ΔS_{0}^{\neq} are the standard free energy of activation, the standard enthalpy of activation and the standard entropy of activation, respectively, for the decomplexation reaction. The symbols k and h in the above equation represent the Boltzmann constant and Plank's constant, respectively. The activation energy values in Table 38 illustrate that the nature of the ligand significantly influences the complexation

Exchange Rates and Thermodynamic Parameters for Release of Cs⁺ From Some Cesium Macrocyclic Complexes in Propylene Carbonate. Table 38.

Ligand	Ea kcal/mole	kbx10 ⁻³ sec ⁻¹ (298°K)	ΔH [#] O kcal/mole	ΔS [≠] cal/K°mole	ΔG_{O}^{\neq} kcal/mole (298°K)
C222B	14.9±0.6	344±38	14.3±0.6	-15±2.0	18.756±0.0004
DCC (A)	8.5±0.5	11±1	7.9±0.5	-14±2.0	11.94±0.05
18C6	8.0±4.0	50±4.0	7.41±4.0	-12.2±0.2	14 ±4.0



reaction. Cryptand-222B has the highest rigidity and also possesses the largest activation energy. In addition, DCC with a substituent, is more rigid than 18C6, and its activation energy is slightly larger. Dibenzo-18C6 has a higher rigidity than DCC but its smaller cavity size and the weaker donor ability of its oxygens makes the complexation with Cs⁺ much weaker. In addition, it may form exclusive complexes in which the cesium ion is not able to penetrate into the center of the ring. This fact may also be the reason that DBC has the fastest exchange rate at room temperature of all the ligands. If the slow exchange limit for DBC complexes in PC could be observed, it would probably have the lowest activation energy if only exclusive complexes are formed. If this assumption is valid then the activation energy for release of Cs⁺ ion from crowns would be generally lower than from cryptands. This is in contrast to the trend of the formation constants, which is 18C6 > DCC > DBC ∿ C222 > C222B. It is not difficult to rationalize the trends caused by rigidity and donor ability of the ligand in regard to the complexation reaction. ligand 18C6 has both flexibility and proper cavity size. Therefore it can form the strongest complexes. other hand, C222B has a greater rigidity and, perhaps, the smallest cavity size, and thus forms the weakest complexes.

The ΔS_0^{\neq} values of all three ligands are negative, the magnitude of this value is usually determined

by factors such as the reorientation of solvent molecules or conformational changes of the ligand. It seems likely that for the case of C222B both factors are involved in the transition state. Therefore complexes with C222B show the largest negative entropies of activation.

(B) SOLVENT EFFECT ON THE EXCHANGE PROCESSES

Lineshape analysis of exchange rates has also been carried out for the complexes of Cs⁺ with 18C6 in pyridine, and C222 in DMF and acetone. The relevant spectra, collected at various temperatures, are shown in Figures 46-48. For the pyridine case the S/N is poor because of the low concentration of the cesium tetraphenylborate (0.01 M was used) and broad linewidth (~400 Hz) of the resonance line. The nonexchanging T₂ values for Cs⁺ in various solvents are listed in Tables 39-41, and are shown graphically in Figures 48 and 49. Again, in these solvents the linewidths of Cs⁺ in the absence of exchange processes are narrow and are dominated by inhomogeniety of the field except at very low temperatures where viscosity broadening starts to become more important. The exchange rates were obtained by fitting the lineshapes with the KINFIT program and the results are listed in Tables 42-44. The Arrhenius plot of log τ vs 1/T for the system 18C6 + Cs⁺ in pyridine is shown in Figure 51. The Arrhenius plots for the cases of C222 in DMF and acetone are complicated (Figures 52,53)

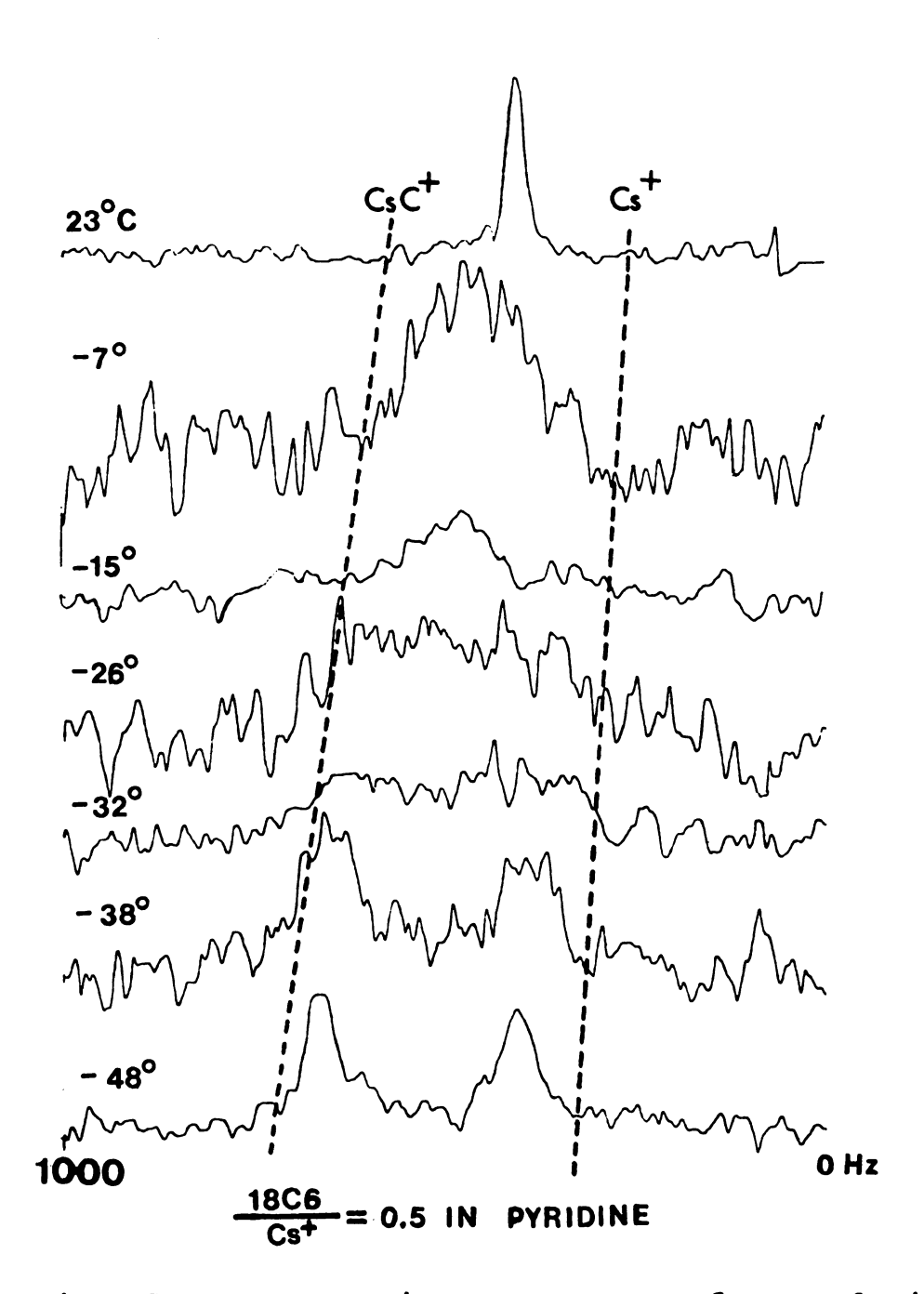


Figure 46. Spectra at various temperature for a solution of 0.01 M CsTPB and 0.005 M 18C6 in pyridine. The linewidth at coalescence were ~400 Hz. This fact and the low concentration lead to the poor S/N. The dotted lines show the chemical shifts of CsC⁺ and Cs⁺ in the absence of exchange.

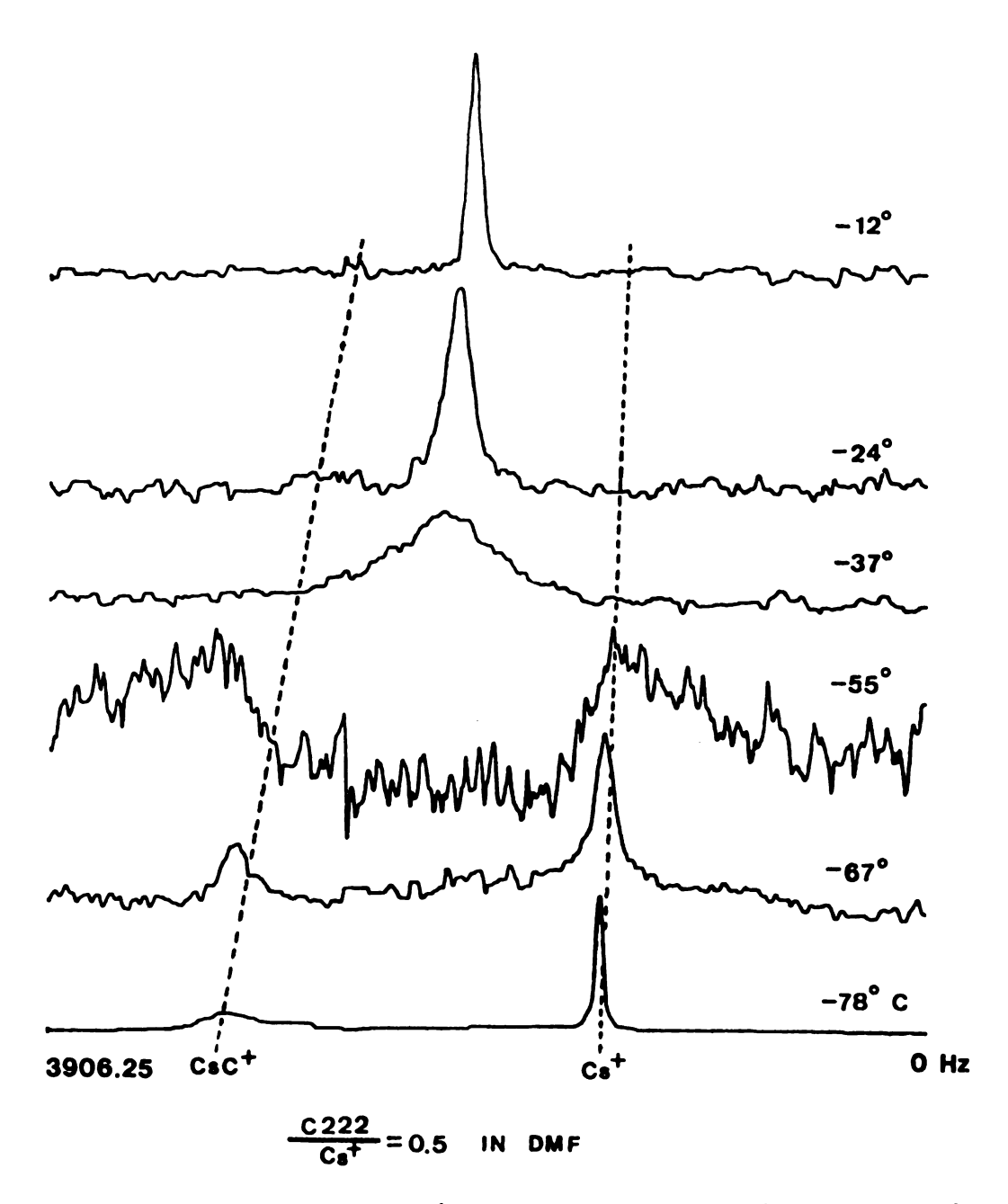


Figure 47. Spectra at various temperatures for a solution containing 0.02 M CsTPB and 0.01 M C222 in DMF. The dotted lines show the chemical shifts of CsC⁺ and Cs⁺ in the absence of exchange.

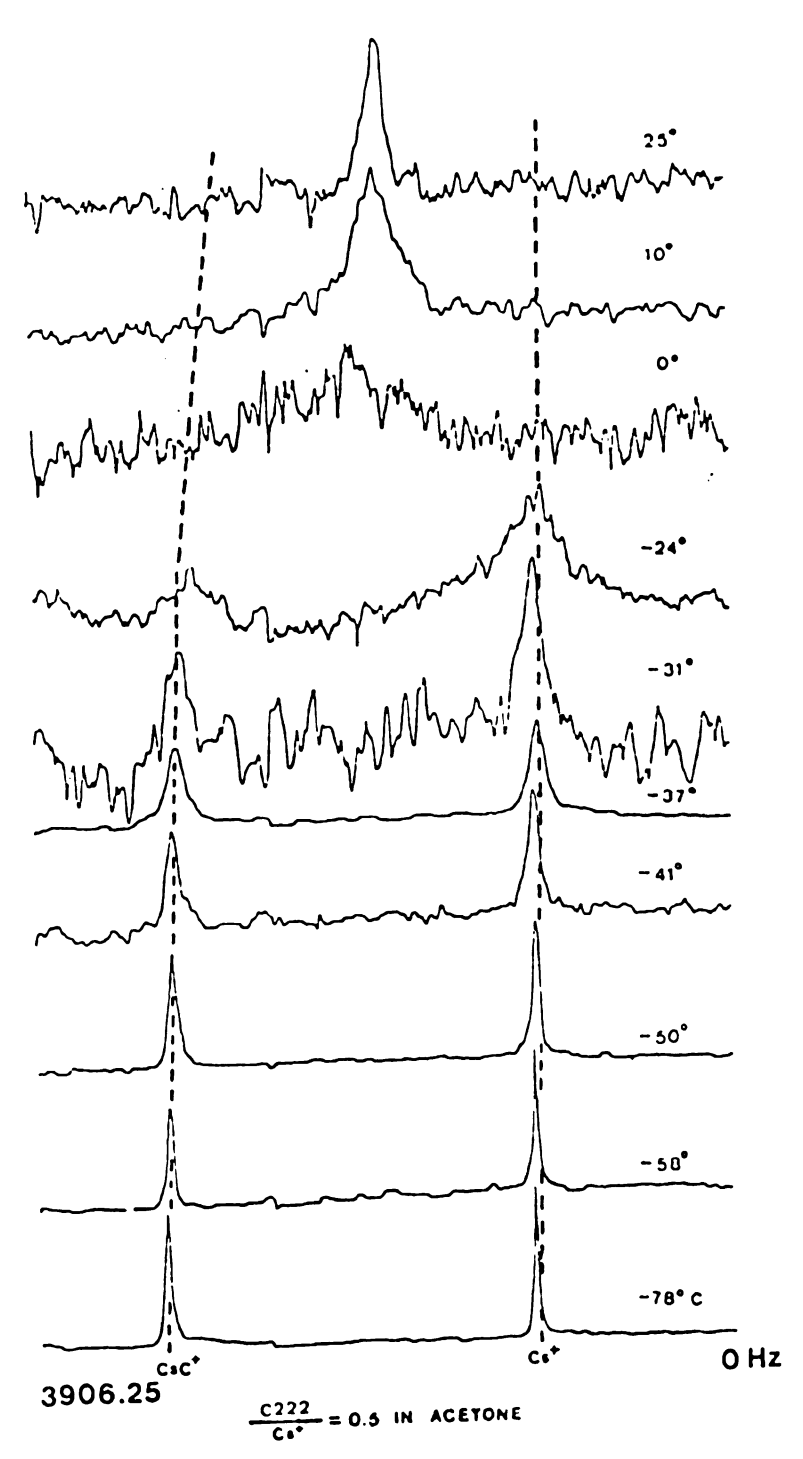


Figure 48. Spectra at various temperature for a solution containing 0.02 M CsTPB and 0.01 M C222 in acetone. The dotted lines show the chemical shifts of CsC⁺ and Cs⁺ in the absence of exchange.

Table 39. Temperature Dependence of the Transverse Relaxation Times of Free and 18C6-Complexed Cesium Cations in Pyridine.

Temperature °C	$^{ ext{Cs}\phi}_{ extbf{4}}^{ extbf{B}}$ $^{ extbf{ iny 2}}_{ ext{2}}(ext{sec})$	Temperature °C	Cs ⁺ ·18C6 T ₂ *(sec)
-47	0.021 (0.003)	-47	0.05 (0.01)
-38	0.035 (0.007)	-38	0.07 (0.01)
-32	0.05 (0.01)	-32	0.07 (0.01)
-26	0.059 (0.007)	-26	0.087 (0.008)
-15	0.087 (0.008)	-15	0.10 (0.01)
-7	0.007 (0.01)	-7	0.07 (0.01)
9	0.08 (0.01)	9	0.08 (0.01)
23	0.072 (0.008)	23	0.10 (0.01)

NOTE: $T_{2(ref)} = T_{2(inh)} = 0.1453 \text{ sec.}$

Table 40. Temperature Dependence of the Transverse Relaxation Time of Free and Complexed (C222) Cesium Cations in DMF

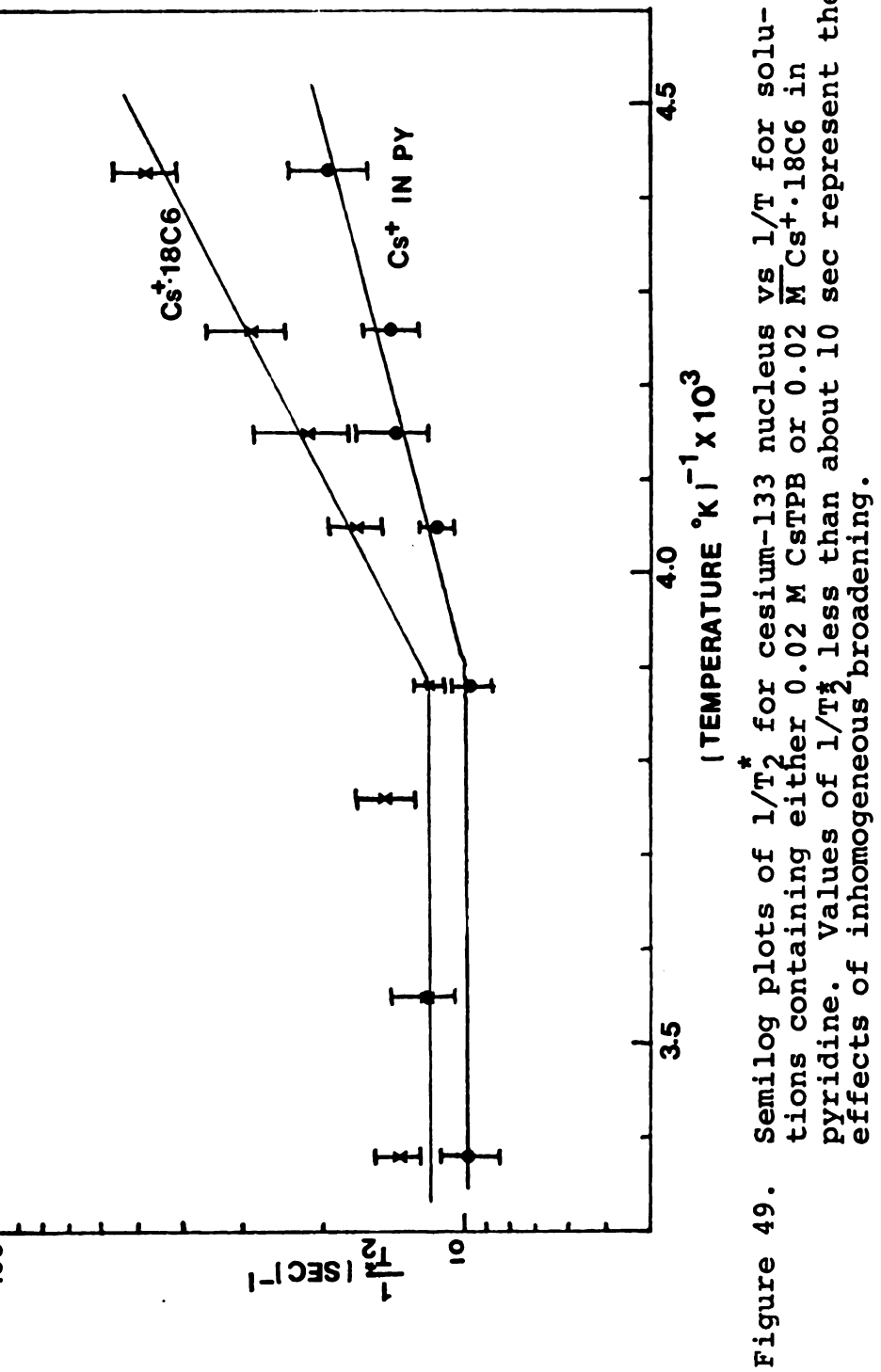
	Temperature °K	T [*] (sec)	
(A)	Cs ⁺		
	297	0.111 (0.009)	
	279	0.12 (0.01)	
	251	0.115 (0.006)	
	234	0.117 (0.007)	
	220	0.104 (0.00)	
	209	0.073 (0.005)	
(B)	Cs [†] ·C222		
	301	0.03 (0.01)	
	287.5	0.0230 (0.009)	
	264.5	0.014 (0.003)	
	243	0.007 (0.001)	
	226	0.004 (0.001)	
	209	0.0019 (0.0005)	

NOTE. $T_{2(ref)} = T_{2(inhomogeneous)} = 0.1305 sec.$

Table 41. Temperature Dependence of the Transverse Relaxation Time and Complexed (C222) Cesium Cations in Acetone.

	Temperature ^o K	T ₂ *(sec)	
(A)	Cs ⁺		
	297	0.11 (0.01)	
	285	0.0 (0.01)	
	273	0.09 (0.01)	
	253	0.084 (0.007)	
	242	0.072 (0.005)	
	232	0.065 (0.005)	
	216	0.082 (0.006)	
	200	0.103 (0.007)	
(B)	Cs ⁺ ⋅C222		
	297	0.067 (0.007)	
	280	0.048 (0.003)	
	273	0.043 (0.006)	
	260	0.03 (0.005)	
	249	0.040 (0.003)	
	236	0.031 (0.004)	
	223	0.028 (0.002)	
	207	0.020 (0.001)	
	195	0.015 (0.001)	

NOTE: $T_{2(ref)} = T_{2(inh)} = 0.1632 \text{ sec.}$



sec represent the

Table 42. Temperature Dependence of the Exchange Time in the Presence of 18C6 in Pyridine and the Corresponding Reciprocal Transverse Relaxation Times of Cs⁺ (A) and CsC⁺ (B).

remperature °C	τ (msec)	$\frac{1}{^{\mathrm{T}}2\mathrm{A}}(\mathrm{sec})$	$\frac{1}{T_{2B}}(sec)$
-47	4.9 (0.7) ^b	19.19	47.39
-38	2.6 (0.5)	15.20	28.65
-32	1.4 (0.2)	13.50	21.65
-26	1.0 (0.2)	11.79	16.95
-15	0.4 (0.1)	9.83	11.49
-7	0.4 (0.1)	9.83	14.58
9	0.14 (0.03)	9.83	12.15
23	0.06 (0.01)	9.92	13.86

 $a_{0.01}$ M CsTPB + 0.005 M 18C6.

bStandard deviation.

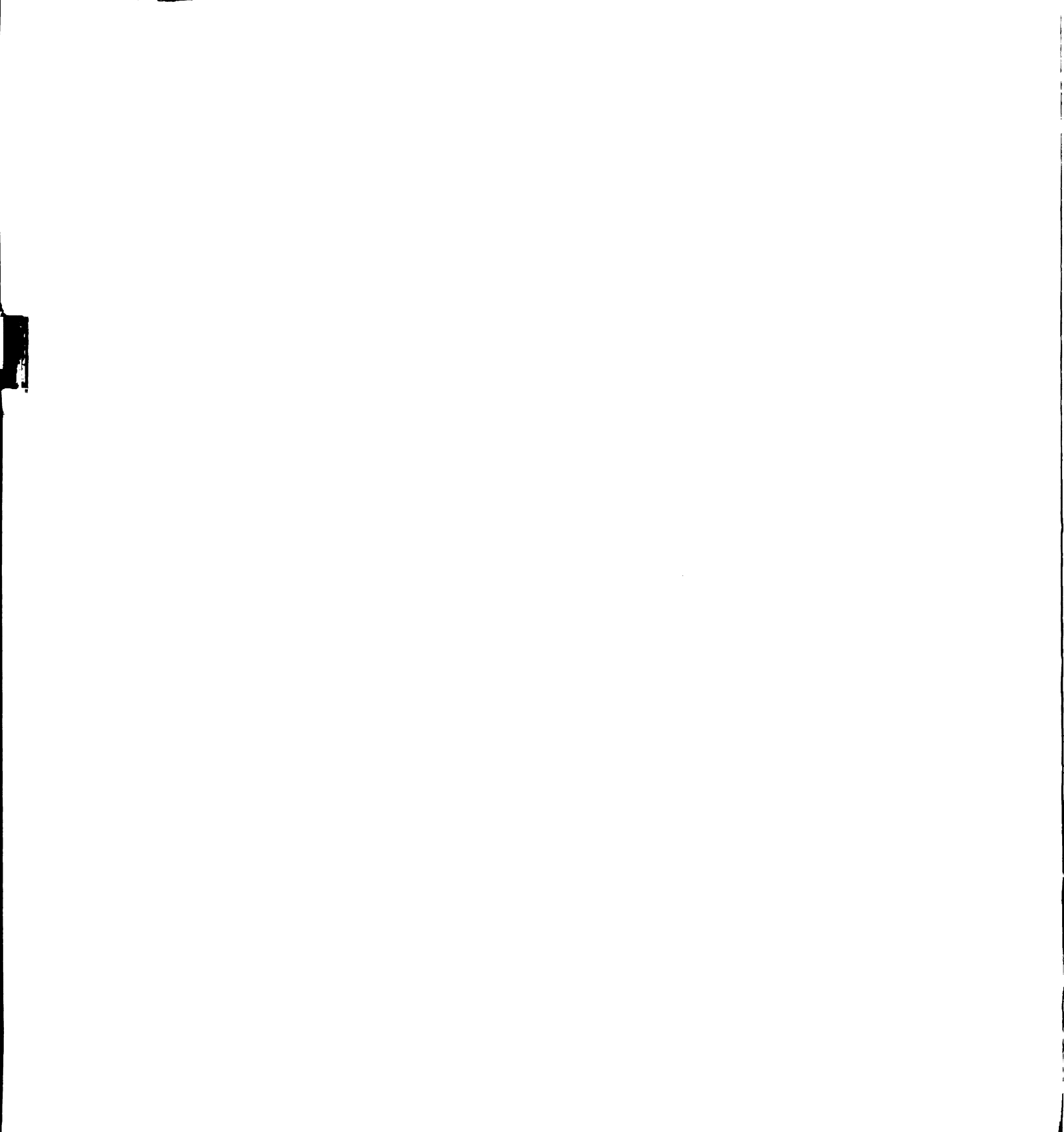


Table 43. Temperature Dependence of the Exchange Time in the Presence of C222 in Acetone and the Corresponding Reciprocal Transverse Relaxation Times of Cs⁺ (A) and CsC⁺ (B).a

			
Temperature °C	τ (msec)	1 T _{2A} (sec)	$\frac{1}{T_{2B}}(sec)$
Experiment No.	<u>1</u>		
10	2.1 (0.2) ^b	0.1042	0.0526
0	16 (8)	0.0971	0.0476
-24	63 (16)	0.769	0.0357
-37	233 (25)	0.0676	0.0299
-50	240 (24)	0.0741	0.0244
-78	1207 (100)	0.1064	0.0147
Experiment No.	2		
*24	1.4 (0.2)	0.0300	0.0244
12	2.2 (0.8)	0.1031	0.0541
*0.7	3.4 (0.5)	0.0276	0.022
-31	107 (17)	0.0718	0.0323
-41	217 (33)	0.0646	0.0282
-58	423 (61)	0.0823	0.0213
-73	1759 (95)	0.1033	0.0161

^{*}Exponential multiplication was used (TC = -5).

^a0.02 CsTPB + 0.01 C222.

bStandard deviation.

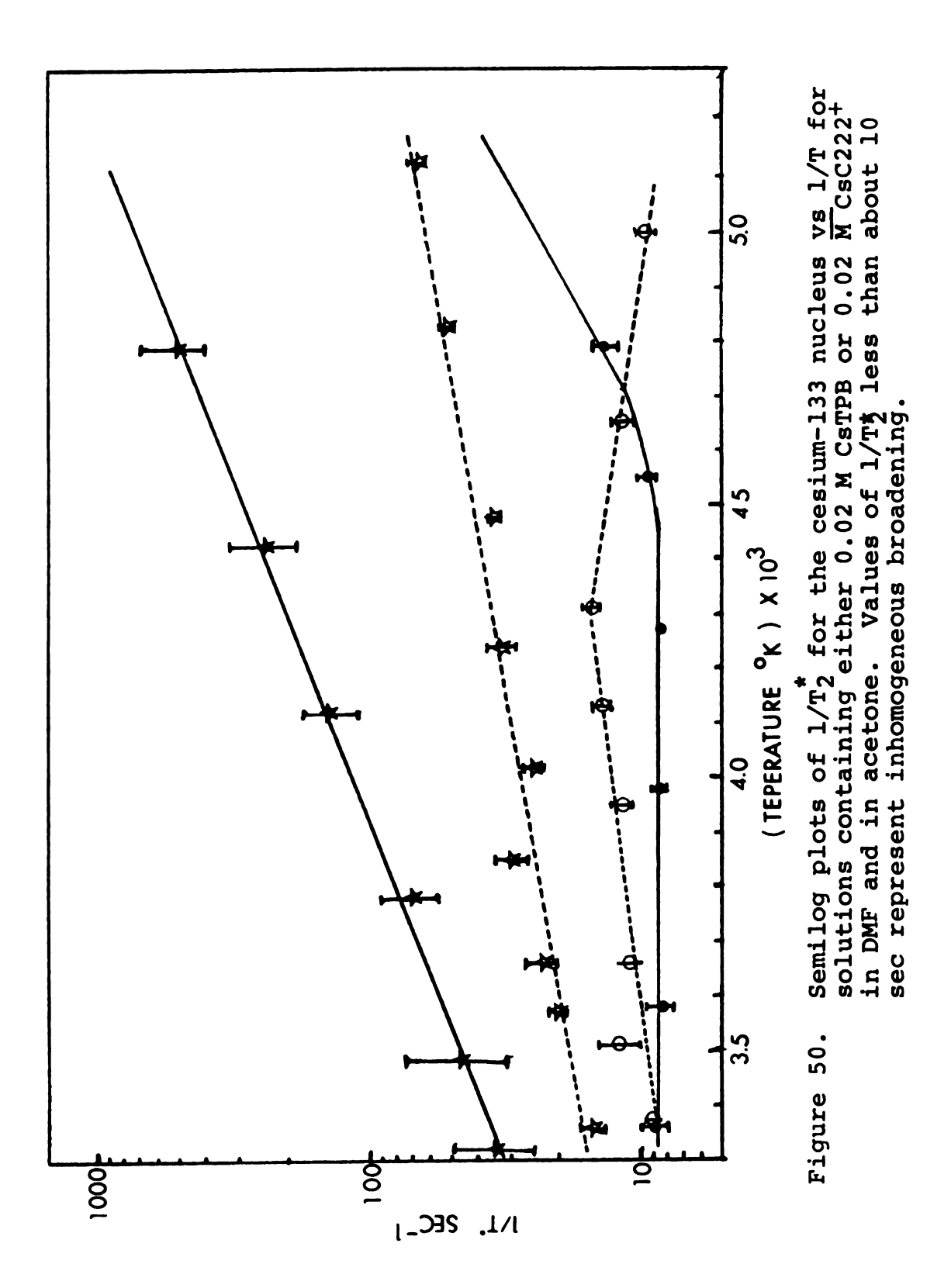
Table 44. Temperature Dependence of the Exchange Time in the Presence of C222 in DMF and the Corresponding Reciprocal Transverse Relaxation Times of Cs⁺ (A) and CsC⁺ (B).a

emperature °C	τ (msec) $x10^2$	$\frac{1}{T_{2A}}(sec)$	$\frac{1}{T_{2B}}(sec)$
-8	0.26(0.02) ^b	0.116	0.0133
-12	0.61 (0.07)	0.1163	0.0119
-20	0.8 (0.2)	0.116	0.0095
-24	1.31 (0.35)	0.1163	0.0085
*-31	1.8 (0.1)	0.116	0.0056
-37	4.9 (0.9)	0.1163	0.0057
*-55	44 (9)	0.0290	0.0086
-67	288 (33)	0.0606	0.0019
-78	1944 (123)	0.0294	0.001

^{*}Exponential multiplication was used (TC = -5)

 $^{^{}a}$ 0.02 M CsTPB + 0.01 M C222.

bStandard deviation.



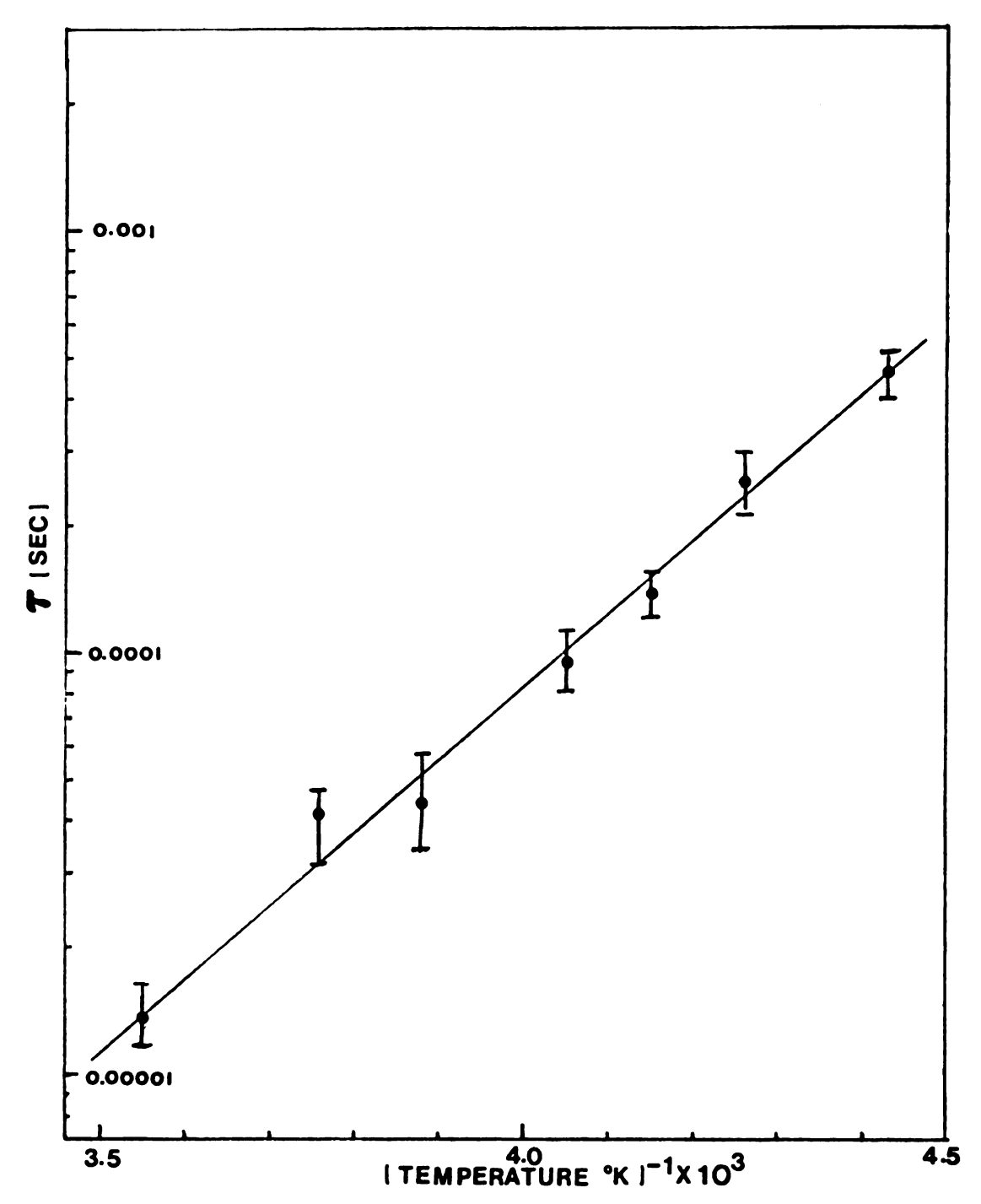


Figure 51. Arrhenius plots of τ (exchange time for Cs⁺ ion from 18C6) in pyridine.

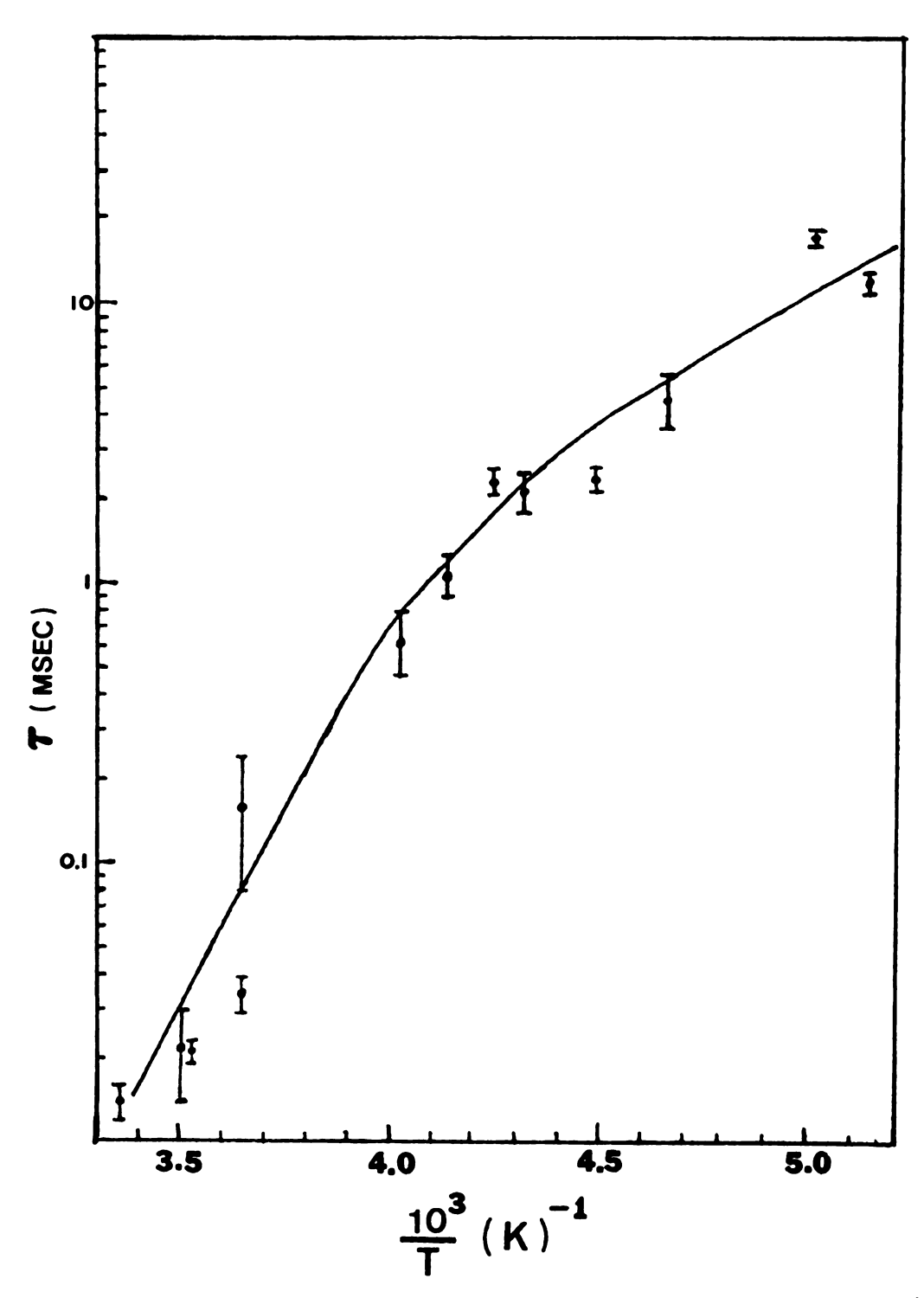


Figure 52. Arrhenius plots of τ (exchange time for Cs⁺ ion from the ligand C222) in acetone solution.

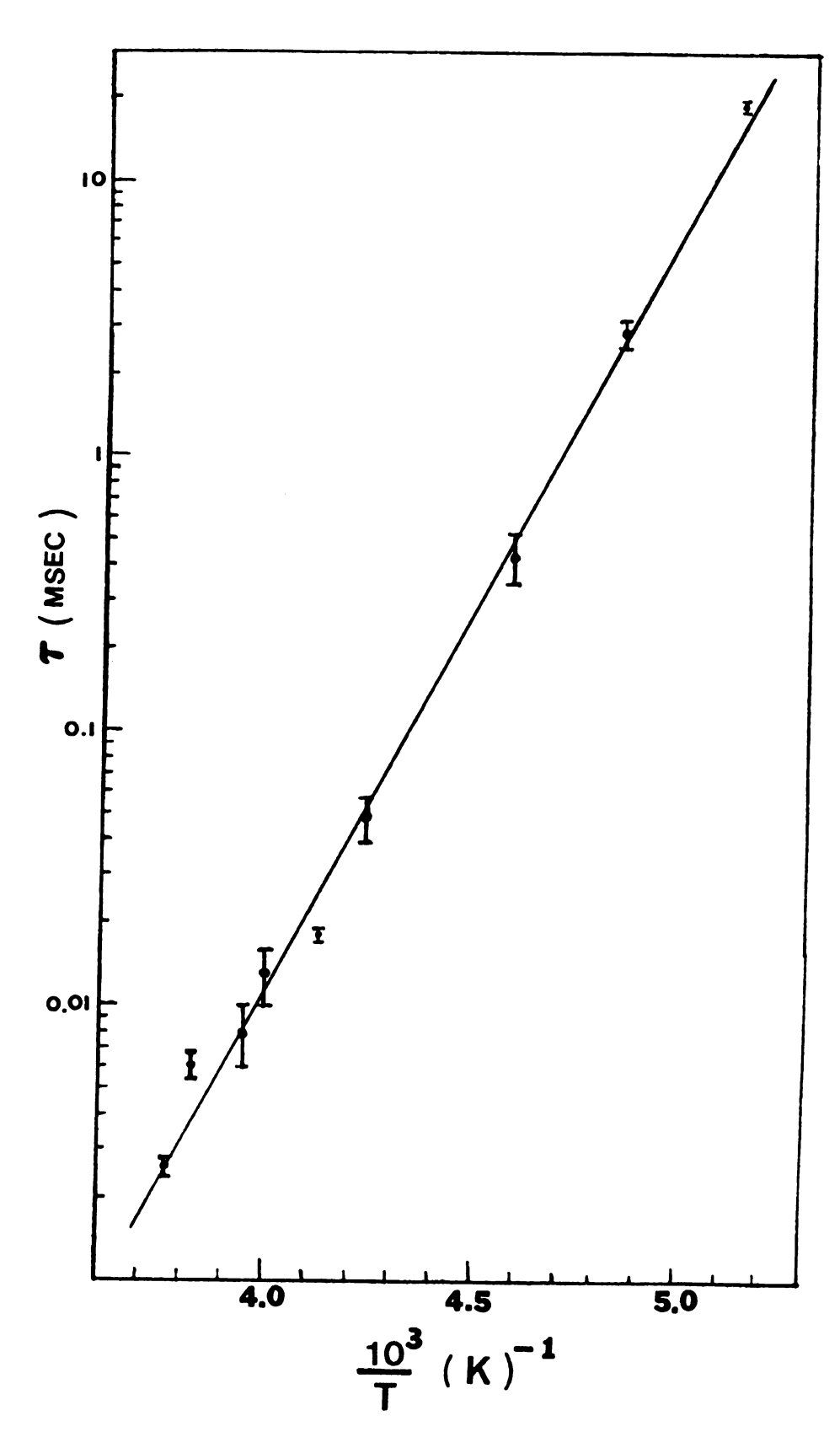


Figure 53. Arrhenius plot of τ (exchange time for Cs⁺ ion from C222) in DMF solution.

and will be discussed in the next chapter.

The activation parameters for the release of Cs⁺ by 18C6 in PC and pyridine are listed in Table 45. The E_a values for both cases are similar; however, the big standard deviations make the meaning of the difference questionable. Previously, Cahen had observed (6) in the Licryptate study that the activation energy increases with increasing donicity, opposite to the overall energy change. Therefore, he concluded that the transition state must involve substantial ionic solvation. In the present study such an effect seems to be small.

(C) DISCUSSION

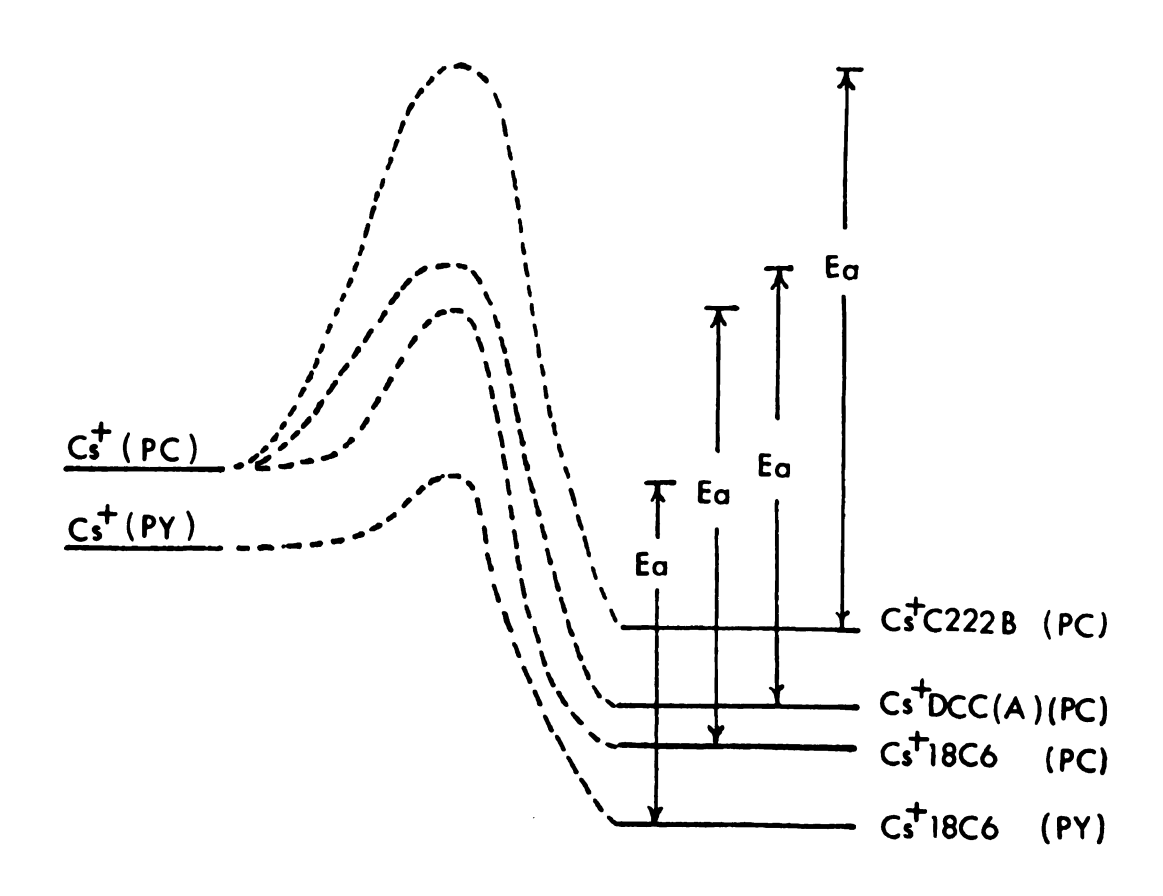
Shporer and coworkers (4,5) studied the dynamics of complexation of Na⁺ by DCC in DMF and methanol and reported E_a values of 8.3 ±1. (Kcal/mole) in both solvents, while for the complexation of Na⁺ or K⁺ with DBC in methanol the E_a values are 12.6 ± 1. (Kcal/mole) for both cations. Therefore, they concluded that the complexation reaction of Na⁺ with DBC has a larger activation energy than with DCC because of the higher steric hinderance of DBC, they also concluded that there is no solvent effect since the activation energies for Na⁺ complexes with DCC in MeOH happen to be the same. The value of E_a found by Shporer and coworkers for Na⁺-DCC in methanol is about the same as we have found for Cs⁺-18C6 in pyridine. However this

Table 45. Exchange Rates and Thermodynamic Parameters of 18C6 Complex Exchange in Propylene Carbonate and Pyridine.

Activation Parameters	PC	Pyridine
		- /
Ea		
(Kcal/mole)	8.0±4.0	8.04±0.27
k _b x10 ⁻³ at 298°K (sec ⁻¹)	50.0±4.0	8.9 ±0.8
H [≠] Kcal/mole)	7.41±4.0	7.5±0.3
s≠		
cal/ K mole)	-12.2 ± 0.2	-15.5±0.2
G≠ o Kcal/mole)		
98°K	14 ±4.0	12.1±0.4

could be coincidental because of the compensation of several factors which affect the activation energy. For instance, 18C6 has less rigidity in the ring than does DCC, but a larger cation such as Cs⁺ might introduce a higher activation energy. Therefore, a coincidence could occur by compensation of the ligand effect and cation effect and solvent effect. In other words, the factors which affect the reaction rate are complex, and conclusions cannot easily be based upon comparisons made with very different systems.

Together the solvent effect and the ligand effect of the complexation reaction can be represented by the reaction profile drawn below:



CHAPTER V

A CESIUM-133 NMR STUDY OF THE COMPLEXATION OF

CESIUM TETRAPHENYLBORATE BY C222:

DISCUSSION OF THE TYPES OF COMPLEXES

I. INTRODUCTION

The diameter of the cesium ion (3.3 Å) is larger than the estimated diameter of the C222 cavity (2.8 Å). However, an X-ray study of the solid complex (55) showed that the cesium ion can be accommodated into the cavity of C222. In the present chapter the discussion will focus on the nature of binding of Cs⁺ to C222 in solution.

II. EVIDENCE FOR TWO TYPES OF CRYPTATE COMPLEXES

Inclusive cryptate complexes were first designated by Lehn (50) with the mathematical symbol $(\underline{e.g.}, M^+ \subset L)$. It was considered that whenever the cavity diameter of the cryptand (L) is larger than or equal to the diameter of the metal ion (M^+) , inclusive complexes are formed in which the cation is situated within the cavity. However, in the present discussion, we need to include other possibilities. The symbol $M^+ \subset L$, will be used to designate a complex in which M^+ is located entirely within the cavity (inclusive complex). By contrast, whenever a complex is formed in which the metal ion only partially penetrates into the cryptand cavity it will be called an exclusive complex and designated as $M^+ \cup L$.

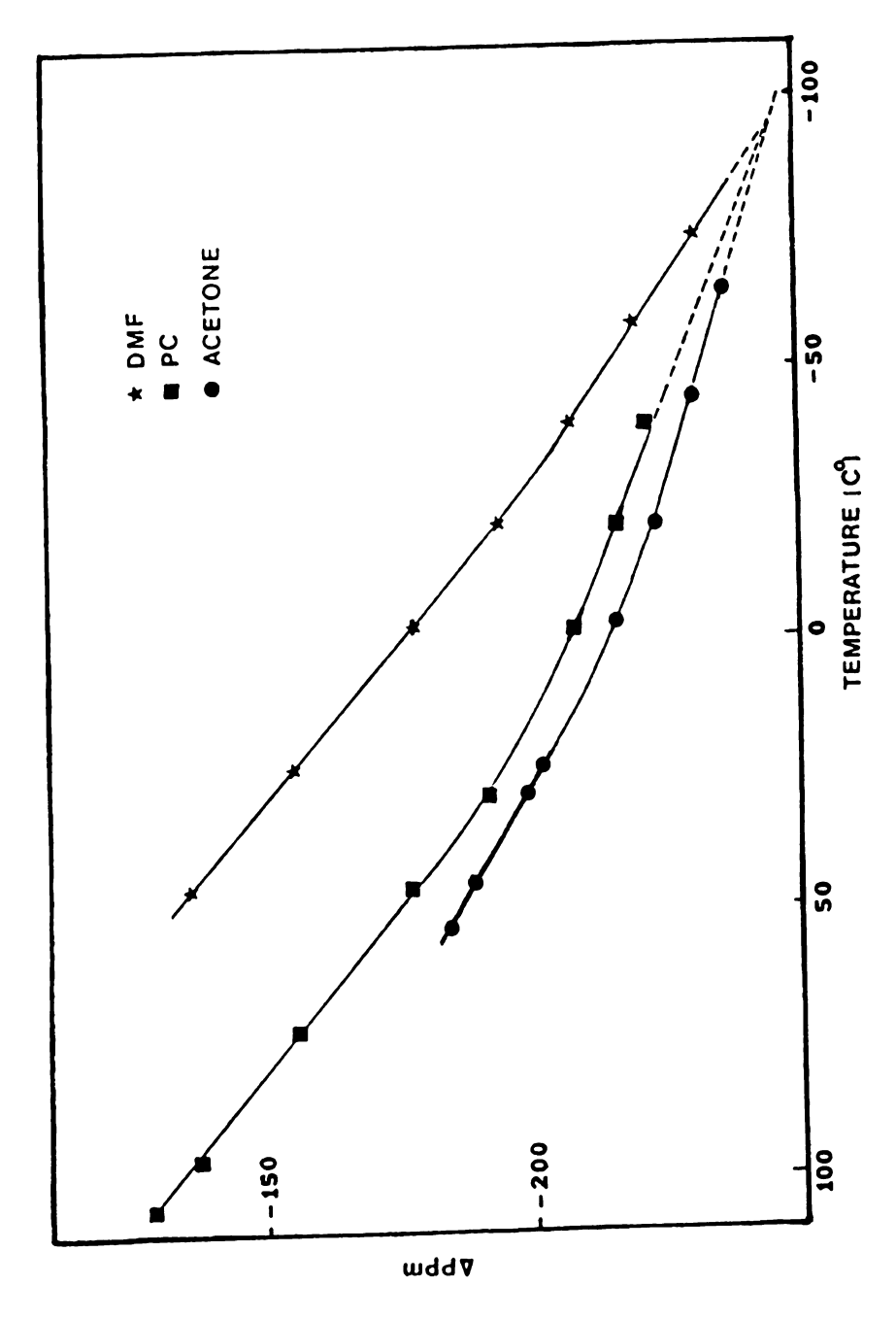
It has already been mentioned in previous chapters that the reaction of Cs⁺ with [2]-cryptands seems to give more than one type of complex. A summary of the observations

which support this speculation are as follows:

(1) The limiting chemical shift of Cs⁺-C222 (measured directly at large ligand/Cs⁺ ratio or obtained as a parameter from data fitting) is very solvent dependent at room temperature as shown below.

Solvent PC Acetone MeCN DMF DMSO Pyridine (Appm) 1 m -193.8 -203.0 -210.4 -155.8 -144.3 -224.3

- (2) The limiting chemical shifts are also temperature dependent, as shown in Figure 54. A special feature is that the extent of variation with temperature decreases at low temperatures eventually extrapolating to the same Cs⁺ chemical shift in all solvents. By contrast Cs⁺ · (18C6)₂ complexes for example, show neither solvent dependence nor temperature dependence of the chemical shift. We would expect Cs⁺ inside of a C222 cavity to be well-shielded from the influence of the solvent.
- (3) The spectra obtained with samples which have only enough C222 to complex half of the Cs⁺ (<u>i.e.</u> C222/(Cs⁺)_t = 0.5) in five solvents were collected at various temperatures including temperatures low enough to be at the slow limit of the exchange process. As shown in Figure 55, the chemical shifts for the complexed Cs⁺ at low temperatues have about the same value. However, in PC and in DMF solutions the linewidth of



A plot of limiting chemical shift of Cs[†]C222 in DMF, PC and acetone vs temperature. The extrapolations (dotted lines) for all three solvents converge to the same value. Figure 54.

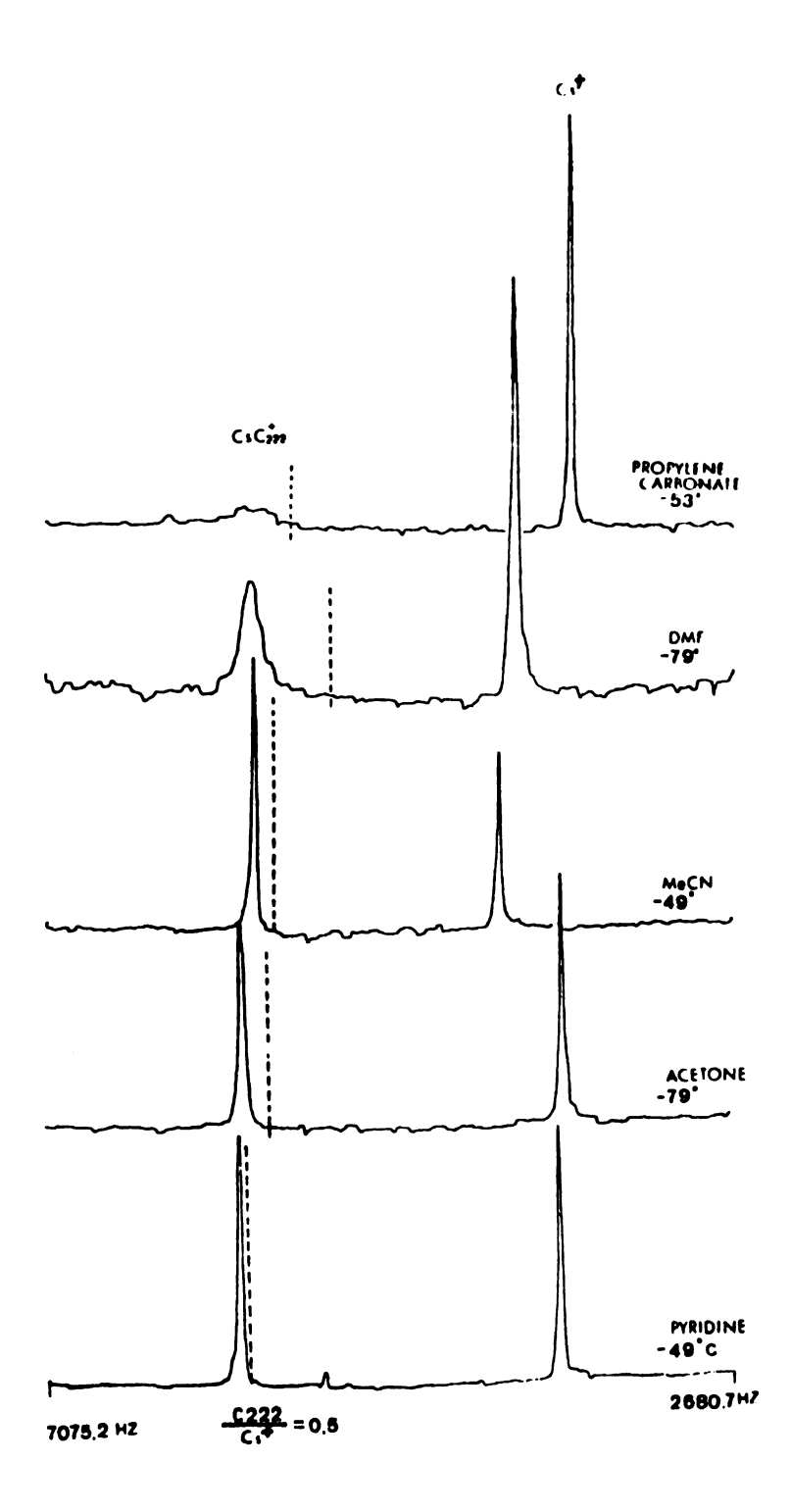


Figure 55. Spectra of solutions which contain the Cs⁺C222 complex and uncomplexed Cs⁺ at low temperatures in five solvents. The dotted lines indicate the resonance frequency of CsC222⁺ at room temperature.

the CsC222⁺ peaks are much broader than in the other solvents. The fact that the chemical shifts of CsC222⁺ are solvent independent at low temperatures is taken to indicate that the complex is inclusive. The broad linewidths of CsC222⁺ in PC and DMF may indicate the presence of slow exchange between the inclusive and the exclusive complexes.

Based on the above observations, an effort was made to examine the data presented in Chapters 3 and 4 to see if they are consistent with the assumption that two types of complexes are found.

The proposed reactions which involve the two types of complexes are as follows:

$$Cs^{+} + C \rightleftharpoons Cs^{+} \cup C \rightleftharpoons Cs^{+} \subset C$$
(exclusive) (inclusive)

where C denotes [2]-cryptand. At a given temperature the observed chemical shift is given by

$$\delta_{obs} = \delta_{F} X_{F} + \delta_{i} X_{i} + \delta_{e} X_{e}$$
 (V.2)

where the subscripts e and i refer respectively to the exclusive and the inclusive complexes. The apparent equilibrium constant, K, is given by

$$K = [CsC^{+}]/[Cs^{+}][C]$$
 (V.3)

while

$$K_1 = [Cs^{\dagger}U C]/[Cs^{\dagger}][C]$$
 (V.4)

and

$$[cs^{\dagger} \subset c] = [cs^{\dagger} \cup c] \cdot \kappa_2 \tag{V.5}$$

80

$$[cs^{+}c]_{total} = [cs^{+}Uc] + [cs^{+}c]$$

$$= K_{1}[cs^{+}][c] + K_{1}K_{2}[cs^{+}][c]$$

$$= [cs^{+}][c]K_{1}[1 + K_{2}] \qquad (v.6)$$

Therefore

$$K = K_1[1 + K_2] \qquad (V.7)$$

It is seen from the above results that at a given temperature, chemical shift studies would not yield separate values of K_1 and K_2 . However, additional information can be obtained from a study of the temperature dependence. Since we can suppress the effect of K_1 by studying the limiting chemical shift at high $(C)/(Cs^+)$ ratios, the temperature dependence

of the limiting shift might reflect the temperature dependence of K_2 and permit its determination. This will only be true if the variations of δ_e and δ_i with temperature are small compared with the variation of the weighted-average limiting chemical shift. From the solvent-independent limiting shift at low temperatures one can find the chemical shift of the inclusive complex (-245 ppm) with some confidence. However, it is difficult to find the characteristic chemical shift for the exclusive complex.

As a first approximation it was assumed that the chemical shift of the 1:1 complex with 18C6 in the solvent under study is the same as the chemical shift of the exclusive complex. Having estimated these two chemical shifts, $\delta_{\rm e}$ and $\delta_{\rm i}$, it is possible to determine ΔH_2 , the enthalpy change due to the conversion of the exclusive to the inclusive complex.

For the limiting case where the analytical concentration of the cryptand is much larger than that of Cs⁺ ion, the concentration of free Cs⁺ must be negligible. Consequently, the observed limiting chemical shift is given by $\delta_{\rm obs}$ = $\delta_{\rm e} X_{\rm e} + \delta_{\rm i} X_{\rm i}$, or

$$\delta_{\text{obs}} = \delta_{e} (1 - X_{i}) + \delta_{i} X_{i} = X_{i} (\delta_{i} - \delta_{e}) + \delta_{e}$$
 (V.8)

so that

$$X_{i} = \frac{\delta_{obs}^{-\delta} e}{\delta_{i}^{-\delta} e}$$
 (V.9)

and

$$x_{e} = \frac{\delta_{i}^{-\delta}obs}{\delta_{i}^{-\delta}e}$$
 (v.10)

Since the concentration of free cesium ions is negligible, only one equilibrium is involved, i.e.,

$$[Cs^{+}U C222] \stackrel{K_{2}}{+} [Cs^{+}C C222]$$
 (V.11)

and

$$K_2 = \frac{X_i}{X_e} = \frac{\delta_{obs} - \delta_e}{\delta_i - \delta_{obs}}$$
 (V.12)

Therefore, from each $\delta_{\rm obs}$ value at a given temperature, a corresponding $\rm K_2$ value can be obtained. From the temperature dependence of $\rm K_2$, the enthalpy change, $\Delta \rm H_2$ can be calculated (Equation III.17) by using the KINFIT program. Since we arbitrarily chose $\delta_{\rm e}$ to be the same as the chemical shift of $\rm Cs^+ \cdot 18C6$, it is important to test the sensitivity of the calculated value of $\Delta \rm H_2$ to the value of $\delta_{\rm e}$ chosen. The highest value used was 20 ppm above the value for the 18C6 complex and the lowest was that found for C222B complexes. The results are given in Table 46.

It is obvious that ΔH_2 is not very sensitive to the choice of δ_e . It is also small and insensitive to the solvent. By using the chemical shift of $Cs^+ \cdot 18C6$ for δ_e , we obtain K_2 at each temperature and from the apparent formation

Table 46. Test of the Dependence of the ΔH_2 Value on δ_e .

δe	ΔH ₂ (Kcal/mole)
8.1	-2.9±0.1
28.	-2.8±0.1
-52.6	-3.3±0.2
6.4	-2.5±0.1
-53.6	-2.7±0.1
-3.37	-2.6±0.1
-51.8	-2.8±0.1
	8.1 28. -52.6 6.4 -53.6 -3.37

constants (listed in Chapter III) at the corresponding temperature, we can also calculate K_1 and thus ΔH_1 . The calculated results are listed in Table 47.

Table 47. Estimated Enthalpies of Formation of the Exclusive (ΔH_1) and Inclusive (ΔH_2) in Acetone, PC and DMF.

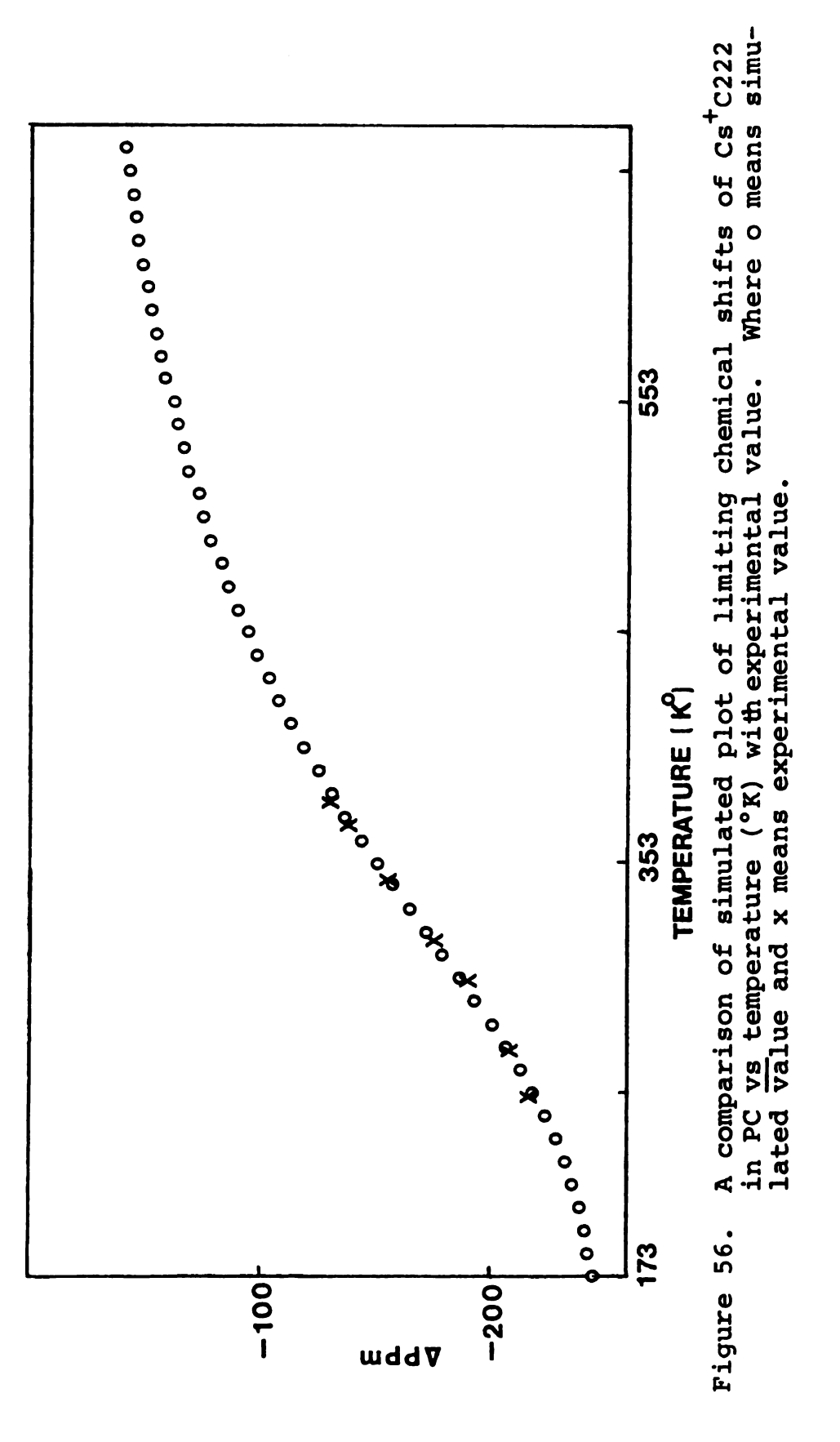
Solvent	ΔH ₁ (Kcal/mole)	ΔH ₂ (Kcal/mole)	ΔH _t (Kcal/mole)
Acetone	-12.9	-2.5	-15.4
PC	-8.6	-2.9	-11.5
DMF	-5.7	-2.6	-8.3

It is interesting to note that ΔH_2 is essentially insensitive to the solvent. This agrees with the model, since, when the exclusive complex is formed, most of the solvent sheath has already been displaced by the cryptand molecule. Simulation of the limiting chemical shift vs. temperature for the range from -100°C to 500°C was done for the three solvents. From Figure 56, a typical example, one can see why it is not possible to obtain δ_2 , ΔH_2 and ΔS_2 by fitting the data with program KINFIT. If the model and the parameters used for simulation are correct, we have examined only a small region of the temperature range over which the inclusive # exclusive equilibrium exists. The required extrapolation to obtain $\delta_{\mathbf{p}}$ is far beyond the temperature region which is susceptable to experiment. From a comparison of ΔH_1 and ΔH_2 and the slow variation of K_2 with temperature, it is also evident why a plot of log K vs 1/T gives a straight line even when K is a function of K_1 and K_2 . The value of ΔH_2 is so small that variations of the inclusive to exclusive ratio with temperature would lead to only a slight curvature of the plot of log K vs 1/T.

It is also interesting to examine the entropy changes. The factors which determine the change of entropy on complexation can be expressed as

$$\Delta S = \Delta S_{S} + \Delta S_{C} + \Delta S_{n} \qquad (V.13)$$

in which $\Delta S_{\mathbf{g}}$ is the net entropy change due to changes in



solvation between the complexed ion, the free salt and the free ligand, $\Delta S_{_{\rm C}}$ is the net entropy change due to conformational changes, and $\Delta S_{_{\rm R}}$ is the change in entropy caused by a change in the total number of particles. In ${\rm Cs}^+-[2]{\rm cryptate}$ complexation, $\Delta S_{_{\rm R}}$ should be nearly independent of the type of complex formed, and it will be left out of the present discussion. The term $\Delta S_{_{\rm S}}$ is probably positive because of the displacement of the well-ordered solvation shell of the cation (except for a highly structured solvent). The $\Delta S_{_{\rm C}}$ term is likely to be negative because of the decrease in the flexibility of the cryptand when it forms a complex. According to these arguments, we expect ΔS to be negative for the conversion of the exclusive to the inclusive complex. This speculation fits the estimated entropy changes given in Table 48.

Table 48. Estimated Entropy Values for the Complexation Reaction at 298°K.

Solvent	ΔS ₁ (e.u.)	ΔS ₂ (e.u.)	ΔS(e.u.)
PC	-13.7	-7.0	-20.7
Acetone	-26.8	-5.6	-32.4
DMF	-11.2	-7.6	-18.8

It is interesting to note that ΔS_1 is strongly solvent dependent, but that ΔS_2 is much less dependent on the solvent.

The existence of two types of complexes in the solution would also be expected to affect the apparent activation energy. Indeed, we obtained anomalous Arrhenius plots as shown in Figures 45 and 52. The curved Arrhenius plots for the acetone and PC cases could result if the exchange process involves more than two sites. If we assume that the reaction actually occurs in two steps as given by Equation V.1 then the activation energy for dissociation of the exclusive complex must be higher than that for the interconversion of the two complexes. This phenomenon is shown by a collapse of the single line at low temperatures into two lines, one of which occurs at the chemical shift value of the free ion. If at low temperatures, the second reaction becomes slow, then a broadening of the line for the complex will occur which will give an anomalously large value of t when only the two-site exchange process is considered. It is simply not valid to use the twosite expression when the rate of conversion to a third site becomes slow.

This speculation is also reinforced by the exchange spectra of Cs⁺C222 in PC and acetone at various temperatures shown in Figures 37 and 48. It is interesting to note that at low temperatures when the exchange rate between free and complexed ions is slow enough to permit observation of

two distinct peaks as the temperature is lowered, the complexed cesium peak is first broad, then narrow and finally again becomes broad. This effect is especially pronounced in PC solutions. The broadening of the signal for the complexed Cs^+ species could be caused by a slowing down of the exchange equilibrium, $[Cs^+ \cup C]^+$ $[Cs^+ \subset C]$ at low temperatures.

The lineshape analysis for DMF solutions at various temperature also shows a broad Cs⁺C222 line at low temperature. However, it was found that the exchange process had not yet reached the slow exchange limit. This may be the reason why the Cs⁺C222 kinetics study in DMF gave a straight-line Arrhenius plot while it was curved in the other two solvents. The activation parameters for the exchange reaction in DMF were therefore calculated.

Table 49. Activation Parameters for the Release of Cs⁺ from Cs⁺C222 in DMF

 $E_a = 13.5 \pm 0.3 \text{ Kcal/mole}$ $(k_b)_{298} = (9 \pm 0.9) \times 10^6 \text{ sec}^{-1}$ $(\Delta G_O^{\neq})_{298} = 7.8 \pm 0.6 \text{ Kcal/mole}$ $\Delta H_O^{\neq} = 12.9 \pm 0.3 \text{ Kcal/mole}$ $\Delta S_O^{\neq} = 17 \pm 1 \text{ (e.u.)}$

CHAPTER VI SUMMARY AND SUGGESTIONS FOR FUTURE STUDIES

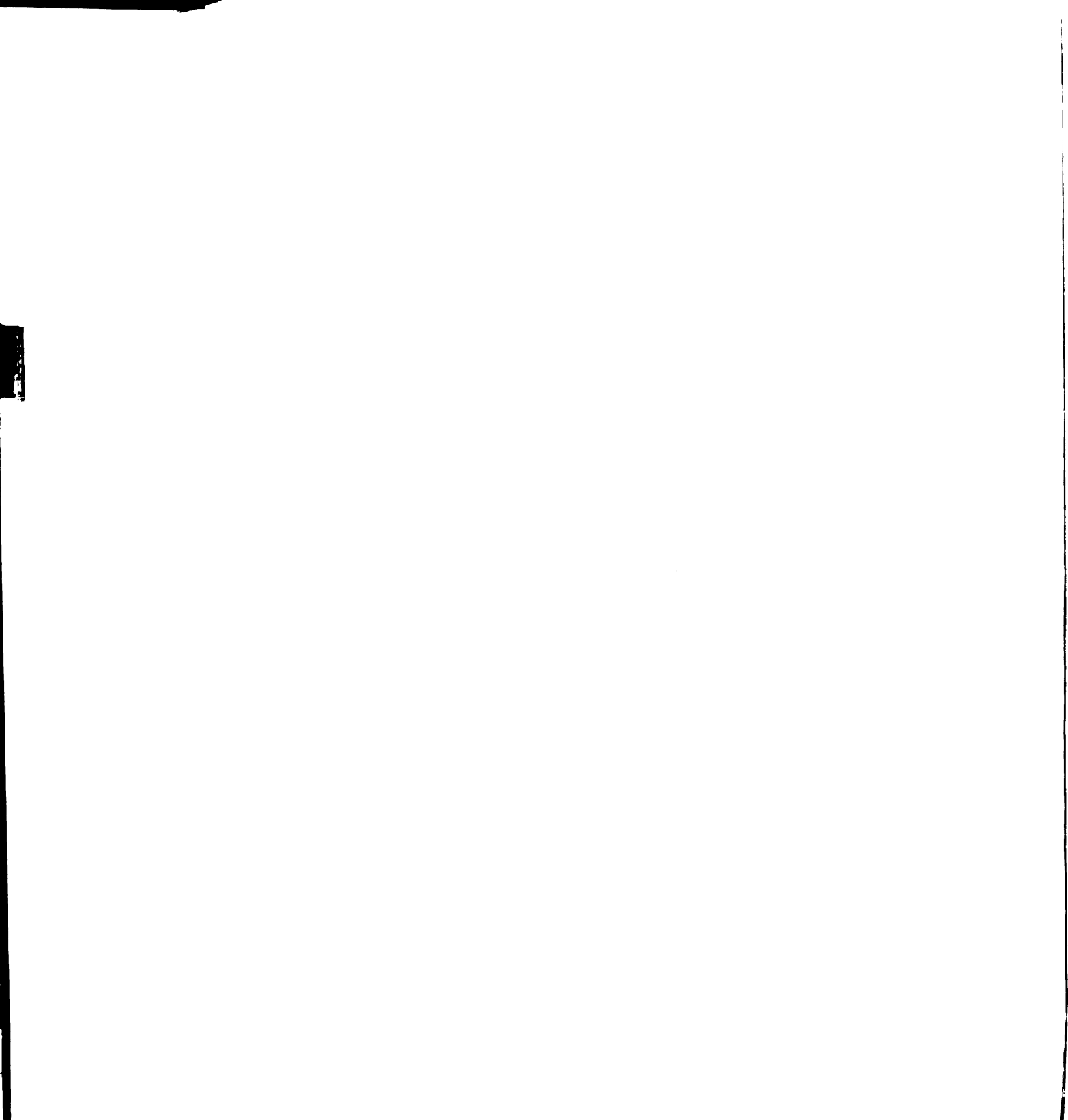
I. SUMMARY

Chemical shifts of the cesium-133 nucleus were measured in six nonaqueous solvents relative to 0.5 M aqueous cesium bromide. Cesium tetraphenylborate (CsTPB), triiodide and thiocynate were used to determine the infinite dilution chemical shifts in pyridine (PY), propylene carbonate (PC), dimethylformamide (DMF), dimethylsulfoxide (DMSO), acetonitrile (MeCN), and acetone. The corresponding ion-pair formation constants were determined from chemical shift-concentration data with the aid of a weighted non-linear least-squares program (KINFIT). The association constant for CsSCN in pyridine is 900±200 while for CsTPB in pyridine it is 370±20, in PC it is 16±7, in MeCN it is 40±10 and in acetone it is 22±3. The uncertainties given are standard deviation estimates.

Cesium-133 NMR studies were also performed on CsTPB complexes with five ligands in six nonaqueous solvents mentioned. These ligands were 18-Crown-6 (18C6), dibenzo-18C6 (DBC), dicyclohexyl-18C6 (DCC), cryptand-222 (C222) and monobenzo-C222 (C222B). These ligands have different topologies and substituents which affect the complexation ability. Cesium tetraphenylborate forms both 1:1 and 2:1 (ligand/Cs⁺) complexes with 18C6 in all six solvents with the first formation constant (K₁) larger than 10³. A new EQN subroutine of the KINFIT program was written to analyze data which show both 1:1 and sandwich complex (2:1) formation.

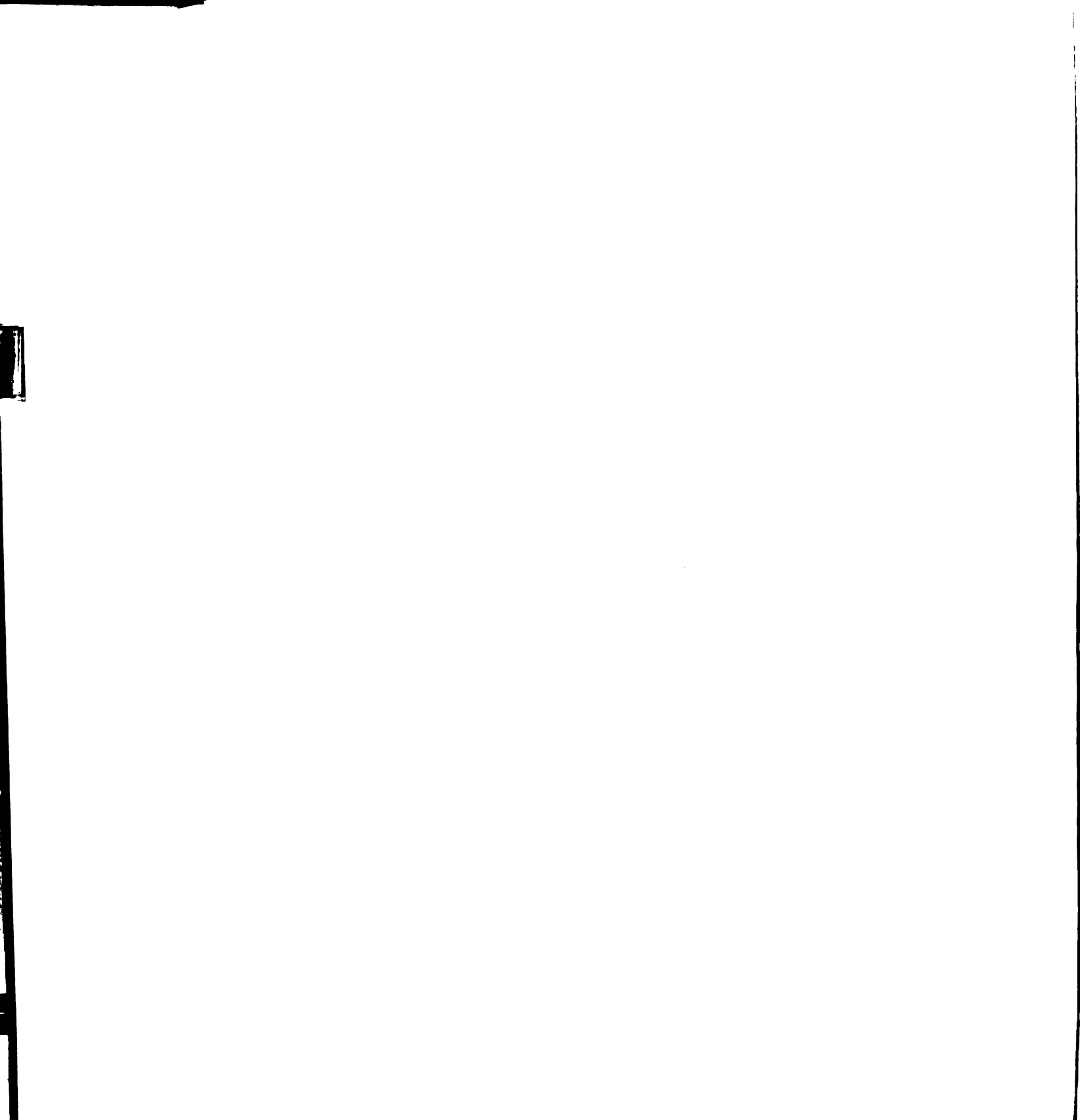
It was found that both K_1 and K_2 are affected by the geometry and substituents of the crown ligands. It was also shown that the solvent plays an important role in the equilibrium process. For example, the K values for 18C6 in six solvents are in pyridine $K_1 > 10^8$, $K_2 = 71\pm1$; in PC $K_1 = (1.5\pm0.6) \times 10^4$, $K_2 = 8\pm2$; in acetone $K_1 > 10^7$, $K_2 =$ 34 ± 0.5 ; in DMF K₁ = (9 ± 3) x 10^3 , K₂ = 2.44 ± 0.05 ; in DMSO $K_1 = (1.1\pm0.1) \times 10^3$, $K_2 = (1\pm0.4)$; in MeCN $K_1 > 10^5$, K_2 = 4.4 ± 0.3 . When substituents are added to the ring of 18C6, the resulting differences in geometry and rigidity affect the K values substantially. The complexation reaction of all three crowns in pyridine can serve as an example, the ligand 18C6 is the most flexible of the three crowns and has the highest \mathbf{K}_1 value, while DBC with the smallest cavity and greatest rigidity has the lowest K_1 value. On the other hand, because of its small cavity and high rigidity, DBC may form a non-symmetric 1:1 complex and this geometry favor the formation of a 2:1 "sandwich" complex. In any event, DBC gives the highest K2 value of the three crowns. Dicyclohexyl-18C6 has a similar cavity size to 18C6 but a higher rigidity of the ring. It has an intermediate K_1 value, but the smallest K_2 value.

A thorough study of 18C6 complexes with CsTPB in pyridine was made at various temperatures (from 25° to -44°C). For the purpose of this study, a new temperature independent reference for all temperatures was designed. Its validity was tested and provided evidence that ion-ion and ion-solvent



interactions are temperature dependent. In this complexation study, conclusive evidence for the 2:1 complex (18C6:Cs⁺) was also found. The values of the first formation constant at various temperatures were too large to be determined by NMR techniques, but K_2 values were determined and used to obtain the enthalpy and entropy changes for the second complexation step. The results are: $\Delta H_2 = -6.2 \pm 0.1$ Kcal/mole $(\Delta G_2^O)_{298} = -2.83 \pm 0.004$ Kcal/mole, $\Delta S_2 = -11.2 \pm 0.3$ e.u. A kinetics study of the decomplexation reaction of Cs⁺·18C6 gave an activation energy of 8 ± 0.3 Kcal/mole.

The formation constants of C222 and C222B complexes were also obtained from the NMR chemical shift data. formation constants for these two ligands showed the same trends with various solvents. For example, the K_1 values for C222 are > 10^5 (PY), (10 ± 1) x 10^3 (PC), (10.8 ± 0.8) x 10^3 (acetone), $(1.5\pm0.1) \times 10^2$ (DMF), (27 ± 3) (DMSO), and (4 ± 1) \times 10⁴ (MeCN). By contrast, the C222B, with a benzo group on one of the ether chains forms weaker complexes with K values ranging from $(5.7\pm0.8) \times 10^3$ (PY) to zero (DMSO). Chemical shift-mole ratio temperature dependent studies were also carried out, as well as studies of kinetics. Both gave evidence for two types of complexes in the solu-The results are interpreted on the basis of the formation of both inclusive and exclusive complexes of Cs⁺ by C222. Enthalpies and entropies of formation were computed by using the KINFIT program and it was found that both quantities are sensitive to the solvent for the



complexation of free cesium ions to form the exclusive complex. The conversion of the exclusive to the inclusive complex is much less sensitive to solvent. The activation energy (E_a) for the loss of Cs⁺ from the Cs⁺C222B complex in PC is 14.9±0.6 Kcal/mole. By comparison, the values obtained from kinetics studies for crown complexes give $E_a = 8.5\pm0.5$ (Kcal/mole) for DCC complexes and $E_a = 8\pm4$ (Kcal/mole), for 18C6 complexes. It appears that the higher rigidity and special geometry of the ligand give C222B the largest activation energy.

II. SUGGESTIONS FOR FUTURE STUDIES

The studies already made lead to the following suggestions for further investigation:

- (1) Calorimetric studies of the complexation reaction can supply some complementary information to the alkali NMR results. A joint study of Cs⁺-C222 in various solvents by calorimetric and NMR lineshape analysis should give more insight into the nature of the complexation reaction.
- (2) It has already been observed that the chemical shift of cesium ion in electrolyte solutions is temperature dependent. By using a temperature independent reference, a series of studies such as K_{ip} for an electrolyte solution and formation constants for complexation

reactions could be made at various temperature and thus one could obtain the corresponding thermodynamic parameters. Also, it may be worthwhile to investigate ion-ion and ion-solvent interactions at different temperatures.

- (3) At present a few studies have been made of the Cs⁺ counter ion effect on formation constants. Therefore, a complete study of cesium salts complexed by [2]-cryptand could be carried out. This information could help to determine the conditions which favor inclusive vs exclusive complexes. It could also be used for the study of competitive complexation reactions such as that between Cs⁺-[2]cryptates and Na⁺-[2]cryptates. Since the latter complexes are usually stronger than those with Cs⁺ the extent of replacement of Cs⁺ by Na⁺ could be used to obtain relative complexation formation constants.
- (4) Preliminary temperature studies of the C222B complexation reaction with Cs⁺ in PC and acetone seem to indicate that the chemical shift of complexed Cs⁺ is not very temperature dependent. Therefore, a thorough temperature study of the Cs⁺-C222B complexation reaction in various solvents may give further information about a system which probably forms only exclusive complexes.
- (5) A lineshape analysis at various temperatures and

concentrations could be made of Cs⁺-[2]cryptate complexation reactions, to determine the order of the decomplexation reaction in low dielectric media. It has long been of interest to find out whether the mechanism of decomplexation involves a unimolecular or a bimolecular process. If C221 or C222B form only exclusive complexes with the Cs⁺ ion, this condition may offer a very favorable situation to test the nature of decomplexation mechanism.



APPENDIX A

DETERMINATION OF ION-PAIR FORMATION CONSTANTS BY THE NMR TECHNIQUE; DESCRIPTION OF THE COMPUTER PROGRAM KINFIT AND SUBROUTINE EON

The equilibrium for an ion pair reaction can be expressed as

$$M^+ + X^- \stackrel{K_{ip}}{\neq} M^+ \cdot X^-$$

and

$$K_{ip} = \frac{\alpha_{(M}^{+} \cdot X^{-})}{\alpha_{M}^{+} \cdot \alpha_{X^{-}}} = K_{c}/\gamma_{\pm}^{2}$$

in which K_{C} is the concentration equilibrium constant and γ_{\pm} is the mean activity coefficient. By using the well known Debye-Hückel equation, γ_{\pm} can be thus calculated as follows:

In this equation Z_+, Z_- are the charges of the ions, I is the molar ionic strength which is $1/2 \sum_i C_i Z_i^2$ (C = Concentration summed over all species in the solution), D is the dielectric constant of the solvent and T and å are the temperature (°K) and the closest distance of approach of the ions in Å.

The observed chemical shift is a population average of those of the free ion and the ion pair; i.e.

$$\delta_{obs} = \delta_{F} X_{F} + \delta_{ip} X_{ip}$$

$$= (\delta_{F} - \delta_{ip}) X_{F} + \delta_{ip}.$$
(A.2)

where $X_F = [Cs^+]/C_T^M$; and C_T^M is the total concentration of Cs^+ in the system. Material balance gives

$$C_{T}^{M} = [Cs^{+}] + [Cs^{+} \cdot x^{-}]$$

$$= [Cs^{+}] + K_{C} [Cs^{+}]^{2}$$

Therefore

$$[Cs^{+}] = \frac{-1 \pm \sqrt{1+4K_{C} C_{T}^{M}}}{2K_{C}}$$

$$x_{F} = \frac{Cs^{+}}{C_{T}^{M}} = \frac{- + \sqrt{1 + 4K_{C} C_{T}^{M}}}{2K_{C} C_{T}^{M}} \quad \text{and} \quad K_{C} = K_{ip}\gamma_{\pm}^{2}$$

So that, finally

$$\delta_{\text{obs}} = \left[\frac{-1 + (1 + 4K_{ip} c_{T}^{M} \cdot \gamma_{\pm}^{2})^{1/2}}{2K_{ip} c_{T}^{M} \cdot \gamma_{\pm}^{2}} \right] (\delta_{F} - \delta_{ip}) + \delta_{ip} (A.3)$$

In order to make computation easier on the CDC 6500 computer, Equation (A.1) was rewritten as:

$$= \exp \left\{ \frac{-\frac{1.823 \times 10^6}{2.303} |z_{+}z_{-}| \sqrt{I}}{[(DT)^{1/2}]^3 [1 + \frac{50.29}{(DT)^{1/2}} (A.4)} \right\}$$

$$= \exp \left\{ \frac{-791600 |z_{+}z_{-}|\sqrt{I}}{[(DT)^{1/2}]^{3}[1 + \frac{50.29}{(DT)^{1/2}} \sqrt[8]{I}]} \right\}$$

Two unknown parameters must be obtained from the fitting procedure. These are the limiting chemical shift of the ion-pair (U(1)) and the activity equilibrium constant (U(2)). The known parameters are introduced as constants; i.e.; const(1) = chemical shift of the free ion, const(2) = (dielectric constant) x (temperature) and const(3) = average distance parameter \mathring{a} . In this study a value was chosen from reference 100. The Fortran expression and deck structure are listed on the next page. It should be noted that in these cases, all K_{ip} values were less than 400; therefore, C_{M}^{T} was used to calculate the ionic strength. However, in general a correction should be made by considering the degree of dissociation.

```
DECK LIST OF ION PAIR FORMATION CONSIANT DETERMINATION
 PNC
JOB CAPO
PASS WORD
HALH *DYE • KINFII4 •
 789
               SURROUTINE FOU

COMMON KOUNT, ITAPE, ITAPE, [WT.LAD. XINCD.NOPT.NOVAR.NOUNG.X.U.ITMAX.KINF1501]
WIX.TFST.LAV.RESID.LAD.ELPS.ITYP.XX.PXTYP.DXII.FOP.FO.FU.P.ZL.TO.EKINF1502
ZIGVAL.XST.T.DT.L.M.IU.Y.DY.VECT.NCSI.CONST.NDAT.JUAT.WOPT.LDPT.

3YYY.CONSIS
COMMON/PLOT/IMFTH
COMMON/PLOT/IMFTH
COMMON/POINT/KOPT.JOPT.XXX
DIMENSION X(4.300).U(20).WIX(4.400).XX(4).FOP(300).FO(300).FU(300)
1.P(30.21).VECT(20.21).71(300).TO(20).EGGVAL(20).XST(300).Y(10).
ZDY(10).CONSIS(50.16).NCSI(50).ISMIN(50).RXTYP(50).DXII(50).IRX(50)
3.MOPI(50).LOPI(50).YYY(50).CONSI(16).XXX(15)
GO TO (2.3.4.5.1.7.8.9.10.11.12) IIYP
ITAPE=60
JIAPE=60
JIAPE=61
WRITE (JTAPE.6)
FORMAT( * DETERMINATION OF K(IP) BY CS-NMR * )
NOUNK=2
RETURN
RETURN
               RETURN
7 CONTINUE
RETURN
A CONTINUE
RETURN
RESIDEST

RETURN

SCONTINUE
RETURN

CONTINUE
RETURN

CONTINUE
RETURN
CONTINUE
RETURN
CONTINUE
          PETURN

OPNTINUE
RETURN
CONTINUE
RETURN
CONTINUE
RETURN
CONTINUE
RETURN
CONTINUE
RETURN
CONTINUE
RETURN
ENO
7<sub>8</sub>
CONTROL CARD
COMMON CARD
CONSTANTS
INTITIAL ESTIMATE
DATA CAPOS
 BLANK CAPO
        H
           9
```

APPENDIX B

DETERMINATION OF COMPLEX FORMATION CONSTANTS BY THE NMR TECHNIQUE; DESCRIPTION OF COMPUTER PROGRAM KINFIT AND SUBROUTINE EQN

(1) DETERMINATION OF FORMATION CONSTANTS FOR A SINGLE STEP REACTION

The equilibrium for a one-to-one complexation reaction can be expressed as

$$M + L \stackrel{+}{\sim} ML \tag{B.1}$$

and the concentration formation constant K will be

$$K = C_{ML}/C_{M} \cdot C_{L}$$
 (B.2)

where C stands for concentration in terms of molarity. In this case we only considered the concentration formation constant since there are no changes in the number of charged species and the concentrations of the reactants are very low (0.01 M). Therefore, we can consider that the mean activity coefficient for the free salt and the complexed cesium are the same.

The method used in this technique makes use of the fact that at the fast exchange limit (on the NMR time scale), the observed chemical shift of M ($\delta_{\rm obs}$) is a weighted average of the characteristic chemical shift of M at each site

(free M and complexed M in bulk solution).

$$\delta_{\text{obs}} = X_{\text{M}} \delta_{\text{M}} + X_{\text{ML}} \delta_{\text{ML}}$$
 (B.3)

where δ_{M} , δ_{ML} are the chemical shift for free and complexed M, respectively in a given solvent, and X_{M} , X_{ML} are the relative mole fractions for each species. Therefore

$$\delta_{\text{obs}} = X_{\text{M}} \delta_{\text{M}} + (1-X_{\text{M}}) \delta_{\text{ML}}$$

$$= X_{\text{M}} (\delta_{\text{M}} - \delta_{\text{ML}}) + \delta_{\text{ML}}$$
(B.4)

The analytical concentration of M is $C_{M}^{T} = C_{M} + C_{ML}$ and for the ligand is $C_{L}^{T} = C_{ML} + C_{L}$ so $C_{ML} = C_{M}^{T} - C_{M}$ $C_{L} = C_{L}^{T} - C_{M}^{T} + C_{M}$ so Then $K = (C_{M}^{T} - C_{M})/(C_{M})(C_{L}^{T} - C_{M}^{T} + C_{M})$ $K C_{M}^{2} + (K C_{L}^{T} - K C_{M}^{T} + 1) C_{M} - C_{M}^{T} = 0$ $C_{M} = \frac{1}{2K} \left\{ -(K C_{L}^{T} - K C_{M}^{T} + 1) \pm \sqrt{(K C_{L}^{T} - K C_{M}^{T} + 1)^{2} + 4K C_{M}^{T}} \right\}$ (B.5)

Since physically $C_{\underline{M}}$ cannot be negative, therefore only the positive root is chosen.

Let

$$D = (K C_{L}^{T} - K C_{M}^{T} + 1)^{2}$$

Then

$$C_{M} = \frac{1}{2K} \{-(K C_{L}^{T} - K C_{M}^{T} + 1) + \sqrt{D + 4K C_{M}^{T}} \}$$

and

$$\delta_{\text{obs}} = \frac{1}{2K \ C_{M}^{T}} \left\{ -(K \ C_{L}^{T} - K \ C_{M}^{T} + 1) + \sqrt{D + 4K \ C_{M}^{T}} \right\} (\delta_{M} - \delta_{ML}) + \delta_{ML}$$
(B.6)

In order to fit this equation, two constants and two parameters are used; namely:

$$u(1) = \delta_{ML}$$
 $u(2) = K$
$$const(1) = C_{M}^{T}$$

$$const(2) = \delta_{M}$$

The above equations expressed in Fortran notation are as follows:

$$A = K C_{M}^{T} = u(2) * const(1)$$

$$B = K C_{L}^{T} = u(2) * xx(1)$$

$$C = \frac{(\delta_{M}^{-}\delta_{ML})}{2K C_{M}^{T}} = (const(2) - u(1))/(2.*A)$$

$$D = (B - A + 1.) ** 2$$

$$S = \delta_{obs} = ((A - B - 1.) + SORT (D + 4.*A))*C + u(1)$$

```
DETERMINATION OF FORMATION CONSTANT
      IIPNC
MET.CM45000.[130.RG2.JC.4...
PW=SECRETSTHE
MAL.MANNER.OME C222. 275 7.
HAL.LEDYE.KIME[]].
SUPPORTINE FOR COMMON KNOWN TITAPE JEACT (THE ACTUACY HOPE NOWARD NORMS KNOWN THANKERN 1282 INTERNATION X (4-10) THE COMMON KNOWN TO THE COMMON TO THE COMMON TO THE COMMON THANKERN THE COMMON THANKERN THE COMMON THANKERN THE COMMON THANKERN THANK
    7
8
9
  BLANK CAPD
    67 A 7
```

A listing of the deck structure is shown on the next page; for details of the format refer to reference (106), Dr. Mark Greenberg's thesis (1974).

(II) DETERMINATION OF FORMATION CONSTANTS FOR A TWO STEP
REACTION

The equilibria for this reaction can be expressed as

$$M^+ + L \stackrel{\rightarrow}{\leftarrow} ML \qquad K_1 = C_{ML} / C_{M} \cdot C_{L}$$
 (B.7)

$$ML^+ + L + ML_2$$
 $K_2 = C_{ML_2}/C_{ML} \cdot C_L$ (B.8)

If the reactions also compete with ion pair formation then the ion pairing reaction should also be considered; i.e.,

$$M^{+} + X^{-} \neq M^{+} \cdot X^{-}$$
 $K_{C} = \frac{C_{MX}}{C_{M} \cdot C_{X}}$ (B.9)

Where C stands for the molarity of the species. Let C_{M}^{T} and C_{L}^{T} denote the total concentration of the metal ion and ligand respectively. Then

$$C_{M}^{T} = C_{M} + C_{ML} + C_{ML_{2}} + C_{MX}$$
 (B.10)

$$C_{L}^{T} = C_{L} + C_{ML} + 2C_{ML_{2}}$$
(B.11)

$$C_{\mathbf{M}}^{\mathbf{T}} = C_{\mathbf{X}}^{\mathbf{T}} = C_{\mathbf{X}} + C_{\mathbf{MX}}$$
 (B.12)

(B.10) can be further written as

$$C_{M}^{T} = C_{M} [1 + K_{1} C_{L} + K_{1} K_{2} C_{L}^{2} + K_{C} C_{X}]$$

Therefore

$$C_{M} = C_{M}^{T}/[1 + K_{1}C_{L} + K_{2}C_{L}^{2} + K_{C}C_{X}]$$
 (B.13)

Equation (B.11) can also be written as

$$\mathbf{C}_{\mathbf{L}}^{\mathbf{T}} = \mathbf{C}_{\mathbf{L}} + \mathbf{K}_{1} \mathbf{C}_{\mathbf{M}} \mathbf{C}_{\mathbf{L}} + 2\mathbf{K}_{1}\mathbf{K}_{2}\mathbf{C}_{\mathbf{M}}\mathbf{C}_{\mathbf{L}}^{2}$$

<u>i.e.</u>,

$$2K_1K_2C_MC_L^2 + C_L\{1 + K_1C_M\} - C_L^T = 0$$

Therefore

$$C_{L} = \frac{-\{1+K_{1}C_{M}\} + \sqrt{(1+KC_{M})^{2}+8K_{1}K_{2}C_{M}C_{L}^{T}}}{4K_{1}K_{2}C_{M}}$$
(B.14)

and (B.12) can be written as

$$C_{\mathbf{M}}^{\mathbf{T}} = C_{\mathbf{X}} + K_{\mathbf{C}}C_{\mathbf{M}}C_{\mathbf{X}}$$

therefore

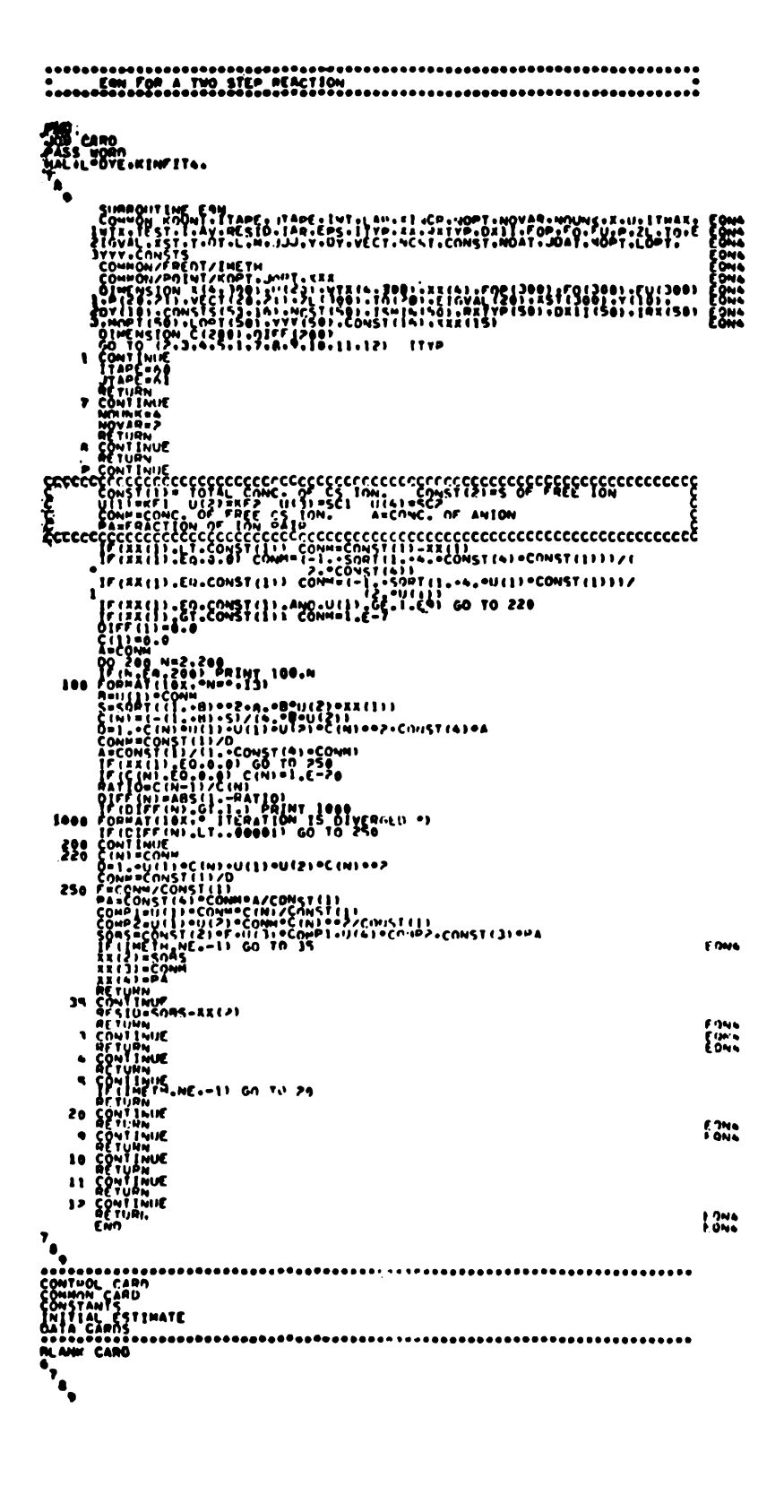
$$C_{X} = C_{M}^{T}/1 + K_{C}C_{M}$$
 (B.15)

Since the observed chemical shift is

$$\delta_{\text{obs}} = \delta_{\text{M}} X_{\text{M}} + X_{\text{ML}} \delta_{\text{ML}} + X_{\text{ML}_2} \delta_{\text{ML}_2} + X_{\text{ip}} \delta_{\text{ip}}$$
 (b.16)

In order to fit the calculated result with the experimental data, an expression for the relative mole fractions of all four species in terms of $C_{\mathbf{M}}^{\mathbf{T}}$ and $C_{\mathbf{T}}^{\mathbf{T}}$ is demanded. However the above equations (B.14-16) are all inter-connected. order to avoid using the solution to a cubic equation to obtain values of $C_{\underline{M}}$ and $C_{\underline{L}}$ and thus $\delta_{\underline{obs}}$, an iteration method was used. This method is achieved by applying a "do loop" in the EQN subroutine. The computer starts the calculation from a given initial estimate and first calculates C_{L} , then uses this newly computed C_{L} value to calculate C_{M} and C_{X} . Then, again these values are used to calculate $\mathbf{C}_{\mathbf{L}}$ and so on until the ratio of the previous $\mathbf{C}_{\mathbf{L}}$ and the current $\mathbf{C}_{\mathbf{L}}$ is almost equal to one. The iteration stops by jumping out of the do loop when the difference between unity and the ratio of the new to the old $C_{\widetilde{\mathbf{L}}}$ values is less than 10^{-5} . Then the current C_{L} , C_{M} , C_{X} values are used to compuete the mole fractions of each component and thus δ_{obs} .

Subroutine EQN of this calculation is listed on the next page. There are four parameters and four constants as follows:



$$u(1) = K_1 \qquad const(1) = C_M^T$$

$$u(2) = K_2$$
 const(2) = δ_F

u(3) = limiting chemical shift of
$$ML^{+}$$
 (δ_{ML}) const(3) = δ_{ip}

u(4) = limiting chemical shift of
$$ML_2^+$$
 (δ_{ML_2}) const(4) = K_C

APPENDIX C

NMR LINESHAPE ANALYSIS FOR TWO-SITE EXCHANGE;
DESCRIPTION OF THE COMPUTER PROGRAM AND SUBROUTINE EQN

The Bloch equations in the double rotating reference frame apply to the macroscopic moment M when all nuclei are acted on by the same field H_O . When two positions in the system under investigation have different screening constants, the simple equations are no longer valid because there are two possible fields and correspondingly two Larmor frequencies, ω_A and ω_B . McConnell (104) therefore modified the equations by assuming that

- (1) All nuclei remain in one state until they make a sudden rapid jump to another, the nuclear precision during the jump being neglected. This implies that a nuclear exchange between positions of the same type will have no effect and we need only consider the interchange between positions of types A and B.
- (2) While a nucleus is in an A position, there is a constant probability τ_A^{-1} per unit time of its making a jump to a B position. Likewise τ_B^{-1} will be the probability of a nucleus in position B jumping to A. Consider the following definitions:

G = A complex moment of magnetization

 H_1 = radiofrequency magnetic field.

 γ = gyromagnetic ratio.

M_O = magnetization in the Z direction at A given site.

 ω_{A} , ω_{B} = chemical shifts (Hz) at sites A and B in the absence of exchange.

 T_{2A} , T_{2B} = Transverse relaxation times of the nuclei at the two sites, in the absence of exchange.

$$\alpha_{A}, \alpha_{B}$$
 are defined as $\alpha_{A} = T_{2A}^{-1} - i(\omega_{A} - \omega)$

$$\alpha_{B} = T_{2B}^{-1} - i(\omega_{B} - \omega)$$

 $\tau_A^{}$, $\tau_B^{}$ are the mean lifetimes on site A and site B, respectively, at a given temperature.

With these definitions, the modified Bloch equations can be expressed as:

$$\frac{dG_{A}}{dt} + \alpha_{A}G_{A} = -i\gamma H_{1}M_{OA} + \tau_{B}^{-1}G_{B} - \tau_{A}^{-1}G_{A}$$
 (C.1)

$$\frac{dG_{B}}{dt} + \alpha_{B}G_{B} = -i\gamma H_{1}M_{OB} + \tau_{A}^{-1}G_{A} - \tau_{B}^{-1}G_{B}$$
 (C.2)

 $\tau_{\rm B}^{-1}{\rm G}_{\rm B}$ represents the rate of increase of ${\rm G}_{\rm A}$ due to transfer of magnetization from B to A sites. Similarly, $\tau_{\rm A}^{-1}{\rm G}_{\rm A}$ is the corresponding rate of loss. For slow passage, it is appropriate to use

$$\frac{dG_A}{dt} = \frac{dG_B}{dt} = 0$$

Let the fractional population in the A and B site be $P_{\mathbf{A}}$

and $\mathbf{P}_{\mathbf{B}}$ which are related to $\boldsymbol{\tau}_{\mathbf{A}}$ and $\boldsymbol{\tau}_{\mathbf{B}}$ through

$$P_A = \frac{\tau_A}{\tau_B + \tau_A}$$
 $P_B = \frac{\tau_B}{\tau_B + \tau_A}$ $P_A + P_B = 1$

then

$$M_{OA} = P_A M_O \qquad M_{OB} = P_B M_O$$

Solve for $G_{\mathbf{A}}$ and $G_{\mathbf{B}}$ by

(1) + (2)
$$\alpha_{A}G_{A} + \alpha_{B}G_{B} = -i\gamma H_{1}M_{0}(P_{A}+P_{B})$$
 (C.3)

(1)-(2)
$$\alpha_{A}G_{A} - \alpha_{B}G_{B} = -i\gamma H_{1}M_{0}(P_{A}-P_{B}) + 2\tau_{B}^{-1}G_{B} - 2\tau_{A}^{-1}G_{A}$$
(C.4)

Then

$$(3) + (4) \quad \alpha_{A}^{G}G_{A} = -i\gamma H_{1}^{M}G_{O}^{P}A + \tau_{B}^{-1}G_{B} - \tau_{A}^{-1}G_{A}$$

$$G_{A} = -\frac{i\gamma H_{1}^{M}G_{O}^{P}A^{T}A}{\alpha_{A}\tau_{A}^{+1}} + \frac{\tau_{A}^{T}G_{B}}{\alpha_{A}\tau_{A}^{+1}}G_{B}$$
(C.5)

(3)-(4)
$$\alpha_B^G = -i\gamma H_1 M_0^P - \tau_B^{-1} G_B + \tau_A^{-1} G_A$$

$$G_{B} = -\frac{i\gamma^{H} 1^{M} 0^{P} B^{T} B}{\alpha_{B} \tau_{B} + 1} + \frac{\tau_{A}^{-1} \tau_{B}}{\alpha_{B} \tau_{B} + 1} G_{A}$$
 (C.6)

Therefore,

$$G_{A} = -\frac{i\gamma H_{1}M_{0}P_{A}\tau_{A}}{\alpha_{A}\tau_{A}+1} + \frac{\tau_{A}\tau_{B}^{-1}}{\alpha_{A}\tau_{A}+1} \left\{ -\frac{i\gamma H_{1}M_{0}P_{B}\tau_{B}}{\alpha_{B}\tau_{B}+1} + \frac{\tau_{A}^{-1}\tau_{B}}{\alpha_{B}\tau_{B}+1} G_{A} \right\}$$

$$G_{A} \left\{ 1 - \frac{1}{(\alpha_{A}\tau_{A}+1)(\tau_{B}\alpha_{B}+1)} \right\} = \frac{-i\gamma H_{1}M_{0}}{(\alpha_{A}\tau_{A}+1)(\alpha_{B}\tau_{B}+1)} \left\{ P_{A}\tau_{A}(\alpha_{B}\tau_{B}+1) + P_{B}\tau_{A} \right\}$$

$$+ P_{B}\tau_{A} \left\{ -i\gamma H_{1}M_{0} - \frac{i\gamma H_{1}M_{0}}{(\alpha_{A}\tau_{A}+1)(\tau_{B}\alpha_{B}+1)} \right\}$$

$$G_{A} = \frac{-i\gamma H_{1}M_{0}}{(\alpha_{A}\tau_{A}+1)(\tau_{B}\alpha_{B}+1)} \left\{ P_{A}\tau_{A} + P_{B}\tau_{A} + P_{A}\tau_{A}\tau_{B}\alpha_{B} \right\}$$

$$-i\gamma H_{1}M_{0}$$

 $= \frac{-1\gamma H_1 M_0}{(\alpha_A \tau_B + 1) (\tau_A \alpha_B + 1) - 1} \{ \tau_A + P_A \tau_A \tau_B \alpha_B \}$

Substitute GA back into (6) to obtain

$$G_{\rm B} = -\frac{{\rm i}\gamma^{\rm H}{\rm 1}^{\rm M}{\rm o}^{\rm \tau}{\rm g}^{\rm P}{\rm B}}{\alpha_{\rm B}\tau_{\rm B}+1} + \frac{\tau_{\rm B}\tau_{\rm A}^{-1}}{\tau_{\rm B}\alpha_{\rm B}+1} \cdot \frac{-{\rm i}\gamma^{\rm H}{\rm 1}^{\rm M}{\rm o}^{\{\tau_{\rm A}+P_{\rm A}\tau_{\rm A}\tau_{\rm B}\alpha_{\rm B}\}}}{(\alpha_{\rm A}\tau_{\rm A}+1)(\tau_{\rm B}\alpha_{\rm B}+1)-1}$$

$$=\frac{-i\gamma H_1 M_0}{(\alpha_A \tau_A + 1)(\alpha_B \tau_B + 1) - 1} \left\{ \frac{P_B \tau_B}{\alpha_B \tau_B + 1} \cdot \frac{(\alpha_A \tau_A + 1)(\alpha_B \tau_B + 1) - 1}{1} \right.$$

$$+\frac{\tau_{B}}{\tau_{B}\alpha_{B}+1}+\frac{P_{A}\tau_{B}^{2}\alpha_{B}}{\tau_{B}\alpha_{B}+1}$$

$$= \frac{-i\gamma^{\rm H}{}_{1}^{\rm M}{}_{\rm O}}{(\alpha_{\rm A}\tau_{\rm A}+1)\;(\alpha_{\rm B}\tau_{\rm B}+1)-1}\; \{P_{\rm B}\tau_{\rm B}(\alpha_{\rm A}\tau_{\rm A}+1)\; -\frac{P_{\rm B}\tau_{\rm B}}{\alpha_{\rm B}\tau_{\rm B}+1}\; +\frac{\tau_{\rm B}}{\tau_{\rm B}\alpha_{\rm B}+1}\\ \\ +\frac{P_{\rm A}\tau_{\rm B}^{2}\alpha_{\rm B}}{\tau_{\rm B}\alpha_{\rm B}+1}\; \}$$

$$= \frac{-i\gamma H_{1}M_{0}}{(\alpha_{A}\tau_{A}+1)(\alpha_{B}\tau_{B}+1)-1} \{ \{P_{B}\tau_{B}\tau_{A}\alpha_{A} + P_{B}\tau_{B} - \frac{P_{B}\tau_{B}}{\alpha_{B}\tau_{B}+1} + \frac{1}{\alpha_{B}\tau_{B}+1} [\tau_{B}(1+P_{A}\tau_{B}\alpha_{B})] \}$$

Therefore

$$\begin{split} G &= G_{A} + G_{B} = u + iv. \\ &= \frac{-i\gamma^{H} 1^{M} 0}{(\alpha_{A} \tau_{A} + 1) (\alpha_{B} \tau_{B} + 1) - 1} \left\{ \tau_{A} + \tau_{A} \tau_{B} (P_{A} \alpha_{B} + P_{B} \alpha_{A}) + \tau_{B} - P_{B} \tau_{B} + P_{B} \tau_{B} \right\} \\ &= \frac{-i\gamma^{H} 1^{M} 0}{(\alpha_{A} \tau_{A} + 1) (\alpha_{B} \tau_{B} + 1) - 1} \left\{ \tau_{A} + \tau_{B} + \tau_{A} \tau_{B} (P_{A} \alpha_{B} + P_{B} \alpha_{A}) \right\}. \end{split}$$

Where u and v are the transverse components of M along and perpendicular to the rotating field H_1 . The v (out-of-phase component) is the one proportional to the absorption intensity.

In order to separate the imaginary part from the real, let

$$\tau = \tau_A \tau_B / (\tau_A + \tau_B)$$

and, therefore,

$$\tau_{A} = \tau/P_{A}$$
 $\tau_{B} = \tau/P_{B}$

$$Y = \frac{G}{-i\gamma H_1 M_0} = \frac{(\tau_A^{+\tau_B}) + \tau_A \tau_B (P_A \alpha_B^{+} P_B \alpha_A)}{\alpha_A \alpha_B \tau_A \tau_B^{+} \alpha_A \tau_A^{+} \alpha_B \tau_B^{+} 1 - 1}$$

$$= \frac{1 + \frac{\tau_A \tau_B}{\tau_A^{+} \tau_B} (P_A \alpha_B^{+} P_B \alpha_A)}{\alpha_A \alpha_B \frac{\tau_A \tau_B}{\tau_A^{+} \tau_B} + \frac{\alpha_A \tau_A^{+} \alpha_B \tau_B}{\tau_A^{+} \tau_B}} = \frac{N}{D}$$

Substitute the expression for α into that for Y to give

$$\begin{split} &N = 1 + \frac{\tau_{A}\tau_{B}}{\tau_{A}^{+}\tau_{B}^{+}} \left\{ P_{A}T_{2B}^{-1} - iP_{A}(\omega_{B}^{-}\omega) + P_{B}T_{2A}^{-1} - iP_{B}(\omega_{A}^{-}\omega) \right\} \\ &= 1 + \frac{\tau_{A}\tau_{B}}{\tau_{A}^{+}\tau_{B}^{+}} \left\{ P_{A}T_{2B}^{-1} + P_{B}T_{2A}^{-1} - i[P_{A}(\omega_{B}^{-}\omega) + P_{B}(\omega_{A}^{-}\omega)] \right\} \\ &= 1 + \tau \{ [P_{A}T_{2B}^{-1} + P_{B}T_{2A}^{-1}] - i[P_{A}\omega_{B}^{-} + P_{B}\omega_{A}^{-}\omega] \right\} \\ &= 1 + \tau \{ [P_{A}T_{2B}^{-1} + P_{B}T_{2A}^{-1}] - i[P_{A}\omega_{B}^{-} + P_{B}\omega_{A}^{-}\omega] \right\} \\ &= \tau [T_{2A}^{-1} - i(\omega_{A}^{-}\omega)][T_{2B}^{-1} - i(\omega_{B}^{-}\omega)] + \frac{\tau_{B}^{-}}{\tau_{A}^{+}\tau_{B}^{-}} [T_{2B}^{-1} - i(\omega_{B}^{-}\omega)] \\ &= \tau \{ T_{2A}^{-1}T_{2B}^{-1} - (\omega_{A}^{-}\omega)(\omega_{B}^{-}\omega) - i[T_{2B}^{-1}(\omega_{A}^{-}\omega) + T_{2A}^{-1}(\omega_{B}^{-}\omega)] \} \\ &+ \{ \frac{\tau_{A}T_{2A}^{-1}}{\tau_{A}^{+}\tau_{B}^{-}} + \frac{\tau_{B}T_{2B}^{-1}}{\tau_{A}^{+}\tau_{B}^{-}} - i[[\frac{\tau_{A}(\omega_{A}^{-}\omega)}{\tau_{A}^{+}\tau_{B}^{-}} + \frac{\tau_{B}(\omega_{B}^{-}\omega)}{\tau_{A}^{+}\tau_{B}^{-}}] \} \\ &= \tau [T_{2A}^{-1}T_{2B}^{-1} - (\omega_{A}^{-}\omega)(\omega_{B}^{-}\omega) + \tau_{B}^{-1}T_{2A}^{-1} + \tau_{A}^{-1}T_{2B}^{-1}] \end{split}$$

$$-i\tau[T_{2B}^{-1}(\omega_{A}-\omega) + T_{2A}^{-1}(\omega_{B}-\omega) + \tau_{B}^{-1}(\omega_{A}-\omega) + \tau_{A}^{-1}(\omega_{B}-\omega)]$$

Let

$$N = 1 + \tau(P_{A}T_{2B}^{-1} + P_{B}T_{2A}^{-1}) - i\tau(P_{A}\omega_{B} + P_{B}\omega_{A}^{-\omega}) = Q - iV$$

$$D = \tau\{T_{2A}^{-1}T_{2B}^{-1} - (\omega_{A}^{-\omega})(\omega_{B}^{-\omega}) + \tau_{B}^{-1}T_{2A}^{-1} + \tau_{A}^{-1}T_{2B}^{-1}\}$$

$$-i\tau\{(\omega_{A}^{-\omega})(T_{2B}^{-1} + \tau_{B}^{-1}) + (\omega_{B}^{-\omega})(T_{2A}^{-1} + \tau_{A}^{-1}) = S - iT$$

$$Y = \frac{Q - iV}{S - iT} = \frac{(Q - iV)(S + iT)}{S^{2} + T^{2}}$$

$$= \frac{QS + VT + i(QT - SV)}{S^{2} + T^{2}} = \frac{QS + VT}{S^{2} + T^{2}} + i\frac{QT - SV}{S^{2} + T^{2}}$$

Then

$$G = -i\gamma H_1 M_0 Y = -\gamma H_1 M_0 \{ -\frac{QT-SV}{S^2+T^2} + i\frac{QS+VT}{S^2+T^2} \}$$

and

$$u = \gamma H_1 M_0 \left\{ \frac{QT-SV}{S^2+T^2} \right\} = \frac{K}{S^2+T^2} [QT-SV]$$

$$v = -\gamma H_1 M_0 \left\{ \frac{QS+VT}{S^2+T^2} \right\} = \frac{-K}{S^2+T^2} (QS+VT)$$

However, in order to eliminate the broadening caused by viscosity, one has to run separate calibration experiments

on the free salt and the completely complexed salt. In this way the correct T_2^{-1} values can be obtained.

The detector is located in the laboratory frame. In conjunction with the rotating frame, My can be expressed as

$$M_{y} = \frac{-\frac{1}{2}M_{o}\gamma^{T}_{2}}{1+T_{2}^{2}(\omega_{o}-\omega)} [2H_{1}\cos_{\omega}t - T_{2}(\omega_{o}-\omega)2H_{1}\sin_{\omega}t]$$

$$= \frac{\Upsilon H_1 M_0 T_2}{1 + T_2^2 (\omega_0 - \omega)} \{\cos \omega t - T_2 (\omega_0 - \omega) \sin \omega t\}$$

where

 $\omega t = \theta_0 + \theta_1 = \text{zero order phase correction} + \text{first}$ order phase correction.

Let

$$K = \gamma H_1 M_0 = u(1)$$

C = Base line correction = u(2)

$$T_2^* = T_2T_{2inh}/T_2+T_{2inh} = u(3)$$
 T_2 : Natural Line width T_{2inh} : Linewidth due to inhomogeneocity

 ω_{O} = peak position (data point number) = u(4)

 θ_{O} = zero order phase correction (degree) = u(5)

Then the above expression for M_{Y} in the FORTRAN 4 language appropriate to the KINFIT program can be written as follows:

Knowing that the frequency can be calculated at a given

data point number and sweep width by the relationship

$$ω$$
 = (data point number) * $\frac{2π*$ sweepwidth memory storage

= (data point number) * PI

and degree = $\frac{\pi}{180}$ rad. = -.017453293 rad.

CAL =
$$u(1)*u(3)/(1+u(3)**2*(u(4)-XX(1))**2*PI**2)*$$

$$(cos(u(5)*0.017453293+XX(1)*.0174532*const(1)/const(2))$$

$$-u(3)*(u(4)-XX(1))*PI*sin(u(5)*0.017453293* \frac{const(1)}{const(2)})$$
+u(2)

where

 $const(1) = \theta_1$ in degree

From this fitting we obtain T_2 for the nonexchange case, and use these T_2 values to calculate τ for the exchange case. Due to the combination of dispersion and absorption mode which are mixed in the observed lineshape the expression for the lineshape becomes

$$M_y = u \sin\theta + v \cos\theta + C$$
 where C is a baseline offset.
 $u = \frac{K}{S^2 + T^2} [QT - SV]$ $v = \frac{-K}{S^2 + T^2} [QS + VT]$

where

$$Q = 1 + \tau(P_{A}T_{2B}^{-1} + P_{B}T_{2A}^{-1})$$

$$V = \tau(P_{A}\omega_{B} + P_{B}\omega_{A} - \omega)$$

$$S = \frac{P_{a}}{T_{2A}} + \frac{P_{B}}{T_{2B}} + \frac{\tau}{T_{2A}T_{2B}} - \tau(\omega_{A}^{-\omega})(\omega_{B}^{-\omega})$$

$$T = P_{A}\omega_{A} + P_{B}\omega_{B} - \omega + \tau(\frac{\omega_{A}^{-\omega}}{T_{2B}} + \frac{\omega_{B}^{-\omega}}{T_{2A}})$$

$$Let K = u(1) \quad C = u(2) \quad \tau = u(3) \quad \theta_{o} = u(4) \quad \Delta = u(5)$$

$$const(1) = P_{A} \text{ (population fraction)} \quad const(2) = T_{2A}^{*}$$

$$const(3) = P_{B} \quad const(4) = T_{2B}^{*} \quad const(5) = \omega_{A}$$

$$const(6) = \omega_{B} \quad const(7) = \theta_{1} \quad const(8) = number point$$

$$Q = 1 + u(3)*(const(1)/const(2) + \frac{const(3)}{const(4)})$$

$$V = u(3)*(const(3)*(const(5)+u(5))+const(1)*(const(6) + u(5))-XX(1))*PI$$

$$S = \frac{const(1)}{const(2)} + \frac{const(3)}{const(4)} + \frac{u(3)}{(const(2)*const(4))} - u(3) + \frac{(const(5)+u(5)-XX(1))*const(3)*((const(6)+u(5)-XX(1))*PI**2}{T}$$

$$T = (const(1)*(const(5)+u(5))+const(3)*((const(6)+u(5)-XX(1))*PI**2$$

$$T = (const(6)+u(5)-XX(1)) * (const(5)+u(5)-XX(1))/const(4)$$

$$+ \frac{(const(6)+u(5)-XX(1))}{const(2)} * PI$$

$$M_{y} = u + iv = \gamma H_{1}M_{0} \quad (R - iI)$$

 $= \frac{K}{c^2 + m^2} [(QS+VT) \cos\theta - (QT-SV) \sin\theta] + C$

```
control of DRCGRAM CONVERT.
MEI*CM45000.TAR.PG2.C2000.JC=00.

PW=ANY 10 CHAPACTERS.

HAL. *ANNER.MEI.

FIN.

1.50.

8
                                                                  105
                                                                                                      066
```

```
OOONEXCHANGE CASE I INCSHAPE ANALYSIS
I(PNC 214715 073176 07 0
MEI.CM45000.T100.RG2.JC3U0.
PW=SECRETSTUF.
HAL:4L*DYE-KIMFIT1.
g
  S CONTINUE PETURN
Ä
À
```

```
EXCHANGE CASE LINESHAME ANALYSIS.
I(PNC 214715 073175 07 0 MEI+CM45000-T100+RG2+JC300+PW=SFCRFTSTUF-MAL+RANNER+HG200)+HAL+L-DYE-KINFITI-
6
789
```

APPENDIX D

DETERMINATION OF THE ACTIVATION ENERGY

For a complexation reaction

(A)
$$k_{t}$$
 (B) $M + L \leftarrow ML$ k_{b}

where M denotes the metal ion and is the nucleus at site A under study, ML denotes the complexed metal ion and is the nucleus at site B. At the fast exchange limits on the NMT time scale one can calculate $K = k_{\rm f}/k_{\rm b}$ from a chemical shiftmole ratio study. At slow and intermediate ranges one can obtain exchange time (τ) values via lineshape analysis. By studying the τ value at various temperatures one can further obtain information about the activation energy as shown in the following way:

The relaxation time τ in a magnetic resonance study is defined as:

$$\frac{1}{\tau_{i}} = \frac{\text{rate of leaving of a nucleus from ith state by exchange}}{\text{number of nuclei in the ith state}}$$

$$\frac{1 \cdot e \cdot}{\tau_{B}} = \frac{dML}{dt}/C_{ML} \qquad \frac{1}{\tau_{A}} = \frac{dM}{dt}/C_{M}$$

while

$$\frac{dML}{dt} = k_b C_{ML} \qquad \frac{dM}{dt} = k_f C_M C_L$$

then

$$\frac{1}{\tau_{B}} = k_{b} \qquad \frac{1}{\tau_{A}} = k_{F}C_{L}$$

Since

$$\tau = \tau_{A} \tau_{B} / (\tau_{A} + \tau_{B})$$

$$P_{A} = \tau_{A} / (\tau_{A} + \tau_{B})$$

$$P_{B} = \tau_{B} / (\tau_{A} + \tau_{B})$$

Therefore

$$\tau = P_A \tau_B = P_B \tau_A$$

$$\frac{1}{\tau_B} = \frac{P_A}{\tau} = k_b \quad \underline{i.e.} \quad \frac{1}{\tau} = \frac{k_b}{P_A} \qquad \tau = \frac{P_A}{k_b}$$

To calculate E_a, a reference value can be used to provide faster convergence; namely,

$$k_b = k_{b(ref)} \exp\left[-\frac{E_a}{R} \left(\frac{1}{T} - \frac{1}{T_{ref}}\right)\right]$$

(instead of $k_b = A \exp[-E_a/RT]$) then

$$const(1) = R = 1.987 cal/mole °K$$

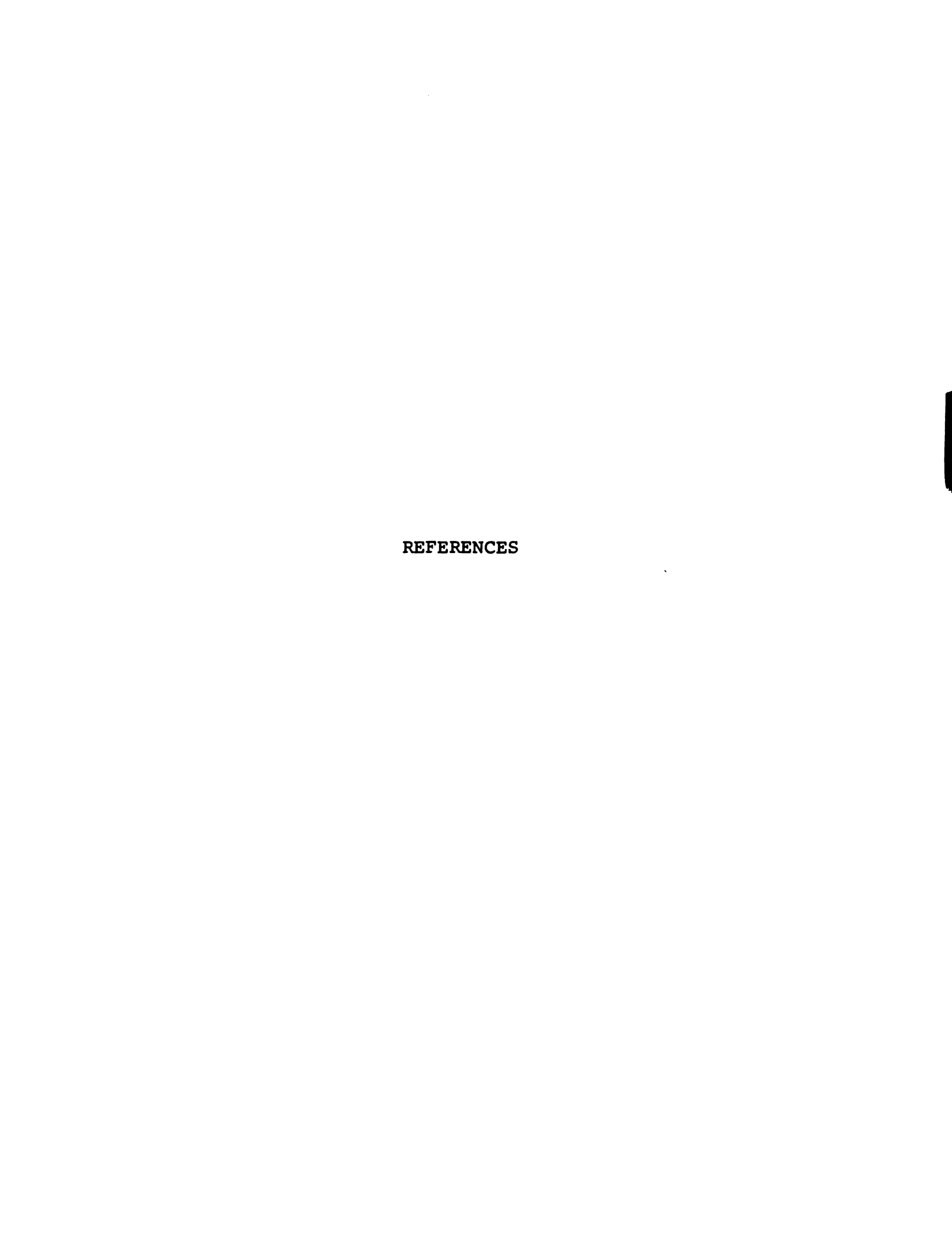
$$XX(1) = T (°K)$$

$$XX(2) = k_h$$

$$u(1) = lnk_b(ref)$$

 $u(2) = E_a$

$$Calc = u(1) - \frac{u(2)}{const(1)} \left(\frac{1}{XX(1)} - \frac{1}{const(2)}\right)$$



- C. J. Pedersen, J. Amer. Chem. Soc. 89, 2495 (1967);
 89, 7017 (1967).
- 2. B. Dietrich, J. M. Lehn, J. P. Sauvage; Tetrahedron Letter 34, 2885 (1969).
- E. Shchori, J. Jagur-Grodzinski, Z. Luz, and M. Shporer,
 J. Amer. Chem. Soc. 93, 7133 (1971).
- 4. E. Shchori, J. Jagur-Grodzinski, and M. Shporer, J. Amer. Chem. Soc. 95, 3842 (1973).
- 5. M. Shporer, Z. Luz, J. Amer. Chem. Soc. 97, 665 (1975).
- 6. Y. M. Cahen, J. L. Dye and A. I. Popov, J. Phys. Chem. 79, 1292 (1975).
- 7. Y. M. Cahen, J. L. Dye and A. I. Popov, J. Phys. Chem. 79, 1289 (1975).
- 8. C. Moore, B. C. Pressman, Biochem. Biophys. Res. Commun. 15, 562 (1964).
- 9. Z. Stefanac, W. Simon, Chimia 20, 436 (1966); J. Microchem. 12, 125 (1967).
- 10. C. J. Pedersen, J. Amer. Chem. Soc. 89, 7017 (1967).
- 11. Ibid, J. Amer. Chem. Soc. 92, 386 (1970).
- 12. D. E. Fenton, M. Mercer, N. S. Poonia, M. R. Truter, Chem. Commun. 66, 1972.
- 13. M. R. Truter, Structure Bonding 16, 71 (1973).
- 14. M. A. Bush, M. R. Truter, J. Chem. Soc. (B) 1440 (1971).
- 15. D. Bright and M. R. Truter, Nature (London), 225, 176 (1970); J. Chem. Soc. (B) 1544 (1970).
- 16. R. M. Izatt, J. H. Rytting, D. P. Nelson, B. L. Haymoore, and J. J. Christensen, Science 164, 443 (1969); J. Amer. Chem. Soc. 93, 1619 (1971).
- 17. H. F. Frensdorff, J. Amer. Chem. Soc. 93, 600 (1971).
- 18. K. H. Wong, G. Konizer, and J. Smid, J. Amer. Chem. Soc. 92, 666 (1970).
- 19. C. J. Pedersen and H. K. Frensdorff, Angew. Chem. Int Ed. Engl. 11, 16 (1972).

- 20. J. Smid, Angew. Chem. Int. Ed. Engl. 11, 112 (1972).
- 21. S. Kopolow, Z. Machacek, U. Takaki and J. Smid, J. Macromol. Sci-Chem. A7(5), 1015 (1973).
- 22. T. E. Hogen-Esch and J. Smid, J. Phys. Chem. <u>79</u>, 233 (1975).
- 23. T. E. Hogen-Esch and J. Smid, J. Amer. Chem. Soc. <u>88</u>, 318 (1966).
- 24. T. Ellingsen and J. Smid, J. Phys. Chem. <u>73</u>, 2712 (1969).
- 25. U. Takaki, T. E. Hogen-Esch, and J. Smid, J. Amer. Chem. Soc., <u>93</u>, 6760 (1971).
- 26. Ting-Po I. and E. Grunwald, J. Amer. Chem. Soc. <u>96</u>, 2879 (1974).
- P. U. Früh, J. T. Clerc, and W. Simon, Helv. Chim. Acta. <u>54</u>, 1445 (1971).
- 28. W. K. Lutz, P. U. Früh, W. Simon, Helv. Chim. Acta. <u>54</u>, 2767 (1971).
- 29. Ch. U. Züst, P. U. Früh and W. Simon, Helv. Chim. Acta. <u>56</u>, **49**5 (1973).
- 30. J. J. Christensen, R. M. Izatt and L. D. Hansen, The Rev. of Sci. Instr. 36, 779 (1965).
- 31. J. J. Christensen, J. Ruckman, D. J. Eatough, and R. M. Izatt, Thermochimica, Acta. 3 (1972) 203, Part I; 219 Part II; 233 Part III.
- 32. R. M. Izatt, D. J. Eatough and J. J. Christensen, Structure and Bonding (Berlin) 16, 161 (1973).
- 33. J. J. Christensen, D. J. Eatough and R. M. Izatt, Chem Rev. <u>74</u>, 151 (1974).
- 34. Hans Jörg Möschler, Hans-Georg Weder and Robert Schwyzer, Helv. Chim. Acta. <u>54</u>, 1437 (1971).
- 35. Ch. U. Züst, P. U. Früh and W. Simon, Helv. Chim. Acta. <u>56</u>, **49**5 (1973).
- 36. H. Diebler, M. Eigen, G. Ilgenfritz, G. Maass and R. Winkler, II. I.C.C.C., Haifa (1968); Pure Appl. Chemistry 20, 93 (1969).

- 37. F. P. Hinz, D. W. Margerum, J. Amer. Chem. Soc. <u>96</u> 4001 (1974).
- 38. F. P. Hinz, D. W. Margerum, Inorg. Chem. 13, 2941 (1974).
- 39. P. B. Chuck, Proc. Nat. Acad. Sci. U.S.A. <u>69</u>, No. 7, 1939 (1972).
- 40. D. F. Evans, S. L. Willington, J. A. Nadis, and E. L. Cussler, J. Solut. Chem. 1, 499 (1972).
- 41. J. M. Lehn, J. P. Sauvage, B. Deitrich, J. Amer. Chem. Soc. 92, 2916 (1970).
- 42. J. M. Ceraso, J. L. Dye, J. Amer. Chem. Soc. <u>95</u>, 4432 (1973).
- 43. (a) J. L. Dye, J. M. Ceraso, Mei Tak Lok, B. L. Barnett, F. J. Tehan, J. Amer. Chem. Soc. 96, 608 (1974).
 - (b) J. M. Ceraso and J. L. Dye, J. Chem. Phys. <u>61</u>, 1585 (1974).
- 44. J. P. Kintzinger, J. M. Lehn, J. Amer. Chem. Soc. <u>96</u>, 3313 (1974).
- 45. J. Cheney, J. M. Lehn, J. P. Sauvage and M. E. Stubbs J. C. S. Chem. Commun. 1100 (1972).
- 46. J. M. Lehn, M. E. Stubbs, J. Amer. Chem. Soc. <u>96</u>, 4011 (1974).
- 47. E. Graf, J. M. Lehn, J. Amer. Chem. Soc. <u>97</u>, 5022 (1975).
- 48. V. W. Loyola, R. G. Wilkins, P. Pizer, J. Amer. Chem. Soc. 97, 7382 (1975).
- 49. H. E. Simmons, C. H. Park, J. Amer. Chem. Soc. <u>90</u>, 2428 (1968).
- 50. J. M. Lehn, Structure Bonding, 16, 1 (1973).
- 51. E. Kauffmann, J. M. Lehn and J. P. Sauvage, Helv. Chim. Acta. 59, 1099 (1976).
- 52. P. D. Moras and R. Weiss, Acta. Cryst. B29, 400 (1973).
- 53. P. D. Moras and R. Weiss, Acta. Cryst. B29, 396 (1973).
- 54. P. D. Moras and R. Weiss, Acta. Cryst. B29, 383 (1973).

- 55. P. D. Moras and R. Weiss, Acta. Cryst. B29, 388 (1973).
- 56. P. D. Moras and R. Weiss, Acta. Cryst. B29, 1382 (1973).
- 57. P. D. Moras and R. Weiss, Acta. Cryst. B29, 1388 (1973).
- 58. R. Wiest and R. Weiss, J. C. S. Chem. Commun. 678 (1973).
- 59. M. Mellinger, J. Fisher and R. Weiss, Angew. Chem. Int. Ed. Engl. 12, 771 (1973).
- 60. J. M. Lehn and J. P. Sauvage, J. Amer. Chem. Soc. <u>97</u>, 6700, (1975).
- 61. B. Dietrich, J. M. Lehn and J. P. Sauvage, J. C. S. Chem. Commun. 15 (1973).
- 62. B. Kaempf, S. Raynal, A. Collet, F. Schué, S. Boileau and J. M. Lehn, Angew. Chem. Int. Ed. Engl. 13, 611 (1974).
- 63. M. A. Komarynsky, S. I. Weissman, J. Amer. Chem. Soc. 97, 1589 (1975).
- 64. M. P. Eastman, D. A. Ramirez, C. D. Jaeger and M. T. Watts, J. Phys. Chem. <u>80</u>, 182 (1976).
- 65. N. F. Ramsey, Phys. Rev. <u>77</u>, 567 (1950).
- 66. N. F. Ramsey, Phys. Rev. <u>78</u>, 699 (1950); <u>83</u>, 540 (1951); <u>86</u>, 243 (1952).
- 67. A. Saika and C. P. Slichter, J. Chem. Phys. <u>22</u>, 26 (1954).
- 68. Y. Yamagata, J. Phys. Soc. Japan, 19, 10 (1964).
- 69. J. Kondo and J. Yamashita, J. Phys. Chem. Solids <u>10</u>, 245 (1959).
- 70. P. O. Löwdin, Adv. Phys. 5, 1, (1956).
- 71. D. Ikenberry and T. P. Das, Phys. Rev. 138A 822 (1965).
- 72. D. W. Hafemeister and W. H. Flygare, J. Chem. Phys. <u>44</u>, 3584 (1966).
- 73. D. W. Hafemeister and W. H. Flygare, J. Chem. Phys. <u>43</u>, 795 (1965).
- 74. D. Ikenberry and T. P. Das, J. Chem. Phys. <u>43</u>, 2199 (1965)

- 75. C. Deverell and Richards, Mol. Phys. 10, 551 (1966).
- 76. C. Deverell, Progr. Nucl. Mag. Resonance. Spectrosc. 4, 278 (1969).
- 77. K. Yosida and T. Moriya, J. Phys. Soc. Japan <u>11</u>, 33 (1956).
- 78. T. P. Das and M. Karplus, J. Chem. Phys. <u>42</u>, 2885 (1965).
- 79. D. Lutz, Physics Letter 25A, 440 (1967).
- 80. H. S. Gutowsky and B. McGarvey, Phys. Rev. <u>91</u>, 81 (1953).
- 81. A. Carrington, F. Dravnicks, M. C. R. Symons, Mol. Phys. 3, 174 (1960).
- 82. J. Halliday, H. D. W. Hill, and R. E. Richards, Chem. Communications, 219 (1969).
- 83. J. D. Halliday, R. E. Richards, F. R. S., and R. R. Sharp, Proc. Roy. Soc. Lond. A. 313, 45 (1969).
- 84. C. Hall, R. E. Richards, F. R. S. and R. R. Sharp, Proc. R. Soc. Lond. A 337, 297 (1974).
- 85. G. W. Gokel, D. J. Cram, C. L. Liotta, H. P. Harris, and F. L. Cook, J. Org. Chem., 39, 2445 (1974).
- 86. B. Dietrich, J. M. Lehn, J. P. Saurage and J. Blanzat Tetrahedron 29 (1973).
- 87. H. K. Fransdorff, J. Amer. Chem. Soc. 93, 4684 (1971).
- 88. R. M. Izatt, J. H. Rytting, D. P. Nelson, B. L. Haymore and J. J. Christensen, J. Amer. Chem. Soc. 93, 1619 (1971).
- 89. Fred J. Tehan, Michigan State University Ph.D. Thesis (1973).
- 90. David L. Wright, Michigan State University Ph.D. Thesis, (1974).
- 91. G. Foex, C. J. Gorter and L. J. Smiths "Constantes Selectionnees, Diamagnetisme et. Paramagnetisme, Relaxation Paramagnetique" Masson & Cie Editeurs, Paris (1957).
- 92. M. S. Greenberg, R. L. Bonder and A. I. Popov, J. Phys. Chem. <u>77</u>, 2449 (1973).

- 93. Y. M. Cahen, Ph.D. Thesis, Michigan State University (1975).
- 94. W. J. DeWitt, Ph.D. Thesis, Michigan State University (1975).
- 95. J. M. Ceraso, Ph.D. Thesis, Michigan State University (1975).
- 96. A. L. VanGeet, J. Amer. Chem. Soc. 94, 5583 (1972).
- 97. E. G. Bloor and R. G. Kidd, Can. J. Chem. <u>46</u>, 3425, (1968).
- 98. R. H. Erlich and A. I. Popov, J. Amer. Chem. Soc. <u>93</u>, 5620 (1971).
- 99. A. I. Popov and N. E. Skelly, J. Amer. Chem. Soc. <u>76</u>, 5309 (1954).
- 100. R. L. Kay, B. J. Hales and G. P. Cuningham, J. Phys. Chem. 71, 3925 (1967).
- 101. V. A. Nicely, J. L. Dye, J. Chem. Ed. 48, 443 (1971).
- 102. J. M. Lehn, J. P. Sauvage, Chem. Commun. 440 (1971).
- 103. H. S. Gutosky, D. W. McCall and C. P. Slichter J. Chem. Phys. 21, 279 (1953).
- 104. H. M. McConnell, J. Chem. Phys. 28, 430 (1958).
- 105. J. W. Cooper "An Introduction to Fourier Transform NMR and the Nicolet 1080 Data System", page 26.
- 106. M. S. Greenberg, Ph.D. Thesis, Michigan State University (1974).